# Historical Contingency in Microbial Ecology and Evolution

by
Reena Debray

A dissertation submitted in partial satisfaction of the
requirements for the degree of
Doctor of Philosophy
in
Integrative Biology
in the
Graduate Division
of the
University of California, Berkeley

Committee in charge:

Professor Britt Koskella, Chair
Professor Mary Power
Professor Rachel Brem

Spring 2023

Abstract

Historical Contingency in Microbial Ecology and Evolution
by
Reena Debray

Doctor of Philosophy in Integrative Biology

University of California, Berkeley

Professor Britt Koskella, Chair

The responses of biological systems to perturbations can depend on past events, a phenomenon known as historical contingency. The fitness of a new species in a community, or of a new mutation in a genome, is always evaluated within the existing context. Identifying historical processes in ecology and evolution has been challenging, as it requires a detailed record of past events. Further, historical contingency can make each instance of community assembly or each mutational sequence appear unique, and potentially not useful for building predictive frameworks. However, a growing body of work reveals that we can, in fact, identify conditions that alter the balance of historical and deterministic processes across systems, and that this understanding can help us interpret puzzling patterns of divergence among populations or communities. My dissertation research explores historical contingency in the ecology and evolution of microorganisms, including bacteria, fungi, and phages. I focus on microbes as a tractable model system for other organisms, an interesting case study when patterns do not align with those of other organisms, and an important component of ecosystems in their own right.

## Table of Contents

# Curriculum vitae

**EDUCATION**

2018–present **University of California, Berkeley**
Integrative Biology Ph.D. program
Advanced to Candidacy April 2020

2014–2018 **Duke University**
Bachelor of Science in Biology, *summa cum laude*
Graduation with High Distinction

**PUBLICATIONS**

*Submitted manuscripts*

9. Marinos, G., Hamerich, I.K., **Debray, R.,** Obeng, N., Petersen, C., Taubenheim, J., Zimmermann, J., Blackburn, D., Samuel, B.S., Dierking, K., Franke, A., Laudes, M., Waschina, S., Schulenburg, H., Kaleta, C. Metabolic model predictions enables targeted microbiome manipulation through precision prebiotics.

8. Mehlferber, E., McCue, K., **Debray, R.**, Kaulbach, G., Ferrel, J., Khanna, R., Koskella, B. Early phyllosphere microbial associations impact plant reproductive success.

*Peer-reviewed publications*

7. **Debray, R.**, Conover, A., Dewald-Wang, E.A., Zhang, X., Koskella, B. Within-host adaptation alters priority effects within the phyllosphere microbiome. *Nature Ecology and Evolution* 7, 725-731.

6. **Debray, R.**, De Luna, N., Koskella, B. 2022. Historical contingency drives compensatory evolution and rare reversal of phage resistance. *Molecular Biology and Evolution*, 39(9): msac182.

5. Mitchem, L., Formica, V., **Debray, R**., Homer, D., Brodie, E.D. 2022. Mycophagous beetle females do not behave competitively during intrasexual interactions in presence of a fungal resource. *Ecology and Evolution* 12(6): e8977.

4. **Debray, R.**, Socolar, Y., Kaulbach, G., Guzman, A., Hernandez, C.A., Curley, R., Dhond, A., Bowles, T., Koskella, B. 2021. Water stress and disruption of mycorrhizas induce parallel shifts in phyllosphere microbiome composition. *New Phytologist* 234(6): 2018-2031.

3. **Debray, R.***, Herbert, R.*, Jaffe, A.L., Crits-Christoph, A., Power, M.E., Koskella, B. 2021. Priority effects in microbiome assembly. *Nature Reviews Microbiology* 20, 109-121.

2. Mitchem, L., **Debray, R.**, Formica, V.A., Brodie, E.D. 2019. Contest interactions and outcomes: relative body size and aggression independently predict contest status. *Animal Behaviour* 157, 43-49.

1. **Debray, R.***, Snyder-Mackler, N.*, Kohn, J., Wilson, M., Barreiro, L., Tung, J. 2019. Social affiliation influences mitochondrial DNA regulation in female rhesus macaques (*Macaca mulatta*). *Biology Letters* 15: 20180643.

**TEACHING**

2022 UCB/PLANTBI22 Microbial Friends and Foes *(Graduate Student Instructor)*

2021 UCB Genomes and Plant Health High School Workshop *(Instructor)*

2021 UCB Genomes and Plant Health Undergraduate Workshop *(Instructor)*

2019 UCB/BIO1A Molecular and Cell Biology *(Graduate Student Instructor)*

**AWARDS AND HONORS**

*Fellowships, Scholarships, and Awards*

2022 Deutscher Akademischer Austauschdienst Research Fellowship– **awarded to top North American Ph.D. students to conduct research in Germany**

2018-2023 NSF Graduate Research Fellowship – **awarded to top Ph.D. students nationally to fund dissertation studies for three years**

2018 Elected to Phi Beta Kappa

2018 Elected to Sigma Xi

2018 Duke University Horn Memorial Prize – **awarded annually to the biology student who has "demonstrated the highest level of academic achievement and promise"**

2017 UC Berkeley Amgen Scholars Program

2017 Barry M. Goldwater Scholarship (Honorable Mention)

2016 NSF Research Experience for Undergraduates Fellowship

2015 Howard Hughes Research Fellowship

*Research Grants*

2022 Berkeley IB Summer Research Award ($2040)

2021 Diversity, Equity, and Inclusion Small Grants Program ($3000)

2021 Berkeley IB Summer Research Award ($2900)

2020 Sigma Xi Grant in Aid of Research ($1000)

2020 Berkeley IB Summer Research Award ($2000)

2019 Sakana and Uplands Foundations Fund ($2500)

2019 Society for the Study of Evolution Lewontin Award ($2500)

2019 Sigma Xi Grant in Aid of Research ($200)

2015 Duke University Undergraduate Research Support Grant ($400)

**PROFESSIONAL SERVICE**

*Diversity, Equity, and Inclusion:* Institutional research on aspects of graduate student-advisor relationships that predict productivity and well-being for students from historically underrepresented backgrounds. **Supported by a DEI award from UC Berkeley**.

*Science Communication*: Writer for Berkeley Science Review (2021-2022) and the AZ Daily Star (2018).

*Peer Review:* New Phytologist, ISME, Molecular Ecology, Proceedings of the Royal Society B, Environmental Microbiology, Microbiology Spectrum, Functional Ecology, The Plant Journal, The American Naturalist, Journal of Evolutionary Biology.

*Conference and Workshop Organizing*: Synthetic Microbiome Communities (November 2022), Microbiome Spring Symposium (May 2022), Technology for Microbiome Sciences (March 2021), Theory for Microbiome Research (November 2020), Model Systems for Microbiome Research (August 2020), Data Science for Microbiome Research (February 2020), Technology for Microbiome Sciences (May 2019), Theory for Microbiome Research (March 2019).

*Committee Membership:* Search committee for Assistant Professor in Global Change Biology.

*Undergraduate Research Mentorship:* Griffin Kaulbach, Haverford College KINSC Scholars Program (2019-2021); Nina De Luna, UC Berkeley Amgen Scholars Program (2019).

*Other Outreach and Mentorship:* NSF Graduate Research Fellowship workshop (2022), Society for the Study of Evolution undergraduate mentoring program (2021), National Alliance on Mental Illness (2016-2018), Females Excelling More in Math, Engineering, and Science (2014-2018).

**PRESENTATIONS**

| | |
|---|---|
| 2023 | **Invited speaker:** Woods Hole History of Biology Seminar (upcoming). Oral presentation. |
| 2022 | Max Planck Meeting in Microbial Communities and Coevolution. **Recipient of Berkeley Graduate Division Travel Grant.** Oral presentation. |
| 2022 | **Invited speaker:** UC Berkeley Center for Theoretical and Evolutionary Genomics. Oral presentation. |
| 2021 | **Invited speaker:** Stanford Eco-Evo Seminars. Oral presentation. |
| 2021 | UC Berkeley Ecology Lunch Seminars. Oral presentation. |
| 2021 | Phyllosphere Fortnight. Oral presentation. |
| 2021 | Society for the Study of Evolution (SSE). Poster presentation. |
| 2020 | Bay Area Ecology and Evolution of Infectious Disease (BAEEID). Poster presentation. |
| 2019 | American Society for Microbiology (ASM) Meeting. Poster presentation. |
| 2017 | Society for Molecular Biology and Evolution (SMBE) Annual Meeting. **Recipient of SMBE Travel Award.** Poster presentation. |
| 2017 | Society for Integrative and Comparative Biology (SICB). **Recipient of NSF REU Travel Award and Charlotte Mangum Student Support Grant.** Poster presentation. |

# 1. Introduction

In many instances, the development of the diversity of life on Earth has hinged on certain critical events happening at the time and place that they did. For example, the eukaryotic cell first originated when an archaeon engulfed a bacterium that gave rise to the mitochondria – an event that has never, to our knowledge, been replicated since (1). The massive asteroid that hit the earth at the end of the Cretaceous Period caused the sudden extinction of non-avian dinosaurs, leaving an evolutionary opportunity for the rapid adaptive radiation of the surviving mammals, including our ancestors (2). Later, the retreat of North African forests was thought to select for primates to descend from the trees and evolve to walk on their hind legs, eventually permitting the development of tool use and the evolution of higher intelligence (3). Stephen Jay Gould famously postulated that if we could rewind the history of life on Earth and rewatch it again and again, the outcomes would likely be different (4). How many times would consciousness evolve again? What about multicellular life? How many times would cells even arise at all?

Gould lamented that "The bad news is that we can't possibly perform the experiment." But in the intervening thirty years, biologists have developed a variety of other creative approaches to explore how historical processes shape ecology and evolution. For example, phylogenetics allows us to reconstruct relationships among lineages and infer what traits their ancestors had, helping us identify when certain traits arise only in the presence of key facilitating mutations (5,6). Geneticists are exploring how gene-gene interactions limit the evolutionary pathways available to organisms, with populations often reaching different local optima on the adaptive landscape depending on the order in which mutations appear (7). Ecologists are investigating how organisms modify their environments, changing which species can colonize after they arrive (8). Biochemists are showing how mutations interact to shape protein function and stability, providing insight into why the effect of a new mutation often depends on the genetic context in which it arises (9,10).

As an experimental biologist, I tackle this question by manipulating historical events in the lab and watching ecological and evolutionary events play out in real time. I use microorganisms as a model system because they allow me to do many things that Gould thought were impossible at the time: preserve populations indefinitely in stasis, resurrect them at any time, and observe community assembly and genetic adaptation within the span of weeks or months (11). In my dissertation research, I used this framework of "replaying" ecology and evolution to provide new insights into five different scientific questions.

In my first chapter, I worked with a diverse team of microbiologists and ecologists to develop new methods for analyzing microbiome sequence data. Unlike plant and animal ecosystems, microbial communities are typically profiled indirectly through sequencing. A particularly common method is to sequence a short section of a highly variable gene to characterize microbiome diversity in a given environment. While this approach – called amplicon sequencing – has revolutionized the microbiome field in the past decade, it is still quite limited. Amplicons do not provide information about genome content, ecosystem function, or even whether the microbial cells they originated from were dead or alive (12). They provide relative, not absolute, abundances of microbial species and often cannot reliably

classify organisms at the species or strain level (13). I developed a framework to identify signatures of priority effects – a phenomenon in which community assembly outcomes depend on historical events such as arrival order – using only the level of species identification that is typically available in such studies (14).

My second chapter tested for priority effects in the lab, expanding beyond ecological effects to incorporate evolutionary changes that occur between arrival of one species and the arrival of another. I introduced bacterial species to tomato plants in varying orders and measured community assembly outcomes. In agreement with the computational data analysis of my first chapter, as well as previous studies (15,16), I found that priority effects were strongest when the species involved overlapped sufficiently in their ecological requirements. I next asked how adaptation to the local environment – a less considered advantage of early arrival – would alter priority effects (17).

In my third chapter, I worked with a team of agroecologists to explore how agricultural management practices impact soil health. We were particularly interested in the response of arbuscular mycorrhizal fungi, which colonize plant roots and assist the plant in a number of ecological services including nutrient and water acquisition, stress tolerance, and fertility (18–20). I harvested leaves from tomato plants grown in full-water and drought conditions, either with or without access to their mycorrhizal symbionts. I found a 25% reduction in biodiversity of both bacteria and fungi when plants were grown without mycorrhizae. To ask whether the plant microbiome can recover from this disturbance, I took an "ecological replay" approach, transplanting microbial communities from either mycorrhizal or non-mycorrhizal plants in the field onto mycorrhizal or non-mycorrhizal plants in the lab (21).

Similarly, my fourth chapter used this field-to-lab transplant approach to test how microbial communities would assemble under different conditions. I was motivated by the observations that viruses of microbes (phages) can maintain microbiome community diversity by preying on abundant species (22,23) and that microbiome diversity often predicts resistance to pathogen infection (24,25) to predict that phages play an indirect role in pathogen defense by maintaining microbiome diversity.

My final chapter tackled a decade-long microbiological puzzle. Bacteria are under frequent parasitism by viruses (bacteriophages), and while they can evolve to evade phage infection, they tend to do so at a cost to growth or reproductive rates (26–28). Since phage-mediated selection pressures are constantly changing as bacteria coevolve, and phage resistance is costly when not in use, resistance mutations should be short-lived in nature (29). Yet surveys of wild bacterial communities often find that they are still resistant to phages that existed months or years in the past (30,31). I hypothesized that bacteria might harbor signatures of historical coevolution because certain resistance mutations are unlikely or even impossible to reverse once they have been required.

Finally, I was fortunate to work on an extremely eye-opening research study focused on mentorship of graduate students in the biological sciences. My collaborators and I surveyed graduate students at the University of California, Berkeley about their advisor's mentoring style and the support they received from their lab and research program more broadly. We aimed to identify mentoring practices that predict graduate student diversity, productivity, and well-being. The results of this study, and commentary on how they can be used to create more supportive and equitable scientific environments, are presented in the Appendix.

# 2. Priority effects in microbiome assembly

Parts of this chapter have been adapted from the following with permission:
Debray, R.*, Herbert, R.A.*, Jaffe, A.L., Crits-Christoph, A., Power, M.E., Koskella, B. 2022. Priority effects in microbiome assembly. *Nature Reviews Microbiology* 20(2): 109-121.
*These authors contributed equally.

## 2.1 Introduction

Decades of ecological theory and field experiments have demonstrated that the initial assembly of ecological communities or their recovery following disturbance can depend on historical processes, including the sequence in which species arrive (32–36). Arrival history influences succession when species that arrive earlier alter resources or environmental conditions in ways that impact species that arrive later, affecting their ability to establish in the community. These interactions, known as priority effects, can generate alternative successional trajectories for whole ecosystems (8). Thus, our knowledge of priority effects in plant and animal communities has critically informed ecological restoration and agricultural practices (37,38).

Until recently, our understanding of historical assembly processes in complex microbial communities has been limited by methodological challenges of characterizing members of microbial communities and their interactions (39). Now, clear evidence of important priority effects in microbiomes is growing and these effects have been shown to influence microbiome assembly across a variety of habitats, including the mammalian gut (40–43) and skin (44), plant foliage (45–47), nectar (15) and roots (48,49), and free-living terrestrial (50) and aquatic (51,52) communities. As microbiome composition is linked to host health and/or ecosystem function in many of these systems (53,54), priority effects represent an important avenue for the management and manipulation of microbiomes in agriculture, conservation and medicine. The rich history of research on priority effects in other systems gives microbial ecologists an excellent framework against which to compare and contrast the assembly of microbial communities. However, key differences in scales of observation, community complexity and life history can limit the direct translation of theoretical predictions to microbiomes.

*Mechanisms of priority effects*

Primary succession (the initial assembly of biota on sterile substrates) and secondary succession (recovery by regrowth and colonization following perturbation) can follow multiple trajectories depending on how early colonists affect later arrivers (32) (Figure **1**). Interactions between early-arriving and late-arriving species can be mediated by trophic resources that are actively metabolized, such as limiting nutrients, or by non-trophic resources, such as micro-environments that provide protection from stress. While priority effects are most often detected during initial assembly or recovery periods, they describe effects of resident community composition on arriving species independent of the time since the habitat was created or disturbed.

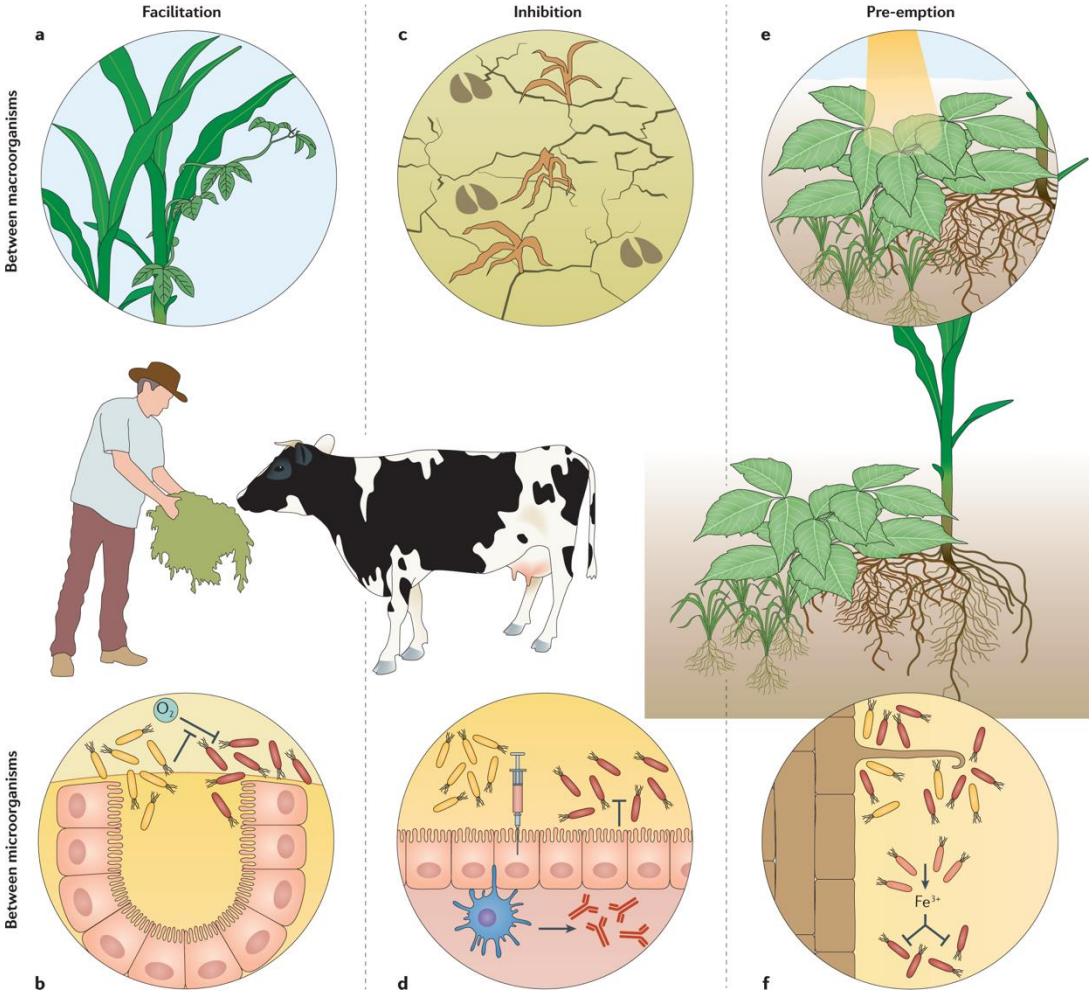


**Figure 1. Priority effects between macroorganisms and between members of their microbiomes in a hypothetical terrestrial ecosystem. a)** Early-planted legume crops facilitate overyielding of grains such as corn through nitrogen sparing (55). **b)** Aerotolerant bacteria facilitate the subsequent colonization of obligate anaerobes in the neonatal intestine by depleting oxygen (56). **c**) Cattle treading affects soil compaction and water retention, inhibiting the germination and growth of new seedlings (57). **d**) Early exposure to pathogens confers cross-immunity to related bacteria in many mammals (58). **e**) Early-arriving plants inhibit the growth of late arrivers through nutrient and light pre-emption (55,59). **f**) Early-arriving, root-associated bacteria can inhibit late-arriving strains through the pre-emption of essential nutrients such as iron (60).

*Niche pre-emption*

Niche pre-emption occurs when an early-arriving organism depletes resources, thereby inhibiting the establishment of a late arriver. Multiple lines of evidence point to niche pre-emption, particularly competition for nutrients (exploitative competition), as an important process in microbiome assembly. Within simplified communities of protozoans, bacteria or yeast, early arrivers are often able to exclude late arrivers in microcosms (15,61,62). Amplicon surveys tracking succession in the *Arabidopsis thaliana* phyllosphere (63) and the infant human gut (64) showed that ecologically similar bacteria tended to occur within the same host population but that individual hosts were dominated by different bacterial species. In the *A. thaliana* study, the spatial arrangement of plants in the greenhouse influenced initial exposure

to microbiota members and strains that established early excluded subsequent strains from occupying the same niche (63).

Furthermore, observed priority effects are often strongest among species that require the same resources (15,62). For example, inoculation order predicted growth among pairs of nectar yeast species with similar amino acid consumption profiles (15). The life history traits of many microorganisms are not well characterized and may not correlate with marker gene sequences. Thus, approaches in metabolic modelling or metagenomic analyses that incorporate microbial function as well as experimental manipulations of arrival order have proved particularly useful in uncovering these complex effects (40,44). The effect of nutrient pre-emption may be altered or prevented by the relative concentrations of other limiting nutrients. For example, algae that are individually superior competitors for either silicate or phosphate can coexist or competitively exclude one another, depending on the concentrations of these nutrients in a nutrient-limited freshwater medium (65). Similarly, competition between bacteria and yeast of the nectar microbiome for amino acids is temperature dependent (66), likely owing, in part, to a shift in the competitors' metabolism. Therefore, broadly speaking, generally inhospitable environments may weaken pre-emptive priority effects in microbial communities by limiting population growth of an early-arriving population and reducing its chances of increasing to a non-invasible density.

Non-trophic resources are also crucial for establishment and thus have the potential to shape priority effects. Niche pre-emption can also occur through competition for space (including through interference competition). For example, ectomycorrhizal fungi compete for space on plant roots (49). In the mouse gut, early-arriving *Bacteroides* strains penetrate and saturate deep colonic crypts, forcing subsequent strains to occupy less protected niches that are cleared by the mouse immune system (41). While simple models of competition often predict the success of superior competitors, accounting for niche pre-emption predicts that species can gain an advantage from arriving early despite characteristics that could otherwise limit their competitive fitness.

*Niche facilitative modification.*

Niche facilitative modification (facilitation) occurs when an early-arriving organism alters the environment in a way that benefits a later-arriving organism. Facilitation is also common in microbial communities, where many strains can metabolize byproducts of other organisms. In particular, the ability of arriving microorganisms to establish can depend on the presence of microorganisms that have broken down large organic molecules into smaller molecules, making otherwise inaccessible nutrients available (40,51). Facilitative priority effects can also be mediated by stress reduction: in harsh environments, such as the plant phyllosphere, arriving strains have a higher probability of survival when they land in multicellular microbial aggregates that have produced extracellular polysaccharides that reduce desiccation stress (67,68). As in niche pre-emption, the ecological interactions that underlie facilitation often depend on resource availability (69), making it likely that facilitative priority effects can also be highly context dependent. In host-associated microbiomes, early arrivers can also facilitate late arrivers by modifying host physiology or immunity. For example, some plant-associated bacteria can modify host tissues to increase nutrient leakage (68).

Furthermore, many microorganisms, particularly pathogens, suppress host immunity as they establish, facilitating colonization by other microorganisms that would have otherwise been recognized by the same immune pathway (45,47,70). Owing to the rapid coevolution of host immune genes and pathogen effectors, the magnitude and direction of this effect can be highly dependent on host and pathogen genotypes. For example, virulent strains of *Xanthomonas perforans* can suppress the tomato immune response and facilitate colonization by *Salmonella enterica*, while avirulent strains of *X. perforans* instead stimulate the immune response and inhibit *S. enterica* (70). Similarly, prior infection by the fungal pathogen *Zymoseptoria tritici* suppresses the wheat immune response and facilitates *Pseudomonas syringae* colonization, but only in a cultivar that is susceptible to *Z. tritici.* In a resistant cultivar, the opposite occurs: *Z. tritici* infection stimulates the wheat immune response and inhibits subsequent colonization by *P. syringae* (45).

Many microorganisms facilitate the dispersal of other species through substrates or around host tissue. For example, the hyphae of osmotrophic fungi create a physical scaffold and a surrounding micro-aqueous environment that enhances the dispersal of motile bacteria such as *Serratia proteamaculans* in cheese rinds (71). In such cases, resident strains benefit new arrivers by increasing their access to their environment.

*Niche inhibitory modification.*

Niche inhibitory modification (inhibition) occurs when an early-arriving species modifies conditions (rather than resource levels) in a way that slows or prevents the establishment of later-arriving species (8,32). Niche inhibitory modification can arise through apparent competition or through interference competition. The best-studied examples of priority effects via apparent competition are mediated by host immunity. Many members of Bacteroidetes and Firmicutes produce short-chain fatty acids in the human gut that stimulate mucus and epithelial cell growth and production of antimicrobial peptides, reducing subsequent colonization by enteric pathogens (72). Conversely, pathogens such as *Salmonella enterica* subsp. *enterica* serovar Typhimurium have been shown to modulate host immune responses to inhibit gut commensals and facilitate their own growth (73). Indeed, although typically considered strictly in terms of molecular interactions with hosts, effector proteins such as Ave1, which is secreted by the fungal plant pathogen *Verticillium dahliae*, can also reduce resident bacterial density in tomato and cotton plants, thus clearing the way for subsequent fungal colonization (74). Pathogens can also remodel the host environment in other ways, such as through necrosis of host tissue, which negatively affect the diversity and composition of microorganisms that can survive in the host (75,76). These effects may help explain the common observation that microbiome diversity is reduced in hosts experiencing disease (53,54).

Apparent competition as a result of shared protozoan or viral predators is likely common in microbiomes and may therefore be an important mechanism by which early-arriving species inhibit subsequent colonization by other species. For example, temperate phages arrive in the microbiome in the genomes of bacterial hosts but can occasionally enter the lytic cycle and infect neighbouring cells, including competitors. The presence of a temperate phage in a resident strain of *Bordetella bronchiseptica* limits colonization by another, phage-sensitive *B. bronchiseptica* strain in pure culture (77). Apparent competition is likely to influence and complicate priority effects in many other ways, as predation can slow the

nutrient depletion or niche construction activities of early-arriving species, select for costly resistance traits and release nutrients sequestered in dormant cells (78). Increasing evidence indicates that viruses of microorganisms can also interact with eukaryotic hosts; for example, lytic production of a Pseudomonas aeruginosa phage increases anti-viral immune responses in the mouse lung, thus suppressing the host response to bacteria (79). These studies highlight the need for future work to characterize the roles of predation and parasitism in microbiome assembly. Finally, direct inhibition in host-associated and environmental communities can occur through bacterially produced compounds. In these cases, interference competition can lead to niche inhibitory modification rather than niche pre-emption because the early arriver degrades an environment for a late arriver without necessarily occupying the space itself. In the mouse caecum, acid production by *Bifidobacterium animalis* subsp. *lactis* reduces pH, creating a non-permissive environment for colitis-inducing Enterobacteriaceae (80). In fermented foods, such as cheese and sourdough, Lactobacillus and Lactococcus species produce bacteriocins with antimicrobial activity against foodborne pathogens such as Salmonella paratyphi (81,82). In the human gut and on human teeth, microaerobic bacteria arrive early in succession and deoxygenate the environment, limiting the establishment of other aerobes while simultaneously facilitating colonization by anaerobes (56,83).

*Functional outcomes of priority effects.*

It is well known that different species can fill similar ecological roles, complicating the interpretation of turnover in community composition across time or space (84). Functional redundancy, when two different taxa perform similar ecosystem functions (for example, as measured in microbiomes by gene content, chemical productivity or host outcomes) is seemingly common in microbial communities (85,86). Nonetheless, microbiome assembly history has been shown to affect community-level and ecosystem-level properties, including biomass distribution (87), decomposition rates (50,62), nutrient cycling (50,88,89), host health (44,45,48,90) and productivity–biodiversity relationships (91). These observations raise the questions of when and how the effects of assembly history are of functional significance.

A helpful framework is to consider species in terms of their resource requirements and environmental impacts (also referred to as guilds or functional groups). Depending on the mechanism, priority effects can occur between species with similar or different resource requirements but are unlikely to affect function when they occur between species from similar functional groups (Figure **2a,b**). However, there are many ways through which priority effects can occur between species with different environmental impacts. Ecologically dissimilar taxa can affect one another by altering resources or environmental conditions, including the abundances of shared predators. Species that differ in most aspects of their requirements and impacts may nevertheless be all limited by an essential resource or, conversely, species with similar requirements may differ in one or a few key genes that translate to different environmental impacts (Figure **2c–e**). The latter case may be especially common in microbial communities, where closely related strains are often distinguished by the presence or absence of entire genes rather than single-nucleotide polymorphisms (92). An important caveat to this framework is that species-rich microbial communities can contain more taxa that perform unique functions as well as those that are functionally redundant than less diverse microbial

communities (93); thus, the consequences of priority effects for ecosystem function are likely to depend on the community context.

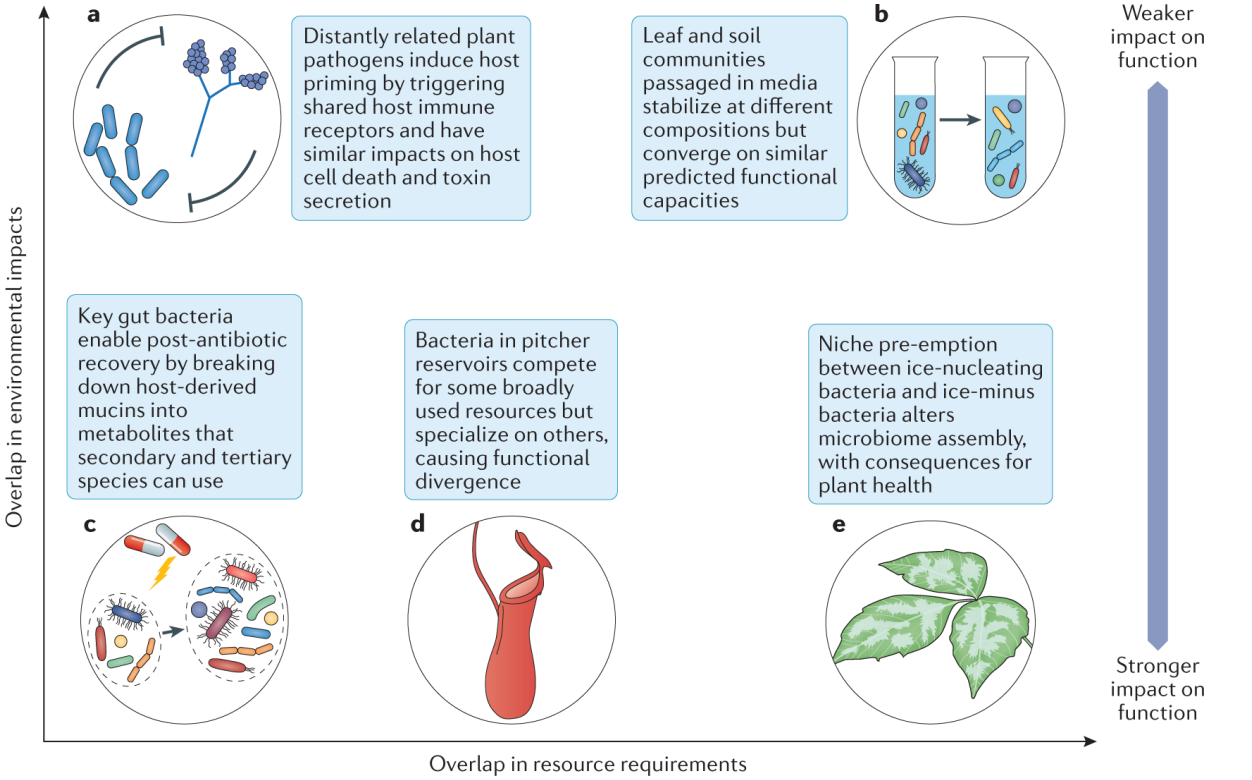


**Figure 2. Examples of priority effects with varying impacts on function**. **a**) Niche inhibitory modification can occur between species with different resource requirements, such as the fungal pathogen *Botrytis cinerea* and the plant pathogen *Pseudomonas syringae*, with similar consequences for host health (94). **b**) Many instances of priority effects between ecologically similar species do not affect microbiome function (95). **c**) Niche modification by early arrivers can facilitate or inhibit the colonization of functionally distinct microorganisms, altering the functional trajectory of the community (40). **d**) Niche pre-emption can occur between ecologically dissimilar species when they compete for a broadly used resource. Serially passaged pitcher plant microbiomes converge on broad functions such as $CO_2$ respiration despite assembly history but diverge on specialized functions such as endochitinase activity (89). **e**) Niche pre-emption between microorganisms that require most of the same resources can still affect function when they differ in a few key traits such as the presence or absence of ice-nucleating proteins that cause frost damage in plants (96).

## 2.2 Materials and Methods

*Detecting microbial priority effects*

Experimental studies that vary the arrival order of individual strains (15,46,50) or entire consortia (42,52,97) can directly measure both the role of priority effects in community assembly and the importance of external factors, such as nutrient availability, for these effects. Experimental manipulations of phyllosphere and mouse gut microbiome assembly showed that most observed priority effects were inhibitory, with only a minority of strains benefiting from facilitation (42,46). In the case of the phyllosphere, individual strain manipulations identified a small number of strains (keystone taxa) that were responsible for most observed priority effects (46). In the mouse gut, priority effects were found to be largely independent of the host immune response, suggesting that direct bacteria–bacteria interactions may comprise the

majority of such effects (42). However, probing the effects of individual strains requires cultivated isolates, whereas only a minority of bacterial species are easily culturable across ecosystems (98). In several cases, difficult-to-culture organisms have only been grown in co-cultures, relying on other microorganisms for compounds such as amino acids, vitamins or siderophores that they do not produce themselves (99,100). This extreme metabolic dependence suggests that uncultured taxa are particularly likely to be sensitive to the presence or absence of other taxa during microbiome assembly. In fact, this may contribute to observations of predominantly inhibitory interactions in laboratory studies (46). As such, despite the clear utility of experimental approaches in probing community assembly mechanisms, measures of priority effects using only culturable strains may miss many interesting or informative cases.

Approaches such as challenging established microbiomes with individual strains to examine invasion success with different resident microbiomes (16,48,101,102) or, conversely, inoculating hosts with specific isolates and then allowing natural colonization (103), are also experimental but can include naturally diverse communities with currently uncultured taxa. For example, wood disks pre-colonized with individual fungal isolates and deposited in leaf litter for 12 months developed different microbiomes depending on the identity of the pre-colonizer (103). These approaches are most informative when strains of interest have already been identified but their interactions within their overall community are not known.

Fully observational datasets have the highest potential to capture realistic microbiome dynamics, especially interactions involving rare and/or uncultured taxa, but can be more difficult to interpret in terms of mechanism or causation. Historically, ecologists have taken advantage of natural phenomena such as island formation or major disturbances to determine how communities assemble when successional dynamics are initiated or reset (104,105). Similarly, microbiome assembly can be measured during initial development of a new host or after disturbances such as antibiotic treatment. Early amplicon surveys showed that infants born by caesarean section acquire a smaller share of their early microbiota from their mothers than infants born by vaginal delivery and signatures of this event persist throughout early life (106,107). While it is not yet possible to rule out dispersal limitation or environmental differences as contributing mechanisms, recent work attributes some of this variation to niche pre-emption between *Bacteroides* (more abundant in vaginally born infants) and *Bifidobacterium* strains (more abundant in infants born by caesarean section). Whichever of these two genera was most abundant contributed the most to human milk oligosaccharide breakdown in the infant gut (64). Observational studies have also revealed that the compositional trajectory of the human gut microbiome after antibiotic perturbation depends on the activities of certain bacteria. Across several human cohorts, taxa associated with antibiotic recovery had genomes enriched for carbohydrate-degrading enzymes, particularly those that degrade host-derived mucins (40). This observation suggests that the initial breakdown of host-derived metabolites can support the growth of secondary or tertiary species (niche facilitative modification) and pave the way to the recovery of pre-antibiotic diversity.

*Re-analyzing data from mammalian gut microbiomes*

Experimental manipulation of arrival order allows direct examination of causative effects, an important and difficult undertaking in complex ecological communities. However, in

the absence of a priori hypotheses about which taxa are expected to interact, searching for a 'needle in the haystack' by individually permuting all strains in a model community can quickly become prohibitively labor-intensive. We reasoned that signatures of priority effects in community sequencing data could be detected in a dataset meeting the following conditions: (i) Repeated sampling from the same individual hosts over time, to quantify how successful species were at establishing after arrival; (ii) Sufficient cohort size to identify species that successfully established in some hosts they colonized but not others; and (iii) High temporal resolution, to test whether variation in the ability of a species to establish in a host was linked to resident microbiome composition prior to its initial colonization. We identified three mammalian gut datasets that met these criteria. One study followed 56 infants from birth through the first three years of life, sampling approximately monthly (108). Another tracked microbiome assembly in 12 mice during the first six months after birth (109), and the final dataset sampled the rumens of 45 cows approximately monthly for the first two years of life (43). We analyzed each dataset separately, as follows:

Within each dataset, we considered OTUs that were detected in at least 20% of hosts for any amount of time. We defined the first arrival of an OTU to a host as the first time at which its relative abundance was greater than zero. We then defined persistence as the proportion of the six-month window after arrival in which the OTU was detected at a relative abundance greater than zero. We thus calculated arrival time and persistence values for every OTU-host pair. For each OTU, we generated a Bray-Curtis dissimilarity matrix in which distances among hosts were based on counts of all other OTUs at the sampling point immediately before the focal OTU was first detected. We used the *adonis* function in the R package "vegan" (110) to identify OTUs for which, across hosts, microbiome composition before arrival predicted persistence.

We considered the possibility that these OTUs were simply responding to aspects of the environment, such as host development, that can be confounded with microbiome composition. To explore this possibility, we repeatedly permuted arrival times across hosts, constructed a Bray-Curtis dissimilarity matrix of resident microbiome composition based on the permuted arrival times, and re-tested the relationship between microbiome composition and persistence. This essentially tested whether microbiome composition at the same stage of development, but in a different host, predicted focal OTU persistence. Across 100 iterations per focal OTU, the permuted data rarely produced test statistics as extreme as the observed values (Figure **S1**). We aimed to identify individual taxa that contributed to observed relationships between microbiome composition and persistence. We focused on focal OTUs for which persistence was significantly associated with resident microbiome composition across hosts after correction for multiple testing. For each focal OTU, we used the negative binomial model implemented in the function *DESeq* (package "DESeq2" (111)) to identify partner OTUs whose relative abundance immediately before arrival of the focal strain predicted persistence of the focal strain. Finally, having identified candidate partner-focal pairs, we asked whether these relationships were phylogenetically structured. To generate a null distribution for each dataset, we resampled the same number of random pairs in each dataset 1000 times and calculated the proportion with the same family-level classification.

*Re-analyzing data from the plant rhizosphere microbiome*

Destructive sampling precludes measurements of microorganismal persistence, and thereby priority effects, within individual hosts. However, we reasoned that evidence of relevant interactions between microorganisms could still be identified in destructively collected datasets, provided they are sufficiently replicated. We identified a study which measured the development of the rice root microbiome in high temporal replication (112). Six rice cultivars were grown unequally across three field experiments in California and Arkansas, U.S.A., and sampled either weekly or biweekly across the plant life cycle. Random forest models were developed ranking the relative abundance of root associated OTUs by their contribution to the prediction of plant age at sampling. 85 plant age-predictive OTUs were identified for each of paired rhizosphere and root endosphere samples. Here, we hypothesized that many of these host age-predictive OTUs impact their surrounding community. For each of the common, biweekly samples, we used the *adonis* function to identify whether any of the 85 endosphere-associated OTUs correlated with the composition of their broader community as a factor nested by plant age at sampling. The relative abundance of 70 of these OTUs were significantly predictive of community composition. To control for the unequal planting of rice varietals in different field trials, we used the same function to conduct an additional PERMANOVA nesting the relative abundance of the OTU of interest by field site, rice cultivar, and plant age at sampling.

## 2.3 Results

With an appropriate observational dataset, it is possible to statistically predict which taxa are of interest and narrow the search space for subsequent experimental validation. Through re-analysis of publicly available data from the succession of human, mouse and cattle intestinal microbiomes, we demonstrate one way in which this can be done. Repeatedly sampling hosts over time captures the arrival times and subsequent persistence of individual taxa (Figure **3a**). With sufficient cohort size, the variation in persistence of individual taxa may be linked to resident microbiome composition before their arrival (Figure **3b,c**). Across datasets, candidate inhibitory priority effects consistently occurred among more closely related taxa than expected by chance (Figure **3d**). This pattern mirrors experimental work in aquatic microcosms (62), nectar yeast communities (15) and probiotic clinical trials (16), in which resident strains limited the subsequent establishment of other, closely related strains.

In many cases, repeated profiling of the same community can be challenging to perform, either as a result of destructive sampling, spatial structure within the microbiome or difficulty in acquiring samples from the same individual hosts over time. When working in a system that does not permit temporal sampling, it is best to draw from a large population of hosts sampled at different times with high temporal resolution. For example, the development of the rice root microbiome was followed by destructively sampling plants weekly or bi-weekly until maturity and senescence, using four plant genotypes unequally grown in field trials at three separate field sites (112). In these high-resolution datasets, strains of interest can be identified by linking the abundance, rather than the persistence, of individual taxa to the composition of the remaining community (Figure **4a**) and then to individual strains therein (Figure **4b**). This approach identified 66 OTUs which were significantly correlated with the composition of their community.

One such OTU (OTU 4453710) was annotated in the original publication as a *Rhodoferax* species, which is compelling, considering the list of plant age-predictive endosphere OTUs also contained three taxa annotated as *Geobacter* species (OTUs 344965, 167822, and 137893). Both genera broadly couple acetate oxidation with dissimilatory metal reduction; and some Rhodoferax species have been previously observed to compete with *Geobacter* spp. for iron and acetate in anoxic subsurface sediments (113). However, some species of *Geobacter*, specifically, are capable of reducing uranium and mercury contaminants, and are therefore relevant to bioremediation of contaminated groundwater (114). Moreover, *Geobacter* spp. have been observed to fix nitrogen and internally colonize diverse plant species (115). Considering that these three plant-age-predictive *Geobacter* OTUs were observed to increase consistently in relative abundance in the rice root endosphere after the shift to plant reproductive growth, when nitrogen demand is highest (116), they may also play a role in promoting plant growth. We plotted the relative abundances of *Rhodoferax* 4453710 against these three *Geobacter* OTUs and observed strong negative correlations across the biweekly samples, although this differed slightly by strain (Figure S2). One explanation for this is host developmental status, as *Rhodoferax* and *Geobacter* were identified as early and late arrivers to the rice rhizobiome, respectively. However, these *Geobacter* OTUs were scarcer in later timepoints (84, 98, and 112 days after planting) when *Rhodoferax* sp. 4453710 was more abundant. This trend was also evident within samples of the rice cultivar "CLXL745" collected from a single field trial in Jonesboro, Arkansas, suggesting that the covariation observed is caused by more than differences in field site or host genotype alone. Alternative factors such as dispersal limitation, environmental heterogeneity, or priority effects via niche preemption could result in such a pattern. However, having identified associations between taxa previously observed to compete is compelling, and at this point it is possible to design complementary laboratory experiments to explicitly test for priority effects involving the identified strains. In general, it is often necessary to integrate multiple pieces of evidence, including mathematical predictions, field observations and laboratory experiments, to fully understand ecological assembly processes in complex systems (117).

## 2.4 Discussion

*Shared insights across systems*

Sufficient theory and data are now available to address the characteristics of priority effects across systems. Although individual priority effects and their underlying mechanisms are likely to be system specific, we can begin to identify general circumstances that affect the likelihood and outcomes of priority effects. Mathematical models have an important role here as they allow the manipulation of parameters that vary across systems (such as resource availability (65), dispersal rates (118), spatial structure (119) and metacommunity structure (120)). Such insights will allow us to move towards a more predictive science and help to determine which principles apply both in communities of microorganisms and those of macroorganisms.

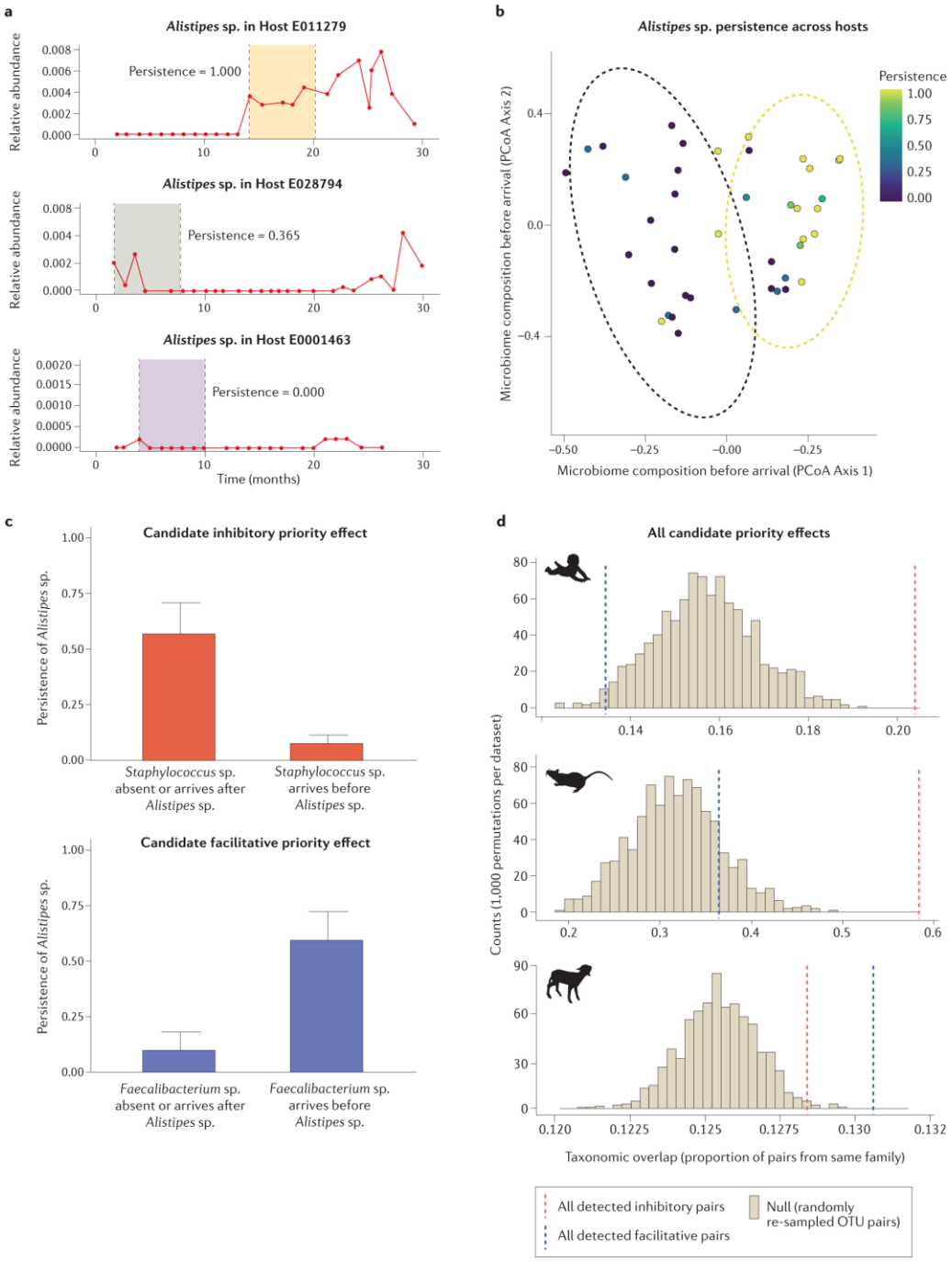


**Figure 3. Approaches for detecting candidate priority effects in time-series microbiome data.** **a**) Repeated sampling of individual hosts allows the calculation of arrival times and persistence values for each host–strain combination (43). Re-analysis of data from infant gut communities sampled monthly for the first 3 years of life (108) revealed variation in persistence of operational taxonomic units (OTUs) among infants. Here, we show the persistence of a representative OTU (OTU17, *Alistipes* sp.) across three infants. Persistence is defined as the proportion of a 6-month period after first arrival (indicated by shaded panels between dashed lines) in which relative abundance was greater than zero. **b**) Variation in the persistence of a single strain across hosts can be associated with resident microbiome composition. Here, we show a principal coordinate analysis (PCoA) in which each point represents microbiome composition immediately prior to the arrival of *Alistipes* sp. (OTU17) in an infant host. Clustering indicates that resident microbiomes associated with high persistence of *Alistipes* sp. were distinct from those associated with low persistence of *Alistipes* sp. Ellipses correspond to 95% confidence intervals based

on k-means clustering. **c**) When the persistence of individual taxa after arrival correlates strongly with resident microbiome composition (as shown in part b), negative binomial regression (111) can be used to identify microbiome features (that is, individual taxa) that differentiate high-persistence and low-persistence outcomes. Here, we show two taxa identified by this approach that predict persistence of *Alistipes* sp. (OTU17). Error bars represent 95% confidence intervals (1.96 times the standard error of the mean). **d**) We applied the approach described in parts **a**–**c** to published temporal microbiome data for mouse (109), human (108) and cattle (43) intestinal microbiomes within the first 1–3 years of life. In each dataset, the observed phylogenetic structure of the predicted OTU pairs was compared to a null distribution generated by measuring the phylogenetic structure of 1,000 permutations of correspondingly sized samples of OTU pairs from the entire dataset. Across all studies, <10 of 1,000 permutations reached or exceeded the level of taxonomic overlap of OTU pairs predicted to engage in inhibitory priority effects (that is, $p < 0.01$ for all datasets). The taxonomic overlap of facilitative priority effects was also higher than expected by chance in the cattle rumen microbiome ($p < 0.001$) but did not differ from chance in the mouse and human gut microbiomes.

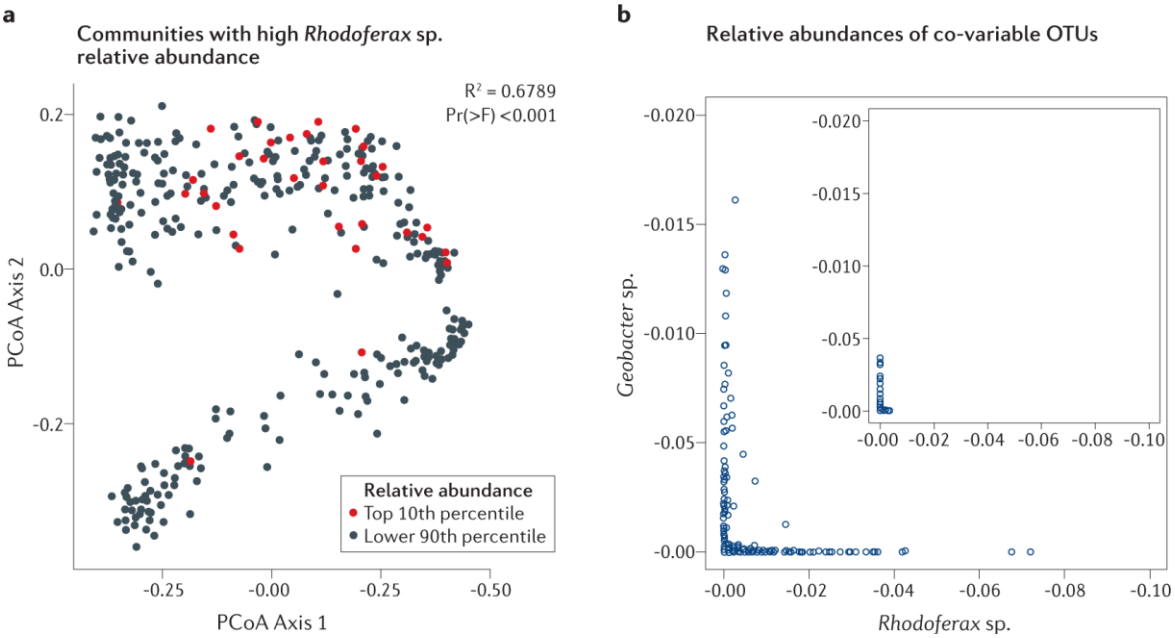


**Figure 4. Identifying strains of interest in destructively sampled microbiome data.** **a**) Destructive sampling of plant hosts over the course of their development allows the identification of strains whose abundance correlates with altered community states. Rice root endosphere samples from three field trials were harvested at common, bi-weekly time points from host germination to senescence (112). In our re-analysis of this published data, nested ANOVA reveals operational taxonomic units (OTUs; such as *Rhodoferax* sp.) whose abundance is significantly correlated with altered community states ($R^2$ and $p$ value of the F statistic (Pr(>F)), top right) despite a predominant effect of host age at sampling. **b**) Co-variance of OTUs reveals candidates potentially involved in niche pre-emption. For example, *Rhodoferax* sp. from part **a** co-varies with several OTUs annotated as *Geobacter* spp. across time points as well as at late time points at which *Geobacter* is predicted to be more fit in this system (for example, at 112 days; inset). That is, the presence of *Rhodoferax* sp. precludes *Geobacter* spp. and vice versa.

*Population dynamics.*

Priority effects are shaped by numerous properties of microbial populations, many of which are likely to interact (Table 1). Large populations or individual sizes of early arrivers commonly strengthen priority effects through niche pre-emption as they deplete resources, including space, more rapidly (121–123). Population density can be especially important in

habitats with only a few favorable microenvironments such as colonic crypts in the mammalian gut (41) and stomata on leaf surfaces (124).

| Parameter | Niche pre-emption | Local adaptation |
|---|---|---|
| Dispersal rate of early arriver | High dispersal rates increase changes of colonizing empty habitats and pre-empting resources (52). | High continuous dispersal can diminish rates of local adaptation of established colonists (118). |
| Lag time between early and late arrivers | The strength of priority effects should scale with lag time until the early-arriving population reaches carrying capacity (52). | The strength of priority effects should scale with lag time for much longer as evolutionary changes occur in the early-arriving population (125). |
| Fitness difference between early and late arrivers | Large fitness differences (i.e. late arriver is a superior competitor) may supersede priority effects (8). | Initial fitness differences should be less important, given sufficient time for early arrivers to adapt (126). |
| Initial size of early-arriving populations | Large initial population sizes buffer against ecological stochasticity and reduce the time needed to effect change on the environment (122). | Large initial population sizes buffer against ecological stochasticity and genetic drift (125). |
| Mutation rate in early-arriving populations | Unknown | High mutation rates facilitate adaptation to the new environment (125) |
| Standing genetic variation in early-arriving populations | Unknown | High standing variation facilitates adaptation to the new environment, especially in cases of short lag time between early and late arrivers (125) |
| Diversity of early-arriving community | May increase niche construction and favor subsequent diversification (including establishment of late-arriving populations) but with diminishing returns as niches are saturated (127). | Adaptation of individual populations can be limited by the presence of other community members, particularly competitors (128). |

The impact of niche modification can also depend on density. Nurse tree canopies in plants (129) and cellular aggregates in bacteria (130) both shield immigrating individuals from heat and ultraviolet stress, with denser populations being more protective. Low to intermediate densities of fermentative bacteria facilitate the growth of photoheterotrophic bacteria but large populations overproduce organic acids, acidifying the environment and changing the interaction from facilitative to inhibitory (131,132). Ectomycorrhizal fungi can facilitate Pinaceae invasion into new environments but only when they are present in high densities (133). Last, host immune modification typically requires sufficient biomass for detection. For example, activation of the plant immunoreceptor FLS2 depends on the dosage of microbial flagellin (134). Similarly, the tolerance of the host mosquito species Aedes aegypti and Aedes albopictus to Dengue virus conferred by the endosymbiotic bacteria Wolbachia depends on the

density of Wolbachia (135). However, not all priority effects are influenced by population density. In many cases, the impacts of the early arriver and the requirements of the late arriver are better predictors of community assembly outcomes than abundance (136). For example, larger phototrophs that use light less efficiently coexist with smaller, more efficient taxa that are less impacted by shading in both terrestrial plant assemblages (137) and microbial communities (138,139). In other cases, small populations of keystone species can, despite their rarity, substantially impact subsequent microbiome colonization (140,141). One such species is the bacterium Porphyromonas gingivalis, a low-abundance member of dental biofilms that can alter oral microbiome composition and cause inflammatory disease (140).

*Spatial and temporal scales.*

The study of priority effects requires a priori understanding of both the spatial and temporal scales of community assembly. Unlike well-mixed liquid lab media, most habitats are physically and chemically heterogeneous. Priority effects among microorganisms therefore depend not only on population density but also on the distribution of individuals in space. Environmental features such as fluid velocity gradients (142), soil granularity (143) and the distribution of free water on surfaces (144) all affect spatial patterns in microbial communities. Although the influence of spatial structure on priority effects in microbiomes has not been well studied, several predictions can be generated from theory and data on contemporaneous strain interactions. Physically structured environments allow individuals to associate more often and more predictably with kin or mutualistic partners and such spatial associations are widely believed to stabilize cooperative traits by excluding non-contributors (145,146). Priority effects that are mediated by metabolites (40,51) may therefore be more pronounced in spatially structured environments, where these products can be retained locally ('privatized') by the partners or consortium. Conversely, theoretical analyses and experiments show that spatial structure can allow competitors to stably coexist over larger spatial scales by occupying different microhabitats (119,147). Early-arriving strains should be slower to saturate all available microhabitats in highly structured environments, weakening their ability to preempt late arrivers. Moreover, depending on whether dispersal to nearby microhabitats is more likely from within the metacommunity or from without, arrival times to microhabitats will vary among strains, blurring the overall patterns of priority effects observed.

Spatial scales of priority effects depend on their underlying mechanisms as well as on properties of the environment (Figure **5a–c**). Many interactions among microorganisms are mediated by secreted compounds, such as metabolites, toxins and enzymes, that are often highly restricted in range (148). Advection (transport of a substance by flow of a fluid) and diffusion are limited by extracellular polysaccharides in biofilms but can occur over longer distances in many settings depending on viscosity and flow in fluids or on porosity and permeability in solid substrates (such as soils, sediments, leaf surfaces and skin). Moreover, in cases where interactions are modulated by host immunity, these effects can be far-reaching relative to cell or aggregate size (45,149). As with spatial distances, the temporal windows across which microorganisms interact can depend on several factors, including host biology (Figure **5d–f**). Microbial populations present in reproductive organs (for example, vaginal and floral populations) can populate offspring and shape microbial succession across host generations (107,150). Similarly, strains that colonize during critical periods of host immune

system development can shape antigen recognition within and across host generations (151,152). Of note, modification of host immunity may be unusual in that, once it has occurred, it may continue to impact community composition regardless of the continued presence or abundance of a causative organism in the community (151).

In many cases, the strength of priority effects increases with the lag time between early and late arrivers (42,52). Given sufficient lag time, priority effects can also be the result of evolution. Though often overlooked, early arrivers may not only pre-empt and monopolize resources but also have more time to adapt to local conditions and/or to diversify (Appendix). Given the potential for long-term changes in fitness in resident species, we might expect priority effects in microbial communities to be longer-lasting (when scaled to generation time) than in their plant and animal counterparts and to involve eco-evolutionary interactions more often.

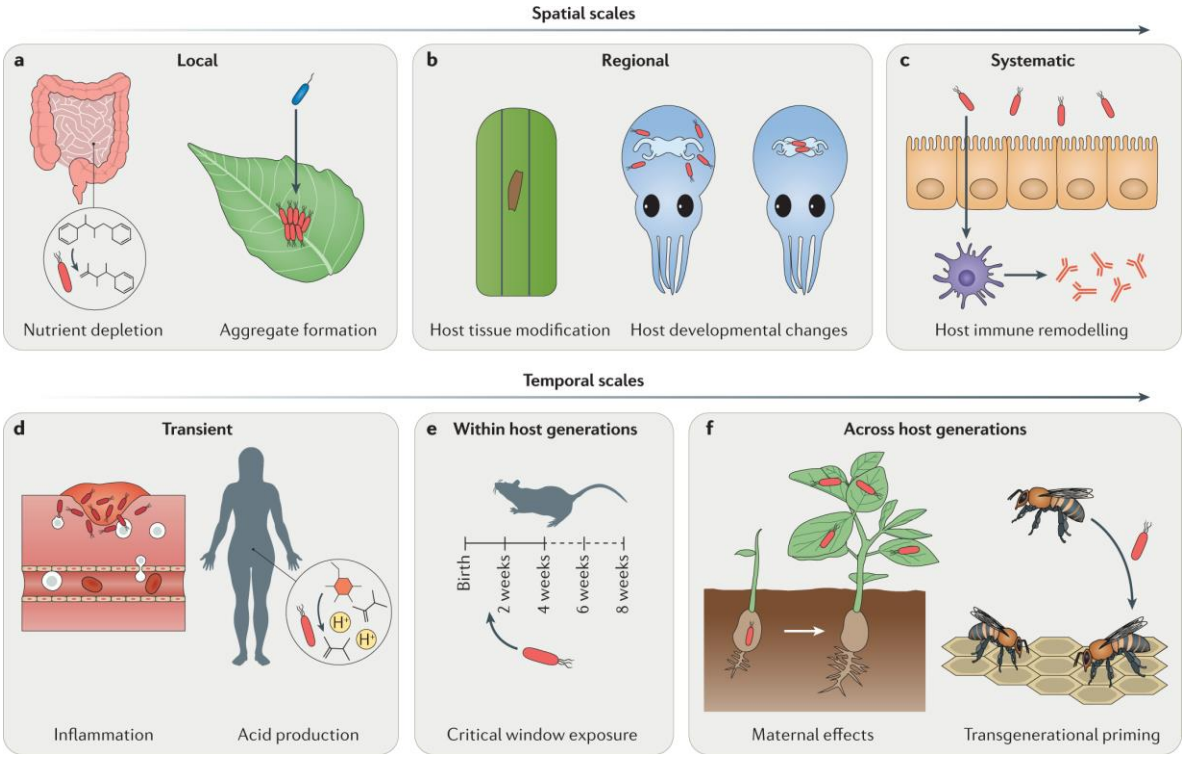


**Figure 5. Priority effects act on a range of spatial and temporal scales.** **a**) Early-arriving microorganisms can alter the local environment in many ways, such as by depleting nutrients or producing extracellular polymeric substances that protect other cells from desiccation (68). **b**) Microorganisms can interact indirectly at greater distances by modifying a shared host organ. Microbial necrosis of plant tissue reduces subsequent microbiome diversity, favoring a minority of taxa that can metabolize diseased tissue (75,76). Bacteria in seawater stimulate Hawaiian bobtail squids to harvest *Vibrio fischeri* symbionts, which trigger the developmental changes that exclude non-symbionts from the squid ocular crypts (153). **c**) Modification of host immune pathways can affect microbial colonization in other host tissues such as between intestinal and lung microbiota (149). **d**) Microorganisms can produce short-term, reversible changes to the host environment, such as transient immune responses or changes in pH in the vaginal microbiome. For example, *Lactobacillus* spp. promote an acidic environment that reduces the colonization success of many common vaginal pathogens (154). **e**) Microbiota exposure within a 'critical window' after birth can permanently shape adaptive immune responses (151). **f**) Microorganisms that colonize hosts can be directly transmitted to offspring (150) or induce heritable changes in immune signaling (152), thereby shaping succession of the offspring microbiome in both cases.

*Dispersal and coalescence.*

An unusual feature of microbial habitats, especially in host-associated systems, is the frequent appearance of pristine or nearly pristine substrates. Both newborn animals and newly emerged seedling hosts are generally sterile or have limited microbial colonization and events such as wounding can make previously microorganism-free host tissue available for colonization within the lifetime of a host. In periods of primary succession, stochastic processes such as birth, death and immigration tend to have a stronger role than later on (43,63,112). These processes may balance or even overwhelm deterministic processes, such as host age, environmental variation or the niche pre-emption and modification processes described in this Review (155).

Another unusual feature of microbiomes compared with plant and animal communities is the frequent occurrence of community coalescence (156) in microbiomes, such as through mixing of freshwater and marine habitats or through close contact between hosts. For example, the skin microbiota of members of opposing teams in roller derby (a high-contact sport) converged during a game (157). In such cases, the resident community will likely have an advantage over the arriving community, but what remains unclear is how much of the observed priority effects at the whole-community scale are the result of individual strain-level effects versus outcomes of community interactions. Experiments that manipulate the dispersal timing of entire communities (52,97), alongside detailed characterizations of pairwise interactions, will reveal whether the traditional concept of priority effects should be expanded to include emergent effects that cannot be captured by pairwise interactions between resident and arriving strains. Finally, although in this Review we have largely focused on how the resident microbiota affect the persistence of new species once they arrive, it may be possible for residents to influence which species arrive to the community in the first place. For example, recent work on floral microbiomes shows that animal pollinators mediate microbial dispersal to flowers and that epiphytic floral microorganisms can in turn alter nectar chemistry and influence future pollinator visits (158). Whether nectar microorganisms can cause priority effects by influencing pollinator recruitment remains to be tested.

*Conclusions and outlook*

Laboratory experiments and field surveys point to priority effects as key, understudied determinants of microbiome assembly and function. Widely used approaches to measuring priority effects each have their associated merits and challenges. Experimental approaches are limited by microbial cultivability and niche predictions, while field-based approaches are limited by the difficulties of repeatedly sampling the same individual host or environment without altering the community. The development and integration of single-cell and multi-omic sequencing technologies (159), imaging mass spectrometry (160), quantitative stable isotope probing (161) and high-resolution cellular imaging techniques (162) will help to answer questions that are beyond the reach of amplicon sequence analyses alone but must still be performed in ways that reflect or reveal the known spatial and temporal scales of priority effects. For example, pairing amplicon and metagenome sequencing provides complementary views of the taxonomic and functional features of the resident microbiome that affect the establishment of new arrivals (16) as well as the functional consequences of priority effects

(40). Lineage tracking within metagenomes over time (163) will help to identify priority effects between closely related strains. Given that niche pre-emption is often strongest among closely related taxa (15,16,62) (Fig. 3), strain-level analyses are likely to uncover many unknown examples of priority effects. Lastly, paired analyses of microbiome dynamics and host metabolomics will shed light on niche modification activities by the resident microbiota (45).

Our current knowledge of priority effects focuses largely on ecological interactions that affect resource availability or stress reduction. However, predation and parasitism are also known to shape community assembly outcomes (164). Multi-kingdom surveys of microbial community succession are becoming more common (165) and, as more are undertaken, they will reveal how assembly history shapes rich, complex environments. When microbial strains consistently coexist and interact over many generations, these interactions have the potential to coevolve. The coevolution of competitors often leads to ecological character displacement (166) as has been observed in Pseudomonas fluorescens populations in microcosms (167). Of course, host-associated microorganisms are unusual in that the environment they inhabit is engaged in ecological and evolutionary processes of its own. How the contrasting timescales of host evolution and the evolution of host-associated microbiota interact to shape priority effects remains to be determined but clues might be gleaned from the study of 'critical windows' in immune recognition across host species (58).

Overall, the existing data make it clear that priority effects shape microbiome assembly and stability. However, the complexity of these systems and the challenges of moving from co-abundance patterns to ecological interactions and functional processes still limit our ability to predict how and when these effects will occur. Among the open questions are: how long-lasting are priority effects? What are the typical spatial and temporal distances over which they occur? And, do our existing ecological models need to be reconsidered in light of differences between microorganisms and macroorganisms? Addressing these questions will be key if we are to leverage our understanding of priority effects to engineer or manipulate microbiomes, for example, by creating disease-suppressive communities or probiotics. Recent evidence that the establishment of probiotic strains can hinder the recovery of gut microbiome diversity (168) highlights the potential problems that can occur if priority effects are not considered as we begin reshaping microbiomes for human, livestock, crop and environmental health.

## 2.5 Appendix

In natural adaptive radiations, community assembly experiments and models, local adaptation and diversification by early arrivers has been shown to limit subsequent colonization by other species (118,125,169). Priority effects through local adaptation are predicted to be most common when nearby habitats are similar enough that immigrants can survive, but different enough that early arrivers can realize fitness gains over time (125). By contrast, priority effects through diversification depends largely on the heterogeneity of the environment and may feedback to further increase environmental heterogeneity (170).

Most known examples of evolutionary priority effects are inhibitory (that is, early arrivers reduce the success of late arrivers), although some exceptions exist. For example, *Daphnia magna* populations that coevolve with predatory fish occupy deeper and darker water layers, freeing up the shallows for late-arriving zooplankton species (169). In general, coevolution with predators or parasites often entails fitness costs associated with

counter-defenses (171), and these adaptations can reduce the competitive ability of early arrivers. Extended coevolution could also cause parasites to specialize on early-arriving strains, making later-arriving strains less susceptible and encouraging community turnover (172).

Despite the mounting evidence for evolutionary priority effects in model microbial systems discussed above, it is unclear how microbial dispersal shapes either the lag time between or standing genetic variation within populations of arriving species in most microbiomes. Our understanding of these factors in natural communities remains limited by the difficulties of tracking strain-level variation in metagenomes. However, recent work in the human gut suggests that the local adaptation of resident microorganisms may limit invasion by new strains. Within 6-month intervals, genetic turnover within metagenomes was largely attributed to selective sweeps within resident populations rather than to replacement by new strains (163). A powerful future approach will thus be to integrate metagenome-based lineage tracking with strain isolation and fitness measurements in the laboratory.

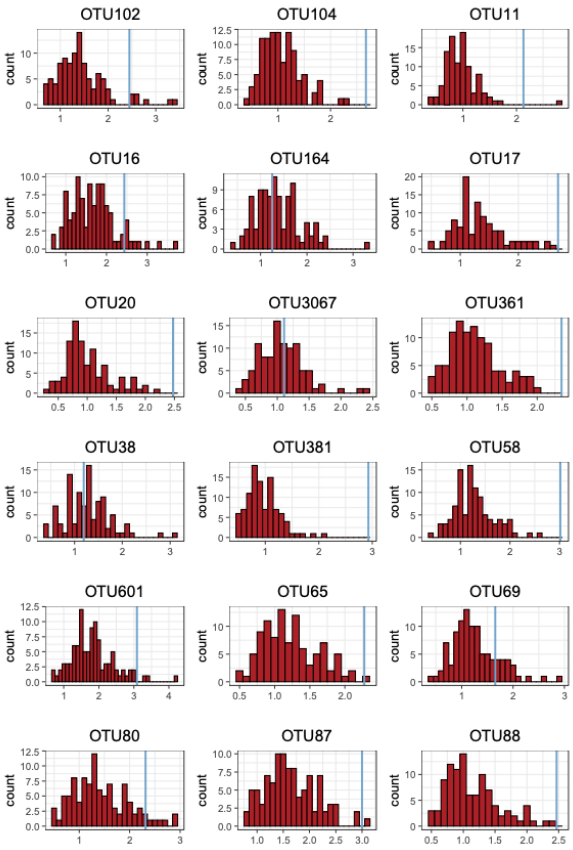


**Figure S1. Permutation of OTU arrival times across hosts.** For OTUs in which persistence was associated with composition of the resident microbiome immediately prior to arrival, we asked whether this relationship could be confounded by other processes related to timing or host development. For each of these focal OTUs, we permuted its arrival times across hosts. We generated a Bray-Curtis dissimilarity matrix in which distances among hosts were based on counts of all other OTUs at the sampling point immediately before the permuted arrival time. Using this dissimilarity matrix based on permuted arrival times, we again tested whether variation in focal OTU persistence was associated with microbiome composition. We repeated this process for 100 iterations per OTU to generate a null distribution. Here, we show the distribution of test statistics based on permuted values (histogram) and the observed test statistic for each OTU (blue line) for 16 representative OTUs in the human gut microbiome.

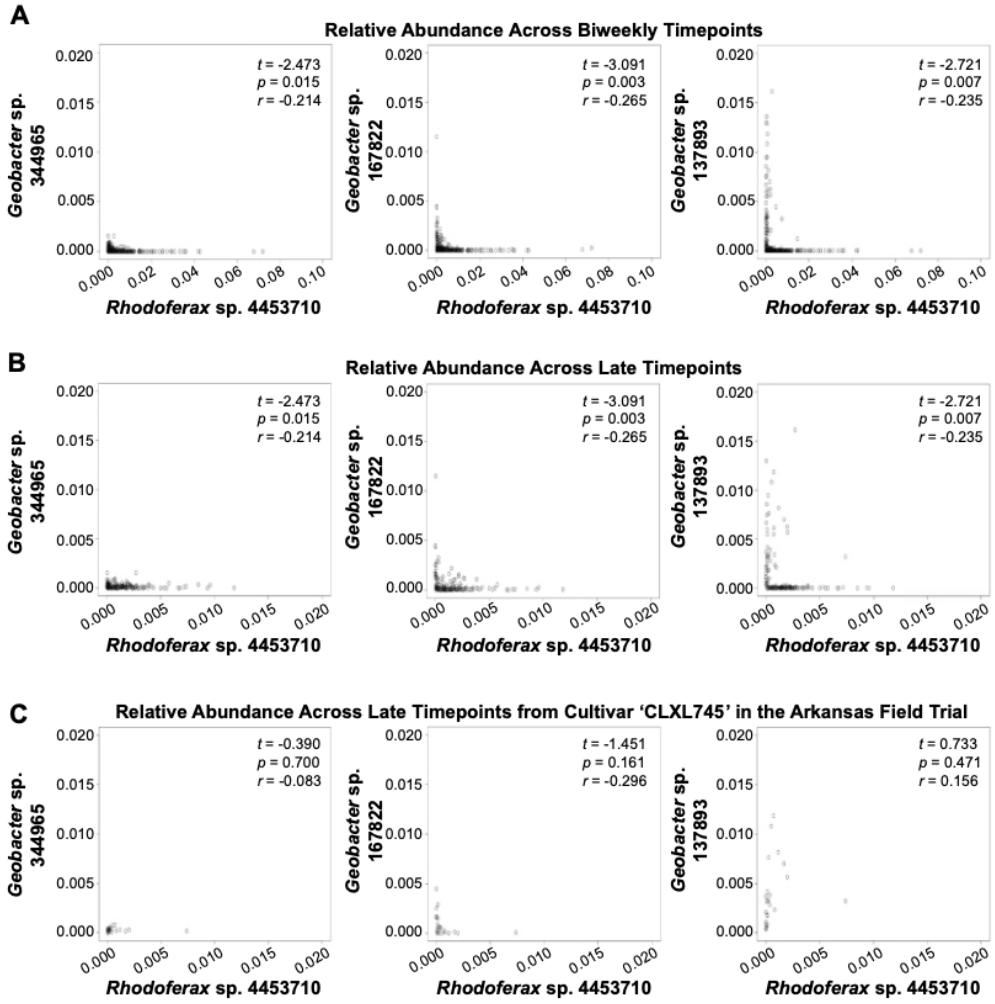


**Figure S2. Relative abundances of OTUs annotated as *Rhodoferax* and *Geobacter*.** We reanalyzed rice root microbiome samples taken from common, biweekly timepoints across three field trials for the relative abundance of two bacterial genera of interest: *Rhodoferax* and *Geobacter*. One *Rhodoferax* and three *Geobacter* OTUs significantly co-varied across all common samples reanalyzed (Pearson's Coefficient, A) as well as within late timepoints (84, 98, and 112 d, B). The relative abundance of two of three *Geobacter* OTUs negatively correlated with that of *Rhodoferax*, although these were not statistically significant (C).

# 3. Rapid evolution alters microbial priority effects

Parts of this chapter have been adapted from the following with permission:
Debray, R., Conover, A., Xuening, Z., Dewald-Wang, E.A., Koskella, B. 2023. Within-host adaptation alters priority effects within the phyllosphere microbiome. *Nature Ecology and Evolution (in press)*

## 3.1 Introduction

Priority effects, an ecological phenomenon whereby community assembly outcomes depend on the order of species arrival, can play a critical role in the assembly, stability, and function of ecological communities (8). Understanding how resident communities resist and/or facilitate invasions by arriving species can be useful for guiding ecosystem restoration and promoting resistance to invasive species (173,174). Systems in which community assembly spans multiple generations open the potential for evolution to play a role as well. This is likely true for microbial communities, suggesting that models recognizing only ecological processes may not sufficiently capture microbiome assembly dynamics (175). Currently, we have little understanding of how microbiomes evolve within hosts, or how within-host selection alters interactions between resident species and invading species.

Prevailing eco-evolutionary models assume that species which colonize hosts early in succession evolve to occupy their niches more efficiently, providing an additional competitive advantage against invaders (125). Early-arriving species would thus resist invasion through both ecological and evolutionary processes, implying that coexistence of competing species should be low, and that communities should be highly resistant to change after initial establishment. Known as the community monopolization hypothesis, this model has received support from several studies of microbial populations evolving in lab culture (176–178). Yet observations of microbiomes in nature often reveal continuous replacement among strains and species (163,179), questioning the extent to which adaptation can increase colonization resistance within hosts.

The phyllosphere, or above-ground plant tissues, provides many advantages for studying microbiome assembly. This plant compartment is clearly delineated from the surrounding environment, supports a diversity of microbial species, and plays an important role both in individual plant fitness and global nutrient cycling (180). To interrogate priority effects in this system, we examined the adaptive potential of the early-colonizing bacterium *Pantoea dispersa* on the leaves of tomato plants (*Solanum lycopersicum*). This species is found on seeds and in the phyllosphere of juvenile and adult plants. In a prior study, *Pa. dispersa* was consistently detected in the microbiomes of two-week-old tomato seedlings (150), suggesting that it experiences ample opportunity in nature to colonize new plants. However, the relationship between *Pa. dispersa* and its host organisms may be context- or strain-dependent. It can promote plant growth and protect against pathogens (150,181), yet has also been reported as an opportunistic pathogen of both plants and animals (182,183).

## 3.2 Materials and Methods

*Bacterial strains and selective markers*

This study included the following bacterial strains: *Pantoea dispersa* strain ZM1 (originally isolated from tomato plants as reported previously (150)), *Pseudomonas protegens* strain ZDW1 (isolated in this study), and *Pseudomonas syringae* pv. tomato DC3000 (provided by Gail Preston, University of Oxford). To distinguish competing populations of *Pantoea dispersa* strain ZM1, antibiotic-resistant strains were selected as follows. 500 µL of overnight culture was inoculated into sterile King's B Medium with either 4 µg/mL rifampicin or 2 µg/mL chloramphenicol. The inoculated culture was incubated overnight at 28°C, and the process was repeated with an increasing antibiotic concentration until resistance was achieved at the final concentration of 20 µg/mL rifampicin or 10 µg/mL chloramphenicol. Strains were then selected for equal competitive ability as their antibiotic-sensitive counterparts *in vitro* by repeatedly co-culturing resistant and sensitive bacteria and measuring the ratios they reached in 24 hours until there were no significant costs of the resistance marker. A single colony of each strain was selected to grow the ancestral stock, which was subsequently used to initiate six experimental evolution populations. This selection procedure resulted in several other genetic differences aside from the antibiotic resistance mutations, which could potentially affect leaf colonization and competition. Since the aim of this process was to generate a closely related and phenotypically distinguishable competitor for focal *Pa. dispersa*, isogenic populations were not required.

*Arrival order experiments*

Tomato seeds (*Solanum lycopersicum* cv. 'Moneymaker') were surface-sterilized in 2.7% bleach (sodium hypochlorite) solution for 20 minutes, then washed three times with 10 mM $MgCl_2$ to remove residual bleach. Each seed was placed in a loosely capped, sterile 15 mL tube with 7 mL of 1% water agar. Tubes were covered in foil and maintained in a 21°C chamber until shoot emergence, then moved to a 28°C growth chamber with a 15h day–9h night cycle.

Seedlings were flooded 9-12 days after planting, depending on the experiment. To prepare inocula, overnight cultures were pelleted at 3500 x *g* and washed with 10 mM $MgCl_2$ to remove residual media. Each culture was diluted to an optical density ($OD_{600}$) of 0.0015, approximately $10^7$ CFU/mL. The surfactant Silwet L-77 was added at a concentration of 0.015% to facilitate leaf colonization. Tubes were immediately placed on an orbital shaker for 4 minutes, then the inocula were poured off and the seedlings were allowed to dry in a biosafety cabinet. Each flooding trial included one or more seedlings treated with only 10 mM $MgCl_2$ and Silwet L-77 to ensure that reagents were sterile.

Three days after the addition of the second species, seedlings were individually weighed and then harvested. Two sterile ceramic beads and 7 mL of 10 mM $MgCl_2$ were added to each tube, and tubes were agitated in a FastPrep-24 5G system (MP Biomedicals, Burlingame, CA, USA) at 4 m/s for 60 seconds to homogenize plant tissue. Leaf homogenate was independently diluted twice per sample, and each replicate dilution series was plated on both rifampicin- and chloramphenicol-supplemented King's B agar plates to distinguish strains in mixed inoculations. Bacterial population sizes were quantified by counting colony-forming units after 2 days of incubation at 28°C.

*Experimental evolution in planta*

An overnight culture of *Pantoea dispersa* was pelleted at 3500 x *g* and washed with 10 mM $MgCl_2$ to remove residual media. Inocula were prepared by resuspending pellets in 10 mM $MgCl_2$ to a bacterial optical density ($OD_{600}$) of 0.0025 and adding 0.015% of the surfactant Silwet L-77 to facilitate leaf colonization. Seedlings were flooded as described above and maintained in the growth chamber for 7 days. At the end of each week, seedlings were collected with sterile forceps into sterile 15-ml Eppendorf tubes and homogenized in sterile 10 mM $MgCl_2$ as above. Leaf homogenate was diluted and plated on rifampicin-supplemented King's B agar plates. For each experimental evolution population, 100 colonies were individually picked from plates, mixed, and grown overnight to generate inocula for the following generation of seedlings.

*Plant symptom quantification*

In all cases where symptoms were measured, seedlings were grown in 15 mL tubes and flooded with bacteria at $OD_{600}$ = 0.0015, as described above. Instead of harvesting three days after inoculation to measure bacterial abundances, these seedlings were maintained in the growth chamber to track symptom development on a daily basis. In accordance with previous plant pathology studies, symptoms were scored blindly with respect to treatment using scores that describe different levels of symptom severity (184). Scores in this study were as follows: no symptoms (level 0), mild speckling (level 1), extensive speckling and/or chlorosis (level 2), and leaf necrosis and/or detachment (level 3). Individual leaflets on the same seedling were scored separately, then combined into an average symptom severity per plant for all analyses and figures to avoid pseudoreplication.

*Genome sequencing*

The six evolved populations of *Pantoea dispersa*, their ancestral stock, and the competitor strain of *Pa. dispersa* were grown overnight in liquid culture to prepare for DNA extraction. Bacterial DNA was extracted using the QIAGEN DNeasy Blood and Tissue Kit. Sample libraries were prepared using the Illumina DNA Prep kit and IDT 10 bp UDI indices and sequenced at an estimated coverage of 133x on an Illumina NextSeq 2000 at SeqCenter (Pittsburgh, PA, USA). Demultiplexing, quality control, and adapter trimming were performed with bcl-convert (v3.9.3). Paired-end reads were filtered and trimmed using Trimmomatic (v0.39). Reads shorter than 25 bp or with an average quality score below 20 in a 4-bp sliding window were discarded. Reads were mapped to the *Pantoea dispersa* genome (entry 22561 in the NCBI genome database) and variants were called using breseq (v0.35.4), a pipeline for identifying fixed and polymorphic genetic variation within microbial populations (185,186). To avoid false positive calls from repetitive elements, mutations were filtered to exclude highly polymorphic regions (five or more mutations in a 50 bp sliding window within a population). All analyses focused on non-synonymous mutations within coding regions of the genome.

*Statistical analyses*

Bacterial population sizes at harvest were determined based on colony counts on selective media. Colony counts of single-species controls were checked for cross-contamination or additional resistance evolution, neither of which was observed in the study. Colony counts were log-transformed prior to statistical analysis to meet assumptions of normality.

We calculated $P_{ij}$, a previously developed metric for quantifying the strength of priority effects (136), as follows. Here, $D(i)_{ji}$ represents the population size reached by species *i* when it was introduced after species *j*, and $D(i)_{ij}$ represents its population size when *i* was introduced before *j*. This coefficient takes on negative values if the population size of species *i* is smaller when arriving after *j* than when arriving before; that is, if competition outcomes between *i* and *j* are arrival order-dependent.

$$P_{ij} = ln\left[\frac{D(i)_{ji}}{D(i)_{ij}}\right]$$

We also calculated an alternative metric $P'_{ij}$, as described below, where $D(i)_{0i}$ and $D(i)_{i0}$ represent the single-species controls of species *i* that were inoculated and sampled at the same time as the corresponding co-colonization treatments:

$$P'_{ij} = ln\left[\frac{D(i)_{ji}}{D(i)_{0i}}\right] - ln\left[\frac{D(i)_{ij}}{D(i)_{i0}}\right]$$

$P'_{ij}$ is similar to $P_{ij}$, but accounts for the growth of species *i* alone. We found the two metrics were highly correlated and gave qualitatively similar results (Figure **S1**).

Plant symptom progression was analyzed by calculating the area under the disease progression curve (AUDPC), a cumulative measure of symptom severity over time (187). Differences in cumulative symptom progression over time were assessed using Welch's t-test that compared the AUDPC across bacterial treatments.

## 3.3 Results

We first asked whether priority effects might play an important role in phyllosphere microbiome assembly by introducing *Pa. dispersa* to tomato seedlings either before, simultaneously with, or after a competitor. To capture a range of expected overlap in niches and potential outcomes on host plant phenotype, we selected the following competitors: i) A closely related strain of the same species *Pa. dispersa*, ii) The plant-protective bacterium *Pseudomonas protegens*, iii) The plant pathogen *Pseudomonas syringae*, a causative agent of bacterial speck and promoter of frost injury in plants (188,189). In the first two cases, the eventual community composition strongly depended on arrival order, indicative of priority effects. In contrast, *Pa. dispersa* and *Ps. syringae* reached similar proportions regardless of their arrival order, possibly reflecting differences in their life cycles and spatial localization in plant tissue (Figure **S2**). *Ps. syringae* inhabits mainly the above-ground tissues of plants. The pathogenic strain used in this study initially colonizes leaf surfaces as a weak epiphyte. Upon reaching a threshold population size, it enters the leaf apoplast, where it has specialized to multiply and cause disease (190). In contrast, *Pa. dispersa* colonizes a wider variety of plant tissues (e.g. roots, leaves, stems, seeds), and has been detected both on plant surfaces (150,191) and within root and stem tissue (181).

As arrival order is inevitably correlated with the amount of time between inoculation and harvest in such experiments, it is possible that early arrival appears advantageous only because of population growth, independent of any interactions with other strains. We excluded this possibility by measuring the growth of each strain on plants in the absence of competition,

which indicated that the duration of the experiment was sufficient for all strains to reach carrying capacity (Figure **S3**). We observed no differences in plant growth across any of these inoculations (Figure **S4**).

To select for increased host association, we repeatedly inoculated tomato seedlings grown in sterile microcosms with replicate populations of *Pa. dispersa* and allowed the bacteria to associate with the plant for one week. Bacteria that successfully colonized the plant were harvested and used to inoculate the next generation of seedlings (Figure **1A**). Following the experimental evolution, we asked whether within-host selection had altered the ability of *Pa. dispersa* to resist invasion and/or invade established populations of competitors (Figure **1B**).

After six weeks of experimental evolution within tomato seedlings, populations of *Pa. dispersa* were significantly more resistant to invasion by *Ps. protegens* than their ancestral counterparts, consistent with the hypothesis that within-host adaptation can strengthen priority effects by early colonizers (Figure **1C**). In contrast, evolved populations of *Pa. dispersa* did not improve their ability to invade established populations of competitors (Figure **1D**). Where evolution of invasion success has been reported in the literature, populations were passaged within cultures that had been pre-conditioned by competitors[5], suggesting that adaptation to the host environment alone may not be sufficient to overcome competition-mediated priority effects. Finally, evolved populations of *Pa. dispersa* were significantly less effective than their progenitors at colonizing plants after the establishment of *Ps. syringae* (Figure **1D**). This final observation was rather unexpected given that *Ps. syringae*, an endophytic plant pathogen, had a substantially different life cycle than the other strains in the study and had not previously shown signs of direct competition with *Pa. dispersa*.

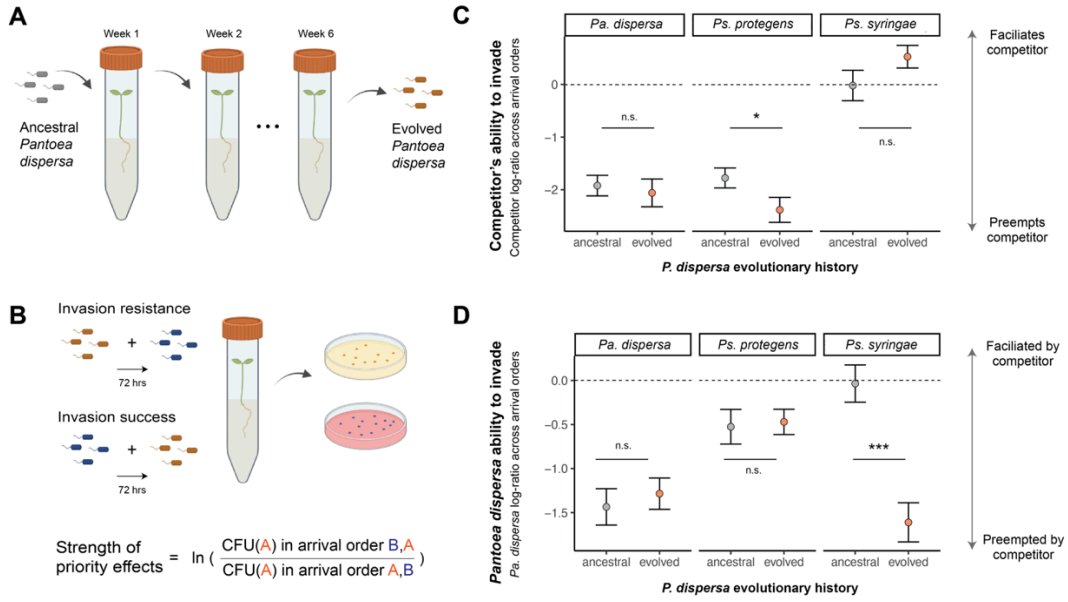


**Figure 1. Within-host evolution of the early colonizer *Pantoea dispersa* alters priority effects among bacterial strains. (a) Schematic of experimental evolution protocol.** Six replicate populations of *Pa. dispersa* were each inoculated onto tomato seedlings via flooding. Seedlings were incubated for 1 week, then harvested to isolate bacteria for the next generation of inoculum. **(b) Schematic of arrival order experiments.** Tomato seedlings were inoculated with either evolved or ancestral *Pa. dispersa* and a competitor (*Pa. dispersa*, *Pseudomonas protegens*, or *Pseudomonas syringae*). Seedlings were harvested 72 hours after the addition of the second strain and plated

on selective media to quantify population sizes. **(c) Competitor's ability to invade in arrival order experiments.** Evolved populations of *Pa. dispersa* were more resistant to invasion by *Ps. protegens* (two-sided t-test, $t = 1.99$, $df = 63.05$, $p = 0.05$). **(d) *Pantoea dispersa* ability to invade in arrival order experiments**. Evolved populations of *Pa. dispersa* were less successful at invading *Ps. syringae* (two-sided t-test, $t = 5.14$, $df = 69.83$, $p < 0.001$). Grid panels in (c) and (d) indicate competitor identity and asterisks indicate level of significance: $0.05 < p \leq 1$ (n.s.); $0.01 < p \leq 0.05$ (*); $0.001 < p \leq 0.01$ (**); $0 < p \leq 0.001$ (***). Error bars represent standard error (n=6 replicates per treatment).

To understand this previously unobserved priority effect between *Ps. syringae* and *Pa. dispersa*, we first examined the colonization dynamics of ancestral and evolved *Pa. dispersa* in the absence of competition. The evolved populations appeared to have undergone a life history shift, reaching higher population sizes than their ancestor but only after a period of slow growth (Figure **2A**). Additionally, many plants inoculated with either ancestral or evolved *Pa. dispersa* showed phenotypes reminiscent of disease, such as specks and chlorosis on cotyledons, that were not present in plants inoculated only with sterile buffer (Figure **2B**). To further examine this phenomenon, we adopted a quantitative assay of leaf symptoms previously used to study plant pathogens[10]. We inoculated plants with either ancestral or evolved populations of *Pa. dispersa* and recorded symptom scores on a daily basis for five days, blindly with respect to treatment. This experiment revealed that evolved *Pa. dispersa* was associated with more pronounced symptom development on leaves (Figure **2C**). We next asked whether it would be possible to leverage priority effects to mitigate the plant symptoms associated with colonization of the evolved *Pa. dispersa*. When a competing strain of *Pa. dispersa* was introduced three days before the evolved strain, symptom progression was reduced, indicating that priority effects can impact not only community composition but also functional properties (Figure **S5**).

On the basis of the above observations, we hypothesized that *Pa. dispersa* had evolved to exploit a new niche on the plant. As the colonization success of evolved *Pa. dispersa* depended on whether *Ps. syringae* had previously established, it seemed plausible that *Pa. dispersa* had shifted towards a more endophytic lifestyle. We inoculated plants with either ancestral or evolved *Pa. dispersa* as before, then sampled populations in a spatially resolved manner as follows: First, plants were submerged in sterile buffer and placed in an ultrasonic bath to dislodge bacterial cells from the leaf surface. Then the sonication buffer was removed and plants were homogenized to isolate the remaining bacterial cells associated with the plant. Ancestral and evolved populations of *Pa. dispersa* reached similar population sizes in the leaf wash, but the evolved populations were more abundant within the leaf homogenate (Figure **2D**-**2E**).

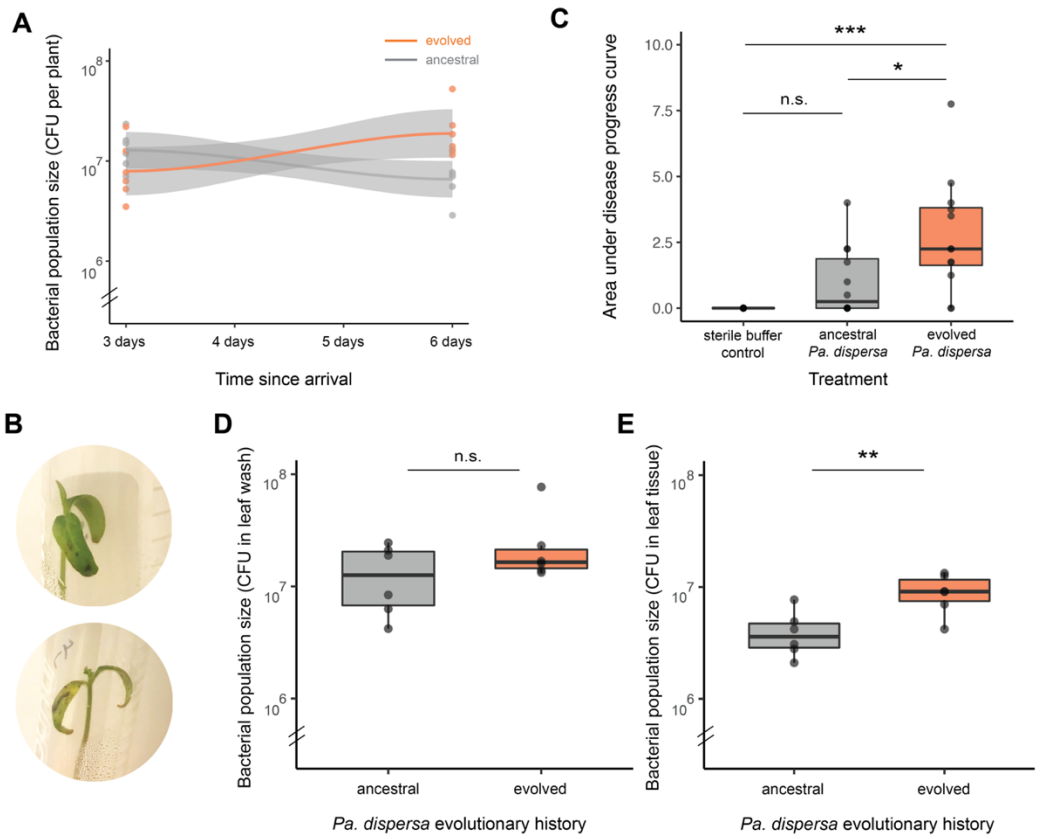


**Figure 2. Changes in *Pantoea dispersa* colonization dynamics over experimental evolution. (a) Life history in the absence of competition.** Population sizes of *Pa. dispersa* after inoculation via flooding. Interaction term between time since arrival and evolutionary history: ANOVA, F = 12.07, df = 1, p = 0.0024. **(b) Images of seedlings inoculated with evolved *Pa. dispersa* populations. (c) Quantitative assay of symptom severity.** A cumulative measure of symptom severity was calculated as the area under the curve of daily symptom scores taken blindly with respect to treatment for 5 days after inoculation. Symptom scores were higher in plants inoculated with evolved *Pa. dispersa* than ancestral *Pa. dispersa* (Tukey HSD, mean difference = 1.77, adjusted p = 0.015) or sterile buffer (Tukey HSD, mean difference = 2.75, adjusted p < 0.001). **(d) Bacterial population sizes on leaf surface.** Seedlings were submerged in sterile buffer, sonicated, and vortexed thoroughly. Population sizes in leaf wash were determined via dilution plating. **(e) Bacterial population sizes in leaf tissue.** Following the sonication described in (d), the remaining bacteria associated with seedlings were isolated by homogenizing the seedling in sterile buffer. Evolved populations reached higher population sizes in the leaf tissue than ancestral populations (two-sided t-test, t = 3.23, df = 9.93, p = 0.0091). Asterisks indicate level of significance: 0.05 < p ≤ 1 (n.s.); 0.01 < p ≤ 0.05 (*); 0.001 < p ≤ 0.01 (**); 0 < p ≤ 0.001 (***). Note truncated y-axes and logarithmic scale in panels (a), (d), and (e). Each experiment included one or more seedlings inoculated with sterile buffer and harvested alongside bacteria-treated plants. No bacterial colonies were recovered from these controls.

Six weeks of experimental evolution within tomato seedlings considerably altered the temporal and spatial colonization dynamics of *Pa. dispersa* populations. Though these changes were small in magnitude, they were sufficient to affect priority effects among bacterial strains as well as the effect of *Pa. dispersa* on its host. Such observed changes could be driven either by genetic adaptation or by non-genetic, plastic shifts in the phenotype of *Pa. dispersa*. To investigate whether our experimentally evolved populations accumulated genetic changes, we deep-sequenced the ancestor of the evolution experiment and the six final populations. We detected a total of 72 mutations across all populations located within 31 genes (Figure **3A**). In

addition to the fixed mutations, a total of 110 other alleles arose to intermediate frequencies but did not fix in any population. In many cases, mutations within the same gene or even at the same position arose repeatedly across populations, suggestive of evolutionary parallelism (Figure **3B**). Mutations arising in parallel across populations tended to reach higher allele frequencies, further suggesting that they were under selection (Figure **3C**).

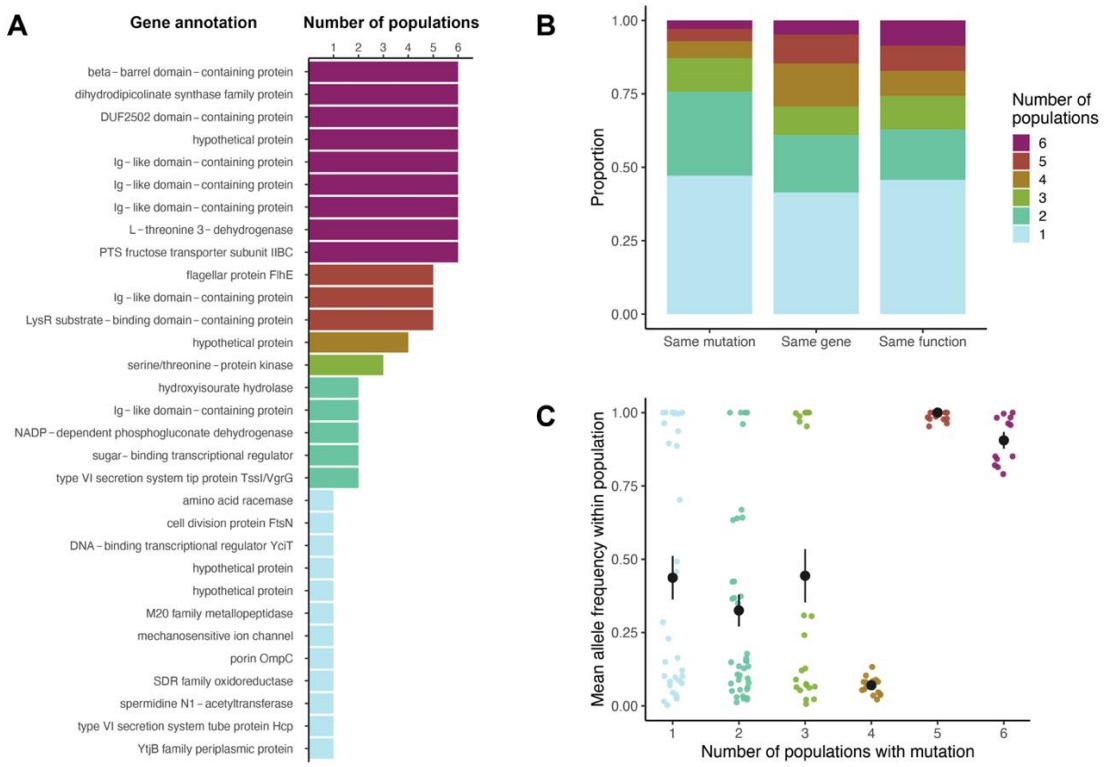


**Figure 3. Genetic changes in *Pantoea dispersa* during experimental evolution. (a) Functional annotations of genes fixed in one or more populations.** Gene product annotations are displayed according to the *Pa. dispersa* genome assembly (NCBI 22561). **(b) Evolutionary parallelism increases across broader levels of categorization.** Leftmost bar indicates the proportion of mutations observed in the experiment that were unique or shared among two, three, four, five, or six populations at any allele frequency. Middle bar indicates the extent of overlap in genes that accumulated mutations, whether they were at the same or different positions. Rightmost bar indicates the extent of overlap in gene annotations that accumulated mutations, whether they were in the same or different genes. **(c) Frequencies of mutations within and across populations.** Mutations arising in parallel tended to reach higher allele frequencies within populations (logistic regression, $z = 4.02$, $df = 212$, $p < 0.001$).

The most common annotation for genes altered in experimental evolution was proteins containing an immunoglobulin (Ig)-like domain. This structure is widespread throughout living organisms and appears in bacterial proteins with a wide range of functions, including adhesion, nutrient uptake, and pathogenic invasion into host cells (192). Other genes were commonly implicated in sugar and amino acid metabolism (e.g. L-threonine 3-dehydrogenase, PTS fructose transporter) and motility (e.g. flagellar protein FlhE), both important aspects of plant-microorganism interactions (180,193).

## 3.4 Discussion

The phenotypic and genetic changes observed in this experiment suggest the evolution of a more intimate association with the plant tissue, possibly mediated by exploitation of plant

stomata or improved persistence within other protected sites on the leaf. As in any experimental evolution study, it is important to consider why, if the observed traits are beneficial and evolve readily, the organism has not already acquired them in nature. *Pa. dispersa* appears to be a widely distributed species that has been isolated from plants, animals, and non-host habitats (182,183,194). It is plausible that improved colonization of tomato seedlings comes with a trade-off at other life stages, on other host species, or in other environments. Another consideration is that the microcosms in this study represent certain conditions (e.g. nutrient limitation, high humidity) that may promote stomatal opening or otherwise make plants particularly vulnerable to exploitation. Indeed, high humidity has previously been shown to promote overgrowth and disease symptoms by endogenous (non-pathogenic) microbiota (195).

Eco-evolutionary models often describe community assembly as a race between local adaptation by resident species and invasion by new species (125,196). They suggest that communities of small, passive dispersers with fast evolutionary rates (such as bacteria) are prone to strong monopolization by early arrivers (125). These predictions are difficult to reconcile, however, with observed fluctuations and replacements in the composition of natural microbial communities. Here, we show that an early colonizer evolved to exploit a new niche within a short time. This niche shift coincided with changes to both the nature and intensity of ecological interactions with other members of the plant microbiome. Although this study did not explicitly link genetic changes to niche occupancy, the observed parallel response to selection across experimental populations suggests the two are related. Our findings imply that the plant environment is sufficiently complex and heterogeneous in chemical and physical structure to present possibilities for microbial populations to adapt beyond simply improving their efficiency within their existing niche space. To understand the predictability of community assembly in microbiomes, it will be critical to further develop theory and data that can fully describe the adaptive landscapes for microbial populations colonizing hosts (197,198).

## 3.5 Appendix

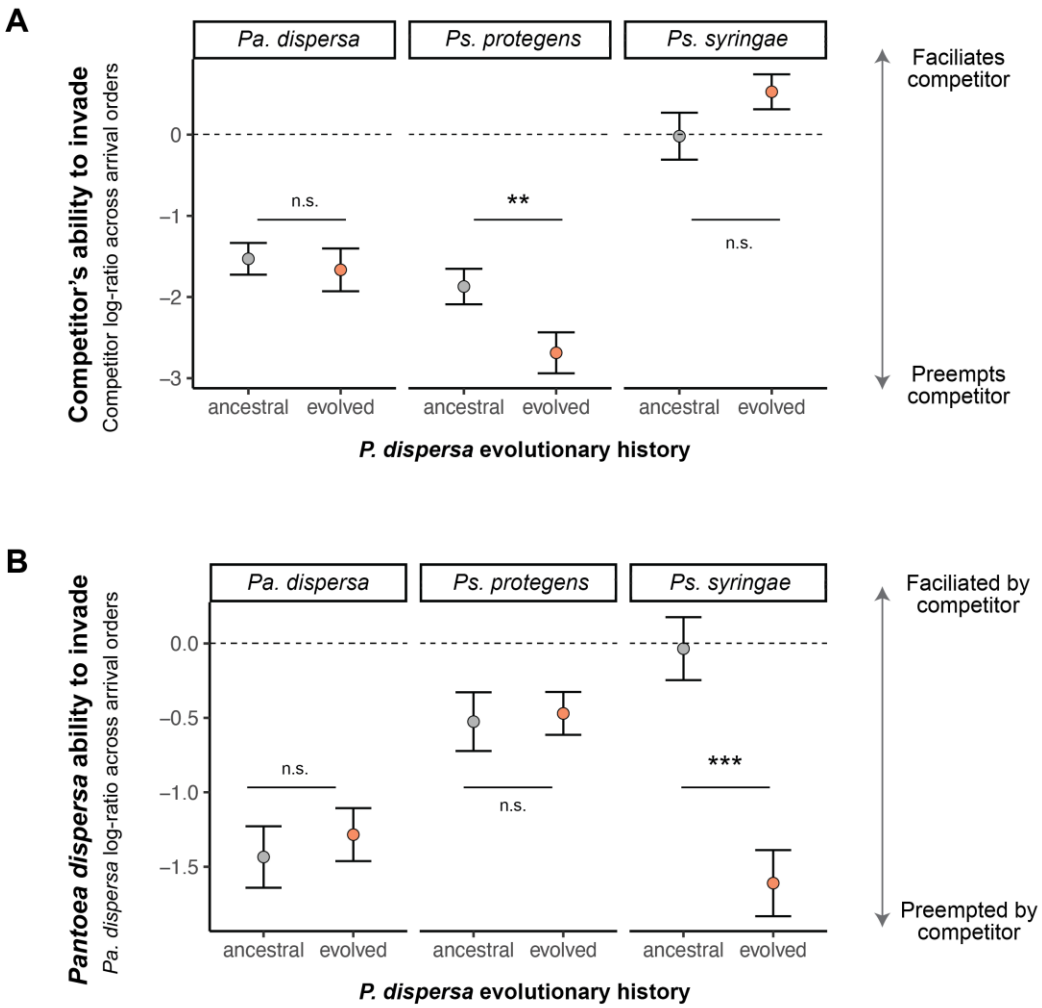


**Figure S1. An alternative measure of priority effects recapitulates effects of experimental evolution. (a) Competitor's ability to invade in arrival order experiments.** Evolved populations of *Pa. dispersa* were more resistant to invasion by *Ps. protegens* (two-sided t-test, t = 2.93, df = 40.58, p = 0.0056). **(d) *Pantoea dispersa* ability to invade in arrival order experiments**. Evolved populations of *Pa. dispersa* were less successful at invading *Ps. syringae* (two-sided t-test, t = 10.18, df = 35, p < 0.001). Grid panels indicate competitor identity and asterisks indicate level of significance: 0.05 < p ≤ 1 (n.s.); 0.01 < p ≤ 0.05 (*); 0.001 < p ≤ 0.01 (**); 0 < p ≤ 0.001 (***). Error bars represent standard error (n=6 replicates per treatment).

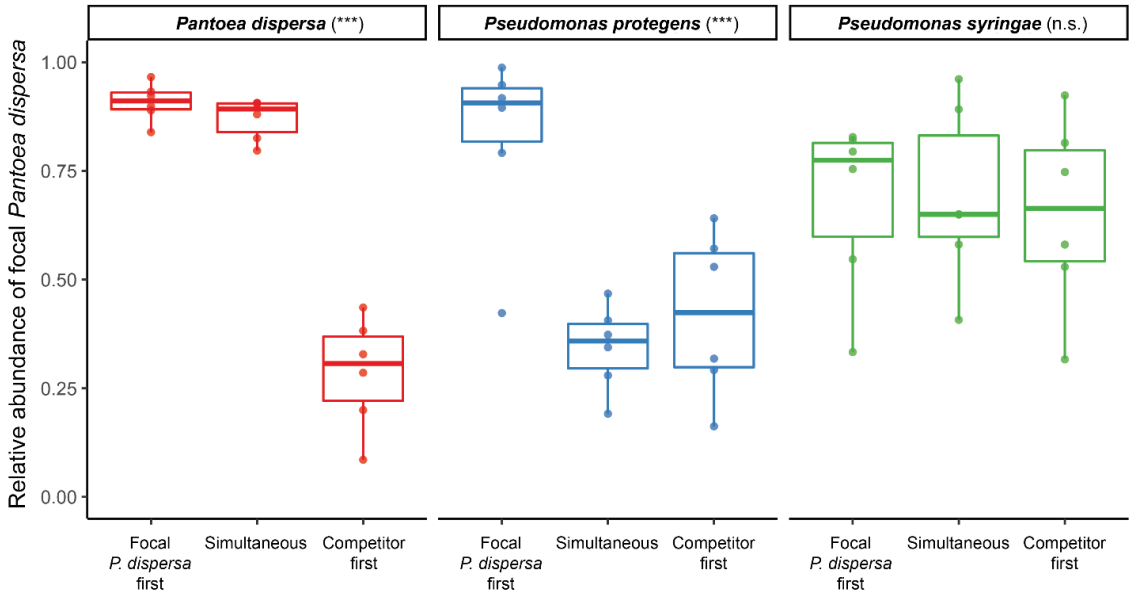


**Figure S2. Priority effects among bacteria in the tomato phyllosphere.** Relative abundance of *Pantoea dispersa* on tomato seedlings when co-inoculated with either *Pantoea dispersa*, *Pseudomonas protegens*, or *Pseudomonas syringae* across varying arrival orders. Seedlings were flooded either with both strains simultaneously or 72 hours apart. Seedlings were harvested another 72 hours after the addition of the final strain, and homogenized plant tissue was plated on selective media to count colonies. Arrival order significantly impacted strain proportions when both strains were *Pa. dispersa* (ANOVA, F = 107.43, df = 34, p < 0.001), or when *Pa. dispersa* was co-inoculated with *Ps. protegens* (ANOVA, F = 13.48, df = 34, p < 0.001), but not when co-inoculated with *Ps. syringae.*

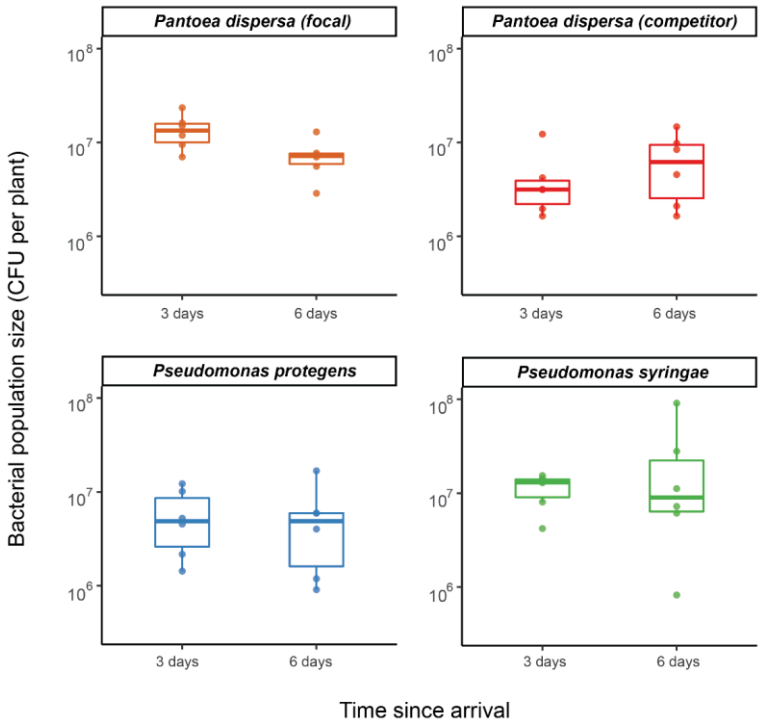


**Figure S3. Experimental duration is sufficient to reach carrying capacity on tomato seedlings.** Population sizes of *Pantoea dispersa*, *Pseudomonas protegens*, and *Pseudomonas syringae* when inoculated individually onto plants. Seedlings were either harvested directly after 72 hours (as a control for the simultaneous co-inoculation

treatments) or flooded with sterile buffer after 72 hours and harvested after 144 hours (as a control for the staggered co-inoculation treatments). At harvest, homogenized plant tissue was plated on selective media to count colonies. None of the strains grew significantly between three and six days after arrival, although the focal strain of *Pa. dispersa* decreased slightly in population size over this time (ANOVA, F = 6.28, df = 10, $p$ = 0.031).

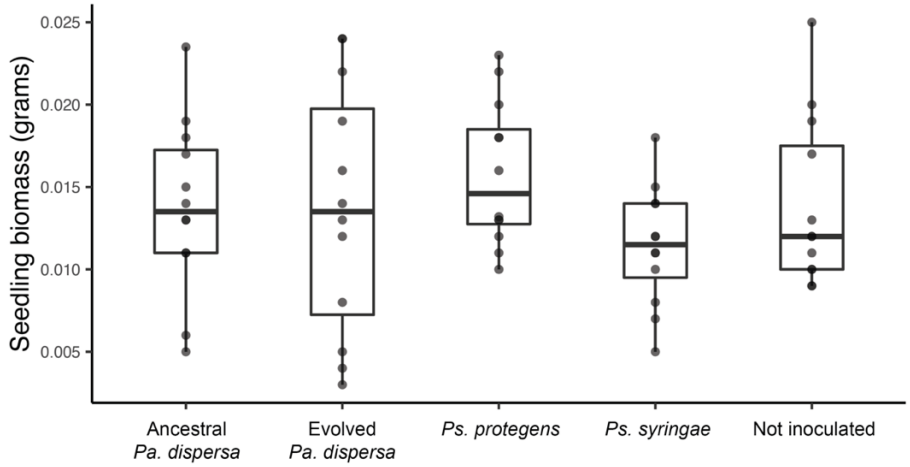


**Figure S4. No differences in seedling biomass across treatments.** Seedlings were weighed at harvest (72 hours after second inoculation). No significant differences were observed with respect to species identity or evolutionary history.

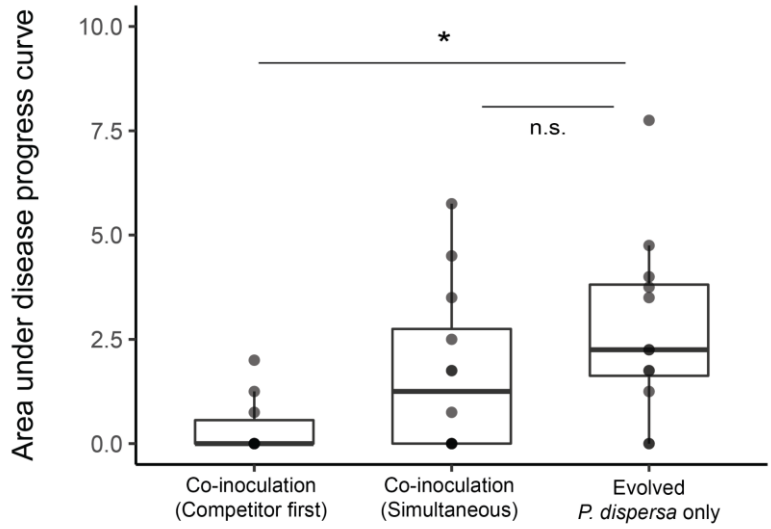


**Figure S5. Consequences of priority effects for plant symptom severity.** Seedlings were inoculated with evolved populations of *Pantoea dispersa*, which were previously associated with lesions and discoloration of the leaf tissue, and a competing strain of *Pa. dispersa* that does not cause such symptoms. A cumulative measure of symptom severity was calculated as the area under the curve of daily symptom scores taken blindly with respect to treatment for 5 days after inoculation. Each evolved population of *Pa. dispersa* was replicated twice in each treatment category (n = 12 seedlings per treatment), but symptom scores were subsequently averaged for each biological replicate to avoid pseudoreplication (n = 6 per treatment in statistical analysis). Co-inoculation with competing *Pa. dispersa* suppressed symptom development, but only if the competing *Pa. dispersa* arrived first (Tukey's HSD, mean difference = 2.35, adjusted p = 0.012). Asterisks indicate level of significance: $0.05 < p \leq 1$ (n.s.); $0.01 < p \leq 0.05$ (*); $0.001 < p \leq 0.01$ (**); $0 < p \leq 0.001$ (***).

# 4. Belowground biodiversity shapes the aboveground plant microbiome

Parts of this chapter have been adapted from the following with permission:
Debray, R., Socolar, Y., Kaulbach, G., Guzman, A., Hernandez, C., Curley, R., Dhond, A., Bowles, T., Koskella, B. 2021. Water stress and disruption of mycorrhizas induce parallel shifts in phyllosphere microbiome composition. *New Phytologist* 234(6): 2018-2031.

## 4.1 Introduction

Disturbances can often force ecological communities into states that are difficult to reverse even when conditions improve, a pheonomenon known as hysteresis (199). Understanding community resilience is critical for guiding the restoration of disturbed communities. In plant ecosystems, the water and nutrient content of soil are among the most important predictors of plant health (200,201). Disturbances that deplete water or alter nutrient composition in soil are expected to increase in frequency and severity with changing climates and altered management practices (202–205). It is therefore crucial to understand how interacting ecological stressors will act in future years to shape plant function. A key piece of the puzzle is how these changes impact plant-associated microbial communities aboveground and belowground, and, in turn, how plant–microbiome interactions buffer or exacerbate these stressors. Plant microbiomes play key roles in plant growth, immune development, and disease resistance (53), and a growing body of work indicates that these associations are vulnerable to disruption under changing global conditions, including climate and agricultural management. Belowground, for example, drought can induce complex changes in microbial dynamics (206–208), including negative to positive impacts on mycorrhizal associations (209,210), which are key drivers of plant performance (20,211). Moreover, increased fertilization via agricultural intensification can cause plants to reduce resource allocations to microbial symbionts such as mycorrhizas and rhizobia, often selecting for less mutualistic strains (212,213). Together, shifts in water availability, soil nutrient content, and mycorrhizal communities in changing environments are likely to alter plant performance, including plant–microbiome interactions.

Although the majority of work in this space has focused on belowground plant–microbe interactions, the microbial communities associated with aboveground plant tissues, known as the phyllosphere, are gaining increased recognition in plant health. These microbiomes have been shown to play roles in nitrogen fixation, tolerance of extreme temperatures, and protection against pathogens (189,214–216). Much like their belowground counterparts, phyllosphere microbiome functions can be disrupted by changes in climate and agricultural management. For example, experimental warming reduces phyllosphere microbial diversity and nitrogen fixation in peat moss (217). Soil fertilization reduces the resistance of phyllosphere communities to invasion by the foliar pathogen *Pseudomonas syringae* (216).Finally, functional genes involved in carbon, nitrogen, phosphorus (P), and sulfur cycling are less abundant in the phyllosphere metagenomes of plants in farmlands than in forests (218). The building evidence makes it clear that plant microbiomes both shape and are shaped by their host plant's response to the local environment. What remains unclear are both how these responses might change

under different or interacting stressors, and whether aboveground and belowground microbial communities impact one another's responses to such stress.

To begin addressing these questions and capture effects of soil conditions on the phyllosphere microbiome, we focused on soil properties that induce systemic changes in plant physiology. Water stress can impact nutrient and biomass allocation, phytohormone production, and toxin accumulation in leaves (201,219,220), while soil fertility can affect nutrient content and acidity of aboveground plant tissues (221,222). Arbuscular mycorrhizal fungi (AMF) colonize plant roots and modulate plant water and nutrient status, leaf gas exchange, and the expression of stress response genes (223,224). We therefore asked how water stress, fertilization, and mycorrhizal colonization affected bacterial and fungal communities in the tomato (*Solanum lycopersicum*) phyllosphere.

Through a combination of field and growth chamber experiments, we found that both plant water stress and disruption of mycorrhizas altered bacterial and fungal composition in the phyllosphere. Upon closer examination, we found that both stressors reduced bacterial richness within plants, homogenized bacterial communities across plants, and increased the evenness of fungal communities. Further, there was a high degree of overlap in the responses of individual indicator taxa to both treatments, suggesting that soil water availability and belowground mycorrhizal associations act in parallel on phyllosphere microbial communities.

## 4.2 Materials and Methods

*Field site and treatments*

The field trial was conducted at the University of California Davis Student Farm (38°32'29.49''N, 121°46'0.94''W), a certified organic farm, during the 2019 growing season (see Appendix for details of field preparation). We conducted our experiment at a certified organic farm to minimize any chances of chemical inputs (e.g. fungicides) directly disrupting the microbial communities we aimed to study. Three treatments, water stress, P fertility, and mycorrhizal associations, were arranged in a split-plot design and assigned to levels in a fertilization gradient (Figure **S1**). Water stress included two levels, fully watered (100% of crop evapotranspiration, $ET_c$) and deficit (50% $ET_c$) irrigation applied in alternating beds, with the deficit beginning 22 d after transplant, and water completely cut to the deficit beds 76 d after transplant. Phosphorus fertility was manipulated as a 12-level gradient of fertilizer established in each irrigation condition (24 plots total). We chose a fertilizer product approved for use in US organic systems. We applied an organic fertilizer, seabird guano (0-11-0, Down to Earth) on the surface of each plot, which was then incorporated with a cultivator a week before planting. The gradient ranged from 0 to 550 g of fertilizer P $m^{-2}$, including duplicate plots of the lowest (0 g P $m^{-2}$) and highest (550 g P $m^{-2}$) treatments (Table **S1**). The 24 experimental plots were each split into two subplots, one with a tomato genotype deficient in mycorrhizal associations (*rmc*, (225)) and another with its wild-type progenitor (76R), for a total of 48 experimental units. Seeds of the 76R and *rmc* genotypes were sourced from plants grown in the glasshouse. To avoid effects of adjacent irrigation treatments, three buffer plants were planted but not sampled between experimental units.

*Sample collection from field*

Soil samples were taken from three depths (0–15, 15–30, and 30–60 cm) at each plot. Gravimetric water content was measured as the difference between soil mass before and after the soils were dried at 105°C. Bioavailable P in soils was measured using the Olsen P method, based on phosphate extraction using sodium bicarbonate solution, at transplant, midseason, and harvest. Stem water potential was measured on one plant per plot, 53 d after transplant. Aboveground biomass was measured at harvest (116 d after transplant) from four plants per plot, of which a subsample was taken for further analysis. Total P in aboveground plant tissue was measured by Murphy–Riley colorimetry following microwave-assisted digestion in nitric acid and hydrogen peroxide.

*Plant care in growth chamber experiments*

We next assessed two of the field trial treatments in a more controlled setting. Surface-sterilized tomato seeds were germinated on sterile agar, then transplanted into pots (see Appendix for growth chamber conditions). In the mycorrhiza experiment, an inoculum containing equal amounts of several arbuscular mycorrhizal fungi taxa (*Gigaspora rosea*, *Gigaspora albida*, *Acaulospora spinosa*, *Rhizophagus intradices*, and *Funneliformis mosseae*) was added to each pot at the transplant stage. Mycorrhizal inoculum was acquired from INVAM (West Virginia University, Morgantown, WV, USA). Half of the inoculum (14 g) was mixed into the potting mix, and the other half was added directly to the seedling transfer site at the top. In the fertilizer experiment, 105.6 mg of P (960 mg fertilizer) was added to half of the pots at the transplant stage, approximating the highest position of the P gradient in the field (550 g P $m^{-3}$, assuming a fertilizer penetration depth of 20 cm). The other half of the pots were not fertilized (0 g P $m^{-3}$). All pots were immediately randomized with respect to treatment and remained under controlled growth chamber conditions for the duration of the experiment.

*Microbiome spray and pathogen challenge in growth chamber*

Three-week-old plants were sprayed with microbial inocula from tomato plant leaves in the field. To track assembly of the same source communities under different conditions, each sample (which corresponded to a single plant in the field) was divided in half and used to generate inocula for two plants. In the mycorrhiza experiment, each field sample was used to inoculate one wild-type plant and one *rmc* plant in the growth chamber. In the P experiment, each field sample was used to inoculate one fertilized and one unfertilized plant in the growth chamber. Each plant was sprayed with 4 ml of microbial inocula at a standardized concentration of $10^4$ colony-forming unit (CFU) $ml^{-1}$.

The purpose of these experiments was two-fold. First, they served as an independent and more controlled test of the treatment effects in the field trial. Pots were completely randomized with respect to treatment, and the paired design allowed direct comparison of plants that received the same microbiota but were grown under different conditions. Second, after allowing communities to establish for 1 wk, we inoculated plants with the bacterial pathogen *P. syringae* pv tomato PT23. *Pseudomonas syringae* can grow to high densities in the tomato genotypes 76R and *rmc* but does not cause disease symptoms. This experiment allowed us to test whether soil conditions had altered microbiome resistance to invasion, a key property of ecological communities that has been shown to vary with nutrient availability (216,226).

Three leaves per plant were inoculated with *P. syringae* at an optical density ($OD_{600}$) of 0.0002 (*c*. $10^5$ CFU $ml^{-1}$) by blunt-end syringe injection into the abaxial side of the leaf. Plants were destructively sampled 24 h after the *P. syringae* challenge. To measure *P. syringae* population density, three hole punches were taken from each of the inoculated leaves and homogenized in sterile buffer using a FastPrep-24 5G sample disruption instrument. *Pseudomonas* density on leaves was obtained through CFU plating and droplet digital polymerase chain reaction (ddPCR). To characterize epiphytic microbial communities, the remaining aboveground plant material, which had been sprayed with microbial inocula but not directly challenged with *P. syringae*, was collected in a 15 ml tube. Microbial communities were isolated through sonication and centrifugation as described earlier. Total bacterial density was obtained through ddPCR with primers for conserved sequences in the 16S rRNA gene. Primer sequences and reaction conditions for ddPCR assays are available in the Appendix.

*DNA extraction and sequencing*

DNA was extracted from microbial communities isolated from the field and both growth chamber experiments. Extractions were performed using the DNeasy PowerSoil kit. Extraction batches of 24 samples were assigned randomly with respect to treatments and included in all statistical models. One extraction in each set of 24 was a negative control. Libraries were prepared by amplifying the V4 region of the 16S rRNA gene and the ITS2 gene (see Appendix for primer sequences). Libraries were amplified, cleaned, and sequenced alongside DNA extraction controls and PCR controls on the Illumina MiSeq platform at Microbiome Insights (Vancouver, BC, Canada).

Reads were analyzed using the recommended DADA2 workflow (227) to infer amplicon sequence variants (ASVs). Taxonomy was assigned using the SILVA and UNITE databases (228,229). Because many internal transcribed spacer (ITS) sequences could not be classified at the kingdom level by UNITE, the hidden Markov model classifier ITSx was used to further delineate ITS sequences and remove nonfungal sequences (230). Thus, 16S variants were filtered to remove chloroplast and mitochondrial sequences. Potential contaminants were filtered based on prevalence in negative controls vs true samples using the package *decontam* (231). Additional details on quality control parameters are available in the Appendix.

*Statistical analysis*

Alpha diversity (species number) and beta diversity (species turnover) were analyzed using ANOVA and permutational multivariate analysis of variance (PERMANOVA) (232) with irrigation regime, plant genotype, soil fertilizer concentration, plant sonication batch, and DNA extraction batch as covariates. When treatments were allowed to interact, none of the interaction terms were significant, and model selection based on Akaike's information criterion favored the model without interactions. Indicator taxa were identified based on Dufrêne and Legendre's indicator value (R package *multipatt*). To independently validate this analysis, we also modeled differential abundance across treatments (R package *edgeR*) (233).

The correlation between bacterial and fungal richness was assessed with Pearson's product correlation coefficient. Partial $R^2$ values were calculated to test whether this correlation could be attributed to shared responses of bacteria and fungi to other variables (R package *rsq*). To test correlations between bacterial and fungal composition, a partial Mantel

test was conducted on their respective Bray–Curtis dissimilarity matrices along with a Euclidean distance matrix of field trial treatments and technical batches. To construct a co-occurrence network, the abundances of the top 500 bacterial taxa and the top 500 fungal taxa were first converted to presence–absence measures (as relative abundances would not be directly comparable across sequencing libraries). The two datasets were combined and the package *rcorr* was used to generate matrices of Pearson's correlations and corresponding *P*-values. After Benjamini–Hochberg correction for multiple testing (false discovery rate (FDR) < 0.1), a network was constructed on significant correlations (R package *igraph*).

While colonization of plants in the growth chamber by field communities was generally high, a subset of plants had low bacterial abundance and a high proportion of ASVs unique to the growth chamber, which appeared to confound estimates of bacterial diversity (Figure **S2**). To address this, ASVs were classified as shared with the field trial or unique to the growth chamber. All analyses were conducted separately on the two categories. In support of this approach, ASVs shared with the field trial generally recapitulated treatment effects observed in the field, while the potential growth chamber contaminants appeared to be randomly distributed with respect to treatment (Figure **S3**). A paired Wilcoxon signed-rank test was used to compare microbiome assembly on plants in the growth chamber that had received the same inoculum from the field.

## 4.3 Results

*Effects of experimental treatments on soil conditions and field plants*

In the field, wild-type plants had significantly higher AMF root colonization than the reduced mycorrhizal genotype (mean 76R = 17%, mean rmc = 11%; 95% confidence interval (CI) for difference in means = (0.60, 11), P = 0.032; Fig. **S4**a). Though there were no significant differences in soil gravimetric water content between fully watered and deficit irrigation plots at the mid-season sampling (51 d after transplant), there was a significant difference in soil water content at all three depths (0–15, 15–30, and 30–60 cm) at harvest (116 d after transplant), and at 53 d after transplant plants grown under deficit irrigation showed a trend toward an increase in stem water potential, i.e. experiencing more water stress (P = 0.07, Fig. **S4**b). Plant biomass from the reduced mycorrhizal genotype had significantly lower P concentrations than the wild-type as measured by percent dry biomass (absolute change of −0.2%, P < 0.001), as did deficit irrigation as compared to fully watered plants (−0.05%, P = 0.01), but the applied fertilizer gradient did not significantly impact P concentration in plant biomass or available soil P (Olsen P) at any of the sampling events (Fig. **S4**c–e). Finally, there were no significant differences in aboveground biomass at harvest among the treatments (data not shown).

*Phyllosphere microbiome composition in field trial*

We next measured the impact of the field trial treatments on microbial community composition in the phyllosphere. Water regime and mycorrhizal associations significantly predicted variation in bacterial and fungal community composition, while the effect of fertilization was marginally significant in fungal communities only (Table **1**).

Shifts in community composition often reflected changes in alpha diversity (species diversity per plant) and beta diversity (heterogeneity within treatments) (full model results in

Tables **S2**, **S3**). Compared to fully watered plants, water-stressed plants harbored lower bacterial richness ($F = 10.468$, df = 72, $p = 0.0018$), lower Shannon diversity ($F = 4.990$, df = 72, $p = 0.029$), and more similar communities to one another ($F = 7.347$, df = 92, $p = 0.0080$).

**Table 1. Full results of permutational multivariate analysis of variance models on Bray–Curtis dissimilarity matrices.**

| **Bacterial community composition** | | | | | | |
|---|---|---|---|---|---|---|
| **Treatment** | **df** | **Sum of squares** | **Mean square** | **F value** | **$R^2$** | **p-value** |
| Irrigation regime | 1 | 0.601 | 0.601 | 1.496 | 0.015 | 0.00079 |
| Genotype | 1 | 0.495 | 0.495 | 1.232 | 0.012 | 0.028 |
| Fertilizer concentration | 1 | 0.455 | 0.455 | 1.133 | 0.011 | 0.112 |
| Plant sonication batch (randomized across treatments) | 12 | 5.763 | 0.480 | 1.196 | 0.145 | <0.0001 |
| DNA extraction batch (randomized across treatments) | 6 | 3.427 | 0.571 | 1.423 | 0.086 | <0.0001 |
| | | | | | | |
| **Fungal community composition** | | | | | | |
| **Treatment** | **df** | **Sum of squares** | **Mean square** | **F value** | **$R^2$** | **p-value** |
| Irrigation regime | 1 | 0.470 | 0.470 | 1.436 | 0.014 | 0.011 |
| Genotype | 1 | 0.482 | 0.482 | 1.473 | 0.015 | 0.0089 |
| Fertilizer concentration | 1 | 0.404 | 0.404 | 1.234 | 0.013 | 0.061 |
| Plant sonication batch (randomized across treatments) | 12 | 4.633 | 0.386 | 1.180 | 0.141 | 0.0003 |
| DNA extraction batch (randomized across treatments) | 6 | 3.388 | 0.564 | 1.726 | 0.103 | <0.0001 |

Simultaneous decreases in alpha and beta diversity often indicate loss of rare species (i.e. species that inhabit some sites, but not others, across a landscape) (234). Accordingly, rare ASVs showed the strongest discrepancies between the full water and deficit treatments (Fig. **S5**). In fungal communities, water stress increased the Shannon diversity index ($F = 7.966$, df = 72, $P = 0.0062$), a combined measure of richness and evenness. Further examination of the individual components revealed that this effect was driven by an increase in evenness under water-limited conditions ($F = 8.495$, df = 72, $P = 0.0047$), while richness was not affected (Fig. **1**).

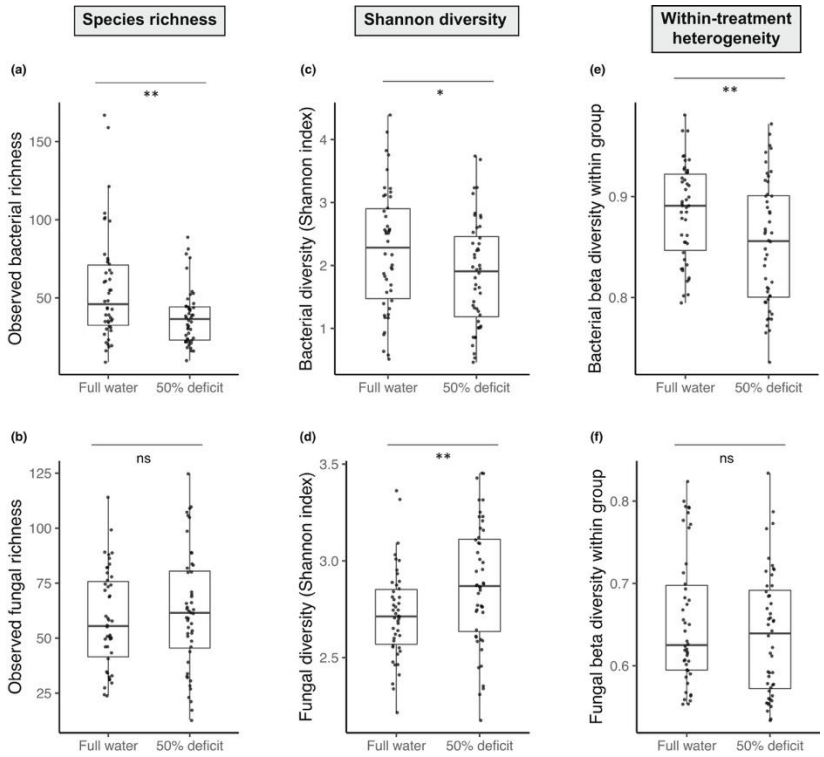


**Figure 1. Water stress reduces bacterial alpha and beta diversity and increases fungal alpha diversity in the tomato phyllosphere. a, b)** Number of amplicon sequence variants (ASVs) per sample. Bacterial richness values were log-transformed before analysis to meet normality and homoscedasticity assumptions. **c, d)** Shannon–Weaver index of combined richness and evenness. **e, f)** Within-group dispersion was quantified by generating a Bray–Curtis dissimilarity matrix. Points represent the mean Bray–Curtis dissimilarity between each sample and other samples within the same treatment group (full water or 50% deficit). The lower and upper hinges of each box plot represent the 25$^{th}$ and 75$^{th}$ percentiles of the data, respectively, while the upper and lower whiskers extend to values within 1.5 times the interquartile range. Levels of significance are indicated as follows: **, $0.001 \leq P < 0.01$; *, $0.01 \leq P < 0.05$; ns, $P \geq 0.05$.

The reduced mycorrhizal (*rmc*) plants harbored lower phyllosphere bacterial richness ($F = 5.203$, df = 72, $P = 0.026$) and more similar communities to one another ($F = 7.548$, df = 92, $p = 0.0072$) than their wild-type counterparts. As with water stress, the strongest discrepancies between wild-type and *rmc* plants were among rare ASVs (Fig. **S6**). The *rmc* plants harbored lower fungal richness ($F = 11.417$, df = 72, $P = 0.0011$) and higher fungal evenness ($F = 13.182$, df = 72, $P < 0.001$) than wild-type plants (Fig. **2**).

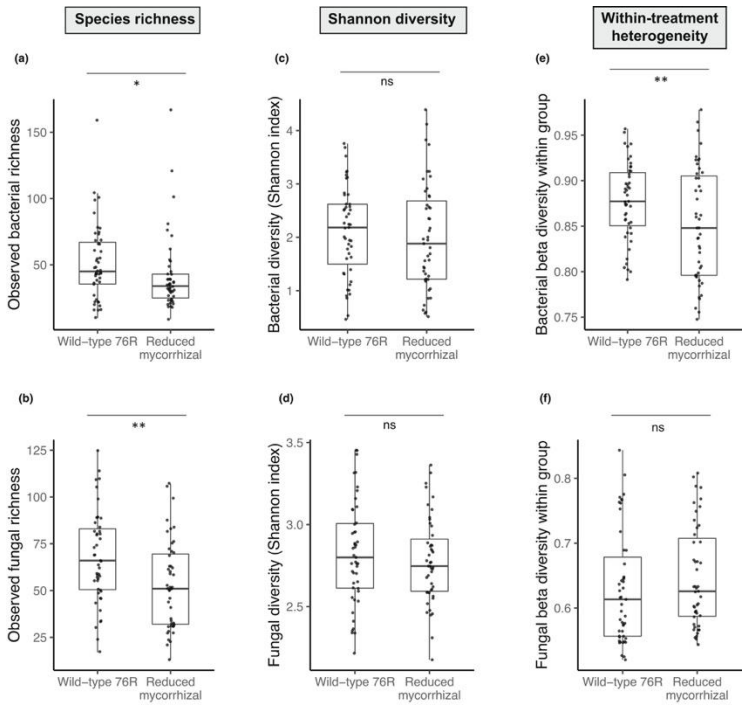


**Figure 2. The *rmc* genotype harbors lower bacterial alpha and beta diversity, and lower fungal alpha diversity, than its wild-type counterpart. a, b)** Number of amplicon sequence variants (ASVs) per sample. Bacterial richness values were log-transformed before analysis to meet normality and homoscedasticity assumptions. **c, d)** Shannon–Weaver index of combined richness and evenness. **e, f)** Within-group dispersion was quantified by generating a Bray–Curtis dissimilarity matrix. Points represent the mean Bray–Curtis dissimilarity between each sample and other samples within the same plant genotype (76R or *rmc*). The lower and upper hinges of each box plot represent the 25$^{th}$ and 75$^{th}$ percentiles of the data, respectively, while the upper and lower whiskers extend to values within 1.5 times the interquartile range. Levels of significance are indicated as follows: **, $0.001 \leq P < 0.01$; *, $0.01 \leq P < 0.05$; ns, $P \geq 0.05$.

Having observed that water limitation and disruption of mycorrhizal associations induced similar changes in bacterial community metrics (i.e. reduction in alpha and beta diversity), we next asked whether similar taxa were affected in both treatments. A PERMANOVA on Bray–Curtis dissimilarity separated the fully watered wild-type plants from plants in deficit and/or reduced mycorrhizal conditions ($P < 0.001$ accounting for effects of P fertilization and sample processing batches), while the remaining combinations of irrigation regime and mycorrhizal associations (wild-type/deficit, *rmc*/full water, *rmc*/deficit) were not statistically different from one another (Fig. **3a,b**). To identify specific taxa affected by each treatment, we calculated Dufrêne and Legendre's indicator value for each bacterial ASV. There was a high degree of overlap in indicator taxa for the full water and wild-type treatments, and in indicator taxa for the water-stressed and reduced mycorrhiza treatments (Fig. **3c**). As indicator species analysis is based on occupancy patterns, we further validated this result using negative binomial regression, a method commonly used to identify taxa associated with treatments based on relative abundance patterns (233). We again found substantial parallels between the effects of irrigation regime and mycorrhizal associations on bacterial community composition (Fig. **S7**). We next examined fungal communities and again observed substantial overlap in the distribution of individual indicator taxa (Fig. **S8**). Finally, we verified that our

results could not be attributed to chance effects during random assignment to plant sonication or DNA extraction batches by comparing the effects of treatments on indicator taxa within, rather than across, technical batches. As expected, treatment effects within batches consistently mirrored those observed within the full dataset (Fig. **S9**).

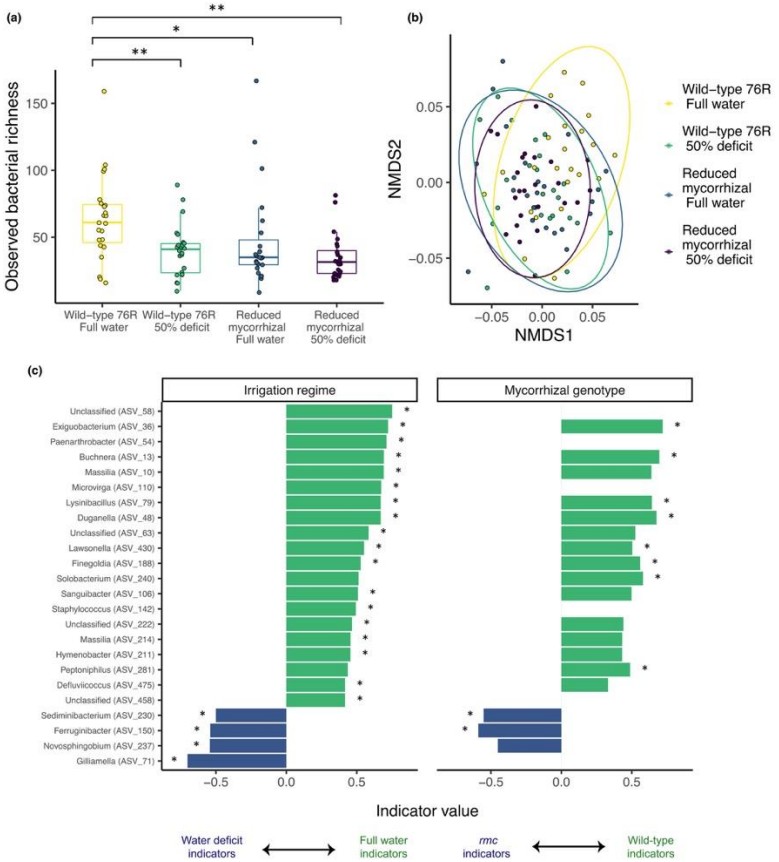


**Figure 3. Water stress and *rmc* genotype induce parallel shifts in bacterial composition. a)** Number of amplicon sequence variants (ASVs) per sample. Bacterial richness values were log-transformed before analysis to meet normality and homoscedasticity assumptions. The lower and upper hinges of each box plot represent the 25 $^{th}$ and 75$^{th}$ percentiles of the data, respectively, while the upper and lower whiskers extend to values within 1.5 times the interquartile range. Levels of significance are indicated as follows: **, $0.001 \leq P < 0.01$; *, $0.01 \leq P < 0.05$; ns, $P \geq 0.05$. **b)** Nonmetric multidimensional scaling (NMDS) ordination of plants in the field trial, colored by irrigation regime and mycorrhizal genotype. Ellipses indicate 95% confidence around groups. **c)** Indicator ASVs identified for irrigation regime (on a wild-type background) or mycorrhizal genotype (on a full water background). Names indicate genus-level classification, with ASV name in parenthesis. Values represent the square root of Dufrêne and Legendre's indicator value. For ease of interpretation, the indicator values of opposing treatments (water deficit vs full water, reduced mycorrhizal vs wild-type) are displayed with opposing signs. Asterisks indicate nominal significance ($P < 0.05$). Missing bars indicate taxa that were too prevalent in both treatments to statistically test association.

By contrast, the fertilizer gradient did not impact bacterial alpha or beta diversity. However, increasing fertilizer concentrations were associated with higher fungal alpha diversity ($F = 4.802$, df = 72, $P = 0.032$) and increased heterogeneity in fungal communities among plants ($F = 6.293$, df = 72, $P = 0.0028$) (Fig. **S10**). Further examination revealed that none of the taxa identified as indicators of fertilization were present in the fertilizer product itself, suggesting that the effect of fertilizer was not directly attributable to the addition of microbes (Table **S4**).

*Cross-kingdom associations*

Next, we asked how bacterial and fungal communities co-associated in our study, and whether these associations changed under water or nutrient limitation. Bacterial richness and fungal richness were highly correlated across plants ($r = 0.482$, df = 92, $P < 0.0001$, Fig. **4a**). The relationship remained significant in an ANOVA model that controlled for the field trial treatments (irrigation regime, mycorrhizal associations and soil fertilizer concentration) and technical effects (plant sonication batch, DNA extraction batch, and number of 16S and ITS reads per sample). Partial $R^2$ calculation indicated that bacterial richness accounted for 16.5% of the variation in fungal richness in this model. Bray–Curtis dissimilarity measures based on bacterial community composition and fungal community composition were correlated as well, including when controlling for field trial treatments and technical batches (partial Mantel statistic = 0.1563, $P = 0.001$).

To assess the contributions of cross-kingdom associations to overall occupancy patterns, we constructed a co-occurrence network for each combination of irrigation regime and plant genotype (Fig. **4b**). Across all treatment combinations, cross-kingdom pairs made up a larger proportion of the significant co-associations than either bacteria–bacteria or fungi–fungi pairs. Across mycorrhizal treatments, water stress decreased the average connectedness of nodes. These differences appeared to be driven by decreases in the number of bacteria–bacteria and bacteria–fungi associations in water-stressed plants (Fig. **4c,d**).

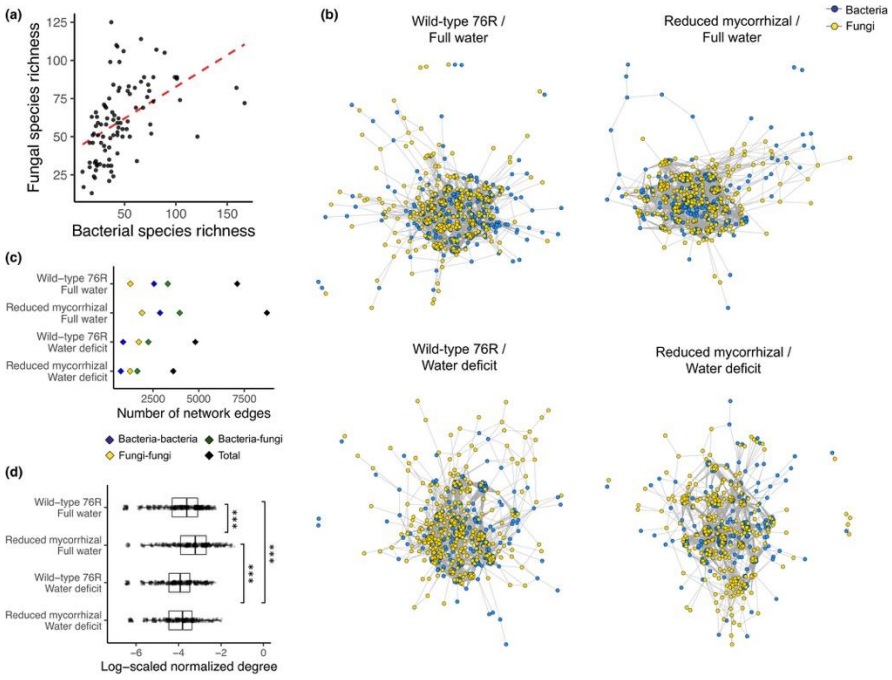


**Figure 4. Correlations between bacterial and fungal composition. a)** Number of amplicon sequence variants (ASVs) per sample. **b)** Co-occurrence networks of top 500 bacterial taxa and top 500 fungal taxa, structured according to Fruchterman and Reingold's force-directed layout algorithm. **c)** Number of network edges (positive and negative), displayed in total and according to the taxonomic identities of the nodes. **d)** Distribution of degree per node (number of positive and negative connections), normalized to total network size and log-transformed. The lower and upper hinges of each box plot represent the 25$^{th}$ and 75$^{th}$ percentiles of the data, respectively, while the upper and lower whiskers extend to values within 1.5 times the interquartile range. Levels of significance are indicated as follows: ***, $P < 0.001$; **, $0.001 \leq P < 0.01$; *, $0.01 \leq P < 0.05$; ns, $P \geq 0.05$.

*Growth chamber experiments*

We next sought to explore phyllosphere microbiome assembly and function in a more controlled setting. Microbial inocula from the field were sprayed onto plants in growth chambers. In the mycorrhiza experiment, wild-type and *rmc* plants in the growth chamber were sprayed with inocula from wild-type or *rmc* plants in the field, or a sterile buffer, for a fully reciprocal design. In the fertilizer experiment, plants treated with fertilizer matching the high and low extremes of the fertilizer gradient were sprayed with inocula from the corresponding positions in the field, or a sterile buffer. In both experiments, each individual sample (corresponding to one plant in the field) was divided in half and used to generate inocula for two plants, one in each growth chamber treatment.

One week after spraying, plants that had been sprayed with field inocula harbored higher absolute microbial abundances compared to plants sprayed only with sterile buffer ($t = 2.181$, df = 19.075, $P = 0.041$). Microbial communities on these plants were primarily composed of ASVs from the field experiment (Fig. **S2**), further validating that the spray treatment was sufficient to alter microbiome composition in the growth chamber.

Compared to their inocula in the field, plants sprayed with field inocula in the growth chamber harbored less diverse bacterial communities (mycorrhiza experiment: $F = 52.369$, df = 17, $P < 0.0001$; fertilizer experiment: $F = 193.307$, df = 17, $P < 0.001$) and underwent a strong shift in bacterial community composition ($P < 0.001$). In the mycorrhiza experiment, bacterial communities remained more similar to their inocula when sprayed onto a plant of the same genotype than a plant of the opposite genotype (Wilcoxon V-statistic = 10, $P = 0.011$). Similarly, bacterial communities in the fertilizer experiment remained more similar when the fertilizer treatment of the field plant matched that of the growth chamber plant (Wilcoxon V-statistic = 8, $P = 0.0061$) (Fig. **5**). The loss of fungal diversity in the growth chamber was much greater, and many plants were dominated by fungal ASVs that were not present in the inoculum (Fig. **S11**), suggesting that the microbiome transplant methods we used were not optimized for fungi. As such, we focused on the bacterial communities in all analyses.

The results of the growth chamber experiments were generally similar to those observed in the field (Fig. **S12-S13**). In the mycorrhiza experiment, *rmc* plants harbored lower bacterial alpha and beta diversity. Surprisingly, *rmc* communities transplanted onto wild-type plants recovered to the point that they were no longer distinguishable from wild-type communities (Fig. **6a**). Preliminary analyses suggested that this recovery could be mediated by the regrowth of small surviving microbial populations that never went extinct and/or dispersal from wild-type neighbors. (Fig. **6b,c**).

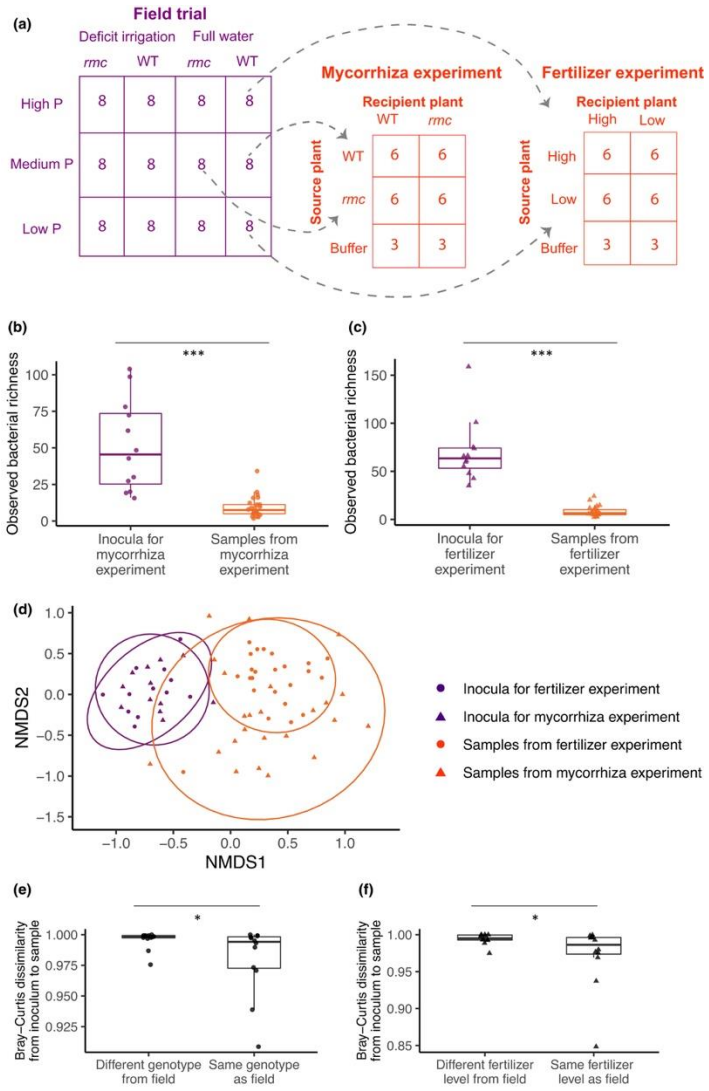


**Figure 5. Diversity and compositional changes from field to growth chamber. a)** Schematic indicating the subset of communities from the field that were transplanted onto plants in the growth chamber, with each cell number representing sample size. Each inoculum was used to inoculate two plants in the growth chamber (one in each treatment column). **b, c)** Number of amplicon sequence variants (ASVs) per sample. Richness values were log-transformed before analysis to meet normality and homoscedasticity assumptions. **d)** Nonmetric multidimensional scaling (NMDS) ordination shows that plants sampled in growth chamber experiments cluster together, away from their inocula. Ellipses indicate 95% confidence around clustering. **e, f)** Bray–Curtis dissimilarity index between each field plant used to generate inocula and its corresponding inoculated plants in the growth chamber. Categories indicate whether the plant in the growth chamber received the same or different experiment treatment as its source plant in the field. Each individual field plant was used to generate inocula for both growth chamber treatments, thus allowing a paired test. The lower and upper hinges of each box plot represent the 25$^{th}$ and 75$^{th}$ percentiles of the data, respectively, while the upper and lower whiskers extend to values within 1.5 times the interquartile range. Levels of significance are indicated as follows: ***, $P < 0.001$, **, $0.001 \leq P < 0.01$; *, $0.01 \leq P < 0.05$; ns, $P \geq 0.05$.

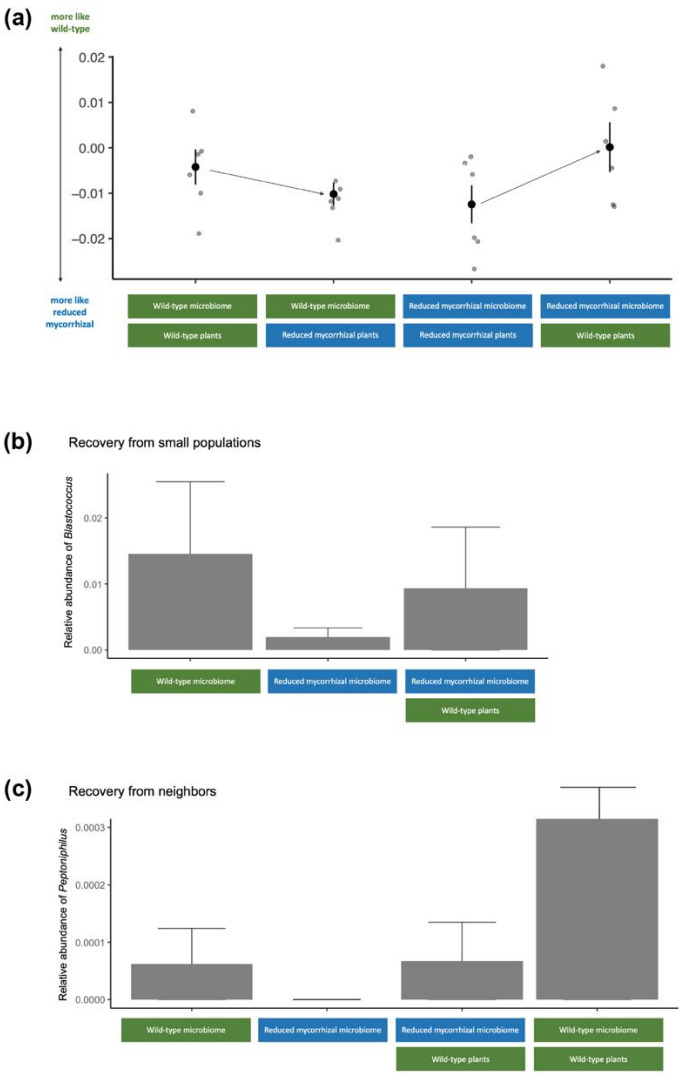


**Figure 6. Recovery of *rmc* microbiomes in the growth chamber. a)** Average Bray-Curtis distance from growth chamber samples to either 76R or *rmc* plants in the field. **b, c)** Relative abundance plots of individual ASVs in the field and growth chamber.

## 4.4 Discussion

Changes in climate and land use threaten plant communities by depleting water and disrupting mycorrhizal communities in the soil (202–204). Many studies have asked how environmental change will affect plant physiology, yet microbiomes can change rapidly and may therefore improve plant resilience to changing environments (235). Systemic changes in nutrient and biomass allocation, defense regulation, leaf structure, and gas exchange in water- and nutrient-limited plants (219,220,236) all suggest that soil conditions are likely to impact aboveground microbiota, with potential consequences for plant health. Here, we tested the effects of irrigation, mycorrhizas, and soil fertility on phyllosphere bacterial and fungal communities.

In the field and growth chamber, water stress and mycorrhizal disruption reduced bacterial richness and homogenized communities across host plants. Together, reduced species

richness and increased homogenization reflect a disproportionate loss of bacterial species with low occupancy across plants (i.e. bacterial species that differentiate individual plants from one another). The phyllosphere environment has harsh temperature fluctuations and low relative humidity compared to the soil or rhizosphere (180,237); low-occupancy species may be less well-adapted to these conditions, and therefore more strongly affected by stressors, than high-occupancy species. Alternatively, low metacommunity occupancy tends to correlate with small local population sizes (Fig. **S14**; (238)), which are often more vulnerable to ecological stochasticity (239,240).

By contrast, fungal community evenness increased under water stress and mycorrhizal disruption, reflecting a relative loss of dominant taxa. One explanation is that a small number of dominant taxa may comprise the majority of actively growing cells, which are more strongly affected by stressors, while rare sequences originate from dormant spores. In support of this explanation, RNA-based and stable isotope-based profiling show that only a minority of fungal sequences represent active populations (241,242) and that this active fraction is more sensitive to disturbance (243).

In general, water stress affected bacterial communities more strongly than fungal communities, a pattern consistent with a large body of work comparing bacterial and fungal drought responses in soil (207,244–248). Interactions between bacteria and fungi may be an important part of the picture as well. We found strong positive correlations between bacterial and fungal composition that persisted when accounting for measured environmental variation. The connectedness of the multi-kingdom network decreased under water-limited conditions despite similar network sizes, largely due to decreases in the numbers of bacteria–fungi and bacteria–bacteria associations. Our ability to draw direct inferences about cross-kingdom interactions in this study is limited, as co-associations can be confounded by environmental heterogeneity or differences between measured and biologically relevant spatial scales (249). However, other work has compiled fascinating examples of interactions between bacteria and fungi (250), and it will be important to see whether and how environmental stressors disrupt such interactions.

We observed a striking parallelism in the responses of microbial communities to water stress and the *rmc* genotype in our study. Based on these observations, we propose that reduced soil moisture and disruption of mycorrhizas both induce systemic stress responses that alter aboveground plant physiology and microbiome composition. Both water limitation and mycorrhizal disruption can induce stomatal closure, reduce specific leaf area, and alter plant nutrient concentration (236,251,252), altering physical and chemical characteristics of the phyllosphere habitat. Interestingly, the effect of water stress in this study was strongest in wild-type plants, and the effect of mycorrhizal disruption was strongest in well-watered plants. In fact, the combined effects of water stress and mycorrhizal disruption were not associated with additional community turnover or loss of microbial diversity compared to either individually. This observation contrasts with previously observed interactions between irrigation and mycorrhizas, where mycorrhizal plants are typically more drought-tolerant (252,253). It is thus possible that mycorrhizas allow plants to access compensatory pathways that buffer their own fitness under water limitation, but do not extend to phyllosphere microbial communities. For example, mycorrhizal tomato plants closed their stomata more quickly than nonmycorrhizal plants under drought conditions in a prior study (254). Rapid stomatal closure in mycorrhizal

plants appeared to minimize plant biomass loss compared to nonmycorrhizal plants, but may have limited microbial access to stomata, an important source of water in the phyllosphere (124,255). It is also possible that an interaction between water stress and mycorrhizas would have emerged if plants were sampled later in the growing season, when water stress was more severe.

Several alternative mechanisms may contribute to the effects of the belowground treatments in this study on phyllosphere microbiome composition. First, microbiome variation between wild-type and reduced mycorrhizal plants could simply reflect host genetic variation, independent of the presence of mycorrhizas. In addition to *CYCLOPS/IPD3*, which confers the reduced mycorrhizal phenotype, the *rmc* deletion spans parts of four other genes (256). At least one of the remaining genes regulates resistance to the root pathogen *Fusarium oxysporum* (257), but we are not aware of any off-target effects on foliar phenotypes or phyllosphere microorganisms. Studies of 76R and *rmc* plants report similar biomass and nutrient uptake in the absence of mycorrhizal fungi (258,259), and *CYCLOPS/IPD3* is not highly expressed in leaf tissue (260,261). Therefore, while our study design does not exclude the possibility of a direct effect of *rmc* on phyllosphere microorganisms, such an effect is at odds with other work on this system.

Another explanation for the effect of the reduced mycorrhizal genotype is that mycorrhizal colonization modifies host immune signaling both locally and systemically (223), tending to increase resistance to necrotrophic pathogens and decrease resistance to biotrophic pathogens (262). This may explain why *P. syringae* colonized wild-type plants more successfully than *rmc* plants in the growth chamber, but it is unclear whether commensal microbiota on the leaf surface interact closely enough with plant cells to be regulated by immune signaling. Bacteria can often grow to high densities on the leaf surface with minimal changes to plant gene expression (263), and the results of studies that directly tested for immune control of phyllosphere microbiome composition have been mixed (264,265).

Soil is thought to be one of many sources of dispersal to the phyllosphere (266), so changes in the soil community could affect the phyllosphere community, independent of systemic plant modifications. However, the taxonomic patterns of enrichment and depletion that we observed in the phyllosphere were markedly different from those previously observed in soil and rhizosphere studies. In soil and rhizosphere habitats, drought is commonly associated with enrichment of many *Actinobacterial* taxa, and depletion of *Acidobacteria, Proteobacteria*, and *Bacteroidetes* (206,208,245). By contrast, we did not observe significant enrichment in any families of *Actinobacteria* (though several were depleted under water-limited conditions), while several *Proteobacteria* and *Bacteroidetes* families were enriched under water stress. Additionally, we would not expect to see parallel responses to water stress and the *rmc* genotype if the effect were driven by dispersal. While mycorrhizas can alter surrounding soil communities, their effects tend to be relatively minor and/or highly localized (258,267).

Although irrigation regime and mycorrhizal associations were the strongest predictors of phyllosphere microbiome composition in our study, we observed some effects of fertilization. Fungal diversity and heterogeneity increased along the fertilization gradient, and bacterial communities remained more similar from the field to the growth chamber if they were transplanted onto a plant grown under the same nutrient conditions. Interestingly, these

effects manifested aboveground even though fertilization did not appear to alter extractable phosphate availability in the soil. In light of this unexpected observation, we suspect that the added P was mainly in an organic form that was not sufficiently mineralized in the time period of the experiment to be detected by our measure of available P (Olsen P), but may have still altered plant physiology or belowground community composition in ways that subsequently impacted aboveground microbial communities. It is also possible that other components of this product, such as added calcium or resident microbiota, contributed to the observed changes in phyllosphere community composition. However, none of the fungal taxa that were enriched in the fertilized plots were detected in the fertilizer product, making it unlikely that the effect of fertilizer was caused by the direct addition of microbes.

Our study demonstrates the effects of soil conditions on the diversity, composition, and distribution of aboveground microbiota. We observed strikingly parallel effects of water stress and mycorrhizal disruption despite differences in their nature (biotic or abiotic), yet these changes were distinct from enrichment patterns previously observed in the soil and rhizosphere. Taken together, our findings are unlikely to be explained by off-target effects of the *rmc* mutation, dispersal from soil, or stochastic colonization of plants in the field. Rather, they indicate that soil conditions induce systemic responses in plants which in turn alter selection on aboveground microbial communities. Our study highlights the importance of phyllosphere microbial communities both as indicators of plant stress and as potential mediators of plant responses to global environmental change.

## 4.5 Appendix

*Methods S1: Field trial preparation and sampling*

Field preparation included spading and bed formation (1.5 m wide from furrow to furrow), followed by feather meal (12 – 0 – 0) banded in at a rate of 40 kg N ha-1 . Experimental plots were established in eight experimental beds with rows of buffer plants between each experimental bed. Transplants were grown in the Westside Transplant facility in Winters, CA. After 9 wk. under certified organic management, seedlings were transplanted on the bed center by hand on 28 April 2019, followed by 1.9 cm of water applied via a single surface drip line in the center of each bed. Transplants that died due to a fungal blight (~100 plants) were replaced in the first three weeks of the experiment. Soil samples were taken at three depths (0-15cm, 15-30cm, 30-60cm) at transplant, midseason (52 days after transplant) and harvest (116 days after transplant).

*Methods S2: Growth chamber experiments*

Seeds were sterilized by swirling in 2.7% bleach for 20 minutes, then washed 3 times with sterile water. 4 seeds per plate were germinated on 1% water agar. Plates were wrapped in aluminum foil for 7 days and stored at 21°C. After 1 week, plants were transferred to individual pots containing Sunshine #4 potting mix, where they were maintained at a 15 h day:9 h night light cycle.

When plants were three weeks old, field communities were used to generate inocula. An aliquot of each sample from the field was thawed and plated on agar to count colonies. Colony counts ranged from $10^4$ – $10^6$ CFU/mL. Each sample from the field was divided in half, then diluted to 104 CFU/mL in 10 mM $MgCl_2$. The surfactant Silwet-L-77 was added at a

concentration of 0.1 µL autoclaved Silwet per 1 mL inocula to facilitate microbial adhesion onto the leaf surface. Each plant was sprayed with 4 mL of inoculum using a 15 mL conical tube fitted with a spray cap. Each plant was sprayed from all angles inside an autoclave bag to contain microbes.

One week after spraying, a frozen stock of *Pseudomonas syringae* pathovar tomato PT23 was grown overnight in King's Broth at 28°C for experimental infections. The overnight culture was diluted in 10 mM $MgCl_2$ to an optical density (OD600) of 0.0002. At 24 hours postinfection, 3 hole punches (6-mm diameter) were taken from each inoculated leaf, for a total of 9 leaf discs per plant. Leaf discs were placed in a FastPrep tube with 1 mL 10 mM $MgCl_2$ and two sterile ceramic beads, then homogenized in the FastPrep-24 5G sample disruption instrument at 4.0 m/s for 40 seconds.

The rest of the aboveground plant tissue was placed in a 15 mL tube. The tube was filled with 10 mM $MgCl_2$ and submerged in a Branson M5800 sonicating water bath for 10 minutes to gently dislodge microbial cells from the leaf surface. Leaf wash was centrifuged at 3500 x g for 10 minutes, resuspended in 600 uL 10 mM $MgCl_2$, and frozen immediately at –20°C for sequencing.

*Methods S3: Droplet digital PCR reaction conditions and primers*

*Pseudomonas* abundance was quantified using the Bio-Rad QX200TM Droplet Digital PCR system. Reaction mixtures were prepared with 11 µL Bio-Rad ddPCR Supermix for Probes (no dUTP), 1.1 µL probe (see below), 4.9 µL molecular grade water, and 5 µL homogenized leaf material. Samples were randomized on the ddPCR plate, with a negative control (replacing the 5 µL template with molecular grade water) in the last well of each column. Droplets were generated according to manufacturer instructions, and the following PCR conditions were used for amplification: 95°C for 10 minutes; 40 cycles of the following: (94°C for 30 seconds, 60°C for 1 minute, 72°C for 1 minute); 98°C for 10 minutes; hold at 12°C. Positive droplet thresholds were set by column, with fluorescence values in the range of the negative control classified as negative. ddPCR primers were adapted from *Pseudomonas* qPCR assays and target a hypervariable region of the 16S rRNA gene (268): Forward 5'- ACTTTAAGTTGGGAGGAAGGG-3'; reverse 5'-ACACAGGAAATTCCACCACCC-3', probe TGCCAGCAGCCGCGG.

Total bacterial abundance was quantified using the Bio-Rad QX200TM Droplet Digital PCR system. Reaction mixtures consisted of 11 µL EvaGreen Supermix, 0.22 µL forward primer (see below), 0.22 µL reverse primer, 5.56 µL molecular grade water, and 5 µL leaf wash. Samples were randomized on the ddPCR plate, with a negative control in the last well of each column. Droplets were generated according to manufacturer instructions, and the following PCR conditions were used for amplification: 95°C for 10 minutes; 40 cycles of the following: (95°C for 30 seconds, 55°C for 30 seconds, 72°C for 2 minutes), 4°C for 5 minutes, 90°C for 5 minutes, hold at 12°C. Positive droplet thresholds were set by column, with fluorescence values in the range of the negative control classified as negative. Conserved sequences in the V3-V4 regions of the 16S rRNA gene were targeted using the following primers: Forward 5'-CCTACGGGNBGCASCAG-3'; reverse 5'-GACTACNVGGGTATCTAATCC-3'.

*Methods S4: Amplicon sequencing workflow and analysis*

The V4 region of the 16S rRNA gene was amplified using 515F/806R primers, with peptide nucleic acids (PNAs) added to limit amplification of plant chloroplast and mitochondrial DNA (Lundberg et al. 2013). The eukaryotic ITS2 gene was amplified using the primers (5'-CCTCCGCTTATTGATATGC-3', 5'-CCGTGARTCATCGAATCTTTG-3'). Reads were analyzed using the recommended DADA2 pipeline with the following parameters. Reads with Ns or >2 "expected errors" (calculated by DADA2 based on quality scores) were removed. 16S reads were truncated at 240 base pairs in the forward direction and 140 base pairs in the reverse direction, or at the first position with a quality score <2. ITS reads shorter than 50 base pairs were removed, or were truncated at the first position with a quality score <2. Amplicon sequence variants (269) were inferred after training the core denoising algorithm on error rates. DADA2 was then used to merge paired reads, on the condition that forward and reverse reads overlap by at least 12 bases. Chimeric sequences were identified as exact reconstructions of segments of two more abundant "parent" sequences, and removed from further analysis. After filtering plant-derived sequences and sequences prevalent in negative controls, the dataset consisted of 1579 bacterial amplicon sequence variants (ASVs) and 1397 fungal ASVs.

**Table S1. Fertilizer gradient in field trial.** Bold values indicate sampling scheme.

| **Position in gradient** | **Fertilizer added ($g/m^2$)** | **Fertilizer added ($g/m^3$)** (assuming penetration depth of 20 cm) |
|---|---|---|
| **1, 2** | **0** | **0** |
| 3 | 40 | 200 |
| 4 | 80 | 400 |
| 5 | 120 | 600 |
| 6 | 160 | 800 |
| 7 | 200 | 1000 |
| **8** | **400** | **2000** |
| **9** | **600** | **3000** |
| 10 | 800 | 4000 |
| **11, 12** | **1000** | **5000** |

**Table S2. Full results of ANOVA models of bacterial and fungal richness.**

| **Treatment** | **df** | **Sum of squares** | **Mean square** | **F value** | **p-value** |
|---|---|---|---|---|---|
| Irrigation regime | 1 | 2.384 | 2.384 | 10.468 | 0.0018 |
| Genotype | 1 | 1.185 | 1.185 | 5.203 | 0.026 |
| Fertilizer concentration | 1 | 0.387 | 0.387 | 1.697 | 0.197 |

| | | | | | |
|---|---|---|---|---|---|
| Plant sonication batch (randomized across treatments) | 12 | 2.729 | 0.227 | 0.998 | 0.459 |
| DNA extraction batch (randomized across treatments) | 6 | 6.765 | 1.127 | 4.951 | 0.00027 |
| | | | | | |
| **Treatment** | **df** | **Sum of squares** | **Mean square** | **F value** | **p-value** |
| Irrigation regime | 1 | 388.5 | 388.5 | 0.902 | 0.345 |
| Genotype | 1 | 4919.1 | 4919.1 | 11.417 | 0.0011 |
| Fertilizer concentration | 1 | 2069.1 | 2069.1 | 4.802 | 0.032 |
| Plant sonication batch (randomized across treatments) | 12 | 8802.5 | 733.5 | 1.702 | 0.084 |
| DNA extraction batch (randomized across treatments) | 6 | 10317.9 | 1.197 | 3.991 | 0.0017 |

**Table S3. Full results of ANOVA models of bacterial and fungal Shannon diversity.**

| **Treatment** | **df** | **Sum of squares** | **Mean square** | **F value** | **p-value** |
|---|---|---|---|---|---|
| Irrigation regime | 1 | 3.047 | 3.047 | 4.990 | 0.029 |
| Genotype | 1 | 0.325 | 0.325 | 0.533 | 0.468 |
| Fertilizer concentration | 1 | 0.076 | 0.076 | 0.124 | 0.726 |
| Plant sonication batch (randomized across treatments) | 12 | 26.670 | 2.222 | 3.640 | 0.00028 |
| DNA extraction batch (randomized across treatments) | 6 | 4.760 | 0.793 | 1.299 | 0.268 |
| | | | | | |
| **Treatment** | **df** | **Sum of squares** | **Mean square** | **F value** | **p-value** |
| Irrigation regime | 1 | 0.5262 | 0.5262 | 7.966 | 0.0062 |
| Genotype | 1 | 0.046 | 0.046 | 0.690 | 0.409 |
| Fertilizer concentration | 1 | 0.040 | 0.040 | 0.610 | 0.437 |
| Plant sonication batch (randomized across treatments) | 12 | 1.336 | 0.111 | 1.685 | 0.088 |
| DNA extraction batch (randomized across treatments) | 6 | 0.973 | 0.162 | 2.453 | 0.032 |

**Table S4. No overlap between taxa enriched in fertilized plants and taxa present in fertilizer.**

| **Fungal taxa enriched at medium or high fertilizer concentrations** |
|---|

| ASV number | Family | Species | Enriched in | Indicator value | p-value |
|---|---|---|---|---|---|
| 25 | Filobasidiaceae | *Filobasidium stepposum* | Medium/high | 0.553 | 0.033 |
| 38 | Filobasidiaceae | *Filobasidium oeirense* | Medium/high | 0.606 | 0.024 |
| 51 | Filobasidiaceae | *Filobasidium stepposum* | Medium/high | 0.464 | 0.022 |
| 95 | Bulleribasidiaceae | *Vishniacozyma dimennae* | Medium/high | 0.564 | 0.018 |
| 103 | Filobasidiaceae | *Naganishia albida* | High | 0.379 | 0.031 |
| 140 | Dothideaceae | Unclassified | Medium | 0.502 | 0.011 |
| 191 | Bulleribasidiaceae | *Vishniacozyma foliicola* | Medium | 0.393 | 0.020 |
| 209 | Filobasidiaceae | *Naganishia albida* | Medium | 0.316 | 0.039 |
| 301 | Pleosporaceae | *Alternaria eureka* | High | 0.393 | 0.014 |
| 333 | Mrakiaceae | *Udeniomyces pyricola* | Medium | 0.365 | 0.005 |
| 436 | Unclassified Myriangiales | Unclassified | High | 0.357 | 0.039 |
| 437 | Dothideaceae | Unclassified | High | 0.354 | 0.035 |
| 474 | Unclassified Pleosporales | Unclassified | Medium | 0.316 | 0.033 |

**Fungal taxa present in fertilizer product**

| ASV number | Family | Species |
|---|---|---|
| 2 | Cladosporiaceae | Unclassified *Cladosporium* |
| 5 | Filobasidiaceae | *Filobasidium stepposum* |
| 16 | Bulleribasidiaceae | *Vishniacozyma victoriae* |
| 394 | Unclassified Phacidiales | *Epithamnolia rangiferinae* |

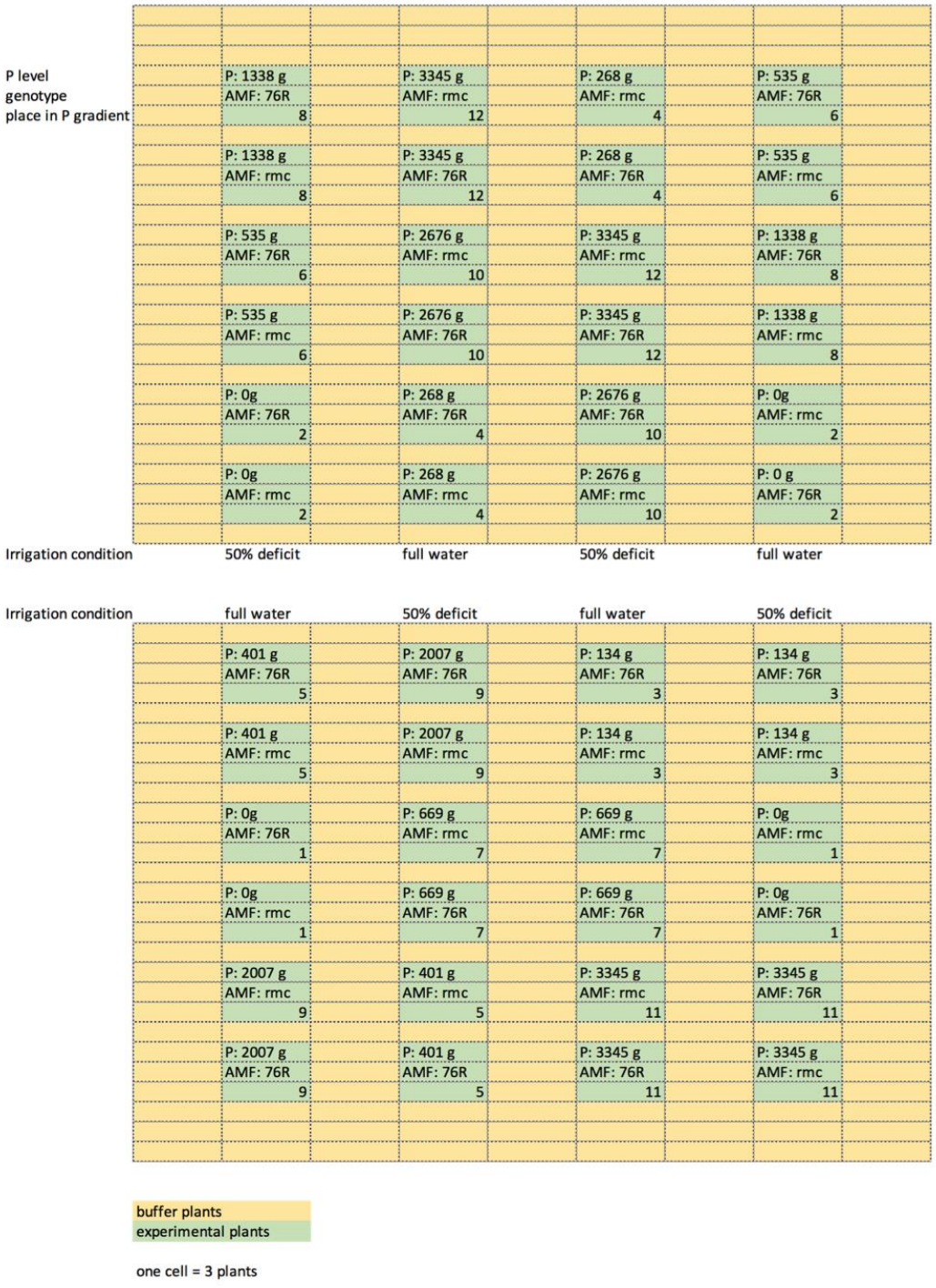


**Figure S1. Experimental design for the field trial.** Plots shown in green included 10 plants and were experimentally manipulated as described within the plot.

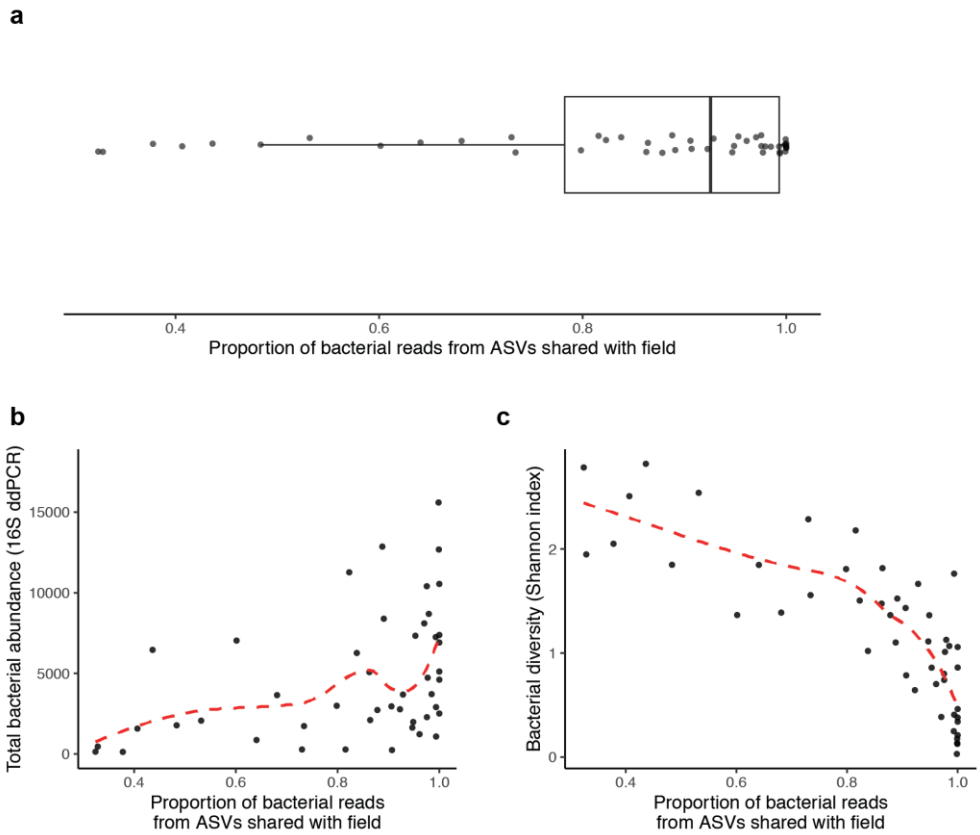


**Figure S2. Colonization of growth chamber plants by field bacterial communities. a)** Bacterial communities on plants in the genotype and phosphorus experiments were composed primarily of taxa from the field trial (median = 92.6%), but in a subset of plants, a large proportion of reads came from taxa unique to the growth chamber. **b)** Plants with a large proportion of growth-chamber-unique reads had low overall bacterial abundance, suggesting that the inocula failed to grow to high densities. **c)** Plants with a large proportion of growth-chamber-unique reads had high diversity despite low bacterial abundance, suggesting that occasional contamination by growth-chamber-unique taxa confounded alpha diversity estimates.

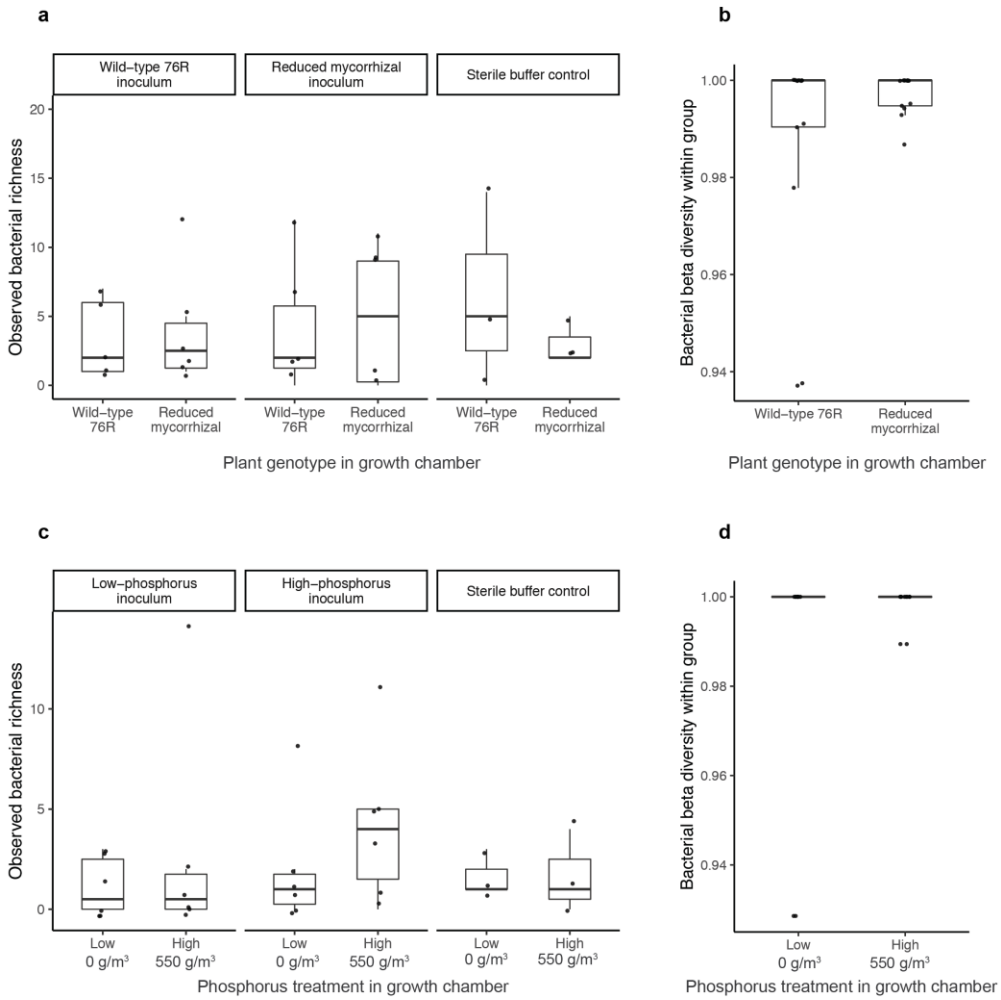


**Figure S3. Growth-chamber-unique taxa are not distributed according to experimental treatments in the growth chamber. a)** Observed bacterial richness in mycorrhizae experiment, as measured by ASV counts of taxa unique to the growth chamber. **b)** Within-group dispersion of bacterial communities was quantified by generating a Bray-Curtis dissimilarity matrix of taxa unique to the growth chamber. Points represent the mean Bray-Curtis dissimilarity between each sample and other samples of the same genotype (76R or reduced mycorrhizal). **c)** Observed bacterial richness in phosphorus experiment, as measured by ASV counts of taxa unique to the growth chamber. **d)** Within-group dispersion of bacterial communities was quantified by generating a Bray-Curtis dissimilarity matrix of taxa unique to the growth chamber. Points represent the mean Bray-Curtis dissimilarity between each sample and other samples within the same treatment group (low, high).

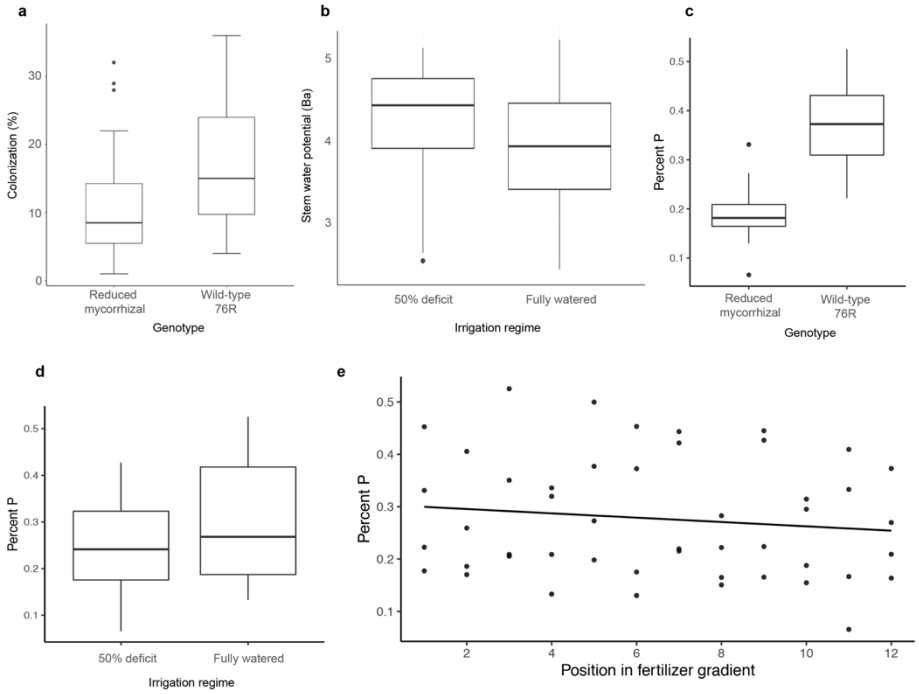


**Figure S4. Effects of field trial treatments on plant phenotypes. a)** Wild-type plants (76R, n=24) show significantly higher root colonization by AMF than reduced mycorrhizal mutants (*rmc,* n=24). **b)** Plants grown under deficit conditions (n=24) show a trend toward higher stem water potential, an indicator of water stress, compared to fully watered plants (n=24). **c)** Wild-type plants (n=24) have a significantly higher P concentration in plant tissue than reduced mycorrhizal mutants (n=24). **d)** Plants grown under deficit conditions (n=24) have significantly lower P concentration in plant tissue than fully watered plants (n=24). **e)** No effect of added fertilizer on the concentration of P in plant tissue, where higher positions on the fertilizer gradient indicate higher concentrations of added fertilizer.

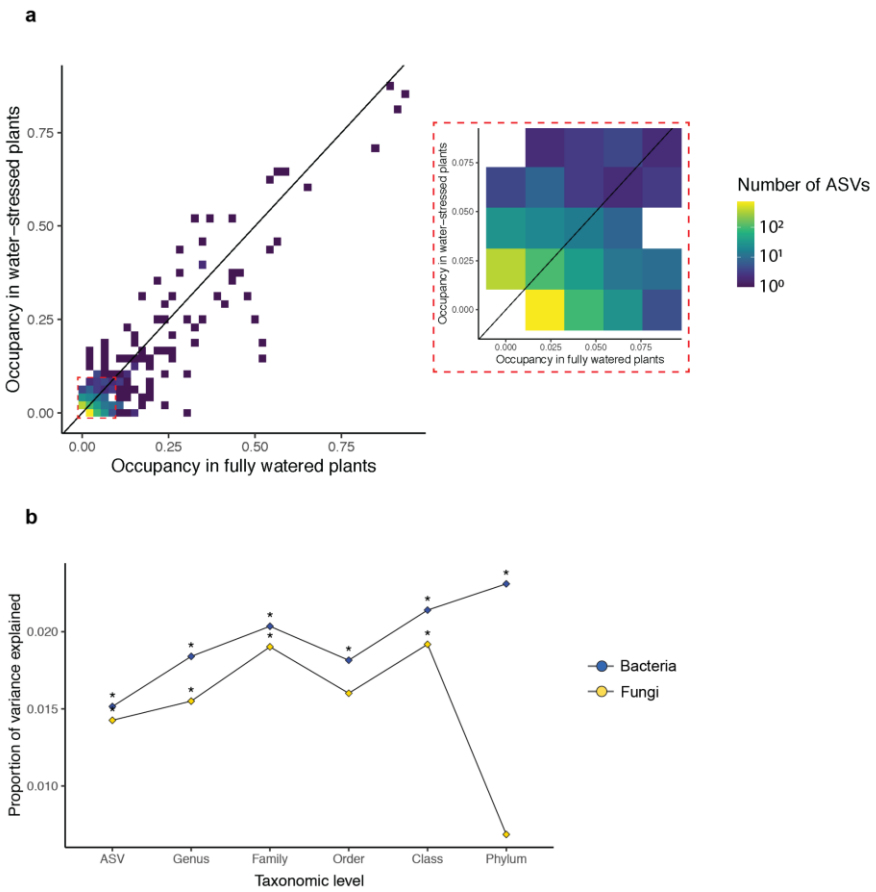


**Figure S5. Effects of water stress are strongest on rare bacterial taxa and persist at broad taxonomic levels. a)** Tile plot describing the relationship between the proportion of fully watered plants and the proportion of drought plants occupied (relative abundance > 0) by each bacterial ASV. Inset depicts bacterial ASVs that were detected on fewer than 10% of plants in either treatment. Many of these ASVs were less frequently detected in the drought treatment than in the full water treatment (as indicated by brighter colors below the diagonal). **b)** Proportion of variance in bacterial or fungal community composition explained by water regime in a model including plant genotype, fertilizer concentration, plant sonication batch, and DNA extraction batch as additional covariates. Asterisks indicate where drought explained a significant portion of variation in a PERMANOVA test.

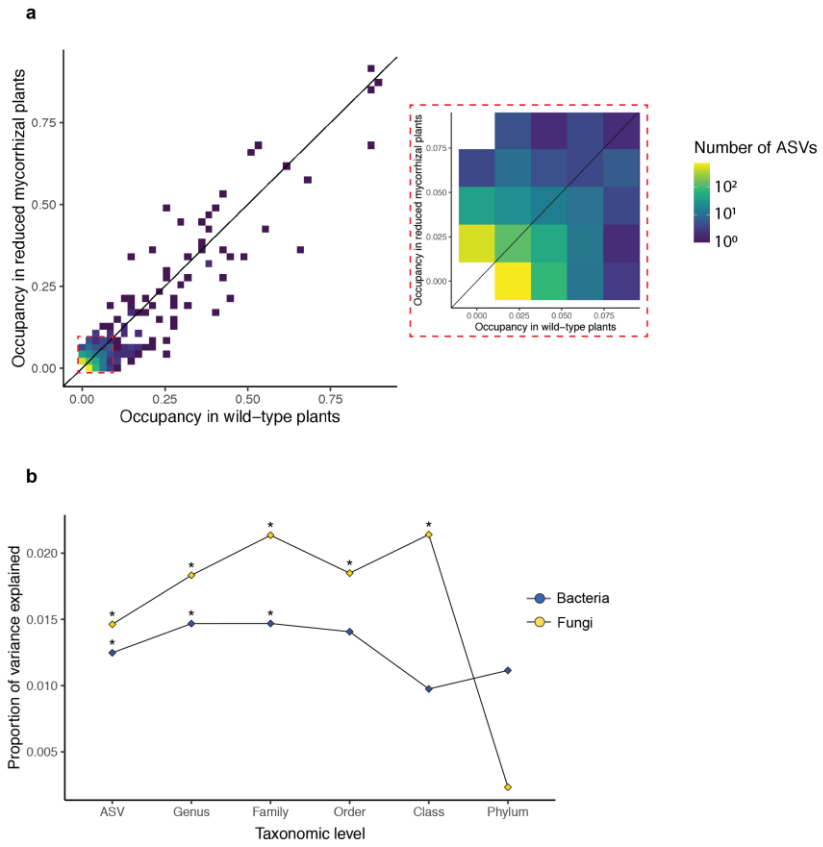


**Figure S6. Effects of the *rmc* genotype are strongest on rare bacterial taxa and persist at broad taxonomic levels.** **a)** Tile plot describing the relationship between the proportion of wild-type plants and the proportion of reduced mycorrhizal plants occupied (relative abundance > 0) by each bacterial ASV. Inset depicts bacterial ASVs that were detected on fewer than 10% of plants in either treatment. Many of these ASVs were less frequently detected in reduced mycorrhizal plants than in wild-type plants (as indicated by brighter colors below the diagonal). **b)** Proportion of variance in bacterial or fungal community composition explained by mycorrhizal genotype in a model including water regime, fertilizer concentration, plant sonication batch, and DNA extraction batch as additional covariates. Asterisks indicate where plant genotype explained a significant portion of variation in a PERMANOVA test.

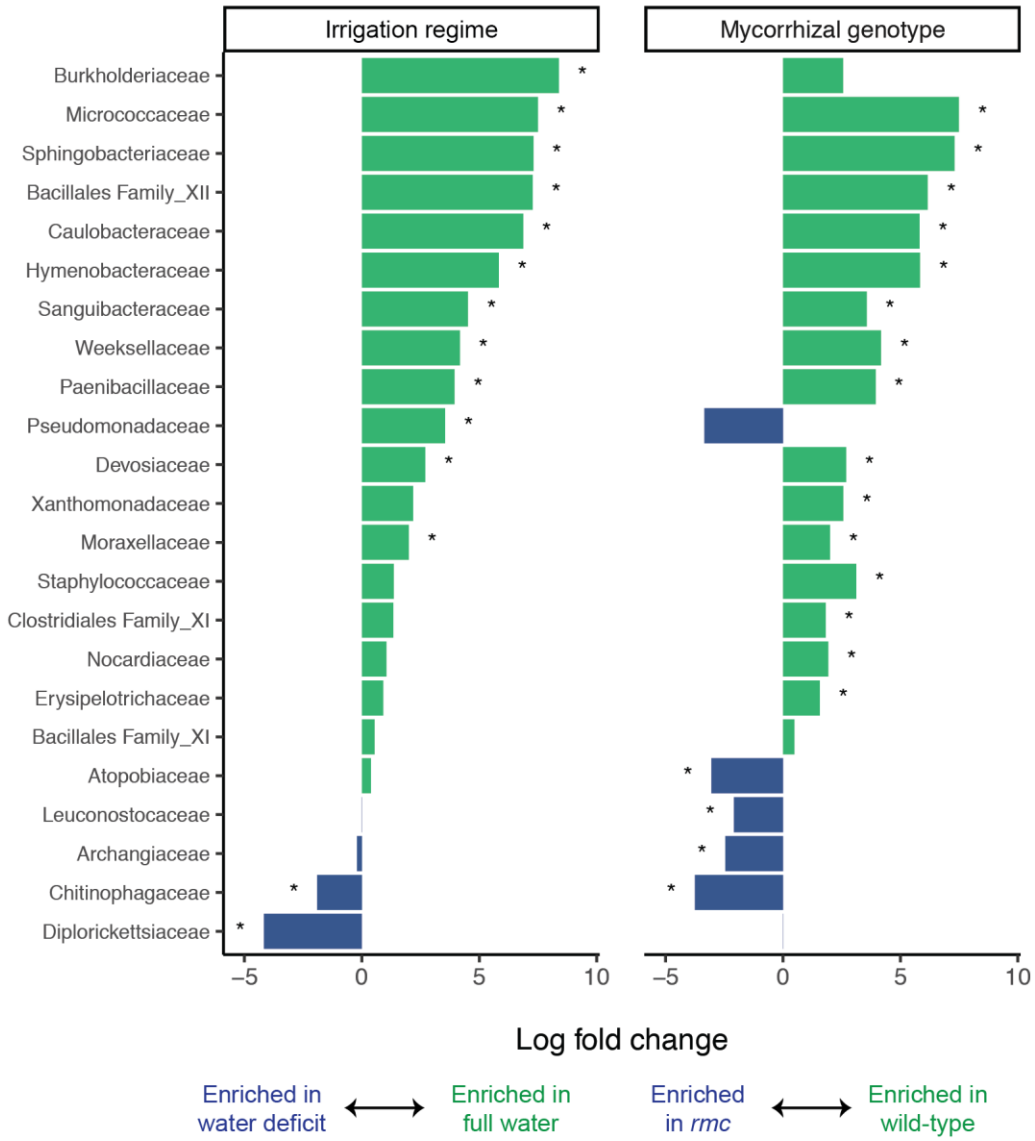


**Figure S7. Negative binomial modeling identifies parallel shifts in bacterial community composition in water stress and *rmc* genotype.** The negative binomial model implemented in the package *edgeR* was used to calculate log fold differences in abundance of bacterial families across water regimes (on a wild-type background) or plant genotypes (on a full water background). Significance was assessed for each family using an analog of Fisher's exact test adapted for overdispersed data, then corrected for multiple testing. Asterisks indicate significance after multiple testing (FDR<0.01).

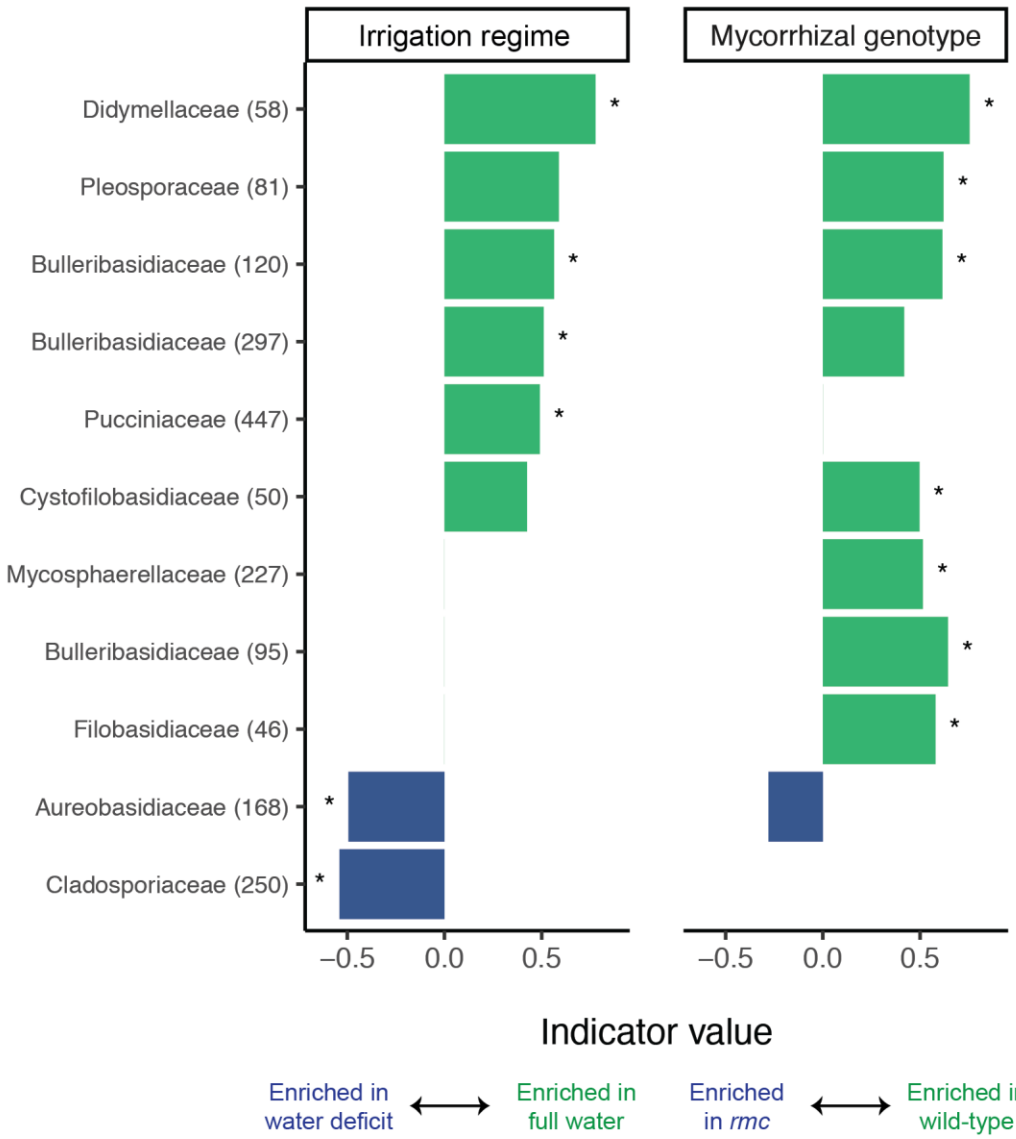


**Figure S8. Overlap in fungal indicator species for water regime and mycorrhizal genotype.** Indicator taxa identified for the water regime (on a wild-type background) or mycorrhizal genotype (on a full water background). Names indicate genus-level classification, with ASV number in parenthesis. Values represent the square root of Dufrêne and Legendre's indicator value. For ease of interpretation, the indicator values of opposing treatments (water deficit vs. full water, reduced mycorrhizal vs. wild-type) are displayed with opposing signs. Asterisks indicate nominal significance ($p<0.05$). Missing bars indicate taxa that were too prevalent in both treatments to statistically test association.

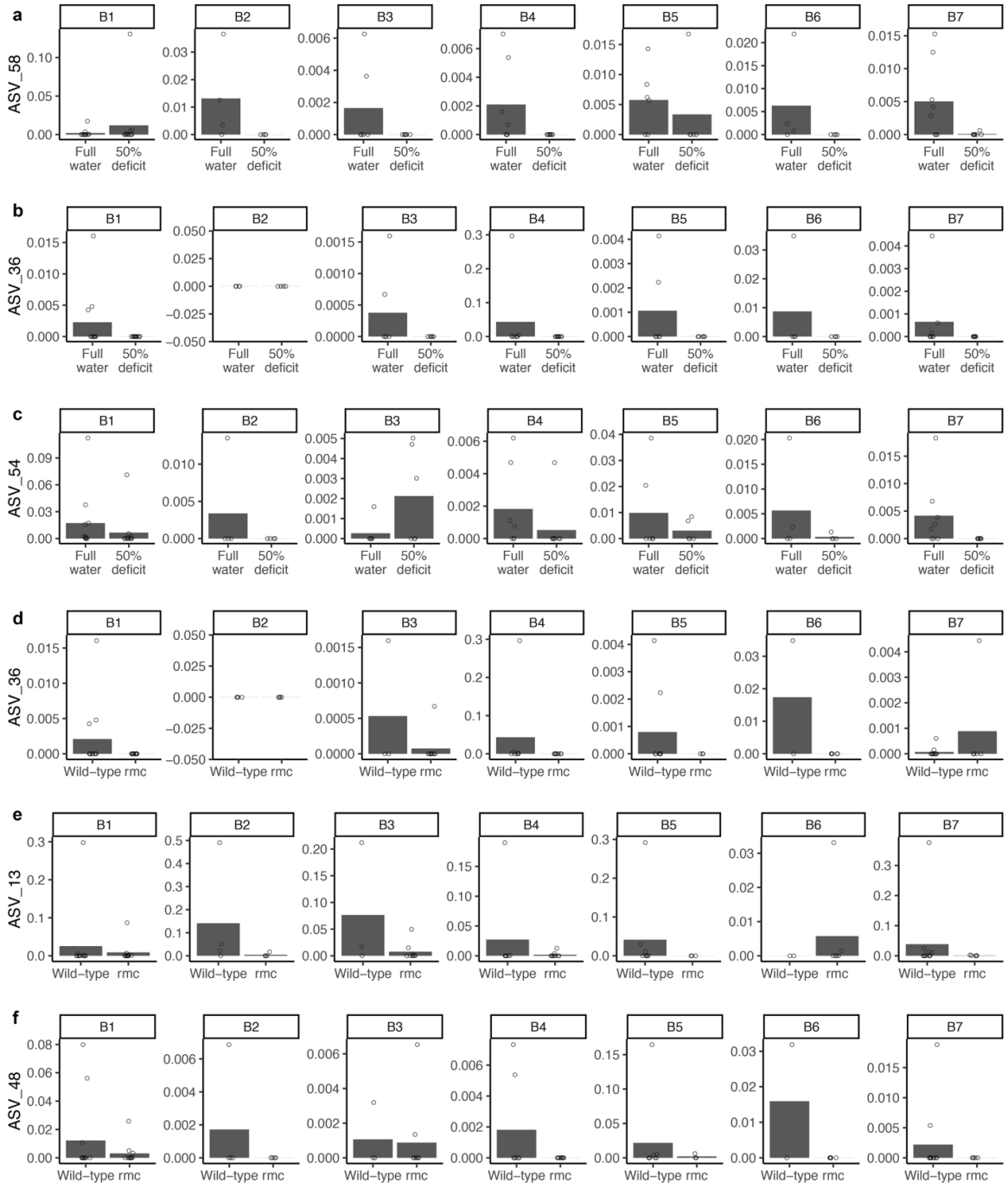


**Figure S9. Treatment effects within batches mirror those observed within the full dataset. a-c)** Distribution of the top three indicator ASVs for irrigation regime within DNA extraction batches. In the full dataset, all three taxa were enriched in fully watered plants compared to water-stressed plants. **d-f)** Distribution of the top three indicator ASVs for mycorrhizal genotype within DNA extraction batches. In the full dataset, all three taxa were enriched in wild-type plants compared to *rmc* plants.

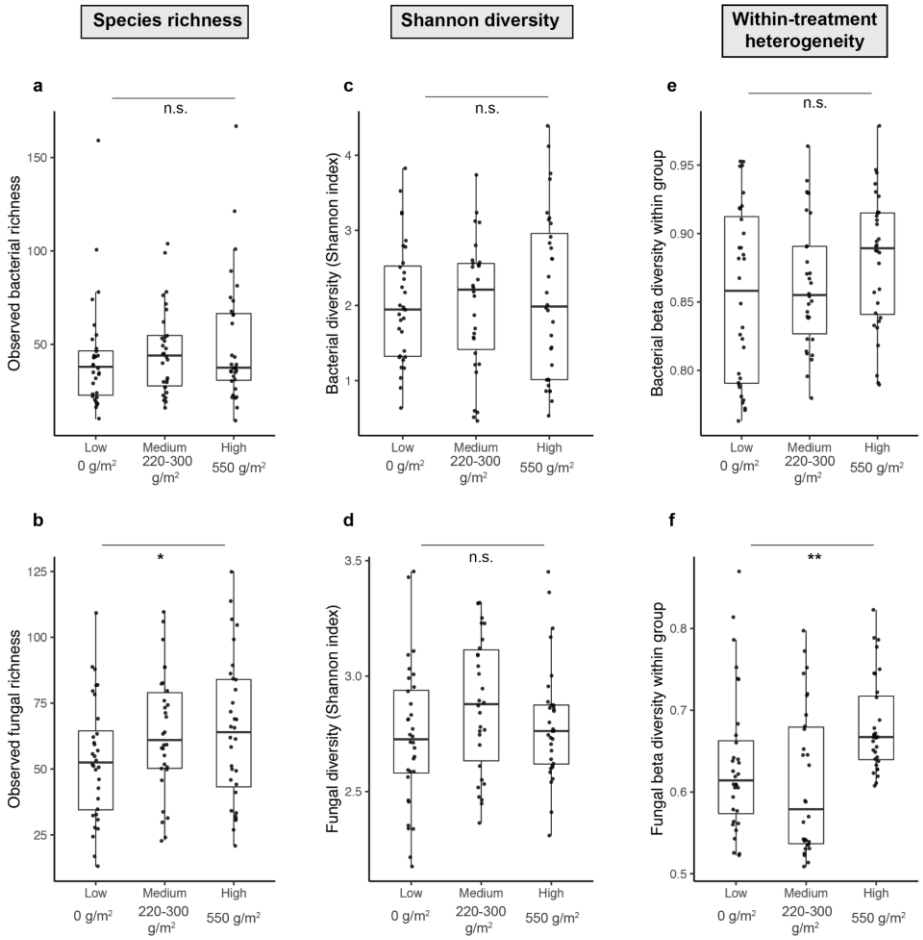


**Figure S10. Phosphorus fertilization increases fungal alpha and beta diversity. a,b)** ASV counts after removing plant sequences and contaminant sequences. Bacterial richness values were log-transformed prior to ANOVA to meet normality and homoscedasticity assumptions. **c,d)** Shannon-Weaver index of combined richness and evenness. **e,f)** Within-group dispersion was quantified by generating a Bray-Curtis dissimilarity matrix. Points represent the mean Bray-Curtis dissimilarity between each sample and other samples within the same treatment group (low, medium, or high).

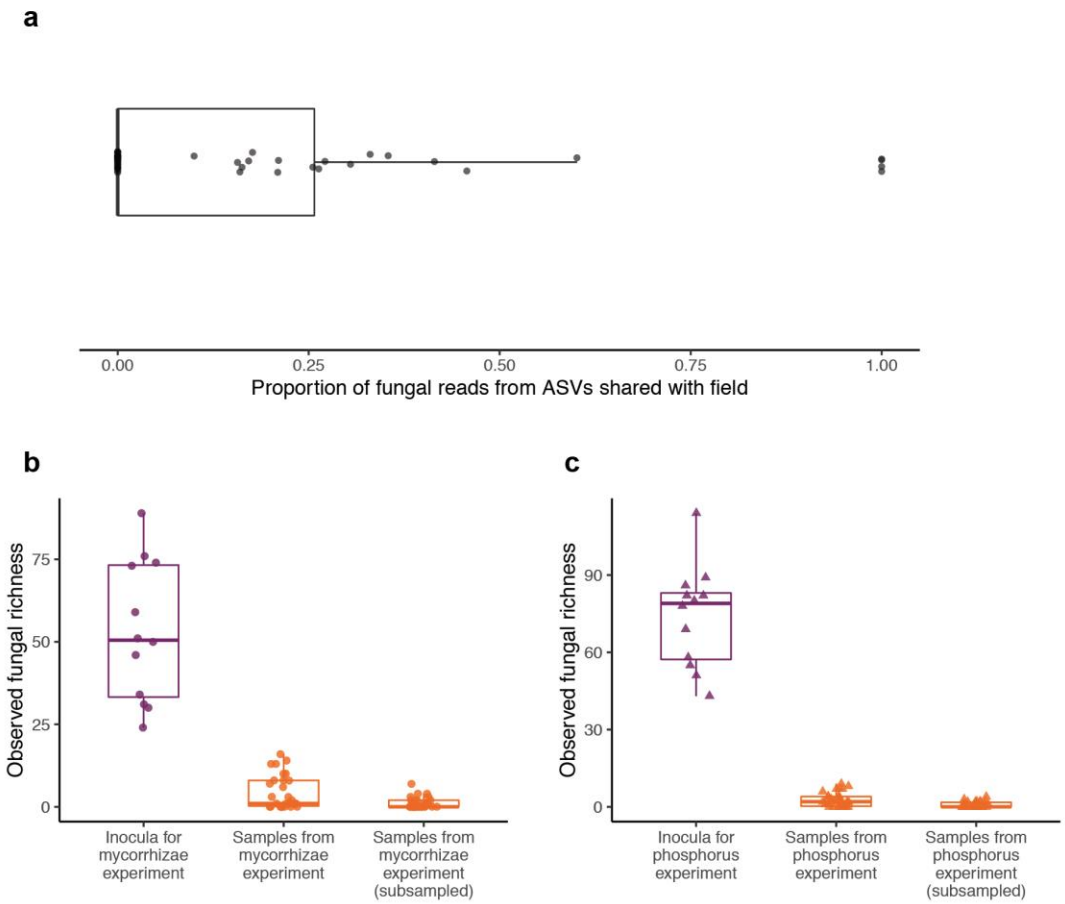


**Figure S11. Colonization of growth chamber plants by field fungal communities. a)** Fungal communities on plants in the genotype and phosphorus experiments were not dominated by taxa from the field, but rather by taxa unique to the growth chamber. **b,c)** Removing taxa unique to the growth chamber for further analysis, as was done in the bacterial microbiome, greatly reduces fungal richness values (most plants had only 0-2 fungal ASVs after subsampling).

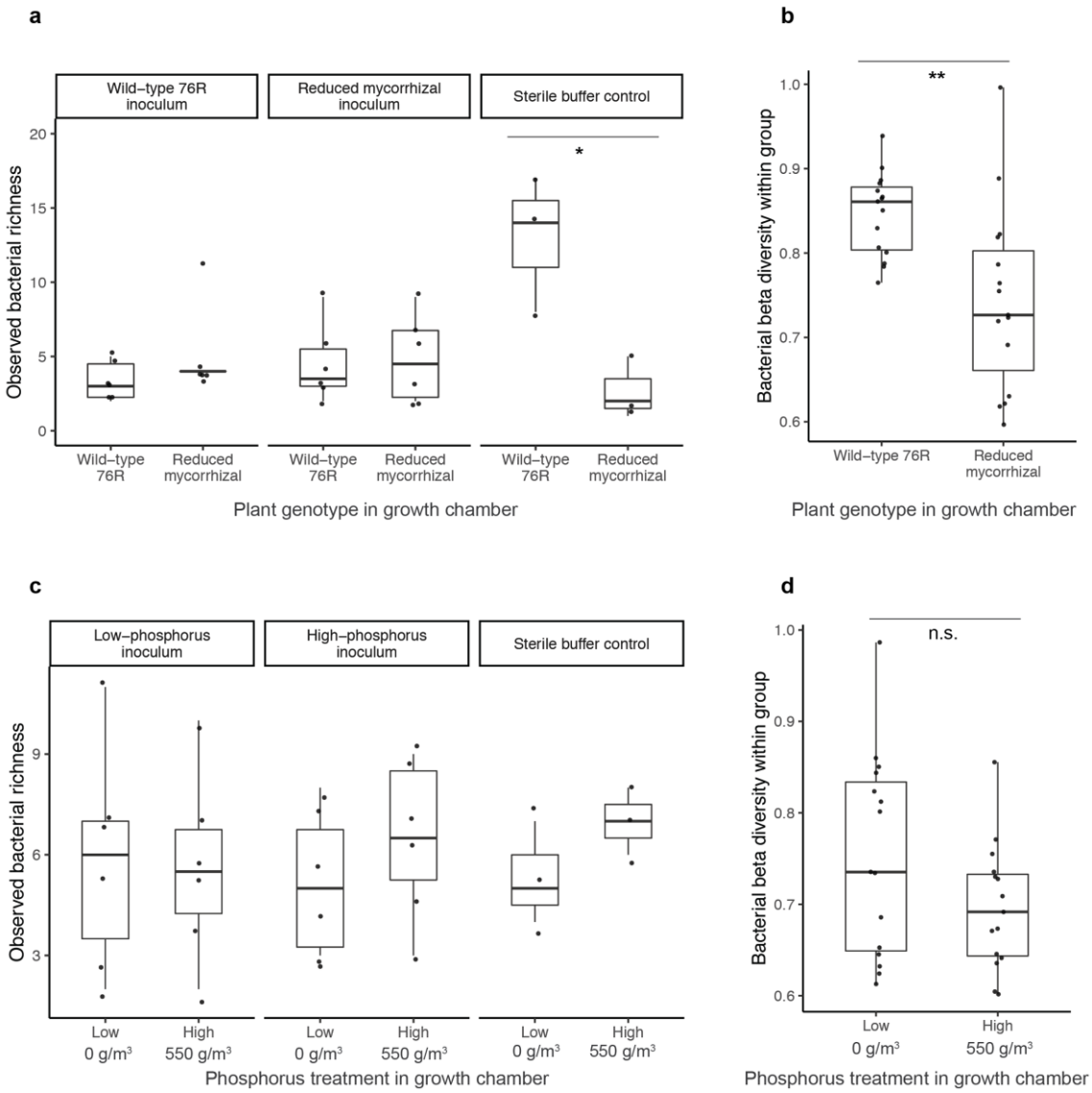


**Figure S12. Growth chamber experiments recapitulate effect of *rmc* genotype, and lack of effect of phosphorus fertilization, on bacterial alpha and beta diversity. a)** Observed bacterial richness in mycorrhizae experiment, as measured by ASV counts after removing chloroplast, mitochondria, and contaminant sequences. Richness values were log-transformed prior to ANOVA to meet normality and homoscedasticity assumptions. **b)** Within-group dispersion of bacterial communities was quantified by generating a Bray-Curtis dissimilarity matrix. Points represent the mean Bray-Curtis dissimilarity between each sample and other samples of the same genotype (76R or reduced mycorrhizal). **c)** Observed bacterial richness in phosphorus experiment, as measured by ASV counts after removing chloroplast, mitochondria, and contaminant sequences. Richness values were log-transformed prior to ANOVA to meet normality assumption. **d)** Within-group dispersion of bacterial communities was quantified by generating a Bray-Curtis dissimilarity matrix. Points represent the mean Bray-Curtis dissimilarity between each sample and other samples within the same treatment group (low, high).

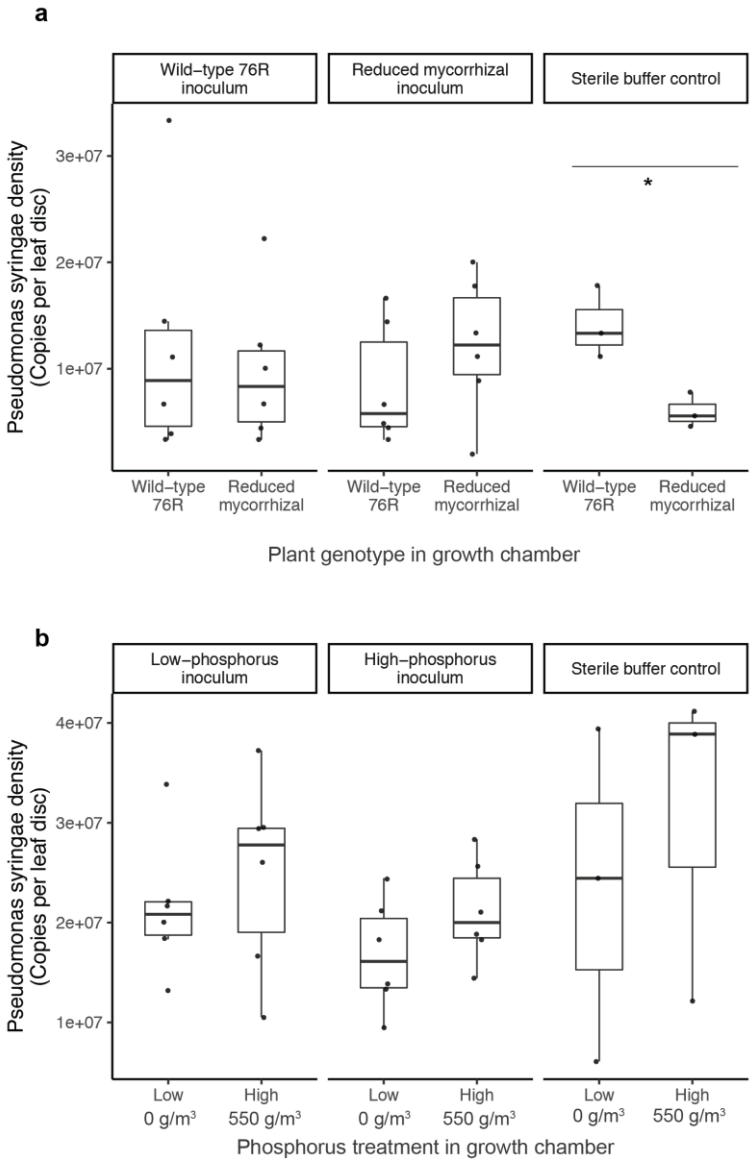


**Figure S13. *Pseudomonas syringae* density on growth chamber plants after experimental infection. a,b)** Colony forming units (CFUs) on leaf discs (6 mm diameter) clipped from leaves experimentally inoculated with *Pseudomonas syringae* pathovar tomato PT23.

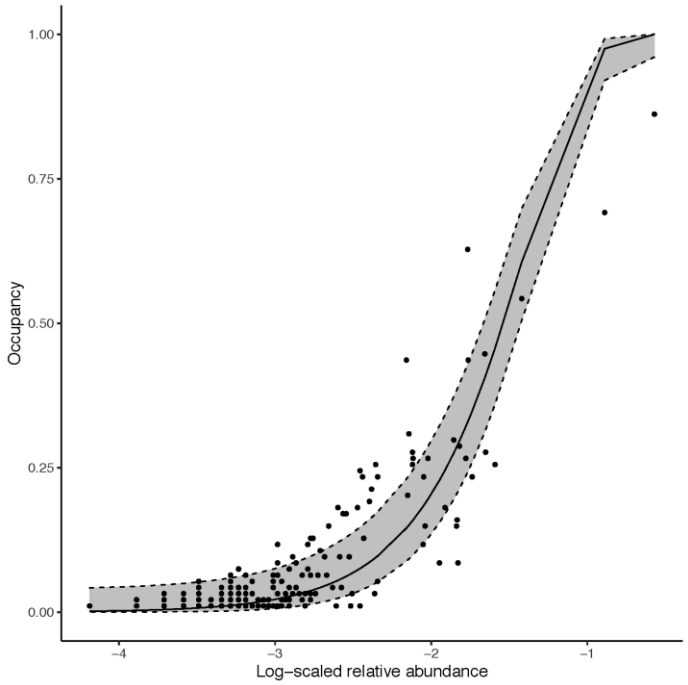


**Figure S14. Occupancy-abundance relationship for bacterial taxa in the field study.** The mean relative abundance of each ASV was plotted against the proportion of plants in which it was detected. The shaded region represents a 95% confidence interval based on the neutral model described by Sloan et al. (270) and implemented in the R package *sncm* by Burns et al. (271).

# 5. The role of phages in microbiome-mediated protection

## 5.1 Introduction

Viruses that infect bacteria, or phages, are abundant and diverse in natural ecosystems. They can be found in all environments that bacteria inhabit and frequently outnumber bacterial cells by 10-100 fold (272–274). Phages play an important ecological role in microbial communities, most notably in nutrient cycling (275). In aquatic environments, for instance, they are responsible for lysing an estimated 10-20% of the bacterial community on a daily basis (276). Because phages tend to specialize on certain bacterial hosts, they can also alter patterns of competition, coexistence, and gene transfer among bacterial species (277–279).

Some phages infect and kill bacteria that are pathogenic to other organisms, such as plants or animals. These phages have long been recognized as an opportunity for managing bacterial pathogens in medicine and agriculture (280). Indeed, mammalian mucosal surfaces are naturally enriched for phages that provide an antimicrobial defense at potential points of entry for pathogens (281,282). Phage-based therapeutics, emerging as an alternative to antibiotics, have been successfully used in a small number of compassionate use cases to treat life-threatening, drug-resistant bacterial infections (283,284). While not yet approved for routine clinical use in most countries, pathogen-targeting phages are considered a promising avenue for managing human, livestock, and crop diseases due to their high specificity and their potential to self-replicate and co-evolve with resistant bacteria (285–288).

While phages that do not directly target bacterial pathogens have received substantially less attention, recent evidence suggests they may also play important roles in susceptibility or resistance to disease (Figure **1**). Many diseases of animals and plants are characterized by altered phage community composition, suggesting that the natural diversity of phages inhabiting these organisms may modulate disease susceptibility (289–291). One possible mechanism by which phages could alter host susceptibility to disease is via a direct interaction between phages and the immune system of the plant or animal host. Phages share some molecular features with mammalian viruses (292), and some have been shown to promote antiviral cytokine production in humans and mice (293,294). A filamentous phage of *Pseudomonas aeruginosa*, Pf, triggered an antiviral pathway that suppressed phagocytosis of bacterial cells, exacerbating the *P. aeruginosa* infection (79). Yet whether phages can interact with or redirect non-mammalian immune systems is not clear.

Another mechanism for phages to influence disease outcomes is by altering the composition of the resident microbiome. Pathogen colonization success is frequently dependent on facilitative or inhibitory interactions with existing bacterial populations (295,296). Phages targeting pathogen-facilitating bacteria are expected to limit disease spread, while phages that target pathogen-inhibiting bacteria are expected to worsen infection severity. In the tomato rhizosphere, variation in the severity of bacterial wilt disease was attributed to the presence of pathogen-inhibiting bacteria and their associated phages. Tomato plants inoculated with these inhibitory bacteria were more resistant to infection by *Ralstonia solanacearum*, but this protective effect vanished in the presence of inhibitor-associated phages (291).

Lastly, phage communities as a whole can maintain bacterial community diversity over time and space by targeting abundant bacterial species. This idea was originally adapted from observations of animal predators and parasites that impose negative frequency-dependent selection on prey or host species (297–299). In microbial communities it is known as the 'kill the winner' hypothesis because any population that reaches sufficiently high density should be followed by a bloom of its specialized phages, which then bring its population size back down and releases nutrients for other, previously rare, bacteria to use (300,301). Several studies in aquatic and terrestrial systems have reported dynamics consistent with the kill-the-winner hypothesis (22,302,303). Of particular relevance here, bacteria from the tomato phyllosphere assembled into more species-rich and more synchronous communities when paired with their phages than when free phages were depleted (22).

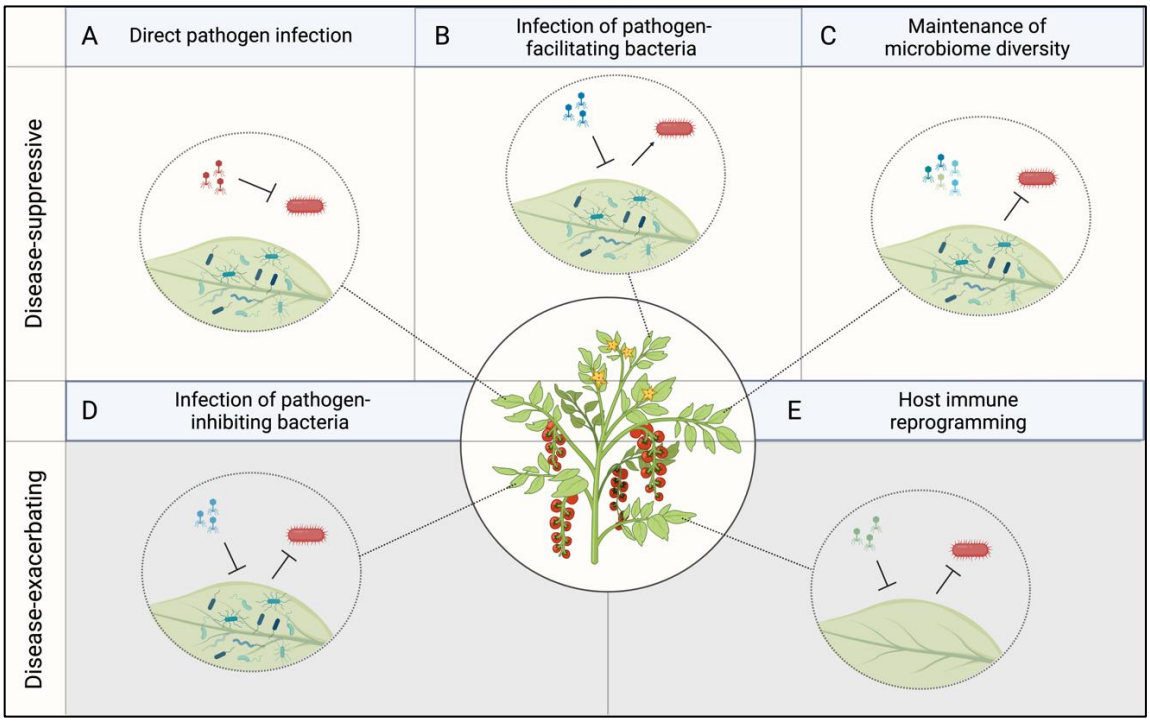


**Figure 1. Mechanisms of phage modulation of pathogen infection.** Phages may suppress disease by **a)** directly reducing pathogen population sizes (283–288), **b)** reducing the population sizes of microbiome members that facilitate pathogen infection, or **c)** maintaining bacterial community diversity and resistance to invasion by preying on abundant bacteria. Phages may facilitate disease by **d)** reducing the population sizes of protective microbiome members (291), or **e)** reprogramming host immunity to trigger an antiviral response and suppress the antibacterial response (currently documented only in mammalian hosts, (79)).

As bacterial community diversity and stability often predicts resistance to pathogen invasion (24,25,304), we hypothesized that phage communities play a role in pathogen defense via community-level regulation of the resident microbiome. We tested this hypothesis using phage community depletion experiments with two different strains of the plant pathogen *Pseudomonas syringae*. *P. syringae* is a generalist bacterial pathogen that infects nearly 200 plant species, including a number of economically important crops such as wheat, barley, soybean, kiwifruit, and tomato (305,306). When we inoculated bacterial communities and

phage communities together onto plants, they were more protective against *P. syringae* pv. tomato than either group was separately. We demonstrated through a series of additional experiments including phage infectivity assays *in vitro*, lipopolysaccharide quantification of the phage filtrate, and reciprocal transplants of phage communities that this effect could not be explained by phage interactions with the plant immune system or by direct effects of phages on *P. syringae* alone. Rather, the protective effect of phages depended on the presence and identity of the bacterial microbiome.

## 5.2 Materials and Methods

*Microbiome sampling from field*

In the first field season (September 2018), leaves were sampled from approximately six-month-old tomato plants at the Student Organic Farm at the University of California, Davis (38°32'20.04" N, 121°44'57.36" W). Leaves were collected from the full range of the height of the plants and placed in a loosely filled bag (35-50 grams of plant material). Bags were transported to the lab and immediately stored at 4°C. Bacteria and phage communities were isolated and frozen within one week of field sampling. These samples were used for the first phage depletion experiment as well as the LPS quantification (Table **1**).

In a subsequent field season (August 2021), leaves were sampled from 16 six-month-old tomato plants at the Student Organic Farm, as well as 6 tomato plants and 6 American black nightshade plants (*Solanum americanum*) at the Vegetable Crops Field at the University of California, Davis (38°32'31.2" N, 121°45'46.8" W). Leaves were transported to the lab on ice, stored at 4°C, and processed within one week of sampling. Of the former group, 10 of these plants were used to generate inocula for the second phage depletion experiment, while the remaining 6 constituted the 'field allopatric' treatment in the local adaptation transplant experiment (Table **1**). Of the latter group, the 6 tomato plants were used to generate inocula for the 'sympatric' and 'neighbor allopatric' treatments, and the 6 American black nightshade plants were used for the 'species allopatric' treatment.

*Isolation of microbial and phage communities*

A buffer solution of 10 mM $MgCl_2$ was added to each bag to cover the leaves, and the Ziploc bags were submerged in a Brandon M5800 sonicating water bath for 10 minutes to gently dislodge microbial cells from the leaf surface. The resulting leaf wash was passed through a coffee filter to remove large plant debris. The leaf wash filtrate was then vacuum filtered through a 0.2 µm membrane to separate cellular microbes (fungi, bacteria) from viral particles.

To release microbial cells, the 0.2 µm filter was transferred to a sterile tube and sonicated in 10 mM $MgCl_2$. Microbial cells were pelleted at 3500 x *g* for 10 minutes, resuspended in 50% glycerol, and stored at -80°C. The filtrate from the 0.2 µm, containing viruses and small molecules, was transferred to an Amicon Ultra-15 filter unit with a 100 kDa molecular weight cutoff. Amicon filters were centrifuged at 4000 x *g* for 25 minutes to isolate and concentrate viruses. The resulting phage fraction was stored at 4°C.

This method of phage isolation and concentration was originally developed to isolate viruses in seawater (307,308) and has been previously adapted to the tomato phyllosphere

(22). It separates the majority of lytic phages from their hosts, but lysogenic phages or lytic phages actively infecting a bacterial cell at the moment of filtration are likely to remain in the bacterial fraction, thus resulting in a "phage-depleted" rather than an entirely phage-free microbial community.

*Phage depletion experiments*

To measure the effect of phage depletion on microbiome-mediated resistance to pathogen colonization, microbial inocula were applied to plant leaves, either with or without their respective phage communities. Briefly, Early Girl tomato seeds (Eden Brothers) were surface sterilized by immersing seeds in 70% ethanol for 1 minute, then swirling seeds in 10 mL of 6% bleach and 10 mL of 0.2% Tween 20 for 20 minutes. Seeds were placed in a petri dish containing 0.8% water agar, then covered and incubated at 21°C in the dark. After germination, plates were maintained in a growth chamber at 24°C and 70% humidity with a 15h day:9h night light cycle. Nine days after planting, seedlings were transferred to pots containing autoclaved potting medium (Profile Porous Ceramic Greens Grade soil amendment, Sierra Pacific Turf Supply). Pots were spatially randomized with respect to treatment for the duration of the experiment.

Three weeks after planting, leaves were sprayed with microbial communities from the field. Microbiome and phage inocula were each standardized to a fixed quantity of plant material from the field so that phage-host ratios in the inocula were the same as those in their natural environment. Inocula were prepared in 4 mL of 10 mM $MgCl_2$, with 0.04 µL of the surfactant Silwet L-77 added to facilitate microbial adhesion to the leaf surface. Leaves were sprayed from all angles using a 15 mL conical tube fitted with a spray cap.

Four weeks after planting (one week after microbiome inoculation), leaves were challenged with *Pseudomonas syringae* pv tomato. Two different strains of *P. syringae* were used in separate experiments: DC3000, a model plant pathogen that infects *Arabidopsis thaliana* as well as tomato plants, and PT23, a closely related pathovar that is more specialized to tomato plants (20). In both cases, an overnight culture of *P. syringae* was pelleted and diluted to an optical density ($OD_{600}$) of 0.0002. The resulting microbial suspension was infiltrated into the abaxial side of the leaf using a blunt-end syringe. At 24 hours post-infection, three hole punches (6-mm diameter) were taken from each leaf. Leaf discs were homogenized in 1 mL 10 mM $MgCl_2$ in a FastPrep-24 5G sample disruption instrument at 4.0 m/s for 40 seconds and stored at -20°C for molecular analysis. Healthy leaves (not challenged with *P. syringae*) were collected, suspended in 10 mM$MgCl_2$, and sonicated, pelleted, and frozen as described above to isolate commensal microbiota.

*Lipopolysaccharide quantification*

The Pierce Chromogenic Endotoxin Quant Kit (ThermoFisher Scientific Cat. #A39553) was used to measure lipopolysaccharide (LPS) concentrations in the phage filtrates. Briefly, amebocyte lysate that binds to LPS was added to samples and incubated at 37°C for 30 minutes. A chromogenic substrate that reacts with the amebocyte proenzyme was added and incubated at 37°C for 6 minutes. Acetic acid was added to stop the reaction, and optical density values were recorded at 405 nm. Absorbance values were adjusted to blanks and LPS concentrations of samples were calculated based on the standard curve.

To assess whether LPS contamination was responsible for the observed effect of phage on disease outcomes *in planta*, the leaves of three-week-old tomato plants were sprayed with either phage communities or varying concentrations of pure LPS from *Escherichia coli.* Leaves were challenged one week after spraying with *P. syringae* and harvested as described above.

*Local adaptation transplant experiment*

Tomato plants were grown and maintained in the growth chamber as described above. The following inocula were applied to three-week-old plants: 1) microbiome only, 2) microbiome with sympatric phages (isolated from the same plant), 3) microbiome with allopatric phages (isolated from a neighboring tomato plant), 4) microbiome with allopatric phages (isolated from a different plant species, American black nightshade, in the same field), and 5) microbiome with allopatric phages (isolated from tomato plants in a different field, approximately 2.3 km away). One week after microbiome inoculation, leaves were challenged with *P. syringae* and harvested as described above.

*Test for direct phage infectivity*

To test whether phage communities contained any phages capable of directly infecting *P. syringae*, co-cultures of *P. syringae* and 100 µL of each phage fraction were incubated in King's B Broth for 24 hours at 28°C. The resulting overnight culture was passed through a 0.2 µm filter to isolate any phages that might have amplified in the presence of *P. syringae*. Next, 200 µL of *P. syringae* overnight culture was mixed with 2 mL of King's B Broth supplemented with 0.6% agar. The soft agar mixture was spread evenly onto petri dishes and allowed to dry, then 30 µL of filtrate from the overnight culture was pipetted on top. Plates were incubated at 28°C and monitored daily for signs of bacterial lysis.

*Quantification of phytopathogen population sizes*

*P. syringae* population sizes on leaves were measured using the Bio-Rad QX200™ Droplet Digital PCR system. Reaction mixtures were prepared using 11 µL Supermix for Probes (no dUTP), 1.1 µL probe (forward 5'- ACTTTAAGTTGGGAGGAAGGG-3'; reverse 5'-ACACAGGAAATTCCACCACCC-3', probe TGCCAGCAGCCGCGG), 5 µL template, and 4.9 µl molecular grade water. Samples were randomized on the plates, with a no-template control in the last well of each column. The following cycling conditions were used for amplification: 95°C for 10 minutes; 40 cycles of the following: (94°C for 30 seconds, 60°C for 1 minute, 72°C for 1 minute); 98°C for 10 minutes; hold at 12°C. Droplet thresholds were set by column based on the fluorescence values in the range of the negative control.

*DNA extraction and sequencing*

In the local adaptation experiment, DNA was extracted from leaves that were not infected by *P. syringae* from the following treatments: microbiomes transplanted in the absence of phages, microbiomes with their sympatric phages, and microbiomes transplanted with phages from a neighboring tomato plant. Extractions were performed using the DNeasy PowerSoil kit in two batches, which were random with respect to treatment and included in all statistical models. Libraries were prepared by amplifying the V4 region of the 16S rRNA gene.

Libraries were amplified, cleaned, and sequenced alongside DNA extraction controls and PCR controls on the Illumina MiSeq platform at Microbiome Insights (Vancouver, BC, CAN).

Reads were analyzed using the recommended DADA2 workflow (Callahan et al. 2016) to infer amplicon sequencing variants. Taxonomy was assigned using the SILVA and UNITE databases (Quast et al. 2013; Kõljalg et al. 2005). Because many ITS sequences could not be classified at the kingdom level by UNITE, the hidden Markov model classifier ITSx was used to further delineate ITS sequences and remove non-fungal sequences (Bengtsson-Palme et al. 2013). 16S variants were filtered to remove the two most abundant ASVs, which corresponded to the chloroplast and the mitochondria sequences, respectively.

## 5.3 Results

*Phages contribute directly and indirectly to microbiome-mediated protection*

To assess the role of natural phage diversity in resistance to pathogen infection, we sampled epiphytic microbial communities from tomato plants at the Student Organic Farm at the University of California, Davis. We used a series of membrane filtration and concentration steps to separate cellular microbes from their associated phages. We transplanted microbial communities, with or without their respective phages, onto juvenile tomato plants which we subsequently challenged with the bacterial pathogen *Pseudomonas syringae* (see Table 1 for a summary of experiments performed). We measured *P. syringae* population sizes within leaf tissue after 24 hours, as this metric can be accurately quantified with droplet digital PCR (310) and correlates with disease epidemiology and plant susceptibility to frost damage (311).

**Table 1. Summary of experiments performed.**

| Experiment | *P. syringae* strain | Treatments | Figure(s) |
|---|---|---|---|
| Phage depletion experiment 1 | PT-23 | Microbiome, microbiome + phages, phages | 2 |
| LPS quantification | PT-23 | 0.3, 0.6, 1.3, 2.5, 5 EU pure *E. coli* LPS | S1 |
| Phage depletion experiment 2 | DC3000 | Microbiome, microbiome + phages, phages | 3 |
| Local adaptation transplant experiment | DC3000 | Microbiome, microbiome + phages, microbiome + phages from neighboring plant, microbiome + phages from different plant species, microbiome + phages from different field | 4, 5 |

In the first phage depletion experiment, the *P. syringae* colonization was significantly reduced in plants treated with the 'microbiome + phages' inocula ($t = 2.11$, $df = 17$, $p = 0.0496$, Figure **2**). Neither the 'microbiome only' or the 'phages only' components were individually protective against *P. syringae* on average, suggesting that this effect was generally contingent on interactions between the phages and their hosts. However, *P. syringae* growth was unusually low in one of the phage-only treatments compared to the others. We hypothesized that this phage community might by chance have contained phages capable of directly infecting *P. syringae*. To test this hypothesis, we co-cultured phage communities with *P. syringae* overnight to amplify any infective phages if they were present, then measured the effect of the

co-culture filtrate on *P. syringae* growth *in vitro*. The lower outlier community in the plant experiment (site F18.5) was the only one to form plaques on agar plates (Figure **2b,c**).

Of note, the significance of the 'microbiome + phages" treatment did not change when the data were reanalyzed to exclude bacteria and phage communities from site F18.5 ($t = 2.73$, $df = 14$, $p = 0.016$), indicating that the protective effect was not solely driven by a direct effect of a single phage community.

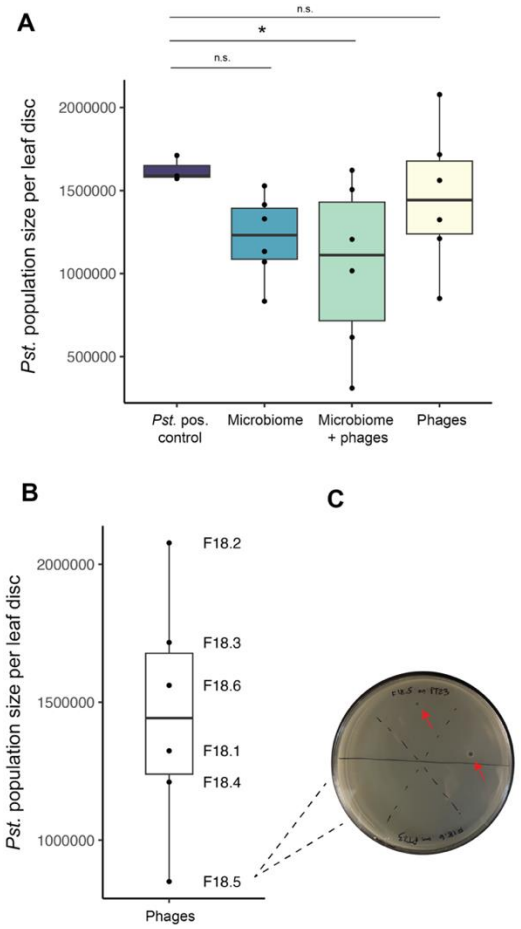


**Figure 2. Microbiome and phage transplant from first field season. a)** Population sizes of *Pseudomonas syringae* pv. tomato strain PT23, 24 hours after blunt-end syringe inoculation into four-week-old tomato plants. Transplant of microbiome and phage communities reduce PT-23 colonization together, but not separately. **b)** Population sizes of PT23 on plants transplanted only with phage communities. **c)** Plaque assay in which phage communities were co-cultured overnight with PT23, filtered through a 0.2 µm membrane, and spotted onto a lawn of PT23 to assess lytic activity.

Ultrafiltration is the most cost-effective method of phage concentration yet available and is commonly used in phage-based industrial applications, but it has the side effect of concentrating molecules larger than the membrane size such as bacterial lipopolysaccharide (LPS) (312). To exclude the possibility that LPS concentration could have triggered a plant immune response, we quantified LPS in the phage filtrates. LPS concentrations in our study ranged from 1-3.5 endotoxin units per milliliter (EU/mL), which fall on the low end of reported LPS levels of phage preparations in other studies (312–314). We next sprayed tomato plants

with pure bacterial LPS in concentrations ranging from 0.3-5 EU/mL to capture the range of concentrations observed in our samples. We challenged the leaves with *P. syringae* and harvested leaves as above. We observed a dose-dependent response: exposure to higher concentrations of LPS was associated with lower colonization of *P. syringae*, suggesting that LPS exposure did indeed trigger plant immunity ($t = 3.99$, $df = 3$, $p = 0.028$; Figure **S1a**), though this appeared to be driven by a large protective effect of the 5 EU/mL dose, with little or no variation among any of the lower doses. LPS concentrations in our phage communities were well below 5 EU/mL, and there was no relationship between LPS content and plant colonization of *P. syringae* in plants treated with phage communities ($t = 0.895$, $df = 3$, $p = 0.436$, Figure **S1b**). This observation again suggested that phages enhanced protection through interactions with their hosts rather than through direct inhibition.

To validate and further generalize the results of the first experiment, we collected tomato leaves in a subsequent field season and repeated the phage depletion process. We sprayed tomato plants with the microbial communities and challenged the leaves with a different *P. syringae* strain, the model plant pathogen DC3000. As before, the *P. syringae* colonization was significantly reduced in plants treated with the 'microbiome + phages' inocula ($t = 2.81$, $df = 35$, $p = 0.008$), while neither component was individually protective (Figure **3a**).

Two phage communities contained phages capable of infecting *P. syringae* (Figure **3b,c**). As before, the effect of the 'microbiome + phages" inocula remained significant when these field sources were excluded from analysis ($t = 2.31$, $df = 35$, $p = 0.029$), indicating that direct infection of *P. syringae* by phage communities was not sufficient to explain the observed pattern.

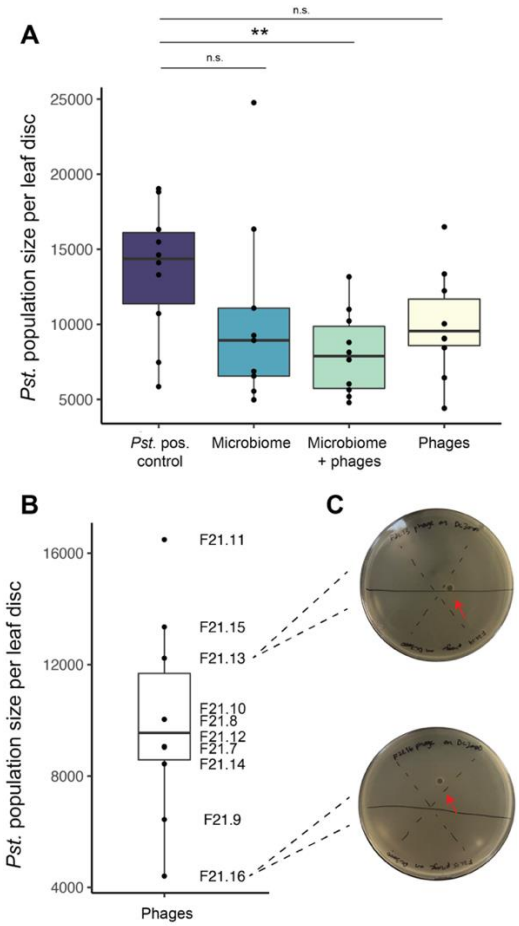


**Figure 3. Microbiome and phage transplant from second field season. a)** Population sizes of *Pseudomonas syringae* pv. tomato strain DC3000, 24 hours after blunt-end syringe inoculation into four-week-old tomato plants. Transplant of microbiome and phage communities reduce DC3000 colonization together, but not separately. **b)** Population sizes of DC3000 on plants transplanted only with phage communities. **c)** Plaque assay in which phage communities were co-cultured overnight with DC3000, filtered through a 0.2 µm membrane, and spotted onto a lawn of DC3000 to assess lytic activity.

*Local adaptation of phages to bacterial hosts*

Next, we designed a reciprocal transplant experiment in which bacterial communities were co-inoculated onto plants with either their sympatric phage communities or other phage communities of varying degrees of allopatry: isolated from a neighboring tomato plant, from a neighboring plant of a different species (American black nightshade), or from tomato plants located in a different field. The purpose of this experiment was twofold. First, it served as an additional measure to exclude the possibility that the protective effect was driven by direct effects of phages or any other components of the phage filtrate on the pathogen or plant immune system. Since phage-bacteria interactions are typically highly specialized (278), if phage communities enhance protection indirectly through interactions with their bacterial hosts, this effect should depend on the origin of the phages and bacteria. The second goal of this experiment was to provide insight into the ecological context of the observed effect. For example, attenuation of the protective effect of phages at increasing levels of allopatry might

indicate that most bacteria are not susceptible to phages from other plant species or at sufficient physical distances.

We found that bacteria paired with phages from neighboring tomato plants were consistently more protective against *P. syringae* than bacteria paired with phages from their own plant (paired t-test, t = 2.82, p = 0.037, Figure **4a**), with one exception. Unlike the other five communities, the bacterial community 'sym5' was more protective when paired with its sympatric phages than with an allopatric phage community (Figure **4b**). We noticed, however, that the 'sym5' phage community was associated with very low *P. syringae* colonization regardless of which bacterial community it was paired with (Figure **4c**). Based on these observations, we hypothesized that 'sym5' contained a *P. syringae*-targeting phage. Indeed, the phage filtrate formed plaques on a bacterial lawn of *P. syringae,* as did "sym4" (Figure **4d**). The difference between phages from neighboring plants and phages from the same plant remained significant when these two field sources were excluded from analysis (paired t-test, t = 3.80, p = 0.032).

For the two more distant forms of allopatry (phages from a different plant species and phages from plants in a different field), there was no difference in protectiveness between sympatric and allopatric phages. We therefore focused the remainder of the analyses on differences between bacteria paired with phages from the same plant and bacteria paired with phages from neighboring tomato plants.

We considered two possible reasons that bacteria would be more resistant to *P. syringae* when paired with allopatric phages than with sympatric phages. Bacteria may coevolve with their sympatric phages closely enough to have evolved some extent of resistance, while remaining susceptible to phages on neighboring plants that they encounter less often. Alternatively, bacteria may be *less* resistant to sympatric phages, to the extent that their abundances are greatly reduced in their presence, reducing their capacity to resist *P. syringae* colonization. To distinguish between these competing hypotheses and further explore the effects of phages on bacterial communities, we sought to characterize the bacterial communities from healthy leaves on the same plants (i.e., not challenged with *P. syringae*). We first verified that these leaves were free from *P. syringae* contamination using droplet digital PCR. The assay detected 0-15 copies of the *Pseudomonas* sequence per 6-mm leaf disc (in comparison to ~10,000 per leaf disc in infected leaves), comparable to baseline levels of *Pseudomonas* probe activity in leaves from plants that were never challenged with *P. syringae* at all (Figure **S2**). We then sequenced the 16S V4 amplicon of communities from the 'microbiome only' transplant, the 'microbiome + sympatric phages' transplant, and the 'microbiome + phages from neighboring plant' transplant.

When transplanted with phages from their own plant, the bacterial communities that established were more diverse than when transplanted alone (t = 2.61, df = 15, p = 0.0195, Figure **5a**). The community compositions they reached after assembly were also more distinct from each other than when they were transplanted alone (i.e. phage-depleted; t = 2.26, df = 15, p = 0.039, Figure **5b**). In contrast, the allopatric phages did not significantly alter alpha diversity or heterogeneity among communities compared to bacteria transplanted alone. Finally, bacteria transplanted with phages from their own plant assembled communities that were more distinct from the 'microbiome only' control than bacteria transplanted with phages from neighboring plants (Figure **5c**).

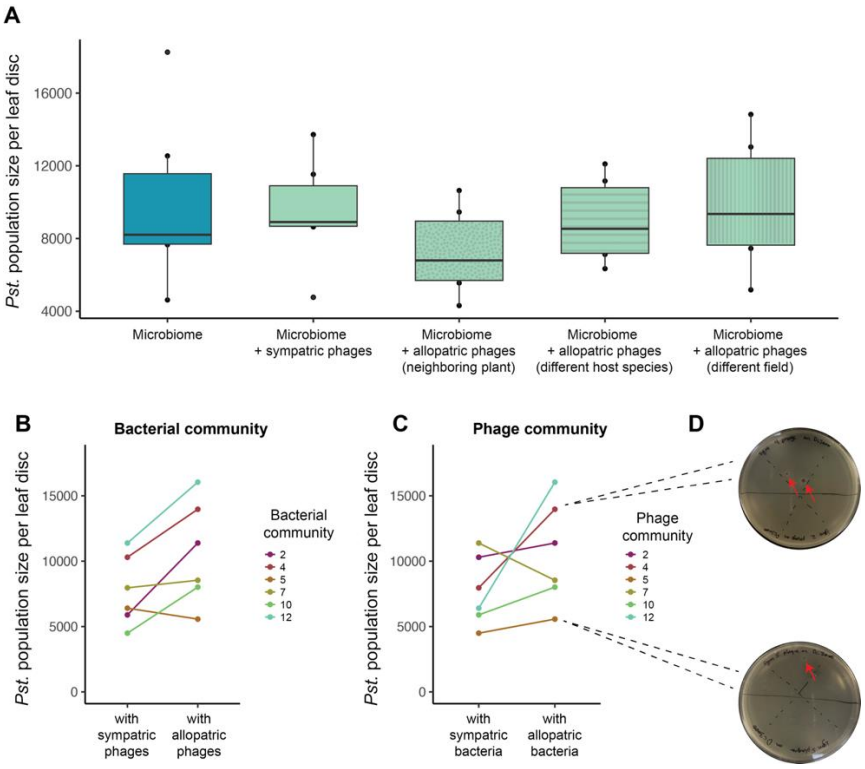


**Figure 4. Effect of phage transplant is locally specific. a)** Population sizes of *Pseudomonas syringae* pv. tomato strain DC3000, 24 hours after blunt-end syringe inoculation into four-week-old tomato plants. **b)** DC3000 population sizes on plants colored by the identity of their source bacterial community. **c)** DC3000 population sizes on plants colored by the identity of their source phage community. **d)** Plaque assay in which phage communities were co-cultured overnight with DC3000, filtered through a 0.2 µm membrane, and spotted onto a lawn of DC3000 to assess lytic activity.

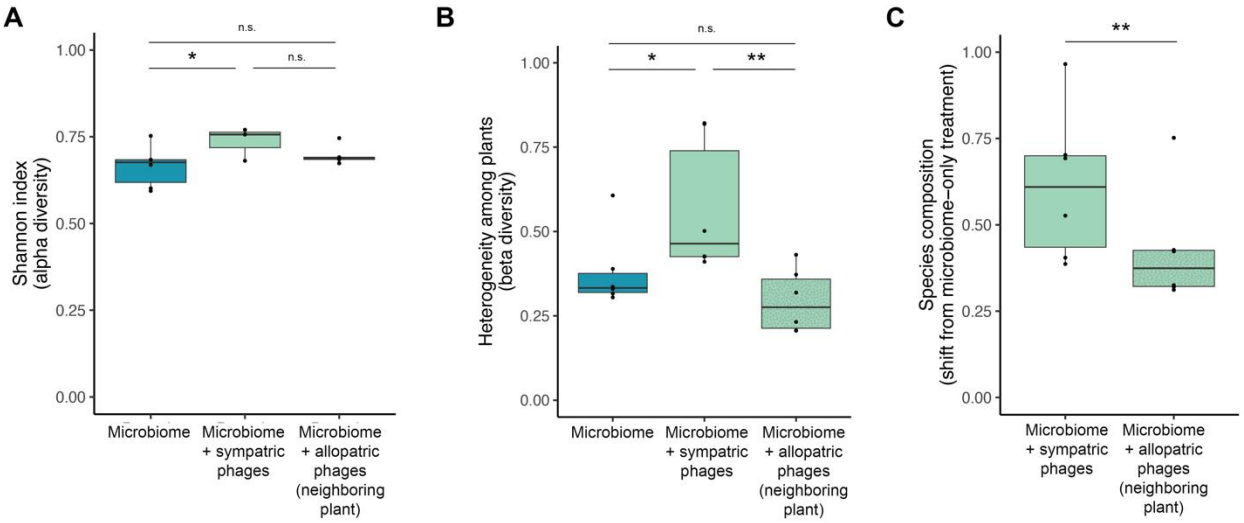


**Figure 5: Amplicon sequencing comparison of sympatric and allopatric phages. a)** Shannon diversity of sequenced bacteria after transplanted alone, with sympatric phages, or with phages from a neighboring plant. **b)** Average

Bray-Curtis distance among plants from the same treatment (bacteria transplanted alone, with sympatric phages, or with phages from a neighboring plant). **c)** Average shift in Bray-Curtis distance from the 'microbiome only' treatment, indicating turnover in species composition.

## 5.4 Discussion

Bacteriophages are diverse and abundant in a variety of habitats and play important roles in the ecology and evolution of bacterial communities (275–277,279). Yet in the context of health and disease, natural phage diversity has largely been overlooked in favor of specific phage strains that target pathogenic bacteria (285,286). Many animal and plant diseases are characterized by altered communities of phages that do not directly target the pathogen involved (289–291). Phages may modulate disease risk by altering the diversity of the resident microbiome and/or by disproportionally reducing the abundances of pathogen-facilitating or pathogen-inhibiting bacterial species. To test these possibilities, we conducted a series of microbiome transplant experiments. We separated microbial and viral communities from leaves collected in the field using size-selective filtration (22,291), then transplanted microbiomes onto a new set of plants in either the absence or presence of their associated phages.

Transplanting microbiomes with their associated phages reduced the subsequent population sizes attained by *P. syringae*, a reflection of infection severity (311). This effect persisted across independent field sampling seasons and against two different strains of *P. syringae*. Although we isolated several *P. syringae*-targeting phages from the field, direct inhibition by individual phages (or other small molecules in the phage filtrate) could not explain the overall effect of transplanting the phage communities, which generally depended on the presence and identity of the bacterial microbiome.

Some of the phage communities that produced plaques on *P. syringae* were associated with unusually low *P. syringae* growth in the plant experiments (e.g., F18.5, F21.16, and sym5), suggesting that they may have reduced *P. syringae* growth via direct infection, though the overall effect remained when these field sites were excluded from analysis. Other phage communities produced plaques *in vitro* but were not notably protective *in planta* (F21.13 and sym4). Our results contrast with a recent report on bacterial wilt resistance in the tomato rhizosphere, where the strongest predictor of disease resistance was the abundance of phages that directly targeted the causative pathogen (291). Several other studies have noted differences in phage ecology between the rhizosphere and the phyllosphere. Phages targeting the pathogen *Erwinia amylovora* can be readily isolated from soil during times of infection, but are often harder to find in the leaves (315,316). Similarly, lytic activity of the phage FRS on *P. syrinage* was low in the tomato phyllosphere despite high rates of lysis *in vitro* (317). The phyllosphere presents a challenging environment to phages due to intense UV exposure and desiccation (180), which may explain why pathogen-targeting phages were not a major contributor to disease resistance in this study.

We next reasoned that if the protective effect of phages depended on specialized interaction with their bacterial hosts, then the effect should vary when host-phage pairs were disrupted. We transplanted microbiomes onto tomato plants either with sympatric phages that were isolated with them, phages from neighboring tomato plants, phages from neighboring American black nightshade plants, or phages from tomato plants growing in a separate field

about 2.3 km away. We observed the strongest protection when bacteria were paired with phages from neighboring plants, as compared to sympatric phages or any of the more distant levels of allopatry.

Two mechanisms might explain the higher effectiveness of allopatric phages. The first scenario assumes that allopatric phages are on average more infective on bacteria than sympatric phages, and therefore have a stronger effect on microbiome composition and diversity. This could occur if bacteria and phages may disperse among neighboring plants often enough for some host-phage pairs to occur, yet too infrequently for bacteria to evolve resistance (318). However, such a pattern would conflict with the general consensus that phages in nature are "ahead" of bacteria in coevolution; in other words, sympatric phages are typically more infective than allopatric phages (319–321). The second explanation assumes that sympatric phages are *more* infective than allopatric phages, reducing bacterial population sizes to the point that they also reduce the protective effect. For example, certain tomato rhizosphere phages target protective bacteria and indirectly exacerbate bacterial wilt disease (291). And when transplanted as a whole, phage communities reduced bacterial community richness in duckweed plants (322).

Upon sequencing the bacterial communities, we found that sympatric phages consistently altered bacterial diversity, heterogeneity, community composition, and total bacterial population sizes more than allopatric phages. These data are more consistent with the second hypothesis – that sympatric phages are generally well-adapted to their hosts – and suggest that local phage communities can reduce the population sizes of protective bacteria. Due to the design of the phage depletion and local adaptation experiments, we had the opportunity to observe the same microbiomes assemble multiple times under different treatments. While microbiomes from different field sources converged towards more similar compositions in the growth chamber, they retained a signature of their source community. Origin in the field was a stronger predictor of eventual community composition than any of the phage treatments. Communities from different field sources also varied systematically in their resistance to *P. syringae* infection. While others have observed inter-host variation in microbiome-mediated resistance to pathogens, the mechanisms are not well-defined, with suspected causes ranging from the strength of resource competition to bile acid metabolism (48,102). Our study did not detect any obvious correlates of diversity or composition to pathogen resistance, though it may be underpowered to do so. Future work should elaborate the extent and causes of natural variation in microbiome resistance to infection.

Our data point to an indirect yet important role for phage communities in plant defense against the pathogen *P. syringae*. This phenomenon was not attributable to direct phage-plant interactions or to other bacterial byproducts in the phage filtrate. Nor could it be explained solely by direct phage infection of *P. syringae*; while this occasionally occurred, the protective role of phages was largely dependent on the presence of the microbiome. Subsequent reciprocal transplants of sympatric and allopatric phages revealed that this effect was strongest with phages from a neighboring plant, even though they altered bacterial community composition less than phages isolated from the same plant. Together, this suggests an emerging picture in which the role of phages in defense is a balance between two competing processes: maintaining community diversity (22) and reducing the population sizes of protective bacteria (291). As the inocula in this study were standardized to the same bacteria-

phage ratios as occurred in nature, an interesting future test of the hypotheses developed in this paper would be to conduct microbiome and phage transplant experiments with varying dilution factors of each component (323,324). Such experiments may identify phage community profiles that are optimal for maintaining an abundant and diverse microbiome.

## 5.5 Appendix

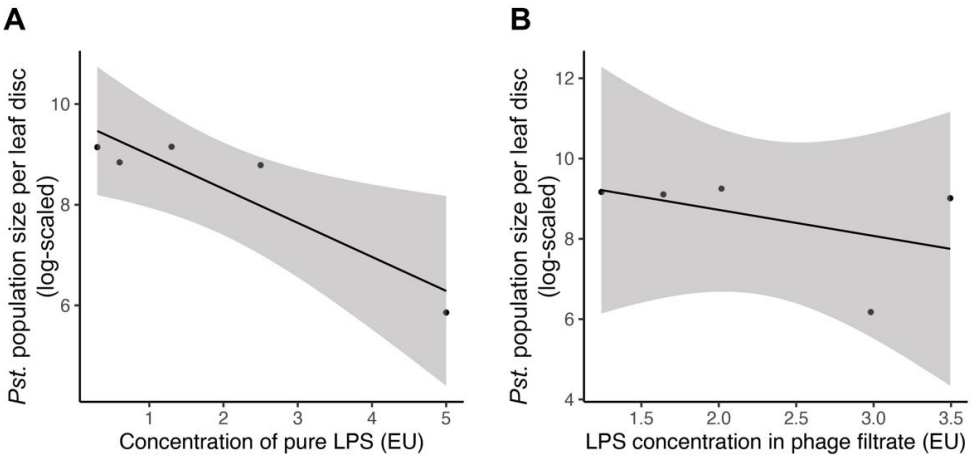


**Figure S1. Protectiveness of phages is not driven by LPS concentration. a)** Population sizes of *Pseudomonas syringae* pv. tomato strain PT23, 24 hours after blunt-end syringe inoculation into four-week-old tomato plants. Plants had been pre-treated with varying concentrations of pure *E. coli* lipopolysaccharide (LPS). **b)** Population sizes of PT23 on plants pre-treated with phages that had been measured for LPS contamination. Values are expressed in EU (endotoxin units per milliliter). One EU is approximately 0.1 ng endotoxin.

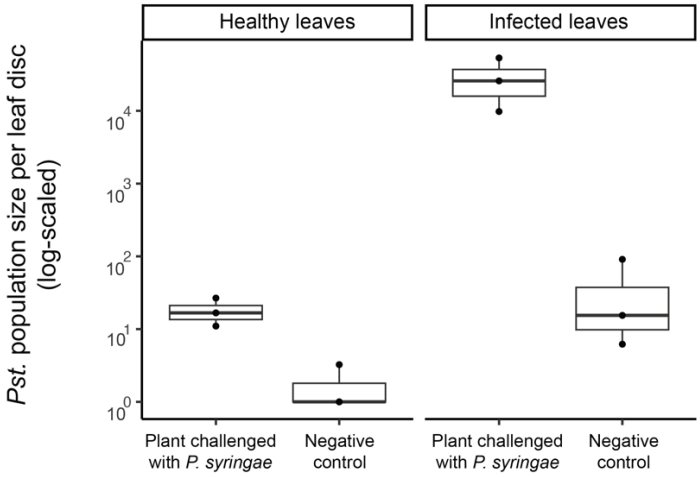


**Figure S2. *Pseudomonas* abundance in healthy and infected leaves.** Population sizes of *P. syringae* were 100-1000 times higher in infected leaves than in healthy leaves.

# 6. Historical contingency in compensatory adaptation

Parts of this chapter have been adapted from the following with permission:
Debray, R., De Luna, N., Koskella, B. 2022. Historical contingency drives compensatory evolution and rare reversal of phage resistance. *Molecular Biology and Evolution* 39(9), msac182.

## 6.1 Introduction

Pathogens are ubiquitous and exert strong selection on their hosts to evade infection (325,326). These selection pressures are constantly in flux, and defense-related traits are often detrimental when pathogens are not present at high levels (327,328). The loss of costly resistance under relaxed selection has been the focus of a plethora of theoretical and empirical studies, in large part because it helps to explain the observed coexistence of resistant and sensitive host types in many natural populations (23,329–331). Whether host populations readily regress to susceptibility after escape from pathogen pressure or retain a signature of their coevolutionary history will depend on several factors, including the environmental conditions and the strength of selection. For example, resistance may persist if it is not costly to maintain; or if compensatory mutations reduce the fitness costs without reversing the trait itself, as is often observed in drug-resistant bacteria (332,333). In other cases, even when reversion to sensitivity would be favorable, it may not be possible if the host population has since acquired other mutations that would be deleterious on the wild-type genetic background (334).

In a more general sense, any mutation that affects an organism's phenotype and is selected for (even temporarily) can alter the selection acting on subsequent mutations, and can therefore shape the evolutionary trajectory of the population. For example, garter snakes that prey on tetrodotoxin-bearing newts have evolved high levels of toxin resistance, but only within lineages that already carried a prior substitution – an ancient modification to a sodium channel that took place long before the newts arose (5). In a laboratory evolution experiment with *Escherichia coli*, different substitutions in a DNA topoisomerase enzyme were shown to have different consequences for the subsequent accumulation of other beneficial mutations. In fact, this second-order selection for evolvability was more important than the initial effects of the substitutions themselves in determining which lineage prevailed in the long term (335). Historical contingencies such as these can make it particularly challenging to interpret patterns of genetic divergence across populations or predict the lasting consequences of short-term coevolutionary interactions.

To explore how previous selection by phages can alter future bacterial evolution, we tracked phage resistance over time in experimental evolution populations of the bacterium *Pseudomonas syringae*. Bacteria and phages are a tractable model system frequently used for studying coevolution in the laboratory (336,337). Phages initiate infection by recognizing and binding to proteins on the surfaces of bacterial cells. Bacteria can evade phages by altering or deleting phage receptors, but in doing so, often compromise other fitness-related traits such as nutrient uptake, adhesion, and virulence (338,339). In these cases, as resistance spreads in a population and phage densities decrease, resistance is predicted to be lost over time as a result of relaxed selection (340). Laboratory fluctuation assays show that the rates of spontaneous

genetic reversion from resistance to susceptibility can be high (341), suggesting that phage sensitivity can (re)emerge within resistant populations.

Despite these predicted dynamics, studies of natural bacterial communities sometimes find that bacteria remain resistant to phages that they co-existed with many months or even years in the past (30,31,342). In cases where laboratory studies propagated resistant bacteria for many generations in the absence of phages, whether phage sensitivity re-emerged has remained inconsistent and difficult to explain (343,344). For example, over 45,000 generations of relaxed selection did not reduce the observed resistance of *Escherichia coli* to T6 phage (343). In contrast, some experimental populations of *Prochlorococcus* became less resistant in the absence of phage, but these changes were difficult to explain in terms of compensatory adaptation, as they often occurred independently of fitness gains (344).

On the basis of these observations, we hypothesized that bacteria can access many different genetic pathways to phage resistance, each with different implications for the subsequent evolutionary potential of the bacteria, including whether they compensate for fitness costs by re-evolving phage sensitivity. To test this idea, we isolated and sequenced *P. syringae* colonies that had evolved resistance across a panel of lytic phages and measured the fitness costs of each resistance mutation. We then used each resistant strain to seed a different population that was experimentally evolved in the absence of phages. Through a series of laboratory evolution experiments, we demonstrate that phage resistance can either be reversible or entrenched depending on the initial genetic path to resistance.

## 6.2 Materials and Methods

*Selection and validation of phage resistance*

*Pseudomonas syringae* pv. tomato DC3000 was obtained from Gail Preston at Oxford. The phage strains FMS, VCM, M5.1, QAC, and SNK were obtained from OmniLytics, Inc., and are considered potential biocontrol agents for plant-pathogenic *Pseudomonas* bacteria. Phage-resistant colonies were selected through soft agar overlays. Briefly, we amplified *P. syringae* in King's B Medium overnight, then mixed bacterial cells with soft agar (King's Broth supplemented with 0.6% agar). The mixture was spread evenly on petri dishes and allowed to dry. Droplets of high titer phage were pipetted on top. Plates were incubated for 48 hours at 28°C. Large clearing zones (plaques) appeared and expanded from the phage droplet sites, and resistant colonies were picked from plaques.

To verify resistance, each bacterial colony was streaked on hard agar plates (King's B Medium supplemented with 1.2% agar), across a high titer line of the phage strain it was isolated on (345). Ancestral DC3000 was also streaked against all phages as a phage-sensitive negative control. Colonies were verified as phage-resistant if bacterial growth was uninterrupted at the phage line (Figure **S1**).

To ensure that colonies were entirely free of phage particles prior to experimental evolution, each colony was streaked on hard agar, and cells were sampled at the end of the streak to seed an overnight culture. The next day, the overnight culture was passed through a 0.22 µm filter. The filtrate was spotted on a mixture of ancestral DC3000 and soft agar, as described above. Plates were incubated for 48 hours at 28°C and checked for plaques. This

entire process was repeated twice, at which point none of the filtrates produced phage plaques.

*Experimental evolution in the absence of phage*

Phage-resistant colonies were passaged in King's Broth media in cell culture plates. Six phage-sensitive populations founded from ancestral DC3000 were passaged alongside phage-resistant colonies to serve as controls for adaptation to the lab environment, and each transfer also included a media-only negative control. Every 3 days, 75 uL of each population (approximately $10^6$ cells) were transferred to a new well with 4 mL of media. At every other transfer (every 6 days), a subset of each population was combined with a 50:50 mixture of King's Broth and glycerol for storage at –80°C. The experiment lasted for 36 days (12 transfers), at which point there were no longer any detectable fitness differences between populations founded from phage-resistant colonies and populations founded from ancestral DC3000. According to previous work, the average doubling time of *Pseudomonas syringae* at this temperature is approximately 1.27 hours (346).

*Resistance and fitness measurements*

On days 12, 24, and 36 of experimental evolution, 100 uL from each culture was sampled, serially diluted, and plated on hard agar. From the dilution level at which individual colonies were visible, 96 colonies were picked from each population. Each colony was streaked against the phage strain that the population was originally isolated on. After two days of incubation at 28°C, colony phenotypes were scored as resistant (uninterrupted bacterial growth across the plate), moderate (partly interrupted bacterial growth), or sensitive (fully interrupted bacterial growth at the intersection with the phage line).

It is possible that populations could contain phage-sensitive cells, yet appear partially resistant on agar due to habitat structure and/or biofilm growth (347,348). We took two measures to combat this possibility. First, while phage-sensitive sub-populations may be able to survive among a larger population of resistant cells, separately streaking 96 colonies from each population should ensure that colonies of entirely sensitive cells are visibly impacted by phages, even in a structured environment. Second, in any populations with colonies scored as moderate or sensitive on agar, resistance was assessed in greater quantitative resolution by measuring bacterial population growth in liquid culture in the presence and absence of phages (Figure **S2**).

To measure population growth rates over the course of experimental evolution, time series growth data was collected using a Molecular Devices VersaMax Microplate Reader. An overnight culture of each population was initially diluted to 0.001 $OD_{600}$ in 200 mL King's Broth. Colonies were randomized with respect to spatial layout, and media-only wells were included as negative controls. The plate was incubated at 28°C for 40 hours with continuous shaking, with optical density readings taken at 600 nm every 5 minutes. These readings were used to fit a logistic growth model with the R package *growthrates* and estimate the intrinsic growth rate $\mu_{max}$ and the final population size $OD_{max}$. To express these values as a proportion of wild-type fitness while controlling for technical effects, the fitted values were extracted from a model that included the day of experimental evolution, the population type (phage-resistant colony or phage-sensitive control), and the location of the well within the plate. While $\mu_{max}$ and $OD_{max}$ were modestly correlated across populations ($r = 0.689$, $p < 0.001$, Figure **S3**), the final

population sizes of resistant populations were close to that of the phage-sensitive ancestor, resulting in only marginally detectable costs of resistance for $OD_{max}$ (one-sample t-test, t = –1.382, *p*= 0.091). This suggests that phage resistance is the most costly during periods of exponential growth; thus, for subsequent analyses we focused on variation in $\mu_{max}$ over time.

*Whole-genome sequencing*

To identify mutations contributing to phage resistance, bacterial DNA was extracted from each phage-resistant clone using the DNeasy Blood and Tissue Kit. Concentrations were measured using a Qubit 3.0 Fluorometer, and samples were concentrated if necessary using an ethanol precipitation to obtain a minimum of 10 ng/uL of DNA per sample. DNA was sequenced at a depth of 300 Mb (estimated coverage of 45.9x) on the Illumina NextSeq 2000 platform at the Microbial Genome Sequencing Center (Pittsburgh, PA, USA). To identify and track the frequencies of mutations that arose during experimental evolution, bacterial DNA was extracted, quantified, and concentrated as described above from populations at day 6 and day 36 of the experiment. DNA was sequenced at a depth of 625 Mb (estimated coverage of 95.6x) as described above.

Paired-end reads were filtered and trimmed using Trimmomatic (349). Reads shorter than 25 base pairs were discarded, and reads with an average quality score below 20 within a 4-base pair sliding window were discarded. Pairs of reads that both passed filtering (>95% of total reads per sample) were retained. Reads were mapped to the *Pseudomonas syringae* pv. tomato DC3000 genome (BioSample accession SAMN02604017 from the Pseudomonas Genome Database) and variants were identified using *breseq* (185,186), a pipeline for identifying genetic variation within microbial populations. Any sites at which the genome of the ancestral strain differed from the reference genome were removed from subsequent analyses. To avoid false positive calls from repetitive regions, mutations were filtered to exclude regions of high polymorphism (five or more mutations in a 50-base pair sliding window within a population at a single time-point).

*Analysis of genomic parallelism*

To quantify the genome-wide parallelism of experimentally evolved populations, a matrix was generated of all genes with newly acquired mutations in each population (i.e. those not already fixed at day 0 of the experiment). The Sørenson-Dice similarity coefficient was calculated for each pair of populations as follows, where $G_1$ represents genes with newly acquired mutations in population 1, and $G_2$ represents genes with newly acquired mutations in population 2.

$$S = \frac{2\,|G_1 \cap G_2|}{|G_1| + |G_2|}$$

Mutations were included if they appeared at any population frequency (they were not required to be fixed), but synonymous and intergenic mutations were excluded. The analysis focused therefore on nonsynonymous point mutations or indels within coding regions.

Following Card et al. (350), the distribution of pairwise Sørenson-Dice values was analyzed using a randomization test. The labels annotating pairs of populations as having the same or different resistance genes were shuffled, and the mean difference was calculated between pairs with the same resistance gene and pairs with different resistance genes. This

process was repeated 10,000 times to generate a null distribution. The true difference in means in the observed data was compared to the null distribution, and the observed difference was considered significant if it was more extreme than the upper 5% of permuted values.

*Replay of experimental evolution*

To assess the repeatability of phage resistance outcomes in the initial evolution experiment, six populations were identified for further study. This list included three populations that re-evolved phage sensitivity in the initial experiment, each paired with the closest possible genetic match that maintained phage resistance. Ten replicates of each population were seeded from samples taken at day 0 of the initial evolution experiment (i.e. before they eventually lost or maintained phage resistance). The resulting sixty populations were maintained in King's Broth media and passaged as described above for 36 days. At this point, 96 colonies were picked from each population, individually streaked against phage, and scored as resistant or sensitive. Resistance was analyzed as a proportion of colonies within each population. Since many populations were either completely resistant or completely sensitive, Welch's t-test for unequal variances was used to compare resistance outcomes in the replay experiment according to their founder populations.

## 6.3 Results

*Single-step selection for phage resistance*

To explore whether the long-term outcomes of phage resistance were contingent on the genetic underpinnings of their initial resistance (and/or the fitness costs associated with resistance), we first generated a panel of phage-resistant bacterial strains. With the aim of generating substantial variation both in resistance mechanisms and in fitness, we used five different *Pseudomonas* phages to select phage-resistant colonies of *Pseudomonas syringae* pv. tomato DC3000 through soft agar overlays. We isolated and sequenced 22 colonies to reveal 17 unique resistance mutations (positions 1184510 and 5662024 each appeared three times in the panel, and one colony had no detectable fixed genetic differences from the ancestor despite apparent phenotypic resistance).

In contrast to the diversity of exact mutations, there was relatively high convergence in the genes in which they were found. The mutations in this study were all located in one of four genes, all involved in biosynthesis of outer membrane lipopolysaccharide molecules: PSPTO_4988 (RfaB family glycosyltransferase), PSPTO_4991 ($Glc^{II}$ glycosyltransferase), and PSPTO_1330 (Glycosyltransferase α-L-Rha), involved in assembling the LPS core structure, and *rfbA* (glucose-1-phosphate thymidylyltransferase) responsible for the O-antigen (351) (Figure **1a**). Resistance mutations included single-nucleotide missense mutations, single-nucleotide nonsense mutations, and insertions and deletions of varying sizes. When resistant mutants were tested in the absence of phages, these strains grew more slowly than their phage-sensitive ancestor, indicating trade-offs between resistance and other aspects of fitness (one-sample t-test, $t = -8.405$, $p < 0.001$, Figure **1b**). Variation in growth rates could not be explained by the genes in which those mutations occurred (ANOVA, $F = 0.673$, $df = 3$, $p = 0.580$), indicating that different resistance mutations in the same gene could have different impacts on fitness. This lack of systematic differences in fitness costs across genes underlying resistance meant that we could tease apart the effects of underlying genetic mechanisms and fitness costs on the

maintenance of phage resistance, as these two predictors were not confounded with each other.

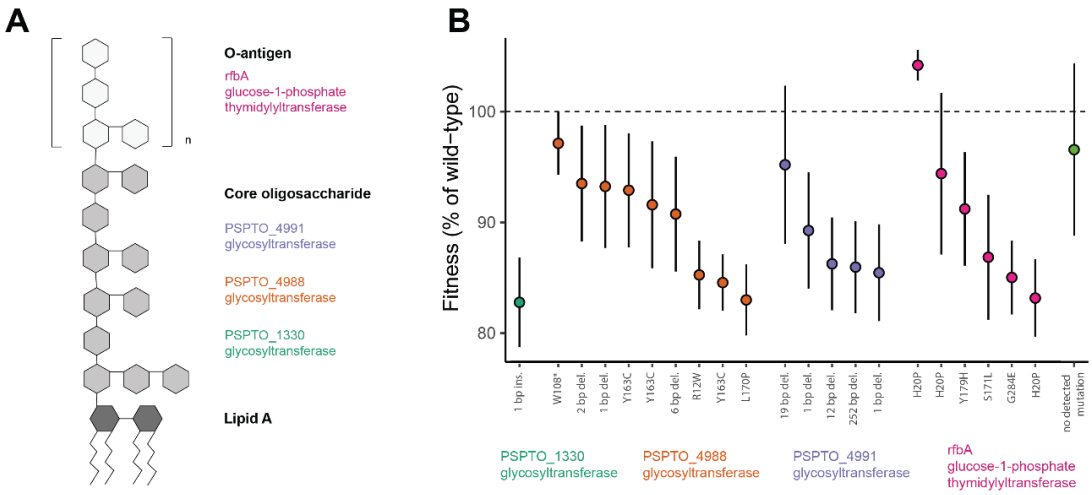


**Figure 1. Genetic mechanisms and fitness costs of phage resistance. (a)** Schematic illustration of the lipopolysaccharide structure, with the genes implicated in phage resistance in this study matched to their corresponding substructures. **(b)** Population growth rates of resistant strains in the absence of phage, based on a logistic model fitted to a 40-hour growth curve (n=22 strains). Error bars represent standard error across technical replicates. Bacterial colonies with resistance mutations in the same gene are denoted by the color scheme. The location and the nature of the mutation is indicated along the x-axis; e.g. R12W indicates a change from arginine to tryptophan at the twelfth position, and W108* indicates a change from tryptophan to a stop codon.

Of note, there was no effect of the identity of the selecting phage on either resistance mechanism or fitness of the bacteria; in fact, different phages often selected for resistance mutations in the same gene or even the exact same resistance mutation (Table **1**). Further, resistance to one phage typically conferred cross-resistance to all other phages in the study, suggesting that the phages in this study used the same receptor. We therefore aggregated data across selecting phages for the analyses in this study. Throughout the manuscript, the name of the population indicates the selecting phage (e.g. “FMS”) and the position of the resistant colony in the original assay for selection of resistance (e.g. “6”).

**Table 1. Genetic mechanisms and evolutionary outcomes of phage-resistant populations**.

| **Population** | **Resistance gene** | **Position of resistance mutation** | **Resistance mutation** | **Outcome in original evolution experiment** |
|---|---|---|---|---|
| FMS6 | *rfbA* | 1183718 | SNP (G284E) | Remained resistant |
| FMS4 | *rfbA* | 1184034 | SNP (Y179H) | Remained resistant |
| VCM4 | *rfbA* | 1184057 | SNP (S171L) | Re-evolved sensitivity |
| MS10 | *rfbA* | 1184510 | SNP (H20P) | Remained resistant |

| | | | | |
|---|---|---|---|---|
| MS2 | *rfbA* | 1184510 | SNP (H20P) | Remained resistant |
| QAC4 | *rfbA* | 1184510 | SNP (H20P) | Remained resistant |
| QAC5 | PSPTO_1330 | 1461031 | 1 bp ins. | Re-evolved sensitivity |
| VCM19 | PSPTO_4988 | 5661617 | 2 bp del. | Remained resistant |
| MS12 | PSPTO_4988 | 5661621 | 1 bp del. | Remained resistant |
| FMS13 | PSPTO_4988 | 5661925 | 6 bp del. | Remained resistant |
| SNK12 | PSPTO_4988 | 5662003 | SNP (L170P) | Remained resistant |
| QAC3 | PSPTO_4988 | 5662024 | SNP (Y163C) | Remained resistant |
| SNK11 | PSPTO_4988 | 5662024 | SNP (Y163C) | Remained resistant |
| VCM17 | PSPTO_4988 | 5662024 | SNP (Y163C) | Remained resistant |
| SNK6 | PSPTO_4988 | 5662188 | SNP (W108*) | Remained resistant |
| MS1 | PSPTO_4988 | 5662478 | SNP (R12W) | Remained resistant |
| FMS12 | PSPTO_4991 | 5664934 | 19 bp del. | Remained resistant |
| FMS9 | PSPTO_4991 | 5665124 | 252 bp del. | Remained resistant |
| SNK7 | PSPTO_4991 | 5665501 | 1 bp del. | Re-evolved sensitivity |
| FMS11 | PSPTO_4991 | 5665743 | 1 bp del. | Remained resistant |
| FMS16 | PSPTO_4991 | 5665890 | 12 bp del. | Remained resistant |

*Multiple evolutionary paths to recover fitness costs*

To test whether phage sensitivity tends to re-evolve in the absence of phages, we inoculated 22 experimental microcosms of King's Broth media each with one of the resistant colonies. We also inoculated 6 microcosms with the phage-sensitive ancestor to assess changes due to overall adaptation to the environment, for a total of 28 experimentally evolving populations. Populations were transferred to fresh media every 3 days for a total of 36 days. Over the course of the experiment, the difference in growth rates between the populations initiated with phage-resistant bacteria and those initiated with phage-sensitive (ancestral) bacteria gradually narrowed, and by the end of the experiment there was no observed fitness difference between the two groups (Figure **2a**). Changes in fitness followed a diminishing returns pattern of adaptation: populations with the lowest initial fitness made the greatest fitness gains over time (ANOVA, $F = 33.226$, $p < 0.001$; Figure **S4**).

Bacterial populations evolved lower levels of resistance to their original selecting phages under relaxed selection, but only rarely. A total of 5 populations (out of 22 initially resistant populations) contained colonies with sensitive, partially resistant, or ambiguous phenotypes on agar plates. We tracked the growth of these clones over time in liquid culture in the presence

or absence of the selecting phage, revealing that 3 of these 5 populations contained phage-sensitive bacteria. (Figure **2b**). Interestingly, the overall increase in bacterial fitness over time could not be attributed to the re-evolution of phage sensitivity alone. While there was a main effect of the day of experimental evolution on bacterial fitness, the rate of change did not differ among populations that re-evolved sensitivity and those that remained resistant (ANOVA, F = 2.146 for the interaction term, $p$ = 0.145). This observation suggested that the resistant populations may be able to access compensatory mutations that lessen the costs of phage resistance without reversing it.

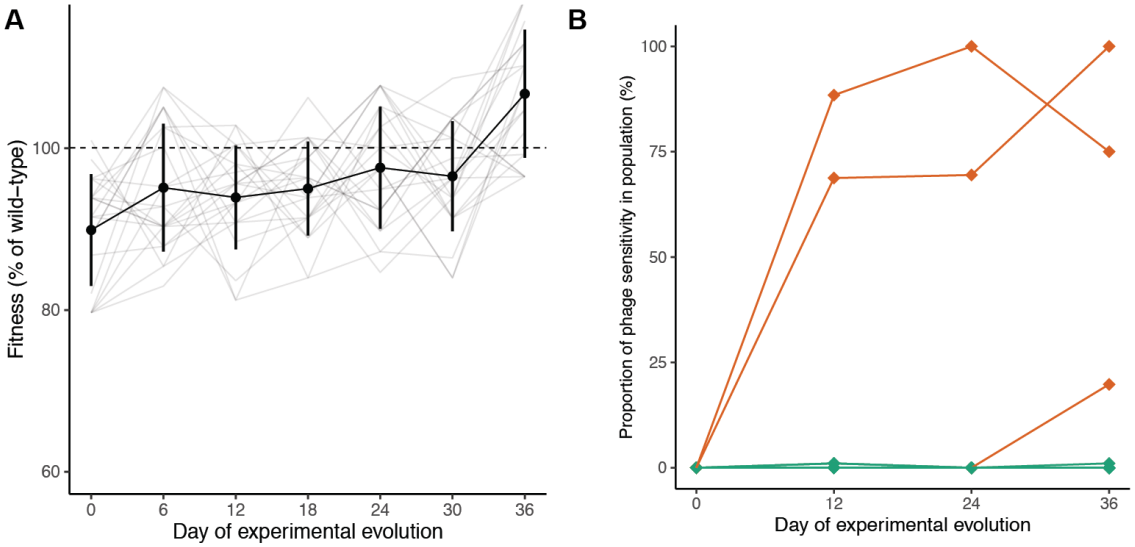


**Figure 2. Phenotypic changes in bacterial populations during experimental evolution in the absence of phages.** **(a)** Population growth rates of populations inoculated with phage-resistant colonies over experimental evolution in the absence of phages, calculated based on optical density measurements in a microplate reader over 40 hours of growth (n=22). Lines represent the trajectories of individual populations over time, while points indicate mean fitness among populations sampled at the same day and error bars indicate standard deviation. Values are normalized to the growth rates of the phage-sensitive control populations sampled at the same point in experimental evolution. **(b)** Proportion of colonies in each population that were scored as phage-sensitive over time, as indicated by disruption in bacterial growth upon encountering phage on an agar plate (n=22 populations with 96 colonies sampled per population). Orange lines indicate populations from which sensitive colonies were isolated and verified in a microplate assay.

We isolated and sequenced the genomes of phage-sensitive colonies to determine how phage sensitivity re-evolved. The population "SNK7", which originally acquired resistance through a single base-pair deletion in the glycosyltransferase-encoding gene PSPTO_4991, later acquired a single base-pair insertion 5 bases away that restored the reading frame. In contrast, the other two populations acquired mutations that fell outside of their initial resistance genes. VCM4, which had become phage-resistant through a substitution in the *rfbA* gene, evolved additional mutations in two other membrane transport proteins. QAC5, which had evolved resistance through a single base-pair insertion in the glycosyltransferase-encoding gene PSPTO_1330, acquired a mutation in a membrane transport protein as well as several intergenic mutations whose function (if any) is unknown.

We had predicted that populations with particularly costly resistance would be most likely to re-evolve sensitivity due to strong selection. However, we did not observe a relationship between initial costs of resistance and the evolution of phage sensitivity (Welch's unequal variances t-test, t = 1.818, $p$ = 0.138). We also asked whether phage sensitivity would be more likely to re-emerge among populations with particular resistance genes. While the unequal distribution of phage resistance outcomes makes it difficult to entirely rule out this possibility, the three populations that re-evolved sensitivity in this study did so from three different initial resistance genes, providing no evidence that trait reversion is historically contingent at the gene level (Table **1**). However, we noticed two important observations that warranted further study.

First, our study included four populations that had originally acquired resistance through large deletions in oligosaccharide synthesis genes, spanning from 6 base pairs to 252 base pairs in length. None of these populations re-evolved sensitivity, whether by re-insertion of the missing sequence or through any other means. Second, by chance our study included two sets of three populations each with identical resistance mutations. In both cases, these genetic triplets all followed the same evolutionary outcome (remaining resistant). Given that re-evolving phage sensitivity was generally rare in this study, it was not apparent whether these two observations were simply probabilistic, or whether they pointed to historical contingency at the level of the individual mutation rather than the resistance gene as a whole. As this experiment was not originally set up to test this possibility, we developed an experimental design that would test the effects of exact resistance mutations on phage resistance outcomes.

*Replay of experimental evolution*

The initial evolution experiment revealed that the identity of the gene conferring phage resistance did not explain whether bacteria remained resistant or re-evolved sensitivity. To ask whether phage resistance outcomes were contingent on the exact resistance mutation instead, we returned to the progenitor frozen stocks of the 3 resistant colonies that had re-evolved sensitivity during experimental evolution. We also included 3 resistant colonies that were never observed to re-evolve sensitivity, selecting the closest possible genetic matches to the colonies that did. For example, colonies VCM4 and MS2 had both originally acquired resistance through point mutations in the *rfbA* gene, yet VCM4 had re-evolved phage sensitivity while MS2 had not.

We used each of these 6 resistant mutants ("founders") to seed 10 replicate populations, resulting in a total of 60 experimentally evolving populations. As above, these populations were maintained in experimental microcosms of King's Broth and transferred every 3 days for 36 days. At the end of the replay experiment, founder identity accounted for the majority of variance among populations in the prevalence of phage sensitivity, with evolutionary stochasticity playing a smaller role. In fact, populations derived from a founder that had re-evolved sensitivity in the original experiment were far more likely to re-evolve sensitivity in the replay experiment as well (Welch's unequal variances t-test, t = 4.744, $p$ < 0.001; Figure **3**).

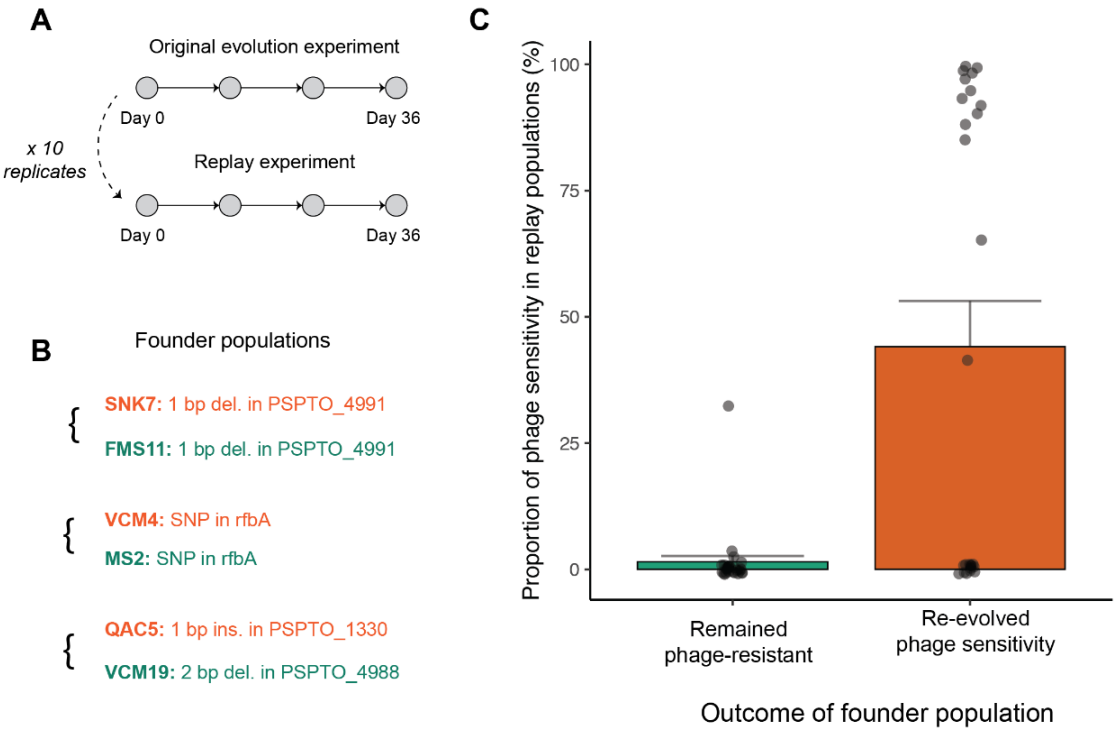


**Figure 3. Phage resistance outcomes in the replay experiment mirror the outcomes of their founding population.** **(a)** Populations in the replay experiment were founded by frozen stocks of resistant colonies prior to their evolution in the absence of phages. Each founder was used to generate 10 replicate populations from genetically identical starting points. **(b)** Resistance mutations of the 6 founders. Each colony that had re-evolved sensitivity in the original experiment (orange) was paired with a genetically similar colony that had remained resistant (green). Of note, QAC5 was the only colony in the study with a mutation in PSPTO_1330, so it was matched with a population that also had a small frameshift mutation, but in a different glycosyltransferase-encoding gene. **(c)** Proportion of colonies in each population that were scored as phage-sensitive after 36 days in the absence of phages, as indicated by disruption in bacterial growth upon encountering phage on an agar plate (n=54 populations with 96 colonies sampled per population).

*Historical contingency in genome evolution*

We pool-sequenced each of the populations of the original evolution experiment after six days of evolution in the absence of phages. To characterize the molecular basis of compensatory evolution in phage-resistant bacteria, we first considered that compensatory mutations in other systems are often related to biochemical protein stability or specialized protein-protein interactions (9,352). We therefore predicted that different mechanisms of resistance would likely require different compensatory mutations to ameliorate their costs. We would then expect populations with the same resistance gene to exhibit greater evolutionary parallelism than populations with different resistance genes. We calculated the Sørenson-Dice similarity coefficient, which describes the proportion of mutated genes that two populations have in common, controlling for their initial genetic backgrounds. We found that populations with the same resistance mechanisms had acquired more similar sets of mutations than populations with different resistance mechanisms (randomization test, $p < 0.001$, Figure **4a**). For example, populations that had originally acquired phage resistance through a mutation in the glycosyltransferase-encoding enzyme PSPTO_4991 evolved particularly similarly to one another, with many genes acquiring mutations in either all or none of the populations (see

Figure **4b** for a diagram of genetic differences between evolved and ancestral populations organized by initial resistance gene).

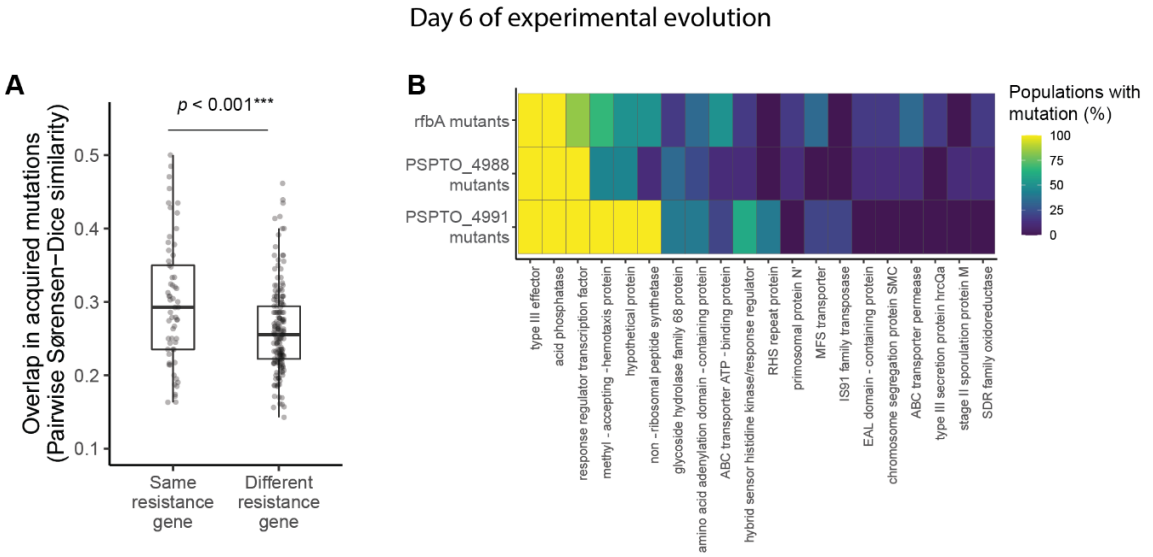


**Figure 4. Genetic contingency in identity of mutated genes during experimental evolution. (a)** Pairwise similarity coefficients among pairs of evolved populations at day 6 of experimental evolution (n=22). Statistical significance was assessed by randomizing whether pairs were labeled as having the same or different resistance genes and recalculating their similarity coefficients for 10,000 permutations. **(b)** Heatmap depicting the relationship between initial resistance genes and mutations acquired during experimental evolution for *rfbA* mutants (n=6), PSPTO_4988 mutants (n=9), and PSPTO_4991 mutants (n=5). Rows represent all populations with resistance mutations in the same gene (note that resistance genes represented by fewer than 2 populations are not pictured, as there was no way to assess parallelism in these cases). Columns represent the top 20 genes that were most frequently mutated across populations by day 6 of experimental evolution. Colors indicate the percentage of populations of each resistance gene that had acquired one or more mutations by day 6 of experimental evolution.

*Effect of history on genome evolution diminishes over time*

To examine adaptation and historical contingency in the longer term, we pool-sequenced each of the populations at the end of the evolution experiment (day 36). By the end of the experiment, the evolving populations had fixed relatively few mutations in protein-coding genes (mean = 0.71 ± 0.66 s.d.), but acquired and maintained polymorphisms at many loci (mean = 22.61 ± 7.20 s.d.). Across all populations, the most frequent mutations occurred in effector proteins, membrane-bound enzymes, and transcription factors. Additionally, several populations had acquired substitutions in the DNA mismatch repair proteins *mutS* or *mutL* during experimental evolution. While none of these mutations fixed within their respective populations, populations with a mutation in *mutS* or *mutL* acquired more fixed mutations or polymorphisms overall than the other populations by the end of the experiment (Student's t-test, t = 2.746, $p$ = 0.005), suggesting that they may contain 'hypermutator' lineages with elevated mutation rates (353,354).

After populations had evolved for a total of 36 days in identical environments, there was no remaining signature of the initial resistance gene on pairwise similarity coefficients (randomization test, $p$ = 0.710, Figure **5**).

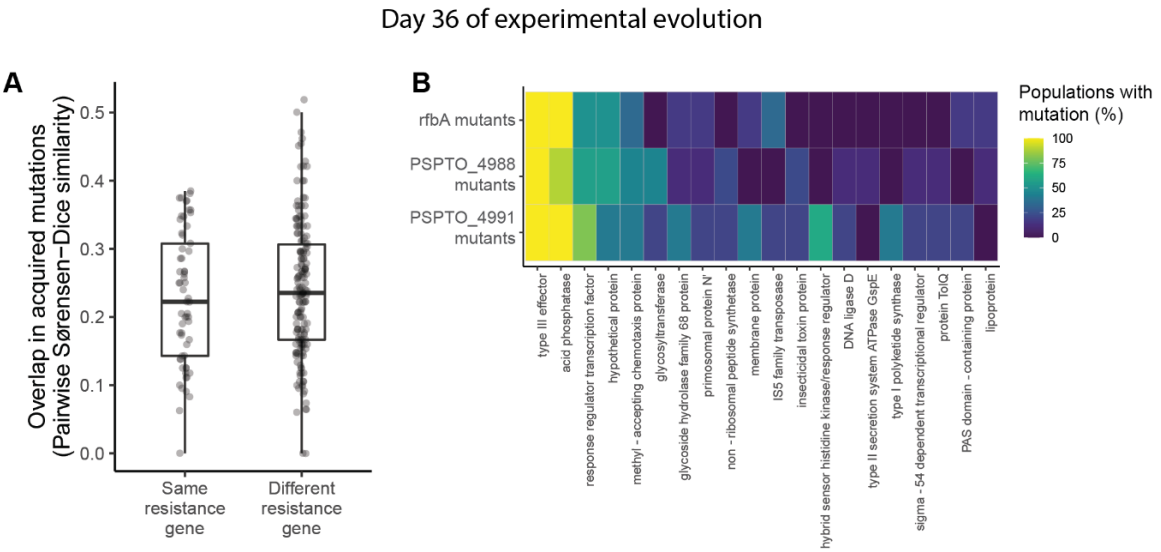


**Figure 5. Genetic contingency is no longer detectable after extended evolution in the absence of phages. (a)** Pairwise similarity coefficients among pairs of evolved populations at day 36 of experimental evolution. Statistical significance was assessed by randomizing whether pairs were labeled as having the same or different resistance genes and recalculating their similarity coefficients for 10,000 permutations. **(b)** Heatmap depicting the relationship between initial resistance genes and mutations acquired during experimental evolution for *rfbA* mutants (n=6), PSPTO_4988 mutants (n=9), and PSPTO_4991 mutants (n=5). Rows represent all populations with resistance mutations in the same gene (note that resistance genes represented by fewer than 2 populations are not pictured, as there was no way to assess parallelism in these cases). Columns represent the top 20 genes that were most frequently mutated across populations by day 36 of experimental evolution. Note that these are not necessarily identical to the top 20 genes identified in Figure **4**. Colors indicate the percentage of populations of each resistance gene that had acquired one or more mutations by day 36 of experimental evolution.

## 6.4 Discussion

Phages are ubiquitous in microbial communities and are expected to play a central role in bacterial evolution, with critical implications for bacteria-bacteria and bacteria-host interactions (277,355). Predation by phages can maintain population and community diversity in their bacterial hosts (356), regulate the dissemination of antibiotic resistance genes (31,357), select for hypermutator strains (358), and alter competitive outcomes among bacterial species (359). Here, we show that even transient exposure to phages can have lasting consequences for the evolutionary trajectories of bacterial populations. Through a series of laboratory evolution experiments, we demonstrate that phage resistance in the bacterium *Pseudomonas syringae* can be reversible or entrenched depending on the original genetic path to resistance.

Phage resistance in our study primarily occurred through mutations in lipopolysaccharide biosynthesis genes, which have been previously implicated in phage resistance in this bacterial species and others (360–364). One population did not appear to have any fixed genetic differences from the ancestor despite its resistant phenotype. Resistance in this case may be conferred by mutations that are not adequately resolved by short-read sequencing, such as copy number variation or sequence region inversions, or through unstable genetic changes such as phase variations (365,366). Of note, this population remained phenotypically resistant throughout the evolution experiment, possibly because it did not experience detectable fitness costs relative to its phage-sensitive ancestor.

Even though the resistance mutations in our study were concentrated within a handful of genes, they occurred at many unique positions and altered the amino acid sequences in a variety of ways, including missense and nonsense substitutions and frameshift mutations of vastly different sizes. Such convergence in resistance mechanisms at the gene level, and diversity at the sequence level, is consistent with the expectation that phage infection relies on specific receptor structures and that recognition can easily be disrupted by modifying or deleting these structures in one of many ways (338). However, resistance was generally costly in the absence of phages, as is often observed in this system and others (26,27,357,362,367).

Costs of resistance may stem from alterations to lipopolysaccharide molecules that destabilize the bacterial membrane or reduce surface adhesion (339). The commonly observed costs of phage resistance suggest that resistance might be selected against in the absence of phage pressure, yet previous studies of this question have produced inconsistent results (28,343,344). When we propagated the bacterial populations for an extended period in the absence of phages, we observed that phage sensitivity re-appeared and swept to high frequencies in several populations but that the majority of populations remained resistant. In the case of one population, this reversion to sensitivity was due to a mutation that restored the reading frame of the original sequence, but in other cases, populations re-evolved phage sensitivity without reversing the original mutation.

The diversity of phage-resistant mutants in this study allowed us to ask whether the re-evolution of phage sensitivity was contingent on the mechanisms and/or costs of phage resistance. Costs of trait maintenance are often expected to predict trait loss under relaxed selection (29,343), yet we did not observe a relationship between the magnitude of fitness costs and the re-evolution of phage sensitivity in our study. This observation, along with the fact that populations that did not re-evolve sensitivity nevertheless improved their fitness to match their phage-sensitive counterparts, suggests the existence of compensatory mutations that reduce the costs of resistance. Compensatory mutations could eventually restore fitness levels to a point where phage sensitivity is no longer advantageous (368–370), or may even be disadvantageous or lethal on the ancestral background, further discouraging reversion of the original trait (371). Therefore, it appears that trade-offs between phage resistance and other aspects of fitness can be strong, yet bacteria are able to access two evolutionary pathways (reversion and compensation) in response.

We hypothesized that the probabilities of these two pathways could be contingent on the genetic mechanism underlying phage resistance. Some traits might have a greater supply of reversion mutations than others; for example, there may be more mutations that restore the ancestral expression levels of a gene than those that reconstitute the exact three-dimensional structure of a receptor (28), or more mutations that reverse duplications than point mutations (341). Similarly, resistance mechanisms may impact bacterial fitness in different ways, thus requiring different sets of compensatory mutations to restore their costs (371). We did not find an overall correlation between the initial resistance gene and whether phage sensitivity re-evolved, but with two important caveats. First, when resistance was acquired through a large deletion in a receptor biosynthesis gene, it was never reversed, whether through a complementary insertion or other mutations. This suggests that the mutations that would reverse such a large change are so vanishingly rare that other compensatory mutations are much more likely to appear first.

Our second observation was that the genetic replicates in the mutant panel (i.e. the populations that independently acquired resistance via the same mutation) all followed the same phenotypic trajectories. Specifically, they all remained resistant throughout experimental evolution in the absence of phage. This suggested that historical contingencies – if they existed here – might be generated not from the identity of the resistance gene, but from the exact genetic sequence. Even within the same resistance gene, some mutations might be more reversible than others. As the original experiment was not explicitly focused on this possibility, we designed a follow-up experiment that "replayed" experimental evolution 10 times per founding genotype (inspired by Stephen Jay Gould's famous thought experiment about replaying the tape of life (4)). Strikingly, we found that the evolutionary outcomes of the populations in our replay experiment closely mirrored those of their founders. Populations whose founders had re-evolved phage sensitivity also tended to re-evolve phage sensitivity at high rates, while populations whose founders had remained resistant tended to remain resistant as well.

Variation in the reversibility of different resistance mutations may occur if different sets of compensatory mutations are required to restore their costs. To explore this possibility, we compared the similarity of acquired mutations among pairs of the experimentally evolving populations. We found that populations with the same initial resistance gene evolved more in parallel with one another than populations with different resistance genes, suggesting that compensatory adaptation in phage-resistant bacteria also depends on evolutionary history. Several other studies have observed greater genomic parallelism among experimental evolution populations with similar starting genotypes for other traits, including in antibiotic resistance evolution (350) and in compensatory adaptation after gene deletion (371). And outside of the laboratory, convergence in sequence evolution appears to be more common among populations with a recent common ancestor than a distant one (372,373). Notably, the effect we observed was strong when the phage selection event was recent, but was no longer detectable after populations had spent an extended period of time in the same environment. Thus, recent historical differences appear to be more important than distant historical differences in shaping subsequent evolution (374–376).

Our study provides evidence for an evolutionary ratchet in bacteria-phage coevolution, where compensatory adaptation enables the persistence of certain resistance mutations even after the original selection pressure has ceased to operate. Why did history constrain evolution in this study, but not in some others (7,377,378)? One important clue may lie in the underlying genetic structure of phage resistance. The phage-sensitive ancestor in this study could mutate to phage resistance through any one of at least 17 individual mutations, including nonsense mutations and large deletions. Phage adsorption relies on highly specific molecular interactions (379), suggesting that there are many ways to change lipopolysaccharide structure to avoid phage recognition, and that at least some of these mutations are not lethal to the cell. In other cases, traits can evolve in parallel across lineages despite their historical differences. For example, several distantly related groups of animals have identical substitutions conferring tetrodotoxin resistance (378). In this case, mutagenic screens have identified additional possible mutations that confer toxin resistance, but these additional mutations are so detrimental to sodium channel performance – an essential function – that they are not

observed in nature (377). The role of history in evolution is therefore likely related to the target size of mutations that confer novel functions yet are not overly disruptive to the original trait.

Our findings add to a growing body of work that selection by phages plays a key role in the ecological and evolutionary dynamics of bacterial communities. Further, many of the bacterial populations in our study acquired mutations in genes known to interact with eukaryotic immune systems. Phage resistance was directly mediated in many cases by changes to lipopolysaccharide molecules, which are recognized by both animal and plant immune systems (380,381), and many populations also acquired mutations in type III effector proteins that underlie bacterial virulence. It will thus be important to characterize whether and how phages are indirectly responsible for shaping coevolution in between bacteria and eukaryotes as well (382).

## 6.5 Appendix

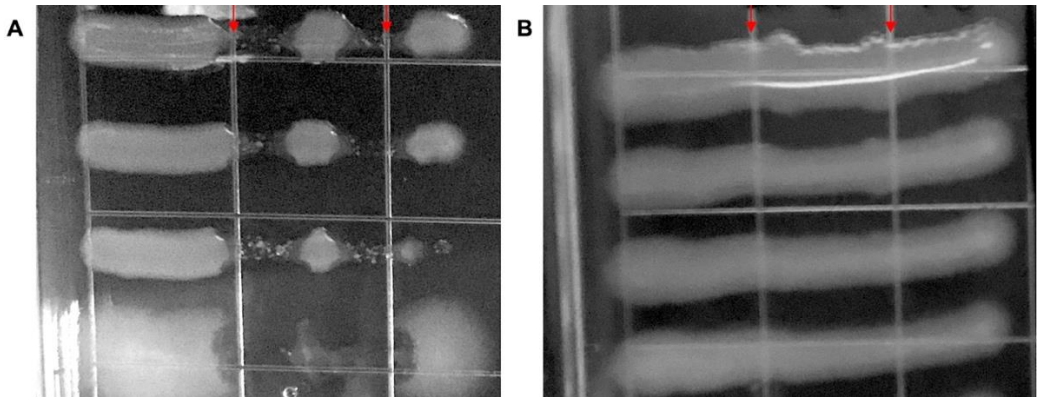


**Figure S1. Assay for phage resistance.** Two droplets of pure phage culture were pipetted at the top of each agar plate and allowed to flow downwards (red arrows). Once the droplets had dried, overnight cultures of bacterial colonies were streaked across the phage lines. Plates were incubated at 28°C for 48 hours, then colonies were scored as **(a)** phage-sensitive if bacterial growth was clearly disrupted at the phage line, or **(b)** phage-resistant if bacteria grew uninterrupted across the plate.

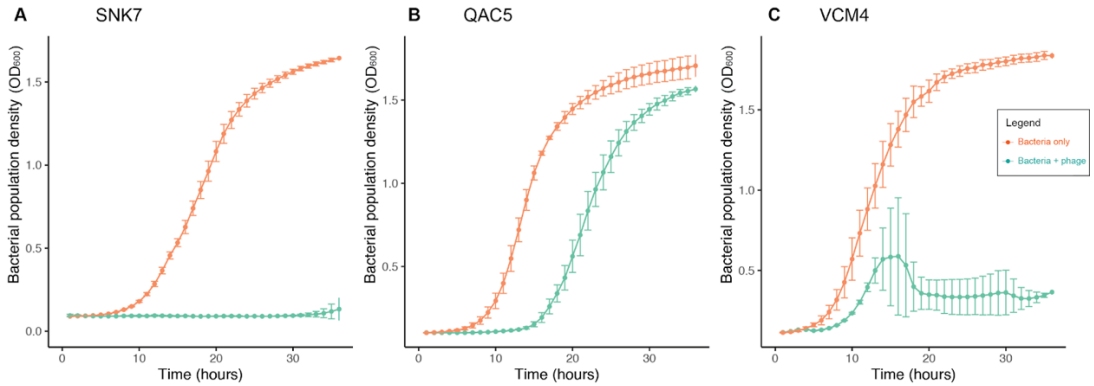


**Figure S2. Validation of phage sensitivity in evolved populations.** Growth curves of individual colonies picked from populations SNK7 **(a)**, QAC5 **(b)**, and VCM4 **(c)**. Either 30 uL of phage (overnight co-culture filtered to exclude bacterial cells) or 30 uL of spent media (overnight bacterial culture filtered to exclude bacterial cells, as a control for how phage propagation changes media composition) was added to each well. Error bars represent the standard deviation of 2-3 technical replicates per colony.

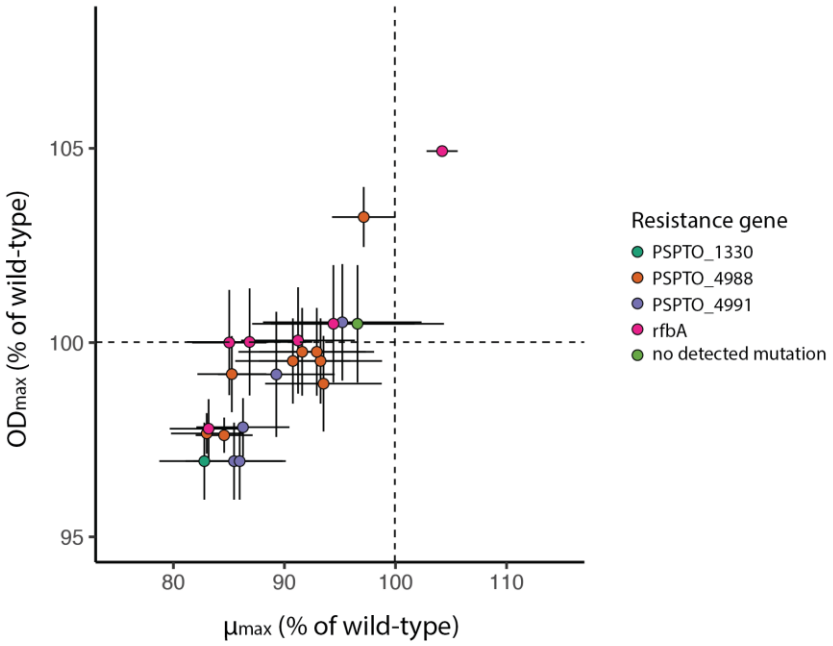


**Figure S3. Fitness costs of phage resistance over varying points in bacterial population growth.** Population growth rates ($\mu_{max}$) and final population sizes ($OD_{max}$) of resistant strains in the absence of phage, based on a logistic model fitted to a 40-hour growth curve (n=22 strains). Error bars represent standard error across technical replicates. Bacterial colonies with resistance mutations in the same gene are denoted by the color scheme.

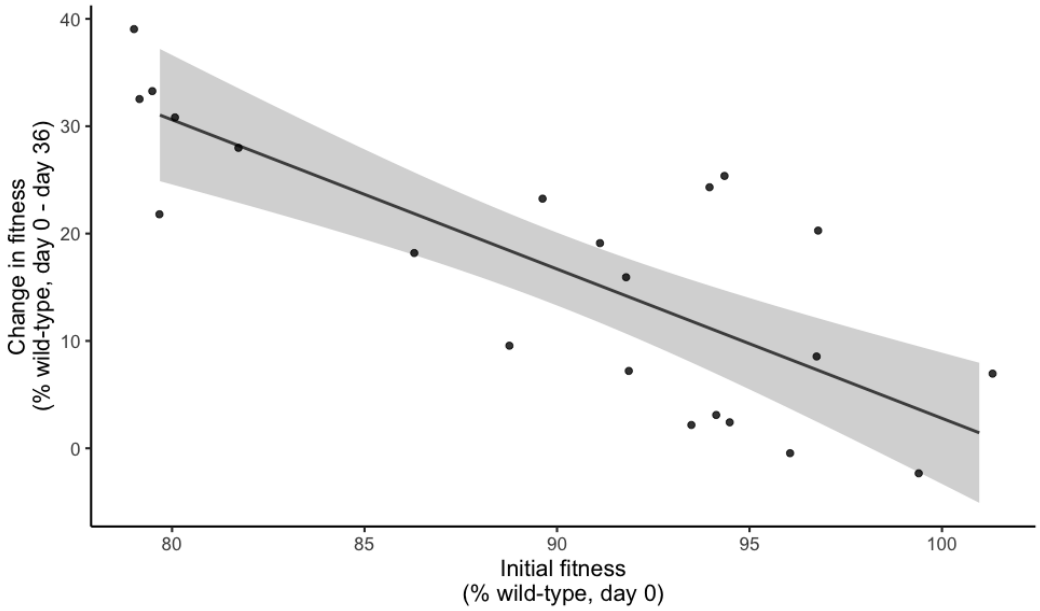


**Figure S4. Diminishing returns in adaptation over time.** Change in fitness (population growth rate) over the entire evolution experiment (days 0-36) as a function of initial fitness.

# 7. Conclusions

The role of historical contingency in ecology and evolution has traditionally received less attention than deterministic factors such as diet, altitude, or temperature. In a 2015 synthesis of research on historical contingency in ecology, Tadashi Fukami identified two possible reasons for this discrepancy (8). First, the study of historical contingency can be challenging in the absence of a detailed record of historical events. Second, identifying instances of historical contingency can make each biological system appear unique – an unsatisfying outcome to biologists that hope to gain generalizable insights into ecology and evolution. Yet with recent research progress, it is becoming clear that there are underlying principles governing when and how biological outcomes are sensitive to history. Fukami likened this to weather forecasting, in which it is difficult to predict how exactly a particular community will develop, but we can forecast a range of possibilities (8).

My dissertation research aimed to characterize these underlying principles that dictate the importance of history in ecology and evolution. I addressed this question with a wide range of approaches, from laboratory experiments to field studies to developing new computational pipelines, because common threads from multiple lines of evidence can help to circumvent their individual limitations. My first two chapters focused on priority effects, the phenomenon in which community assembly trajectories depend on the order of species arrival. Through both re-analysis of time-series data from animal gut microbiomes in early life (Chapter 1) and arrival order manipulations of plant microbiomes in the lab (Chapter 2), I found the strongest signatures of priority effects among closely related species that presumably compete for similar resources (14,17). This pattern has been observed in other systems (15,16), and has led to suggestions that priority effects may not be very important to ecosystem function if they result in the substitution of functionally equivalent species (95). But in my arrival order experiments, I found that bacteria with similar ecological requirements at times had very different effects on host fitness. Arrival order variation between competing species of bacteria, when one was a pathogen, affected the extent of symptom progression on the plant leaves (17).

In my following two chapters, I isolated bacterial communities from tomato plants in the field and transplanted them onto plants in the lab, asking how the same species pool would assemble under different ecological conditions. In the agricultural field trial focused on soil mycorrhizae (Chapter 3), I found that disrupting plant-mycorrhizal associations in the soil led to a ~25% loss of microbial biodiversity in the leaves. Next, I transplanted leaf microbial communities from mycorrhizal and non-mycorrhizal plants onto mycorrhizal and non-mycorrhizal plants in the lab to ask whether the leaf microbiome could recover when mycorrhizal associations were restored. Across all treatments, the leaf microbiomes shifted from their source inocula to more closely resemble the microbiome of the typical plant type that they were currently associated with. This suggested that in this case, history was not a long-term factor in shaping in microbiome composition – possibly because regrowth of small local populations and/or dispersal from neighboring plants facilitated recovery. In Chapter 4, I used a similar approach to explore how phages impact bacterial community ecology. I transplanted bacteria in the absence of any phages, in the presence of their sympatric (local) phages, and in the presence of phages from other environments. Sympatric phages had the

strongest effects on bacterial biodiversity, yet allopatric phages had the strongest effects on pathogen resistance, suggesting that the relationship between microbiome diversity and host health is more complicated than often assumed (53). Of note, the strongest predictor of both plant microbiome composition and disease resistance in the lab was the original species composition of their source inocula in the field, suggesting that historical processes play an important role in shaping microbiome composition and function.

My final chapter showed that bacteria can evolve resistance to phages through any of a number of genetic mutations (my experiment uncovered at least 17, but many others have been documented (384)). Yet some phage resistance mutations were reversible in the absence of phage, while others remained entrenched despite being equally costly. The identity of the initial resistance gene also predicted the pattern of mutations that populations acquired throughout the rest of the genome (385). How bacteria resolved the costs of phage resistance mechanisms was clearly an event that is sensitive to history (the history of which phage resistance mutation they happened to fix in the population). This was due in part to the fact that so many different mutations were able to confer resistance, and in part because each resistance mutation had different consequences for subsequent evolution. But why are there so many genetic paths to phage resistance? The answer seems to lie in the ecology of phage-bacteria interactions. All of the phages in this study recognized the lipopolysaccharide receptor, and all of the resistance mutations were involved in altering, distorting, or deleting the receptor to prevent phages from binding to it (338,363). Just as host recognition by phages is referred to a "lock-and-key" mechanism (385,386), bacteria have many ways to change the locks.

My findings add to a growing body of genetic, biochemical, ecological, comparative, and philosophical work that is uncovering a role for history in the generation and maintenance of biological diversity. Only three decades after the publication of Gould's *Wonderful Life*, we are already succeeding in capturing the essence of the grand evolutionary experiment that Gould declared impossible. My future research will continue to explore the intersection of ecological and evolutionary processes in microbial communities. But instead of assembling microbiomes from the bottom up or replaying community assembly in the lab, I will be tracking microbiome composition, stability, and evolution within hosts in the wild (387). This work will provide insights into community and metacommunity dynamics over much longer time periods than I measured in my dissertation research, raising the unanswered question of whether (and how) historical processes have long-lasting effects on microbiomes and their hosts.

## References


1. Martin WF, Garg S, Zimorski V. Endosymbiotic theories for eukaryote origin. Philos Trans R Soc B Biol Sci. 2015 Sep 26;370(1678):20140330.

2. Raup DM. Biological Extinction in Earth History. Science. 1986 Mar 28;231(4745):1528–33.

3. Prost JH. Origin of bipedalism. Am J Phys Anthropol. 1980;52(2):175–89.

4. Gould SJ. Wonderful life: the Burgess Shale and the Nature of History. WW Norton & Company; 1990.

5. McGlothlin JW, Kobiela ME, Feldman CR, Castoe TA, Geffeney SL, Hanifin CT, et al. Historical contingency in a multigene family facilitates adaptive evolution of toxin resistance. Curr Biol. 2016;26(12):1616–21.

6. Heywood JJN. Explaining patterns in modern ruminant diversity: contingency or constraint? Biol J Linn Soc. 2010 Apr 1;99(4):657–72.

7. Weinreich DM, Delaney NF, DePristo MA, Hartl DL. Darwinian evolution can follow only very few mutational paths to fitter proteins. science. 2006;312(5770):111–4.

8. Fukami T. Historical Contingency in Community Assembly: Integrating Niches, Species Pools, and Priority Effects. Annu Rev Ecol Evol Syst. 2015 Dec 4;46:1–23.

9. Bridgham JT, Ortlund EA, Thornton JW. An epistatic ratchet constrains the direction of glucocorticoid receptor evolution. Nature. 2009;461(7263):515–9.

10. Harms MJ, Thornton JW. Historical contingency and its biophysical basis in glucocorticoid receptor evolution. Nature. 2014 Aug;512(7513):203–7.

11. Kawecki TJ, Lenski RE, Ebert D, Hollis B, Olivieri I, Whitlock MC. Experimental evolution. Trends Ecol Evol. 2012 Oct 1;27(10):547–60.

12. Nguyen NH, Smith D, Peay K, Kennedy P. Parsing ecological signal from noise in next generation amplicon sequencing. New Phytol. 2015;205(4):1389–93.

13. Liwinski T, Leshem A, Elinav E. Breakthroughs and Bottlenecks in Microbiome Research. Trends Mol Med. 2021 Apr 1;27(4):298–301.

14. Debray R, Herbert RA, Jaffe AL, Crits-Christoph A, Power ME, Koskella B. Priority effects in microbiome assembly. Nat Rev Microbiol. 2022 Feb;20(2):109–21.

15. Peay KG, Belisle M, Fukami T. Phylogenetic relatedness predicts priority effects in nectar yeast communities. Proc R Soc B Biol Sci. 2011 Jul 20;279(1729):749–58.

16. Maldonado-Gómez MX, Martínez I, Bottacini F, O'Callaghan A, Ventura M, van Sinderen D, et al. Stable Engraftment of Bifidobacterium longum AH1206 in the Human Gut Depends on Individualized Features of the Resident Microbiome. Cell Host Microbe. 2016 Oct 12;20(4):515–26.

17. Debray R, Conover A, Zhang X, Dewald-Wang EA, Koskella B. Within-host adaptation alters priority effects within the tomato phyllosphere microbiome. Nat Ecol Evol. 2023 May;7(5):725–31.

18. Douds DD, Millner PD. Biodiversity of arbuscular mycorrhizal fungi in agroecosystems. Agric Ecosyst Environ. 1999 Jun 1;74(1):77–93.

19. Chen M, Arato M, Borghi L, Nouri E, Reinhardt D. Beneficial Services of Arbuscular Mycorrhizal Fungi – From Ecology to Application. Front Plant Sci. 2018. 9: 1270.

20. Latef AAHA, Hashem A, Rasool S, Abd_Allah EF, Alqarawi AA, Egamberdieva D, et al. Arbuscular mycorrhizal symbiosis and abiotic stress in plants: A review. J Plant Biol. 2016 Oct 1;59(5):407–26.

21. Debray R, Socolar Y, Kaulbach G, Guzman A, Hernandez CA, Curley R, et al. Water stress and disruption of mycorrhizas induce parallel shifts in phyllosphere microbiome composition. New Phytol. 2022;234(6):2018–31.

22. Morella NM, Gomez AL, Wang G, Leung MS, Koskella B. The impact of bacteriophages on phyllosphere bacterial abundance and composition. Mol Ecol. 2018;27(8):2025–38.

23. Rodriguez-Brito B, Li L, Wegley L, Furlan M, Angly F, Breitbart M, et al. Viral and microbial community dynamics in four aquatic environments. ISME J. 2010;4(6):739–51.

24. Hu J, Wei Z, Friman VP, Gu S hua, Wang X fang, Eisenhauer N, et al. Probiotic Diversity Enhances Rhizosphere Microbiome Function and Plant Disease Suppression. mBio. 2016 Dec 13;7(6):e01790-16.

25. Becker CG, Longo AV, Haddad CFB, Zamudio KR. Land cover and forest connectivity alter the interactions among host, pathogen and skin microbiome. Proc R Soc B Biol Sci. 2017 Aug 23;284(1861):20170582.

26. Burmeister AR, Sullivan RM, Lenski RE. Fitness costs and benefits of resistance to phage Lambda in experimentally evolved Escherichia coli. In: Evolution in Action: Past, Present and Future. Springer; 2020. p. 123–43.

27. Koskella B, Lin DM, Buckling A, Thompson JN. The costs of evolving resistance in heterogeneous parasite environments. Proc R Soc B Biol Sci. 2012;279(1735):1896–903.

28. Wielgoss S, Bergmiller T, Bischofberger AM, Hall AR. Adaptation to parasites and costs of parasite resistance in mutator and nonmutator bacteria. Mol Biol Evol. 2016;33(3):770–82.

29. Lahti DC, Johnson NA, Ajie BC, Otto SP, Hendry AP, Blumstein DT, et al. Relaxed selection in the wild. Trends Ecol Evol. 2009;24(9):487–96.

30. Dewald-Wang EA, Parr N, Tiley K, Lee A, Koskella B. Multiyear time-shift study of bacteria and phage dynamics in the phyllosphere. Am Nat. 2022;199(1):126–40.

31. LeGault KN, Hays SG, Angermeyer A, McKitterick AC, Johura F tuz, Sultana M, et al. Temporal shifts in antibiotic resistance elements govern phage-pathogen conflicts. Science. 2021;373(6554):eabg2166.

32. Connell JH, Slatyer RO. Mechanisms of Succession in Natural Communities and Their Role in Community Stability and Organization. Am Nat. 1977 Nov;111(982):1119–44.

33. Shulman MJ, Ogden JC, Ebersole JP, McFarland WN, Miller SL, Wolf NG. Priority Effects in the Recruitment of Juvenile Coral Reef Fishes. Ecology. 1983;64(6):1508–13.

34. Alford RA, Wilbur HM. Priority Effects in Experimental Pond Communities: Competition between Bufo and Rana. Ecology. 1985;66(4):1097–105.

35. Grman E, Suding KN. Within-Year Soil Legacies Contribute to Strong Priority Effects of Exotics on Native California Grassland Communities. Restor Ecol. 2010;18(5):664–70.

36. Almany GR. Priority Effects in Coral Reef Fish Communities. Ecology. 2003;84(7):1920–35.

37. Mariotte P, Mehrabi Z, Bezemer TM, De Deyn GB, Kulmatiski A, Drigo B, et al. Plant–Soil Feedback: Bridging Natural and Agricultural Sciences. Trends Ecol Evol. 2018 Feb 1;33(2):129–42.

38. Suding KN, Gross KL, Houseman GR. Alternative states and positive feedbacks in restoration ecology. Trends Ecol Evol. 2004 Jan 1;19(1):46–53.

39. Sprockett D, Fukami T, Relman DA. Role of priority effects in the early-life assembly of the gut microbiota. Nat Rev Gastroenterol Hepatol. 2018 Apr;15(4):197–205.

40. Chng KR, Ghosh TS, Tan YH, Nandi T, Lee IR, Ng AHQ, et al. Metagenome-wide association analysis identifies microbial determinants of post-antibiotic ecological recovery in the gut. Nat Ecol Evol. 2020 Sep;4(9):1256–67.

41. Lee SM, Donaldson GP, Mikulski Z, Boyajian S, Ley K, Mazmanian SK. Bacterial colonization factors control specificity and stability of the gut microbiota. Nature. 2013 Sep;501(7467):426–9.

42. Martínez I, Maldonado-Gomez MX, Gomes-Neto JC, Kittana H, Ding H, Schmaltz R, et al. Experimental evaluation of the importance of colonization history in early-life gut microbiota assembly. Ley RE, Garrett WS, editors. eLife. 2018 Sep 18;7:e36521.

43. Furman O, Shenhav L, Sasson G, Kokou F, Honig H, Jacoby S, et al. Stochasticity constrained by deterministic effects of diet and age drive rumen microbiome assembly dynamics. Nat Commun. 2020 Apr 20;11(1):1904.

44. Cheong JZA, Johnson CJ, Wan H, Liu A, Kernien JF, Gibson ALF, et al. Priority effects dictate community structure and alter virulence of fungal-bacterial biofilms. ISME J. 2021 Jul;15(7):2012–27.

45. Seybold H, Demetrowitsch TJ, Hassani MA, Szymczak S, Reim E, Haueisen J, et al. A fungal pathogen induces systemic susceptibility and systemic shifts in wheat metabolome and microbiome composition. Nat Commun. 2020 Apr 20;11(1):1910.

46. Carlström CI, Field CM, Bortfeld-Miller M, Müller B, Sunagawa S, Vorholt JA. Synthetic microbiota reveal priority effects and keystone strains in the Arabidopsis phyllosphere. Nat Ecol Evol. 2019 Oct;3(10):1445–54.

47. Halliday FW, Penczykowski RM, Barrès B, Eck JL, Numminen E, Laine AL. Facilitative priority effects drive parasite assembly under coinfection. Nat Ecol Evol. 2020 Nov;4(11):1510–21.

48. Wei Z, Yang T, Friman VP, Xu Y, Shen Q, Jousset A. Trophic network architecture of root-associated bacterial communities determines pathogen invasion and plant health. Nat Commun. 2015 Sep 24;6(1):8413.

49. Kennedy PG, Peay KG, Bruns TD. Root tip competition among ectomycorrhizal fungi: Are priority effects a rule or an exception? Ecology. 2009;90(8):2098–107.

50. Fukami T, Dickie IA, Paula Wilkie J, Paulus BC, Park D, Roberts A, et al. Assembly history dictates ecosystem functioning: evidence from wood decomposer communities. Ecol Lett. 2010;13(6):675–84.

51. Enke TN, Datta MS, Schwartzman J, Cermak N, Schmitz D, Barrere J, et al. Modular Assembly of Polysaccharide-Degrading Marine Microbial Communities. Curr Biol. 2019 May 6;29(9):1528-1535.e6.

52. Svoboda P, Lindström ES, Ahmed Osman O, Langenheder S. Dispersal timing determines the importance of priority effects in bacterial communities. ISME J. 2018 Feb;12(2):644–6.

53. Trivedi P, Leach JE, Tringe SG, Sa T, Singh BK. Plant–microbiome interactions: from community assembly to plant health. Nat Rev Microbiol. 2020 Nov;18(11):607–21.

54. Shreiner AB, Kao JY, Young VB. The gut microbiome in health and in disease. Curr Opin Gastroenterol. 2015 Jan;31(1):69–75.

55. Gillhaussen P von, Rascher U, Jablonowski ND, Plückers C, Beierkuhnlein C, Temperton VM. Priority Effects of Time of Arrival of Plant Functional Groups Override Sowing Interval or Density Effects: A Grassland Experiment. PLOS ONE. 2014 Jan 31;9(1):e86906.

56. Gibbons SM, Kearney SM, Smillie CS, Alm EJ. Two dynamic regimes in the human gut microbiome. PLOS Comput Biol. 2017 Feb 21;13(2):e1005364.

57. Ferrero AF. Effect of compaction simulating cattle trampling on soil physical characteristics in woodland. Soil Tillage Res. 1991 Feb 1;19(2):319–29.

58. Gensollen T, Iyer SS, Kasper DL, Blumberg RS. How colonization by microbiota in early life shapes the immune system. Science. 2016;352(6285):539–44.

59. Maron JL, Jefferies RL. Bush Lupine Mortality, Altered Resource Availability, and Alternative Vegetation States. Ecology. 1999;80(2):443–54.

60. Eng T, Herbert RA, Martinez U, Wang B, Chen JC, Brown JB, et al. Iron Supplementation Eliminates Antagonistic Interactions Between Root-Associated Bacteria. Front Microbiol 2020;11:1742.

61. Long ZT, Karel I. Resource specialization determines whether history influences community structure. Oikos. 2002;96(1):62–9.

62. Tan J, Pu Z, Ryberg WA, Jiang L. Species phylogenetic relatedness, priority effects, and ecosystem functioning. Ecology. 2012;93(5):1164–72.

63. Maignien L, DeForce EA, Chafee ME, Eren AM, Simmons SL. Ecological Succession and Stochastic Variation in the Assembly of Arabidopsis thaliana Phyllosphere Communities. mBio. 2014 Jan 21;5(1):e00682-13.

64. Yassour M, Vatanen T, Siljander H, Hämäläinen AM, Härkönen T, Ryhänen SJ, et al. Natural history of the infant gut microbiome and impact of antibiotic treatment on bacterial strain diversity and stability. Sci Transl Med. 2016 Jun 15;8(343):343ra81-343ra81.

65. Tilman D. Resource Competition between Plankton Algae: An Experimental and Theoretical Approach. Ecology. 1977;58(2):338–48.

66. Tucker CM, Fukami T. Environmental variability counteracts priority effects to facilitate species coexistence: evidence from nectar microbes. Proc R Soc B Biol Sci. 2014 Mar 7;281(1778):20132637.

67. Poza-Carrion C, Suslow T, Lindow S. Resident Bacteria on Leaves Enhance Survival of Immigrant Cells of Salmonella enterica. Phytopathology®. 2013 Apr;103(4):341–51.

68. Monier JM, Lindow SE. Aggregates of Resident Bacteria Facilitate Survival of Immigrant Bacteria on Leaf Surfaces. Microb Ecol. 2005 Apr 1;49(3):343–52.

69. Piccardi P, Vessman B, Mitri S. Toxicity drives facilitation between 4 bacterial species. Proc Natl Acad Sci. 2019 Aug 6;116(32):15979–84.

70. Potnis N, Soto-Arias JP, Cowles KN, van Bruggen AHC, Jones JB, Barak JD. Xanthomonas perforans Colonization Influences Salmonella enterica in the Tomato Phyllosphere. Appl Environ Microbiol. 2014 May 15;80(10):3173–80.

71. Zhang Y, Kastman EK, Guasto JS, Wolfe BE. Fungal networks shape dynamics of bacterial dispersal and community assembly in cheese rind microbiomes. Nat Commun. 2018 Jan 23;9(1):336.

72. Chang PV. Chemical Mechanisms of Colonization Resistance by the Gut Microbial Metabolome. ACS Chem Biol. 2020 May 15;15(5):1119–26.

73. Borton MA, Sabag-Daigle A, Wu J, Solden LM, O'Banion BS, Daly RA, et al. Chemical and pathogen-induced inflammation disrupt the murine intestinal microbiome. Microbiome. 2017 Apr 27;5(1):47.

74. Snelders NC, Rovenich H, Petti GC, Rocafort M, van den Berg GCM, Vorholt JA, et al. Microbiome manipulation by a soil-borne fungal plant pathogen using effector proteins. Nat Plants. 2020 Nov;6(11):1365–74.

75. Foster JL, Fogleman JC. Bacterial succession in necrotic tissue of agria cactus (Stenocereus gummosus). Appl Environ Microbiol. 1994 Feb;60(2):619–25.

76. O'Keeffe KR, Halliday FW, Jones CD, Carbone I, Mitchell CE. Parasites, niche modification and the host microbiome: A field survey of multiple parasites. Mol Ecol. 2021;30(10):2404–16.

77. Joo J, Gunny M, Cases M, Hudson P, Albert R, Harvill E. Bacteriophage-mediated competition in Bordetella bacteria. Proc R Soc B Biol Sci. 2006 Mar 30;273(1595):1843–8.

78. Fernández L, Rodríguez A, García P. Phage or foe: an insight into the impact of viral predation on microbial communities. ISME J. 2018 May;12(5):1171–9.

79. Sweere JM, Van Belleghem JD, Ishak H, Bach MS, Popescu M, Sunkari V, et al. Bacteriophage trigger antiviral immunity and prevent clearance of bacterial infection. Science. 2019 Mar 29;363(6434):eaat9691.

80. Veiga P, Gallini CA, Beal C, Michaud M, Delaney ML, DuBois A, et al. Bifidobacterium animalis subsp. lactis fermented milk product reduces inflammation by altering a niche for colitogenic microbes. Proc Natl Acad Sci. 2010 Oct 19;107(42):18132–7.

81. Topisirovic L, Kojic M, Fira D, Golic N, Strahinic I, Lozo J. Potential of lactic acid bacteria isolated from specific natural niches in food production and preservation. Int J Food Microbiol. 2006 Dec 1;112(3):230–5.

82. Vuyst LD, Leroy F. Bacteriocins from Lactic Acid Bacteria: Production, Purification, and Food Applications. Microb Physiol. 2007;13(4):194–9.

83. ten Cate JM. Biofilms, a new approach to the microbiology of dental plaque. Odontology. 2006 Sep 1;94(1):1–9.

84. Mouillot D, Villéger S, Parravicini V, Kulbicki M, Arias-González JE, Bender M, et al. Functional over-redundancy and high functional vulnerability in global fish faunas on tropical reefs. Proc Natl Acad Sci. 2014 Sep 23;111(38):13757–62.

85. Louca S, Polz MF, Mazel F, Albright MBN, Huber JA, O'Connor MI, et al. Function and functional redundancy in microbial systems. Nat Ecol Evol. 2018 Jun;2(6):936–43.

86. Huttenhower C, Gevers D, Knight R, Abubucker S, Badger JH, Chinwalla AT, et al. Structure, function and diversity of the healthy human microbiome. Nature. 2012 Jun;486(7402):207–14.

87. Zhang QG, Zhang DY. Colonization Sequence Influences Selection and Complementarity Effects on Biomass Production in Experimental Algal Microcosms. Oikos. 2007;116(10):1748–58.

88. Dickie IA, Fukami T, Wilkie JP, Allen RB, Buchanan PK. Do assembly history effects attenuate from species to ecosystem properties? A field test with wood-inhabiting fungi. Ecol Lett. 2012;15(2):133–41.

89. Bittleston LS, Gralka M, Leventhal GE, Mizrahi I, Cordero OX. Context-dependent dynamics lead to the assembly of functionally distinct microbial communities. Nat Commun. 2020 Mar 18;11(1):1440.

90. Boyle JA, Simonsen AK, Frederickson ME, Stinchcombe JR. Priority effects alter interaction outcomes in a legume–rhizobium mutualism. Proc R Soc B Biol Sci. 2021 Mar 10;288(1946):20202753.

91. Fukami T, Morin PJ. Productivity–biodiversity relationships depend on the history of community assembly. Nature. 2003 Jul;424(6947):423–6.

92. Medini D, Donati C, Tettelin H, Masignani V, Rappuoli R. The microbial pan-genome. Curr Opin Genet Dev. 2005 Dec 1;15(6):589–94.

93. Wagg C, Schlaeppi K, Banerjee S, Kuramae EE, van der Heijden MGA. Fungal-bacterial diversity and microbiome complexity predict ecosystem functioning. Nat Commun. 2019 Oct 24;10(1):4841.

94. Gong BQ, Guo J, Zhang N, Yao X, Wang HB, Li JF. Cross-Microbial Protection via Priming a Conserved Immune Co-Receptor through Juxtamembrane Phosphorylation in Plants. Cell Host Microbe. 2019 Dec 11;26(6):810-822.e7.

95. Goldford JE, Lu N, Bajić D, Estrela S, Tikhonov M, Sanchez-Gorostiaga A, et al. Emergent simplicity in microbial community assembly. Science. 2018 Aug 3;361(6401):469–74.

96. Lindemann J. Competition Between Ice Nucleation-Active Wild Type and Ice Nucleation-Deficient Deletion Mutant Strains of *Pseudomonas syringae* and *P. fluorescens* Biovar I and Biological Control of Frost Injury on Strawberry Blossoms. Phytopathology. 1987;77(6):882.

97. Rummens K, De Meester L, Souffreau C. Inoculation history affects community composition in experimental freshwater bacterioplankton communities. Environ Microbiol. 2018;20(3):1120–33.

98. Steen AD, Crits-Christoph A, Carini P, DeAngelis KM, Fierer N, Lloyd KG, et al. High proportions of bacteria and archaea across most biomes remain uncultured. ISME J. 2019 Dec;13(12):3126–30.

99. Imachi H, Nobu MK, Nakahara N, Morono Y, Ogawara M, Takaki Y, et al. Isolation of an archaeon at the prokaryote–eukaryote interface. Nature. 2020 Jan;577(7791):519–25.

100. D'Onofrio A, Crawford JM, Stewart EJ, Witt K, Gavrish E, Epstein S, et al. Siderophores from Neighboring Organisms Promote the Growth of Uncultured Bacteria. Chem Biol. 2010 Mar 26;17(3):254–64.

101. Christian N, Herre EA, Mejia LC, Clay K. Exposure to the leaf litter microbiome of healthy adults protects seedlings from pathogen damage. Proc R Soc B Biol Sci. 2017 Jul 5;284(1858):20170641.

102. Alavi S, Mitchell JD, Cho JY, Liu R, Macbeth JC, Hsiao A. Interpersonal Gut Microbiome Variation Drives Susceptibility and Resistance to Cholera Infection. Cell. 2020 Jun 25;181(7):1533-1546.e13.

103. Hiscox J, Savoury M, Müller CT, Lindahl BD, Rogers HJ, Boddy L. Priority effects during fungal community establishment in beech wood. ISME J. 2015 Oct;9(10):2246–60.

104. Losos JB, Jackman TR, Larson A, Queiroz K de, Rodríguez-Schettino L. Contingency and Determinism in Replicated Adaptive Radiations of Island Lizards. Science. 1998 Mar 27;279(5359):2115–8.

105. Glitzenstein JS, Harcombe PA, Streng DR. Disturbance, Succession, and Maintenance of Species Diversity in an East Texas Forest. Ecol Monogr. 1986;56(3):243–58.

106. Dominguez-Bello MG, Costello EK, Contreras M, Magris M, Hidalgo G, Fierer N, et al. Delivery mode shapes the acquisition and structure of the initial microbiota across multiple body habitats in newborns. Proc Natl Acad Sci. 2010 Jun 29;107(26):11971–5.

107. Bäckhed F, Roswall J, Peng Y, Feng Q, Jia H, Kovatcheva-Datchary P, et al. Dynamics and Stabilization of the Human Gut Microbiome during the First Year of Life. Cell Host Microbe. 2015 May 13;17(5):690–703.

108. Guittar J, Shade A, Litchman E. Trait-based community assembly and succession of the infant gut microbiome. Nat Commun. 2019 Feb 1;10(1):512.

109. Kozich JJ, Westcott SL, Baxter NT, Highlander SK, Schloss PD. Development of a Dual-Index Sequencing Strategy and Curation Pipeline for Analyzing Amplicon Sequence Data on the MiSeq Illumina Sequencing Platform. Appl Environ Microbiol. 2013 Sep;79(17):5112–20.

110. Dixon P. VEGAN, a package of R functions for community ecology. J Veg Sci. 2003;14(6):927–30.

111. Love MI, Huber W, Anders S. Moderated estimation of fold change and dispersion for RNA-seq data with DESeq2. Genome Biol. 2014 Dec 5;15(12):550.

112. Edwards JA, Santos-Medellín CM, Liechty ZS, Nguyen B, Lurie E, Eason S, et al. Compositional shifts in root-associated bacterial and archaeal microbiota track the plant life cycle in field-grown rice. PLOS Biol. 2018 Feb 23;16(2):e2003862.

113. Mahadevan R, Palsson BØ, Lovley DR. In situ to in silico and back: elucidating the physiology and ecology of Geobacter spp. using genome-scale modelling. Nat Rev Microbiol. 2011 Jan;9(1):39–50.

114. Anderson RT, Vrionis HA, Ortiz-Bernad I, Resch CT, Long PE, Dayvault R, et al. Stimulating the In Situ Activity of Geobacter Species To Remove Uranium from the Groundwater of a Uranium-Contaminated Aquifer. Appl Environ Microbiol. 2003 Oct;69(10):5884–91.

115. Elbeltagy A, Ando Y. Expression of nitrogenase gene (nifH) in roots and stems of rice, Oryza sativa, by endophytic nitrogenfixing communities. Afr J Biotechnol. 2008;7(12).

116. Fageria NK. Plant Tissue Test for Determination of Optimum Concentration and Uptake of Nitrogen at Different Growth Stages in Lowland Rice. Commun Soil Sci Plant Anal. 2003 Mar 1;34(1–2):259–70.

117. Chappell CR, Fukami T. Nectar yeasts: a natural microcosm for ecology. Yeast. 2018;35(6):417–23.

118. Loeuille N, Leibold MA. Evolution in Metacommunities: On the Relative Importance of Species Sorting and Monopolization in Structuring Communities. Am Nat. 2008 Jun;171(6):788–99.

119. Vallespir Lowery N, Ursell T. Structured environments fundamentally alter dynamics and stability of ecological communities. Proc Natl Acad Sci. 2019 Jan 8;116(2):379–88.

120. Wittmann MJ, Fukami T. Eco-Evolutionary Buffering: Rapid Evolution Facilitates Regional Species Coexistence despite Local Priority Effects. Am Nat. 2018 Jun;191(6):E171–84.

121. Eitam A, Blaustein L, Mangel M. Density and intercohort priority effects on larval Salamandra salamandra in temporary pools. Oecologia. 2005 Nov 1;146(1):36–42.

122. Woody ST, Ives AR, Nordheim EV, Andrews JH. Dispersal, Density Dependence, and Population Dynamics of a Fungal Microbe on Leaf Surfaces. Ecology. 2007;88(6):1513–24.

123. Wein T, Dagan T, Fraune S, Bosch TCG, Reusch TBH, Hülter NF. Carrying Capacity and Colonization Dynamics of Curvibacter in the Hydra Host Habitat. Front Microbiol. 2018; 9:443.

124. Remus-Emsermann MNP, Lücker S, Müller DB, Potthoff E, Daims H, Vorholt JA. Spatial distribution analyses of natural phyllosphere-colonizing bacteria on Arabidopsis thaliana revealed by fluorescence in situ hybridization. Environ Microbiol. 2014;16(7):2329–40.

125. Urban MC, De Meester L. Community monopolization: local adaptation enhances priority effects in an evolving metacommunity. Proc R Soc B Biol Sci. 2009 Dec 7;276(1676):4129–38.

126. De Meester L, Vanoverbeke J, Kilsdonk LJ, Urban MC. Evolving Perspectives on Monopolization and Priority Effects. Trends Ecol Evol. 2016 Feb 1;31(2):136–46.

127. Madi N, Vos M, Murall CL, Legendre P, Shapiro BJ. Does diversity beget diversity in microbiomes? Weigel D, Kemen E, Wolfe BE, editors. eLife. 2020 Nov 20;9:e58999.

128. Castledine M, Padfield D, Buckling A. Experimental (co)evolution in a multi-species microbial community results in local maladaptation. Ecol Lett. 2020;23(11):1673–81.

129. Tewksbury JJ, Lloyd JD. Positive interactions under nurse-plants: spatial scale, stress gradients and benefactor size. Oecologia. 2001 May 1;127(3):425–34.

130. Monier JM, Lindow SE. Differential survival of solitary and aggregated bacterial cells promotes aggregate formation on leaf surfaces. Proc Natl Acad Sci. 2003 Dec 23;100(26):15977–82.

131. LaSarre B, McCully AL, Lennon JT, McKinlay JB. Microbial mutualism dynamics governed by dose-dependent toxicity of cross-fed nutrients. ISME J. 2017 Feb;11(2):337–48.

132. McCully AL, LaSarre B, McKinlay JB. Growth-independent cross-feeding modifies boundaries for coexistence in a bacterial mutualism. Environ Microbiol. 2017;19(9):3538–50.

133. Nuñez MA, Horton TR, Simberloff D. Lack of belowground mutualisms hinders Pinaceae invasions. Ecology. 2009;90(9):2352–9.

134. Fürst U, Zeng Y, Albert M, Witte AK, Fliegmann J, Felix G. Perception of Agrobacterium tumefaciens flagellin by FLS2XL confers resistance to crown gall disease. Nat Plants. 2020 Jan;6(1):22–7.

135. Lu P, Bian G, Pan X, Xi Z. Wolbachia Induces Density-Dependent Inhibition to Dengue Virus in Mosquito Cells. PLoS Negl Trop Dis. 2012 Jul 24;6(7):e1754.

136. Vannette RL, Fukami T. Historical contingency in species interactions: towards niche-based predictions. Ecol Lett. 2014;17(1):115–24.

137. Onoda Y, Saluñga JB, Akutsu K, Aiba S ichiro, Yahara T, Anten NPR. Trade-off between light interception efficiency and light use efficiency: implications for species coexistence in one-sided light competition. J Ecol. 2014;102(1):167–75.

138. Burson A, Stomp M, Greenwell E, Grosse J, Huisman J. Competition for nutrients and light: testing advances in resource competition with a natural phytoplankton community. Ecology. 2018;99(5):1108–18.

139. Malerba ME, Palacios MM, Palacios Delgado YM, Beardall J, Marshall DJ. Cell size, photosynthesis and the package effect: an artificial selection approach. New Phytol. 2018;219(1):449–61.

140. Hajishengallis G, Liang S, Payne MA, Hashim A, Jotwani R, Eskan MA, et al. Low-Abundance Biofilm Species Orchestrates Inflammatory Periodontal Disease through the Commensal Microbiota and Complement. Cell Host Microbe. 2011 Nov 17;10(5):497–506.

141. Herren CM, McMahon KD. Keystone taxa predict compositional change in microbial communities. Environ Microbiol. 2018;20(6):2207–17.

142. Battin TJ, Kaplan LA, Newbold JD, Cheng X, Hansen C. Effects of Current Velocity on the Nascent Architecture of Stream Microbial Biofilms. Appl Environ Microbiol. 2003 Sep;69(9):5443–52.

143. Tecon R, Ebrahimi A, Kleyer H, Erev Levi S, Or D. Cell-to-cell bacterial interactions promoted by drier conditions on soil surfaces. Proc Natl Acad Sci. 2018 Sep 25;115(39):9791–6.

144. Wal A van der, Tecon R, Kreft JU, Mooij WM, Leveau JHJ. Explaining Bacterial Dispersion on Leaf Surfaces with an Individual-Based Model (PHYLLOSIM). PLOS ONE. 2013 Oct 4;8(10):e75633.

145. Pande S, Kaftan F, Lang S, Svatoš A, Germerodt S, Kost C. Privatization of cooperative benefits stabilizes mutualistic cross-feeding interactions in spatially structured environments. ISME J. 2016 Jun;10(6):1413–23.

146. Momeni B, Waite AJ, Shou W. Spatial self-organization favors heterotypic cooperation over cheating. Tautz D, editor. eLife. 2013 Nov 12;2:e00960.

147. Hol FJH, Galajda P, Woolthuis RG, Dekker C, Keymer JE. The idiosyncrasy of spatial structure in bacterial competition. BMC Res Notes. 2015 Jun 17;8(1):245.

148. Dal Co A, van Vliet S, Kiviet DJ, Schlegel S, Ackermann M. Short-range interactions govern the dynamics and functions of microbial communities. Nat Ecol Evol. 2020 Mar;4(3):366–75.

149. Dang AT, Marsland BJ. Microbes, metabolites, and the gut–lung axis. Mucosal Immunol. 2019 Jul 1;12(4):843–50.

150. Morella NM, Zhang X, Koskella B. Tomato Seed-Associated Bacteria Confer Protection of Seedlings Against Foliar Disease Caused by Pseudomonas syringae. Phytobiomes J. 2019 Jan;3(3):177–90.

151. Scharschmidt TC, Vasquez KS, Truong HA, Gearty SV, Pauli ML, Nosbaum A, et al. A Wave of Regulatory T Cells into Neonatal Skin Mediates Tolerance to Commensal Microbes. Immunity. 2015 Nov 17;43(5):1011–21.

152. Sadd BM, Kleinlogel Y, Schmid-Hempel R, Schmid-Hempel P. Trans-generational immune priming in a social insect. Biol Lett. 2005 Sep;1(4):386–8.

153. Nyholm SV, McFall-Ngai M. The winnowing: establishing the squid–vibrio symbiosis. Nat Rev Microbiol. 2004 Aug;2(8):632–42.

154. O'Hanlon DE, Moench TR, Cone RA. Vaginal pH and Microbicidal Lactic Acid When Lactobacilli Dominate the Microbiota. PLOS ONE. 2013 Nov 6;8(11):e80074.

155. Zhou J, Ning D. Stochastic Community Assembly: Does It Matter in Microbial Ecology? Microbiol Mol Biol Rev. 2017 Oct 11;81(4):e00002-17.

156. Rillig MC, Antonovics J, Caruso T, Lehmann A, Powell JR, Veresoglou SD, et al. Interchange of entire communities: microbial community coalescence. Trends Ecol Evol. 2015 Aug 1;30(8):470–6.

157. Meadow JF, Bateman AC, Herkert KM, O'Connor TK, Green JL. Significant changes in the skin microbiome mediated by the sport of roller derby. PeerJ. 2013 Mar 12;1:e53.

158. Vannette RL. The Floral Microbiome: Plant, Pollinator, and Microbial Perspectives. Annu Rev Ecol Evol Syst. 2020;51(1):363–86.

159. Pachiadaki MG, Brown JM, Brown J, Bezuidt O, Berube PM, Biller SJ, et al. Charting the Complexity of the Marine Microbiome through Single-Cell Genomics. Cell. 2019 Dec 12;179(7):1623-1635.e11.

160. Watrous JD, Dorrestein PC. Imaging mass spectrometry in microbiology. Nat Rev Microbiol. 2011 Sep;9(9):683–94.

161. Hungate BA, Mau RL, Schwartz E, Caporaso JG, Dijkstra P, van Gestel N, et al. Quantitative Microbial Ecology through Stable Isotope Probing. Appl Environ Microbiol. 2015 Nov;81(21):7570–81.

162. Tropini C, Earle KA, Huang KC, Sonnenburg JL. The Gut Microbiome: Connecting Spatial Organization to Function. Cell Host Microbe. 2017 Apr 12;21(4):433–42.

163. Garud NR, Good BH, Hallatschek O, Pollard KS. Evolutionary dynamics of bacteria in the gut microbiome within and across hosts. PLOS Biol. 2019 Jan 23;17(1):e3000102.

164. Braga LPP, Spor A, Kot W, Breuil MC, Hansen LH, Setubal JC, et al. Impact of phages on soil bacterial communities and nitrogen availability under different assembly scenarios. Microbiome. 2020 Apr 6;8(1):52.

165. Rao C, Coyte KZ, Bainter W, Geha RS, Martin CR, Rakoff-Nahoum S. Multi-kingdom ecological drivers of microbiota assembly in preterm infants. Nature. 2021 Mar;591(7851):633–8.

166. Schluter D, Price TD, Grant PR. Ecological Character Displacement in Darwin's Finches. Science. 1985 Mar;227(4690):1056–9.

167. Zee PC, Fukami T. Priority effects are weakened by a short, but not long, history of sympatric evolution. Proc R Soc B Biol Sci. 2018 Jan 31;285(1871):20171722.

168. Suez J, Zmora N, Zilberman-Schapira G, Mor U, Dori-Bachash M, Bashiardes S, et al. Post-Antibiotic Gut Mucosal Microbiome Reconstitution Is Impaired by Probiotics and Improved by Autologous FMT. Cell. 2018 Sep 6;174(6):1406-1423.e16.

169. Pantel JH, Duvivier C, Meester LD. Rapid local adaptation mediates zooplankton community assembly in experimental mesocosms. Ecol Lett. 2015;18(10):992–1000.

170. Fukami T, Beaumont HJE, Zhang XX, Rainey PB. Immigration history controls diversification in experimental adaptive radiation. Nature. 2007 Mar;446(7134):436–9.

171. Rigby MC, Hechinger RF, Stevens L. Why should parasite resistance be costly? Trends Parasitol. 2002 Mar 1;18(3):116–20.

172. Koskella B. Phage-Mediated Selection on Microbiota of a Long-Lived Host. Curr Biol. 2013 Jul 8;23(13):1256–60.

173. Weidlich EWA, Nelson CR, Maron JL, Callaway RM, Delory BM, Temperton VM. Priority effects and ecological restoration. Restor Ecol. 2021;29(1):e13317.

174. Young TP, Stuble KL, Balachowski JA, Werner CM. Using priority effects to manipulate competitive relationships in restoration. Restor Ecol. 2017;25(S2):S114–23.

175. Koskella B, Hall LJ, Metcalf CJE. The microbiome beyond the horizon of ecological and evolutionary theory. Nat Ecol Evol. 2017 Nov;1(11):1606–15.

176. Nadeau CP, Farkas TE, Makkay AM, Papke RT, Urban MC. Adaptation reduces competitive dominance and alters community assembly. Proc R Soc B Biol Sci. 2021 Feb 24;288(1945):20203133.

177. Chappell CR, Dhami MK, Bitter MC, Czech L, Herrera Paredes S, Barrie FB, et al. Wide-ranging consequences of priority effects governed by an overarching factor. Coleman ML, Schuman MC, Bittleston LS, editors. eLife. 2022 Oct 27;11:e79647.

178. Piccardi P, Alberti G, Alexander JM, Mitri S. Microbial invasion of a toxic medium is facilitated by a resident community but inhibited as the community co-evolves. ISME J. 2022 Dec;16(12):2644–52.

179. Meyer KM, Porch R, Muscettola IE, Vasconcelos ALS, Sherman JK, Metcalf CJE, et al. Plant neighborhood shapes diversity and reduces interspecific variation of the phyllosphere microbiome. ISME J. 2022 May;16(5):1376–87.

180. Vorholt JA. Microbial life in the phyllosphere. Nat Rev Microbiol. 2012 Dec;10(12):828–40.

181. Jiang L, Jeong JC, Lee JS, Park JM, Yang JW, Lee MH, et al. Potential of Pantoea dispersa as an effective biocontrol agent for black rot in sweet potato. Sci Rep. 2019 Nov 8;9(1):16354.

182. Toh WK, Loh PC, Wong HL. First Report of Leaf Blight of Rice Caused by Pantoea ananatis and Pantoea dispersa in Malaysia. Plant Dis. 2019 Jul;103(7):1764–1764.

183. Asai N, Koizumi Y, Yamada A, Sakanashi D, Watanabe H, Kato H, et al. Pantoea dispersa bacteremia in an immunocompetent patient: a case report and review of the literature. J Med Case Reports. 2019 Feb 13;13(1):33.

184. Rajendran DK, Park E, Nagendran R, Hung NB, Cho BK, Kim KH, et al. Visual Analysis for Detection and Quantification of Pseudomonas cichorii Disease Severity in Tomato Plants. Plant Pathol J. 2016 Aug;32(4):300–10.

185. Deatherage DE, Barrick JE. Identification of Mutations in Laboratory-Evolved Microbes from Next-Generation Sequencing Data Using breseq. In: Sun L, Shou W, editors. Engineering and Analyzing Multicellular Systems: Methods and Protocols. 2014;1151:165-188.

186. Deatherage DE, Traverse CC, Wolf LN, Barrick JE. Detecting rare structural variation in evolving microbial populations from new sequence junctions using breseq. Front Genet. 2015;5:468.

187. Jeger MJ, Viljanen-Rollinson SLH. The use of the area under the disease-progress curve (AUDPC) to assess quantitative disease resistance in crop cultivars. Theor Appl Genet. 2001 Jan 1;102(1):32–40.

188. Yunis H. Two Sources of Resistance to Bacterial Speck of Tomato Caused by *Pseudomonas tomato*. Plant Dis. 1980;64(9):851.

189. Lindow SE, Arny DC, Upper CD. Bacterial Ice Nucleation: A Factor in Frost Injury to Plants. Plant Physiol. 1982 Oct;70(4):1084–9.

190. Xin XF, Kvitko B, He SY. Pseudomonas syringae: what it takes to be a pathogen. Nat Rev Microbiol. 2018 May;16(5):316–28.

191. Völksch B, Sammer U. Characterization of the Inhibitory Strain Pantoea sp. 48b/90 with Potential as a Biocontrol Agent for Bacterial Plant Pathogens. In: Fatmi M, Collmer A, Iacobellis NS, Mansfield JW, Murillo J, Schaad NW, et al., editors. Pseudomonas syringae Pathovars and Related Pathogens – Identification, Epidemiology and Genomics. 2008.

192. Bodelón G, Palomino C, Fernández LÁ. Immunoglobulin domains in Escherichia coli and other enterobacteria: from pathogenesis to applications in antibody technologies. FEMS Microbiol Rev. 2013 Mar 1;37(2):204–50.

193. Haiko J, Westerlund-Wikström B. The Role of the Bacterial Flagellum in Adhesion and Virulence. Biology. 2013 Dec;2(4):1242–67.

194. Selvakumar G, Kundu S, Joshi P, Nazim S, Gupta AD, Mishra PK, et al. Characterization of a cold-tolerant plant growth-promoting bacterium Pantoea dispersa 1A isolated from a sub-alpine soil in the North Western Indian Himalayas. World J Microbiol Biotechnol. 2008 Jul 1;24(7):955–60.

195. Xin XF, Nomura K, Aung K, Velásquez AC, Yao J, Boutrot F, et al. Bacteria establish an aqueous living space in plants crucial for virulence. Nature. 2016 Nov;539(7630):524–9.

196. Vanoverbeke J, Urban MC, Meester L. Community assembly is a race between immigration and adaptation: eco-evolutionary interactions across spatial scales. Ecography. 2016 Sep;39(9):858–70.

197. Lieberman TD. Detecting bacterial adaptation within individual microbiomes. Philos Trans R Soc B Biol Sci. 2022 Oct 10;377(1861):20210243.

198. Wong DPGH, Good BH. Quantifying the adaptive landscape of commensal gut bacteria using high-resolution lineage tracking. bioRxiv; 2022. p. 2022.05.13.491573. Available from: https://www.biorxiv.org/content/10.1101/2022.05.13.491573v1

199. Beisner B, Haydon D, Cuddington K. Alternative stable states in ecology. Front Ecol Environ. 2003;1(7):376–82.

200. Pautasso M, Dehnen-Schmutz K, Holdenrieder O, Pietravalle S, Salama N, Jeger MJ, et al. Plant health and global change – some implications for landscape management. Biol Rev. 2010;85(4):729–55.

201. Gupta A, Rico-Medina A, Caño-Delgado A. The physiology of plant responses to drought. Science. 2020;368(6488):266–9.

202. St.Clair SB, Lynch JP. The opening of Pandora's Box: climate change impacts on soil fertility and crop nutrition in developing countries. Plant Soil. 2010 Oct 1;335(1):101–15.

203. Pritchard SG. Soil organisms and global climate change. Plant Pathol. 2011;60(1):82–99.

204. Seidl R, Thom D, Kautz M, Martin-Benito D, Peltoniemi M, Vacchiano G, et al. Forest disturbances under climate change. Nat Clim Change. 2017 Jun;7(6):395–402.

205. Bowles TM, Atallah SS, Campbell EE, Gaudin ACM, Wieder WR, Grandy AS. Addressing agricultural nitrogen losses in a changing climate. Nat Sustain. 2018 Aug;1(8):399–408.

206. Naylor D, DeGraaf S, Purdom E, Coleman-Derr D. Drought and host selection influence bacterial community dynamics in the grass root microbiome. ISME J. 2017 Dec;11(12):2691–704.

207. de Vries FT, Griffiths RI, Bailey M, Craig H, Girlanda M, Gweon HS, et al. Soil bacterial networks are less stable under drought than fungal networks. Nat Commun. 2018 Aug 2;9(1):3033.

208. Xu L, Naylor D, Dong Z, Simmons T, Pierroz G, Hixson KK, et al. Drought delays development of the sorghum root microbiome and enriches for monoderm bacteria. Proc Natl Acad Sci. 2018 May;115(18):E4284–93.

209. Rillig MC, Treseder KK, Allen MF. Global Change and Mycorrhizal Fungi. In: van der Heijden MGA, Sanders IR, editors. Mycorrhizal Ecology. Berlin, Heidelberg: Springer; 2003. p. 135–60. (Ecological Studies).

210. Verbruggen E, Toby Kiers E. Evolutionary ecology of mycorrhizal functional diversity in agricultural systems. Evol Appl. 2010;3(5–6):547–60.

211. Smith SE, Read DJ. Mycorrhizal Symbiosis. Academic Press; 2010. 815 p.

212. Johnson NC. Can Fertilization of Soil Select Less Mutualistic Mycorrhizae? Ecol Appl. 1993;3(4):749–57.

213. Weese DJ, Heath KD, Dentinger BTM, Lau JA. Long-term nitrogen addition causes the evolution of less-cooperative mutualists. Evolution. 2015 Mar 1;69(3):631–42.

214. Fürnkranz M, Wanek W, Richter A, Abell G, Rasche F, Sessitsch A. Nitrogen fixation by phyllosphere bacteria associated with higher plants and their colonizing epiphytes of a tropical lowland rainforest of Costa Rica. ISME J. 2008 May;2(5):561–70.

215. Hubbard M, Germida J j., Vujanovic V. Fungal endophytes enhance wheat heat and drought tolerance in terms of grain yield and second-generation seed viability. J Appl Microbiol. 2014;116(1):109–22.

216. Berg M, Koskella B. Nutrient- and Dose-Dependent Microbiome-Mediated Protection against a Plant Pathogen. Curr Biol. 2018 Aug 6;28(15):2487-2492.e3.

217. Carrell AA, Kolton M, Glass JB, Pelletier DA, Warren MJ, Kostka JE, et al. Experimental warming alters the community composition, diversity, and N2 fixation activity of peat moss (Sphagnum fallax) microbiomes. Glob Change Biol. 2019;25(9):2993–3004.

218. Xiang Q, Chen QL, Zhu D, Yang XR, Qiao M, Hu HW, et al. Microbial functional traits in phyllosphere are more sensitive to anthropogenic disturbance than in soil. Environ Pollut. 2020 Oct 1;265:114954.

219. Moles TM, Mariotti L, De Pedro LF, Guglielminetti L, Picciarelli P, Scartazza A. Drought induced changes of leaf-to-root relationships in two tomato genotypes. Plant Physiol Biochem. 2018 Jul 1;128:24–31.

220. Zhou R, Yu X, Zhao T, Ottosen CO, Rosenqvist E, Wu Z. Physiological analysis and transcriptome sequencing reveal the effects of combined cold and drought on tomato leaf. BMC Plant Biol. 2019 Aug 27;19(1):377.

221. Fageria NK, Filho MPB. Dry-Matter and Grain Yield, Nutrient Uptake, and Phosphorus Use-Efficiency of Lowland Rice as Influenced by Phosphorus Fertilization. Commun Soil Sci Plant Anal. 2007 May 1;38(9–10):1289–97.

222. Wang ZH, Li SX, Malhi S. Effects of fertilization and other agronomic measures on nutritional quality of crops. J Sci Food Agric. 2008;88(1):7–23.

223. Liu J, Maldonado-Mendoza I, Lopez-Meyer M, Cheung F, Town CD, Harrison MJ. Arbuscular mycorrhizal symbiosis is accompanied by local and systemic alterations in gene expression and an increase in disease resistance in the shoots. Plant J. 2007;50(3):529–44.

224. Gerlach N, Schmitz J, Polatajko A, Schlüter U, Fahnenstich H, Witt S, et al. An integrated functional approach to dissect systemic responses in maize to arbuscular mycorrhizal symbiosis. Plant Cell Environ. 2015;38(8):1591–612.

225. Barker SJ, Stummer B, Gao L, Dispain I, O'Connor PJ, Smith SE. A mutant in Lycopersicon esculentum Mill. with highly reduced VA mycorrhizal colonization: isolation and preliminary characterisation. Plant J. 1998;15(6):791–7.

226. Baumgartner M, Pfrunder-Cardozo KR, Hall AR. Microbial community composition interacts with local abiotic conditions to drive colonization resistance in human gut microbiome samples. Proc R Soc B Biol Sci. 2021 Mar 24;288(1947):20203106.

227. Callahan BJ, McMurdie PJ, Rosen MJ, Han AW, Johnson AJA, Holmes SP. DADA2: High-resolution sample inference from Illumina amplicon data. Nat Methods. 2016 Jul;13(7):581–3.

228. Kõljalg U, Larsson KH, Abarenkov K, Nilsson RH, Alexander IJ, Eberhardt U, et al. UNITE: a database providing web-based methods for the molecular identification of ectomycorrhizal fungi. New Phytol. 2005;166(3):1063–8.

229. Quast C, Pruesse E, Yilmaz P, Gerken J, Schweer T, Yarza P, et al. The SILVA ribosomal RNA gene database project: improved data processing and web-based tools. Nucleic Acids Res. 2012 Nov 27;41(D1):D590–6.

230. Bengtsson-Palme J, Ryberg M, Hartmann M, Branco S, Wang Z, Godhe A, et al. Improved software detection and extraction of ITS1 and ITS2 from ribosomal ITS sequences of fungi and other eukaryotes for analysis of environmental sequencing data. Methods Ecol Evol. 2013;4(10):914–9.

231. Davis NM, Proctor DM, Holmes SP, Relman DA, Callahan BJ. Simple statistical identification and removal of contaminant sequences in marker-gene and metagenomics data. Microbiome. 2018 Dec 17;6(1):226.

232. Anderson MJ. A new method for non-parametric multivariate analysis of variance. Austral Ecol. 2001;26(1):32–46.

233. Robinson MD, McCarthy DJ, Smyth GK. edgeR: a Bioconductor package for differential expression analysis of digital gene expression data. Bioinformatics. 2010 Jan 1;26(1):139–40.

234. Socolar JB, Gilroy JJ, Kunin WE, Edwards DP. How Should Beta-Diversity Inform Biodiversity Conservation? Trends Ecol Evol. 2016 Jan;31(1):67–80.

235. Suryanarayanan TS, Shaanker RU. Can fungal endophytes fast-track plant adaptations to climate change? Fungal Ecol. 2021 Apr 1;50:101039.

236. Bowles TM, Barrios-Masias FH, Carlisle EA, Cavagnaro TR, Jackson LE. Effects of arbuscular mycorrhizae on tomato yield, nutrient uptake, water relations, and soil carbon dynamics under deficit irrigation in field conditions. Sci Total Environ. 2016 Oct 1;566–567:1223–34.

237. Knief C, Delmotte N, Chaffron S, Stark M, Innerebner G, Wassmann R, et al. Metaproteogenomic analysis of microbial communities in the phyllosphere and rhizosphere of rice. ISME J. 2012 Jul;6(7):1378–90.

238. Gaston KJ. What is rarity? In: Gaston KJ, editor. Rarity. Dordrecht: Springer Netherlands; 1994. p. 1–21. (Population and Community Biology Series).

239. Shoemaker LG, Sullivan LL, Donohue I, Cabral JS, Williams RJ, Mayfield MM, et al. Integrating the underlying structure of stochasticity into community ecology. Ecology. 2020;101(2):e02922.

240. Lynch M, Conery J, Burger R. Mutation Accumulation and the Extinction of Small Populations. Am Nat. 1995;146:4.

241. Cardoso DC, Sandionigi A, Cretoiu MS, Casiraghi M, Stal L, Bolhuis H. Comparison of the active and resident community of a coastal microbial mat. Sci Rep. 2017 Jun 7;7(1):2969.

242. Che R, Deng Y, Wang W, Rui Y, Zhang J, Tahmasbian I, et al. Long-term warming rather than grazing significantly changed total and active soil procaryotic community structures. Geoderma. 2018 Apr 15;316:1–10.

243. Che R, Wang S, Wang Y, Xu Z, Wang W, Rui Y, et al. Total and active soil fungal community profiles were significantly altered by six years of warming but not by grazing. Soil Biol Biochem. 2019 Dec 1;139:107611.

244. Yuste J c., Peñuelas J, Estiarte M, Garcia-Mas J, Mattana S, Ogaya R, et al. Drought-resistant fungi control soil organic matter decomposition and its response to temperature. Glob Change Biol. 2011;17(3):1475–86.

245. Barnard RL, Osborne CA, Firestone MK. Responses of soil bacterial and fungal communities to extreme desiccation and rewetting. ISME J. 2013 Nov;7(11):2229–41.

246. Ochoa-Hueso R, Collins SL, Delgado-Baquerizo M, Hamonts K, Pockman WT, Sinsabaugh RL, et al. Drought consistently alters the composition of soil fungal and bacterial communities in grasslands from two continents. Glob Change Biol. 2018;24(7):2818–27.

247. Preece C, Verbruggen E, Liu L, Weedon JT, Peñuelas J. Effects of past and current drought on the composition and diversity of soil microbial communities. Soil Biol Biochem. 2019 Apr;131:28–39.

248. Sun Y, Chen HYH, Jin L, Wang C, Zhang R, Ruan H, et al. Drought stress induced increase of fungi:bacteria ratio in a poplar plantation. CATENA. 2020 Oct 1;193:104607.

249. Blanchet FG, Cazelles K, Gravel D. Co-occurrence is not evidence of ecological interactions. Ecol Lett. 2020;23(7):1050–63.

250. Scherlach K, Graupner K, Hertweck C. Molecular Bacteria-Fungi Interactions: Effects on Environment, Food, and Medicine. Annu Rev Microbiol. 2013;67(1):375–97.

251. Easlon HM, Richards JH. Drought response in self-compatible species of tomato (Solanaceae). Am J Bot. 2009;96(3):605–11.

252. Augé RM, Toler HD, Saxton AM. Arbuscular mycorrhizal symbiosis alters stomatal conductance of host plants more under drought than under amply watered conditions: a meta-analysis. Mycorrhiza. 2015 Jan 1;25(1):13–24.

253. Al-Karaki G, McMichael B, Zak J. Field response of wheat to arbuscular mycorrhizal fungi and drought stress. Mycorrhiza. 2004 Aug 1;14(4):263–9.

254. Lazcano C, Barrios-Masias FH, Jackson LE. Arbuscular mycorrhizal effects on plant water relations and soil greenhouse gas emissions under changing moisture regimes. Soil Biol Biochem. 2014 Jul;74:184–92.

255. Beattie GA, Lindow SE. Bacterial Colonization of Leaves: A Spectrum of Strategies. Phytopathology®. 1999 May;89(5):353–9.

256. Larkan NJ, Ruzicka DR, Edmonds-Tibbett T, Durkin JMH, Jackson LE, Smith FA, et al. The reduced mycorrhizal colonisation (rmc) mutation of tomato disrupts five gene sequences including the CYCLOPS/IPD3 homologue. Mycorrhiza. 2013 Oct 1;23(7):573–84.

257. Prihatna C, Barbetti MJ, Barker SJ. A Novel Tomato Fusarium Wilt Tolerance Gene. Front Microbiol. 2018;9:1226.

258. Cavagnaro TR, Jackson LE, Six J, Ferris H, Goyal S, Asami D, et al. Arbuscular Mycorrhizas, Microbial Communities, Nutrient Availability, and Soil Aggregates in Organic Tomato Production. Plant Soil. 2006 Apr 1;282(1):209–25.

259. Facelli E, Smith SE, Facelli JM, Christophersen HM, Andrew Smith F. Underground friends or enemies: model plants help to unravel direct and indirect effects of arbuscular mycorrhizal fungi on plant competition. New Phytol. 2010;185(4):1050–61.

260. Messinese E, Mun JH, Yeun LH, Jayaraman D, Rougé P, Barre A, et al. A Novel Nuclear Protein Interacts With the Symbiotic DMI3 Calcium- and Calmodulin-Dependent Protein Kinase of Medicago truncatula. Mol Plant-Microbe Interactions®. 2007 Aug;20(8):912–21.

261. Yano K, Yoshida S, Müller J, Singh S, Banba M, Vickers K, et al. CYCLOPS, a mediator of symbiotic intracellular accommodation. Proc Natl Acad Sci. 2008 Dec 23;105(51):20540–5.

262. Azcón-Aguilar C, Barea JM, Gianinazzi S, Gianinazzi-Pearson V, editors. Mycorrhizas - Functional Processes and Ecological Impact. Berlin, Heidelberg: Springer Berlin Heidelberg; 2009.

263. Vogel C, Bodenhausen N, Gruissem W, Vorholt JA. The Arabidopsis leaf transcriptome reveals distinct but also overlapping responses to colonization by phyllosphere commensals and pathogen infection with impact on plant health. New Phytol. 2016;212(1):192–207.

264. Bodenhausen N, Bortfeld-Miller M, Ackermann M, Vorholt JA. A Synthetic Community Approach Reveals Plant Genotypes Affecting the Phyllosphere Microbiota. PLOS Genet. 2014 Apr 17;10(4):e1004283.

265. Chen T, Nomura K, Wang X, Sohrabi R, Xu J, Yao L, et al. A plant genetic network for preventing dysbiosis in the phyllosphere. Nature. 2020 Apr;580(7805):653–7.

266. Copeland JK, Yuan L, Layeghifard M, Wang PW, Guttman DS. Seasonal Community Succession of the Phyllosphere Microbiome. Mol Plant-Microbe Interactions®. 2015 Mar;28(3):274–85.

267. Marschner P, Baumann K. Changes in bacterial community structure induced by mycorrhizal colonisation in split-root maize. Plant Soil. 2003 Apr 1;251(2):279–89.

268. Bergmark L, Poulsen PHB, Al-Soud WA, Norman A, Hansen LH, Sørensen SJ. Assessment of the specificity of Burkholderia and Pseudomonas qPCR assays for detection of these genera in soil using 454 pyrosequencing. FEMS Microbiol Lett. 2012 Aug 1;333(1):77–84.

269. Callahan BJ, McMurdie PJ, Holmes SP. Exact sequence variants should replace operational taxonomic units in marker-gene data analysis. ISME J. 2017 Dec;11(12):2639–43.

270. Sloan WT, Lunn M, Woodcock S, Head IM, Nee S, Curtis TP. Quantifying the roles of immigration and chance in shaping prokaryote community structure. Environ Microbiol. 2006;8(4):732–40.

271. Burns AR, Stephens WZ, Stagaman K, Wong S, Rawls JF, Guillemin K, et al. Contribution of neutral processes to the assembly of gut microbial communities in the zebrafish over host development. ISME J. 2016 Mar;10(3):655–64.

272. Chibani-Chennoufi S, Bruttin A, Dillmann ML, Brüssow H. Phage-Host Interaction: an Ecological Perspective. J Bacteriol. 2004 Jun 15;186(12):3677–86.

273. Marsh P, Wellington EMH. Phage-host interactions in soil. FEMS Microbiol Ecol. 1994 Nov 1;15(1–2):99–107.

274. Wigington CH, Sonderegger D, Brussaard CPD, Buchan A, Finke JF, Fuhrman JA, et al. Re-examination of the relationship between marine virus and microbial cell abundances. Nat Microbiol. 2016 Jan 25;1(3):1–9.

275. Emerson JB, Roux S, Brum JR, Bolduc B, Woodcroft BJ, Jang HB, et al. Host-linked soil viral ecology along a permafrost thaw gradient. Nat Microbiol. 2018 Aug;3(8):870–80.

276. Suttle CA. The significance of viruses to mortality in aquatic microbial communities. Microb Ecol. 1994 Sep 1;28(2):237–43.

277. Koskella B, Brockhurst MA. Bacteria–phage coevolution as a driver of ecological and evolutionary processes in microbial communities. FEMS Microbiol Rev. 2014;38(5):916–31.

278. Koskella B, Meaden S. Understanding bacteriophage specificity in natural microbial communities. Viruses. 2013;5(3):806–23.

279. Koskella B, Taylor TB. Multifaceted Impacts of Bacteriophages in the Plant Microbiome. Annu Rev Phytopathol. 2018;56(1):361–80.

280. Carlton RM. Phage therapy: past history and future prospects. Arch Immunol Ther Exp (Warsz). 1999;47(5):267–74.

281. Barr JJ, Auro R, Furlan M, Whiteson KL, Erb ML, Pogliano J, et al. Bacteriophage adhering to mucus provide a non–host-derived immunity. Proc Natl Acad Sci. 2013 Jun 25;110(26):10771–6.

282. Barr JJ, Youle M, Rohwer F. Innate and acquired bacteriophage-mediated immunity. Bacteriophage. 2013 Jul 11;3(3):e25857.

283. Schooley RT, Biswas B, Gill JJ, Hernandez-Morales A, Lancaster J, Lessor L, et al. Development and Use of Personalized Bacteriophage-Based Therapeutic Cocktails To Treat a Patient with a Disseminated Resistant Acinetobacter baumannii Infection. Antimicrob Agents Chemother. 2017 Sep 22;61(10):e00954-17.

284. Chan BK, Turner PE, Kim S, Mojibian HR, Elefteriades JA, Narayan D. Phage treatment of an aortic graft infected with Pseudomonas aeruginosa. Evol Med Public Health. 2018 Jan 1;2018(1):60–6.

285. Doss J, Culbertson K, Hahn D, Camacho J, Barekzi N. A Review of Phage Therapy against Bacterial Pathogens of Aquatic and Terrestrial Organisms. Viruses. 2017 Mar;9(3):50.

286. Balogh B, Jones JB, Iriarte FB, Momol MT. Phage Therapy for Plant Disease Control. Curr Pharm Biotechnol. 2010 Jan 1;11(1):48–57.

287. Kortright KE, Chan BK, Koff JL, Turner PE. Phage Therapy: A Renewed Approach to Combat Antibiotic-Resistant Bacteria. Cell Host Microbe. 2019 Feb 13;25(2):219–32.

288. Wang X, Wei Z, Yang K, Wang J, Jousset A, Xu Y, et al. Phage combination therapies for bacterial wilt disease in tomato. Nat Biotechnol. 2019 Dec;37(12):1513–20.

289. Wagner J, Maksimovic J, Farries G, Sim WH, Bishop RF, Cameron DJ, et al. Bacteriophages in Gut Samples From Pediatric Crohn's Disease Patients: Metagenomic Analysis Using 454 Pyrosequencing. Inflamm Bowel Dis. 2013 Jul 1;19(8):1598–608.

290. Norman JM, Handley SA, Baldridge MT, Droit L, Liu CY, Keller BC, et al. Disease-Specific Alterations in the Enteric Virome in Inflammatory Bowel Disease. Cell. 2015 Jan 29;160(3):447–60.

291. Yang K, Wang X, Hou R, Lu C, Fan Z, Li J, et al. Rhizosphere phage communities drive soil suppressiveness to bacterial wilt disease. Microbiome. 2023 Feb 1;11(1):16.

292. Federici S, Nobs SP, Elinav E. Phages and their potential to modulate the microbiome and immunity. Cell Mol Immunol. 2021;18(4):889–904.

293. Li Y, Fu X, Ma J, Zhang J, Hu Y, Dong W, et al. Altered respiratory virome and serum cytokine profile associated with recurrent respiratory tract infections in children. Nat Commun. 2019 May 23;10(1):2288.

294. Dufour N, Delattre R, Chevallereau A, Ricard JD, Debarbieux L. Phage Therapy of Pneumonia Is Not Associated with an Overstimulation of the Inflammatory Response Compared to Antibiotic Treatment in Mice. Antimicrob Agents Chemother. 2019 Jul 25;63(8):e00379-19.

295. Li M, Wei Z, Wang J, Jousset A, Friman VP, Xu Y, et al. Facilitation promotes invasions in plant-associated microbial communities. Ecol Lett. 2019;22(1):149–58.

296. Wei Z, Gu Y, Friman VP, Kowalchuk GA, Xu Y, Shen Q, et al. Initial soil microbiome composition and functioning predetermine future plant health. Sci Adv. 2019 Sep 25;5(9):eaaw0759.

297. Hoy SR, MacNulty DR, Metz MC, Smith DW, Stahler DR, Peterson RO, et al. Negative frequency-dependent prey selection by wolves and its implications on predator–prey dynamics. Anim Behav. 2021 Sep 1;179:247–65.

298. Greenwood JJD, Elton RA. Analysing Experiments on Frequency-Dependent Selection by Predators. J Anim Ecol. 1979;48(3):721–37.

299. Allen JA, Greenwood JJD, Clarke BC, Partridge L, Robertson A, Clarke BC, et al. Frequency-dependent selection by predators. Philos Trans R Soc Lond B Biol Sci. 1997 Jan;319(1196):485–503.

300. Rodriguez-Valera F, Martín-Cuadrado AB, Rodriguez-Brito B, Pasic L, Thingstad TF, Rohwer F, et al. Explaining microbial population genomics through phage predation. Nat Preced. 2009 Jul 29;1–1.

301. Thingstad TF. Elements of a theory for the mechanisms controlling abundance, diversity, and biogeochemical role of lytic bacterial viruses in aquatic systems. Limnol Oceanogr. 2000;45(6):1320–8.

302. Rodriguez-Brito B, Li L, Wegley L, Furlan M, Angly F, Breitbart M, et al. Viral and microbial community dynamics in four aquatic environments. ISME J. 2010 Jun;4(6):739–51.

303. Bouvier T, Del Giorgio PA. Key role of selective viral-induced mortality in determining marine bacterial community composition. Environ Microbiol. 2007 Feb;9(2):287–97.

304. Harrison XA, Price SJ, Hopkins K, Leung WTM, Sergeant C, Garner TWJ. Diversity-Stability Dynamics of the Amphibian Skin Microbiome and Susceptibility to a Lethal Viral Pathogen. Front Microbiol. 2019;10.

305. Rooney WM, Grinter RW, Correia A, Parkhill J, Walker DC, Milner JJ. Engineering bacteriocin-mediated resistance against the plant pathogen Pseudomonas syringae. Plant Biotechnol J. 2020 May;18(5):1296–306.

306. Zembek P, Danilecka A, Hoser R, Eschen-Lippold L, Benicka M, Grech-Baran M, et al. Two Strategies of Pseudomonas syringae to Avoid Recognition of the HopQ1 Effector in Nicotiana Species. Front Plant Sci. 2018;9:978.

307. Schwalbach MS, Hewson I, Fuhrman JA. Viral effects on bacterial community composition in marine plankton microcosms. Aquat Microb Ecol. 2004 Feb 4;34(2):117–27.

308. Wilcox R, Fuhrman J. Bacterial viruses in coastal seawater: lytic rather than lysogenic production. Mar Ecol Prog Ser. 1994;114:35–45.

309. Meaden S, Koskella B. Adaptation of the pathogen, Pseudomonas syringae, during experimental evolution on a native vs. alternative host plant. Mol Ecol. 2017;26(7):1790–801.

310. Morella NM, Yang SC, Hernandez CA, Koskella B. Rapid quantification of bacteriophages and their bacterial hosts in vitro and in vivo using droplet digital PCR. J Virol Methods. 2018 Sep 1;259:18–24.

311. Hirano SS, Upper CD. Population Biology and Epidemiology of Pseudomonas Syringae. Annu Rev Phytopathol. 1990;28(1):155–77.

312. Bonilla N, Rojas MI, Cruz GNF, Hung SH, Rohwer F, Barr JJ. Phage on tap–a quick and efficient protocol for the preparation of bacteriophage laboratory stocks. PeerJ. 2016 Jul 26;4:e2261.

313. Bourdin G, Schmitt B, Marvin Guy L, Germond JE, Zuber S, Michot L, et al. Amplification and Purification of T4-Like Escherichia coli Phages for Phage Therapy: from Laboratory to Pilot Scale. Appl Environ Microbiol. 2014 Feb 15;80(4):1469–76.

314. Branston SD, Wright J, Keshavarz-Moore E. A non-chromatographic method for the removal of endotoxins from bacteriophages. Biotechnol Bioeng. 2015;112(8):1714–9.

315. Erskine JM. Characteristics of Erwinia amylovora bacteriophage and its possible role in the epidemiology of fire blight. Can J Microbiol. 1973 Jul;19(7):837–45.

316. Gill JJ, Svircev AM, Smith R, Castle AJ. Bacteriophages of Erwinia amylovora. Appl Environ Microbiol. 2003 Apr;69(4):2133–8.

317. Hernandez CA, Koskella B. Phage resistance evolution in vitro is not reflective of in vivo outcome in a plant-bacteria-phage system*. Evolution. 2019 Dec 1;73(12):2461–75.

318. Vogwill T, Fenton A, Brockhurst MA. How does spatial dispersal network affect the evolution of parasite local adaptation? Evolution. 2010 Jun 1;64(6):1795–801.

319. Vos M, Birkett PJ, Birch E, Griffiths RI, Buckling A. Local Adaptation of Bacteriophages to Their Bacterial Hosts in Soil. Science. 2009 Aug 14;325(5942):833–833.

320. Koskella B. Bacteria-Phage Interactions across Time and Space: Merging Local Adaptation and Time-Shift Experiments to Understand Phage Evolution. Am Nat. 2014 Aug;184(S1):S9–21.

321. Lopez Pascua L, Gandon S, Buckling A. Abiotic heterogeneity drives parasite local adaptation in coevolving bacteria and phages. J Evol Biol. 2012;25(1):187–95.

322. Tan J, Wei N, Turcotte MM. Trophic interactions in microbiomes influence plant host population size and ecosystem function. bioRxiv; 2023. p. 2023.03.06.531362. Available from: https://www.biorxiv.org/content/10.1101/2023.03.06.531362v1

323. Abedon ST. Phage therapy dosing: The problem(s) with multiplicity of infection (MOI). Bacteriophage. 2016 Jul 2;6(3):e1220348.

324. Ossowicki A, Raaijmakers JM, Garbeva P. Disentangling soil microbiome functions by perturbation. Environ Microbiol Rep. 2021;13(5):582–90.

325. Stenseth N, Smith JM. Coevolution in ecosystems: Red Queen evolution or stasis? Evolution. 1984;870–80.

326. Gómez JM, Verdú M, Perfectti F. Ecological interactions are evolutionarily conserved across the entire tree of life. Nature. 2010 Jun;465(7300):918–21.

327. Clay K, Kover PX. The Red Queen hypothesis and plant/pathogen interactions. Annu Rev Phytopathol. 1996;34(1):29–50.

328. Sheldon BC, Verhulst S. Ecological immunology: costly parasite defences and trade-offs in evolutionary ecology. Trends Ecol Evol. 1996;11(8):317–21.

329. Waterbury JB, Valois FW. Resistance to co-occurring phages enables marine Synechococcus communities to coexist with cyanophages abundant in seawater. Appl Environ Microbiol. 1993;59(10):3393–9.

330. Stahl EA, Dwyer G, Mauricio R, Kreitman M, Bergelson J. Dynamics of disease resistance polymorphism at the Rpm1 locus of Arabidopsis. Nature. 1999;400(6745):667–71.

331. Lourenço M, Chaffringeon L, Lamy-Besnier Q, Pédron T, Campagne P, Eberl C, et al. The spatial heterogeneity of the gut limits predation and fosters coexistence of bacteria and bacteriophages. Cell Host Microbe. 2020;28(3):390–401.

332. Faria VG, Martins NE, Paulo T, Teixeira L, Sucena É, Magalhães S. Evolution of Drosophila resistance against different pathogens and infection routes entails no detectable maintenance costs. Evolution. 2015;69(11):2799–809.

333. Durão P, Balbontín R, Gordo I. Evolutionary Mechanisms Shaping the Maintenance of Antibiotic Resistance. Trends Microbiol. 2018 Aug;26(8):677–91.

334. Shah P, McCandlish DM, Plotkin JB. Contingency and entrenchment in protein evolution under purifying selection. Proc Natl Acad Sci. 2015;112(25):E3226–35.

335. Woods RJ, Barrick JE, Cooper TF, Shrestha U, Kauth MR, Lenski RE. Second-order selection for evolvability in a large Escherichia coli population. Science. 2011;331(6023):1433–6.

336. Brockhurst MA, Morgan AD, Fenton A, Buckling A. Experimental coevolution with bacteria and phage: the Pseudomonas fluorescens—Φ2 model system. Infect Genet Evol. 2007;7(4):547–52.

337. Dennehy JJ. What can phages tell us about host-pathogen coevolution? Int J Evol Biol. 2012;2012.

338. Dy RL, Richter C, Salmond GP, Fineran PC. Remarkable mechanisms in microbes to resist phage infections. Annu Rev Virol. 2014;1:307–31.

339. Mangalea MR, Duerkop BA. Fitness trade-offs resulting from bacteriophage resistance potentiate synergistic antibacterial strategies. Infect Immun. 2020;88(7):e00926-19.

340. Koskella B. Resistance gained, resistance lost: an explanation for host–parasite coexistence. PLoS Biol. 2018;16(9):e3000013.

341. Chaudhry WN, Pleška M, Shah NN, Weiss H, McCall IC, Meyer JR, et al. Leaky resistance and the conditions for the existence of lytic bacteriophage. PLoS Biol. 2018;16(8):e2005971.

342. Koskella B, Parr N. The evolution of bacterial resistance against bacteriophages in the horse chestnut phyllosphere is general across both space and time. Philos Trans R Soc B Biol Sci. 2015;370(1675):20140297.

343. Meyer JR, Agrawal AA, Quick RT, Dobias DT, Schneider D, Lenski RE. Parallel changes in host resistance to viral infection during 45,000 generations of relaxed selection. Evol Int J Org Evol. 2010;64(10):3024–34.

344. Avrani S, Lindell D. Convergent evolution toward an improved growth rate and a reduced resistance range in Prochlorococcus strains resistant to phage. Proc Natl Acad Sci. 2015;112(17):E2191–200.

345. Burlage RS, Atlas R, Stahl D, Sayler G, Geesey G. Techniques in microbial ecology. Oxford University Press on Demand; 1998.

346. Young JM, Luketina RC, Marshall AM. The effects on temperature on growth in vitro of Pseudomonas syringae and Xanthomonas pruni. J Appl Bacteriol. 1977;42(3):345–54.

347. Testa S, Berger S, Piccardi P, Oechslin F, Resch G, Mitri S. Spatial structure affects phage efficacy in infecting dual-strain biofilms of Pseudomonas aeruginosa. Commun Biol. 2019;2(1):1–12.

348. Simmons EL, Bond MC, Koskella B. Biofilm Structure Promotes Coexistence of Phage-Resistant and Phage-Susceptible. MSystems 5 3. 2020;

349. Bolger AM, Lohse M, Usadel B. Trimmomatic: a flexible trimmer for Illumina sequence data. Bioinformatics. 2014;30(15):2114–20.

350. Card KJ, Thomas MD, Graves JL, Barrick JE, Lenski RE. Genomic evolution of antibiotic resistance is contingent on genetic background following a long-term experiment with Escherichia coli. Proc Natl Acad Sci. 2021 Feb 2;118(5):e2016886118.

351. Kutschera A, Schombel U, Schwudke D, Ranf S, Gisch N. Analysis of the structure and biosynthesis of the lipopolysaccharide core oligosaccharide of Pseudomonas syringae pv. tomato DC3000. Int J Mol Sci. 2021;22(6):3250.

352. Gong LI, Suchard MA, Bloom JD. Stability-mediated epistasis constrains the evolution of an influenza protein. Elife. 2013;2:e00631.

353. Shaver AC, Dombrowski PG, Sweeney JY, Treis T, Zappala RM, Sniegowski PD. Fitness Evolution and the Rise of Mutator Alleles in Experimental Escherichia coli Populations. Genetics. 2002 Oct 1;162(2):557–66.

354. Harris KB, Flynn KM, Cooper VS. Polygenic adaptation and clonal interference enable sustained diversity in experimental Pseudomonas aeruginosa populations. Mol Biol Evol. 2021;38(12):5359–75.

355. Thurber RV. Current insights into phage biodiversity and biogeography. Curr Opin Microbiol. 2009;12(5):582–7.

356. Weinbauer MG, Rassoulzadegan F. Are viruses driving microbial diversification and diversity? Environ Microbiol. 2004;6(1):1–11.

357. Burmeister AR, Fortier A, Roush C, Lessing AJ, Bender RG, Barahman R, et al. Pleiotropy complicates a trade-off between phage resistance and antibiotic resistance. Proc Natl Acad Sci. 2020;117(21):11207–16.

358. Pal C, Maciá MD, Oliver A, Schachar I, Buckling A. Coevolution with viruses drives the evolution of bacterial mutation rates. Nature. 2007;450(7172):1079–81.

359. Bohannan BJ, Lenski RE. Linking genetic change to community evolution: insights from studies of bacteria and bacteriophage. Ecol Lett. 2000;3(4):362–77.

360. Picken RN, Beacham IR. Bacteriophage-resistant mutants of Escherichia coliK12. Location of receptors within the lipopolysaccharide. Microbiology. 1977;102(2):305–18.

361. Evans TJ, Ind A, Komitopoulou E, Salmond GPC. Phage-selected lipopolysaccharide mutants of Pectobacterium atrosepticum exhibit different impacts on virulence. J Appl Microbiol. 2010;109(2):505–14.

362. Meaden S, Paszkiewicz K, Koskella B. The cost of phage resistance in a plant pathogenic bacterium is context-dependent. Evolution. 2015;69(5):1321–8.

363. Kulikov EE, Golomidova AK, Prokhorov NS, Ivanov PA, Letarov AV. High-throughput LPS profiling as a tool for revealing of bacteriophage infection strategies. Sci Rep. 2019 Feb 27;9(1):2958.

364. Holtappels D, Kerremans A, Busschots Y, Van Vaerenbergh J, Maes M, Lavigne R, et al. Preparing for the KIL: Receptor analysis of Pseudomonas syringae pv. porri phages and their impact on bacterial virulence. Int J Mol Sci. 2020;21(8):2930.

365. Kircher M, Kelso J. High-throughput DNA sequencing–concepts and limitations. Bioessays. 2010;32(6):524–36.

366. Bull JJ, Vegge CS, Schmerer M, Chaudhry WN, Levin BR. Phenotypic resistance and the dynamics of bacterial escape from phage control. PloS One. 2014;9(4):e94690.

367. Scanlan PD, Buckling A, Hall AR. Experimental evolution and bacterial resistance:(co) evolutionary costs and trade-offs as opportunities in phage therapy research. Bacteriophage. 2015;5(2):e1050153.

368. Teotónio H, Rose MR. Perspective: reverse evolution. Evolution. 2001;55(4):653–60.

369. McCandlish DM, Shah P, Plotkin JB. Epistasis and the dynamics of reversion in molecular evolution. Genetics. 2016;203(3):1335–51.

370. Pennings PS, Ogbunugafor CB, Hershberg R. Reversion is most likely under high mutation supply when compensatory mutations do not fully restore fitness costs. G3. 2022;12(9):jkac190.

371. Rojas Echenique JI, Kryazhimskiy S, Nguyen Ba AN, Desai MM. Modular epistasis and the compensatory evolution of gene deletion mutants. PLoS Genet. 2019;15(2):e1007958.

372. Conte GL, Arnegard ME, Peichel CL, Schluter D. The probability of genetic parallelism and convergence in natural populations. Proc R Soc B Biol Sci. 2012;279(1749):5039–47.

373. Goldstein RA, Pollard ST, Shah SD, Pollock DD. Nonadaptive amino acid convergence rates decrease over time. Mol Biol Evol. 2015;32(6):1373–81.

374. Travisano M, Mongold JA, Bennett AF, Lenski RE. Experimental tests of the roles of adaptation, chance, and history in evolution. Science. 1995;267(5194):87–90.

375. Yen P, Papin JA. History of antibiotic adaptation influences microbial evolutionary dynamics during subsequent treatment. PLoS Biol. 2017;15(8):e2001586.

376. Santos-Lopez A, Marshall CW, Haas AL, Turner C, Rasero J, Cooper VS. The roles of history, chance, and natural selection in the evolution of antibiotic resistance. Elife. 2021;10:e70676.

377. Feldman CR, Brodie Jr ED, Brodie III ED, Pfrender ME. Constraint shapes convergence in tetrodotoxin-resistant sodium channels of snakes. Proc Natl Acad Sci. 2012;109(12):4556–61.

378. Toledo G, Hanifin C, Geffeney S, Brodie III ED. Convergent evolution of tetrodotoxin-resistant sodium channels in predators and prey. Curr Top Membr. 2016;78:87–113.

379. Sharma RS, Mishra V, Mohmmed A, Babu CR. Phage specificity and lipopolysaccarides of stem-and root-nodulating bacteria (Azorhizobium caulinodans, Sinorhizobium spp., and Rhizobium spp.) of Sesbania spp. Arch Microbiol. 2008;189(4):411–8.

380. Triantafilou M, Triantafilou K. Invited review: the dynamics of LPS recognition: complex orchestration of multiple receptors. J Endotoxin Res. 2005;11(1):5–11.

381. Newman MA, Dow JM, Molinaro A, Parrilli M. Invited review: priming, induction and modulation of plant defence responses by bacterial lipopolysaccharides. J Endotoxin Res. 2007;13(2):69–84.

382. Wahida A, Tang F, Barr JJ. Rethinking phage-bacteria-eukaryotic relationships and their influence on human health. Cell Host Microbe. 2021;29(5):681–8.

383. Mutalik VK, Adler BA, Rishi HS, Piya D, Zhong C, Koskella B, et al. High-throughput mapping of the phage resistance landscape in E. coli. PLOS Biol. 2020 Oct 13;18(10):e3000877.

384. Debray R, De Luna N, Koskella B. Historical Contingency Drives Compensatory Evolution and Rare Reversal of Phage Resistance. Mol Biol Evol. 2022 Sep 1;39(9):msac182.

385. Gordillo Altamirano FL, Barr JJ. Unlocking the next generation of phage therapy: the key is in the receptors. Curr Opin Biotechnol. 2021 Apr 1;68:115–23.

386. Beckett SJ, Williams HTP. Coevolutionary diversification creates nested-modular structure in phage–bacteria interaction networks. Interface Focus. 2013 Dec 6;3(6):20130033.

387. Alberts SC, Altmann J. The Amboseli Baboon Research Project: 40 years of continuity and change. In: Long-term field studies of primates. Springer; 2012. p. 261–87.

# Appendix A: Identifying inequities in mentorship and addressing student needs

*Summary of motivation and methods*

Most graduate students view the relationship with their faculty advisor as the single most important factor in their graduate experience. Faculty support is instrumental in applying for funding, accessing departmental resources, planning research projects, and obtaining letters of recommendation. While the importance of this relationship is universal, students vary widely in their specific needs and expectations. Mentorship is a key priority for efforts to improve diversity in science both because poor or inequitable mentorship can exacerbate existing disparities and because effective mentorship can help students overcome them.

Results of graduate student surveys in the Integrative Biology department implicate student-faculty relationships as a key area of need for building an inclusive community. In a 2020 department-wide survey, the majority of students (81.1%) had experienced discrimination or microaggressions perpetrated by faculty. Few indicated that they were willing to share experiences of discrimination with their advisor (5.9%), compared to sharing with their peers (86.9%), or keeping the experience to themselves (36.9%). These reports indicate the need for better mentoring in IB, yet past surveys have not identified mentoring practices that predict student outcomes, or asked how these needs vary across student backgrounds.

In response to a funding call for projects that would improve diversity and equity in the IB department, we conducted a research study on effective mentorship. In consultation with the UCB Division of Equity and Inclusion and the UCB Committee for the Protection of Human Subjects, we developed a 71-question survey that asked respondents to evaluate their advisors, research groups, and departments on a five-point scale and solicited quantitative and qualitative measures of their productivity and well-being. We administered the survey to current graduate students in the Integrative Biology, Plant and Microbial Biology, Molecular and Cell Biology, and Environmental Science, Policy, and Management departments. Our sample size of 129 respondents (~24% response rate) generally reflected the underlying gender and racial proportions of the graduate programs that we surveyed (Tables 1-3).

*Experiences within and across departments*

IB (and in some cases ESPM) students consistently rated their experiences lower than students in PMB and MCB. This was true for a range of aspects including the culture of research groups, inclusion and belonging in the department as a whole, and self-assessed career preparedness after graduate school (Figure 1). Within the IB department, students associated with museums had different experiences than students in unaffiliated labs.

Museum-affiliated labs were smaller, yet students in museums reported a stronger sense of belonging and better peer support, potentially reflecting a sense of inter-lab community in museums. However, students in museum-affiliated labs also reported being more negatively impacted by lab and/or travel restrictions during COVID-19 (Figure 2). This might reflect the difficulty of social distancing in large, shared spaces or the possibility that museum-

affiliated researchers are more involved in fieldwork, live animal care, or other activities impacted by COVID-19 restrictions.

*Experiences of students from varying backgrounds*

Several groups of students were significant less likely than their counterparts to experience supportive relationships with their advisors or inclusive research environments: i) Female students, ii) Students who started their graduate degree after the age of 30, and iii) Non-traditional students, e.g. parents or caregivers, first-generation students, students with a disability, or veterans (these categories were all grouped together to protect anonymity of respondents) (Figures 3-5). These discrepancies may reflect direct effects (e.g. unconscious bias towards female students, social activities that conflict with childcare duties) and/or indirect effects (e.g. students that start their degree later in life are often from less privileged backgrounds and have faced other barriers to success). Indeed, the effects of multiple marginalized identities on student experiences were compounded (Figure 6).

It is important to mention that the three categories identified above were among the most statistically tractable demographic groups in our survey. For example, when selecting their gender identity, most respondents fell into one of two groups, and sample sizes for those groups were close to evenly distributed. In contrast, the racial identity question had many categories, students often selected multiple identities, and subgroups had uneven distributions, making it potentially difficult to analyze responses in ways that meaningfully reflected their lived experiences. Additionally, some students elected not to provide any specific identification factors in certain demographic questions (i.e., they elected "Prefer not to disclose" as a response). These students consistently reported less support from their advisors, labs, and departments than students who answered the questions, suggesting that the unhappiest graduate students did not even trust the survey (Figures 7-8). True effects of race, ethnicity, or sexual orientation may therefore be masked due to these data collection and analysis challenges.

*Representation by advisors*

The vast majority (86.5%) of respondents reported that they identified with a demographic that had been historically underrepresented in the biological sciences (such as gender, race, first-generation, etc.). We asked these respondents whether their advisor was also a member of that demographic group. Students who felt represented by their advisors were happier and more productive by nearly every metric we measured: they felt their advisors were more empathetic, that they understood what their advisors expected of them, that they belonged in their graduate program, and that they were prepared for an academic or non-academic career after graduate school. They published more frequently and presented at more conferences, felt that their research was more meaningful, and were more likely to report that they were on track to graduate within normative time (Figure 9). Notably, students who did not share any demographic identities with their advisors but rated their advisors highly on empathy tended to be similarly happy and productive as students who did feel represented by their advisors. This observation suggests that non-minority advisors can be highly effective mentors to students from minority backgrounds provided that they are open to learning about issues they have not personally experienced.

*Advising practices*

The overall quality of the student-advisor relationship consistently ranked among the top predictors of research progress, self-assessed career preparedness, well-being, and sense of belonging in science. To identify specific aspects of effective advisors, we asked students to evaluate their advisor on a range of qualities, some relating to empathy and kindness and others relating to structure, feedback, and helpfulness. Students who rated their advisors highly on empathy and kindness felt their labs were more inclusive, more collaborative, and had better conflict resolution. They felt more satisfied overall with their mentorship than students who rated their advisors low on kindness. Students who rated their advisors highly on structure and feedback published more often, felt their research was more meaningful, and felt more prepared for academic and non-academic careers (Figure 10). Of note, while kindness and feedback had explanatory value for different outcome variables, there was no trade-off between the two. In fact, most students who thought their advisors were honest and helpful also found them to be kind, and vice versa.

In both the empathy/kindness and structure/feedback evaluations, a large proportion of variance was attributable to a single variable – the availability of advisors to their students. Students who frequently met with their advisors reported a better understanding of what was expected of them, a higher sense of inclusion and belonging, and better preparedness for their post-graduate career. Meeting frequency was closely related to how meetings were scheduled: students saw their advisors more often and were happier with their meeting schedule if they could drop into their advisor's office briefly or had regular standing meetings (Figures 11-12). This distinction was especially important for female graduate students, who reported the least satisfaction with as-needed meetings. Female students who could only see their advisors on an as-needed basis also rated their labs low on equity, perhaps suggesting that advisors with this system were not equally available to all lab members (Figure 13). Lastly, group size influenced meeting frequency, with graduate students in the largest and smallest labs seeing the least of their advisors (Figure 14). In large labs, faculty likely face constraints on their time and/or delegate supervision to postdocs and senior graduate students. At the other end of the spectrum, we hypothesized that labs headed by faculty who invest less in mentoring might face challenges with recruitment and/or retention, eventually resulting in fewer members. In support of this possibility, students who were dissatisfied with their advisors came on average (though not exclusively) from smaller labs.

*Informal mentorship*

We asked respondents about the quality and quantity of their connections outside of their formal advising relationship. In general, students reported high levels of support from peers or near-peers on issues pertaining to research practices, scientific careers, and personal issues such as discrimination or work-life balance. Far fewer reported that they had received such advice from faculty, especially on personal issues. Be it advice from faculty members, collaborations with other labs, or support from other graduate students in the program, informal mentorship reduced or closed gaps in outcomes between students with good or poor relationships with their formal dissertation advisors (Figure 15). This suggests a path forward

for community building, particularly for students who are dissatisfied with their advising experience.

*Outlook*

The survey results highlight several potential opportunities for improving graduate experiences overall, but especially for those students that are reporting the lowest satisfaction and worst outcomes. Our study provides evidence of improved mentoring, research and career preparedness as well as improved sentiments of increased inclusion and equity associated with regularly scheduled meetings. Several findings from this study also point to the importance of community engagement and informal mentoring channels for graduate student experiences and outcomes. Facilitating connections for secondary mentors (both faculty and near-peer and especially in the smallest and largest lab groups), by improving collaborative environments, community inclusion and engagement may narrow the gap for those graduate students that are less satisfied with their primary mentoring experience. Finally, our results support the continued prioritization of faculty diversity. Graduate students represented by their primary advisor have improved outcomes and experiences in lab culture, inclusion, research progress and career preparedness.

**Table 1. Sample sizes and response rates by department. Enrollment is based on Spring 2022 data from the UC Berkeley Office of Planning and Analysis (OPA).**

| Department | Our study | UCB enrollment | Est. response rate |
|---|---|---|---|
| Integrative Biology (IB) | 42 | 114 | 36.8% |
| Molecular and Cell Biology (MCB) | 41 | 215 | 19.1% |
| Plant and Microbial Biology (PMB) | 24 | 92 | 26.1% |
| Environmental Science, Policy, and Management (ESPM) | 22 | 117 | 18.8% |

**Table 2. Sample sizes and response rates by gender, based on Spring 2022 data from the UC Berkeley OPA.**

| Gender identity (this study) | Composition of this study | Gender identity (UCB categories) | Composition of participating departments |
|---|---|---|---|
| Female | 56.6% | Female | 58.0% |
| Male | 27.1% | Male | 41.6% |
| Non-binary | 5.4% | Non-binary | 0.4% |
| Female, Non-binary | 3.1% | | |
| Male, Non-binary | 0.8% | | |
| NA / prefer not to disclose | 5.4% | | |

**Table 3. Sample sizes and response rates by race, based on Spring 2022 data from the UC Berkeley OPA.**

| Racial identity (this study) | Composition of this study | Racial identity (UCB categories) | Composition of participating departments |
|---|---|---|---|
| White/Caucasian | 50.4% | White/Other | 54.0% |
| East Asian/South Asian/Pacific Islander | 16.3% | Asian | 16.3% |
| Black | 4.7% | International | 10.4% |
| Native/Indigenous | 0.8% | Underrepresented Minority | 20.0% |
| Multiracial | 10.1% | | |
| NA / prefer not to disclose | 9.5% | | |

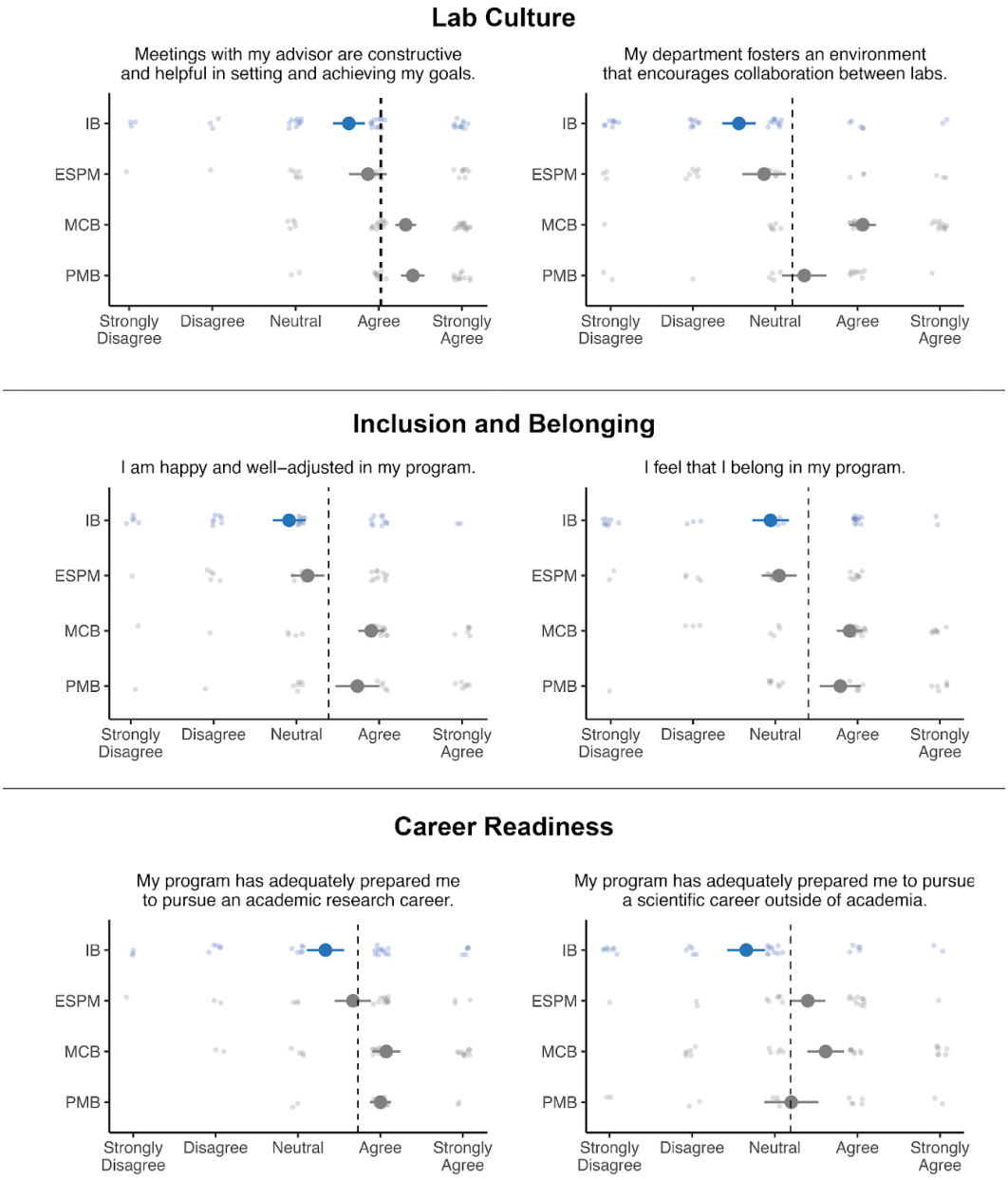


**Figure 1. Variation in graduate experiences across departments.** IB graduate students (blue) rated their graduate experiences lower than students in other departments (grey), including in the quality of meetings with their advisors (Tukey HSD post-hoc test, IB-PMB p = 0.019, IB-MCB p = 0.018), collaborations among labs (IB-MCB p<0.001), happiness (IB-PMB p = 0.032, IB-MCB p = 0.001), sense of belonging (IB-PMB p = 0.038, IB-MCB p = 0.003), readiness for an academic career (IB-MCB p = 0.031), and readiness for a non-academic career (IB-MCB p = 0.014). Summary bars represent means and standard errors by department, while dashed lines represent the mean response of all students in the study.

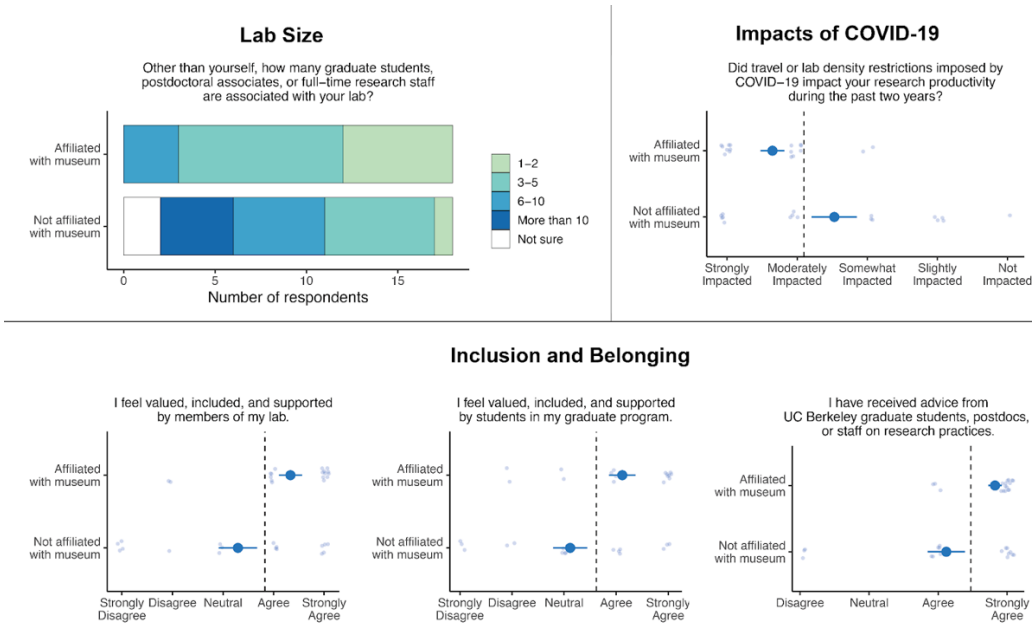


**Figure 2. Variation in experiences of IB students by museum affiliation.** IB labs affiliated with museums were smaller than labs not affiliated with museums (chi-squared test, $X^2$ = 10.671, p = 0.031). IB students affiliated with museums reported more inclusive and supportive experiences within their labs (generalized linear mixed model, ß = 1.194, p = 0.005) and graduate program (ß = 1.079, p = 0.005) and were more likely to report support from peers on research (ß = 0.712, p = 0.014). IB students affiliated with museums reported more hardship due to COVID-19 (ß = 1.002, p = 0.005).

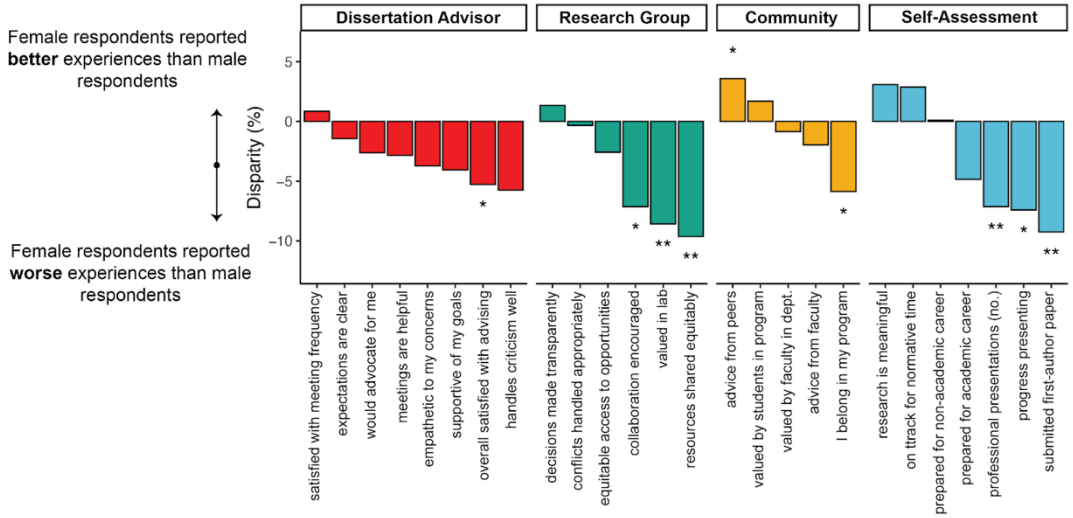


**Figure 3. Disparities in experiences of male and female graduate students.** We aimed to provide an overall view of differences among demographic groups. For each item with a quantitative response, the average difference between the response of each female graduate student and each male graduate student was computed. This distribution was compared to zero (the null hypothesis, that no differences exist across genders) using a one-sample t-test with degrees of freedom equal to the number of female graduate students minus one. The resulting plot shows areas of significant disparity between male and female graduate students, but also categories in which many differences are non-significant but trend in the same direction (e.g. experiences with dissertation advisor), patterns which may also be informative.

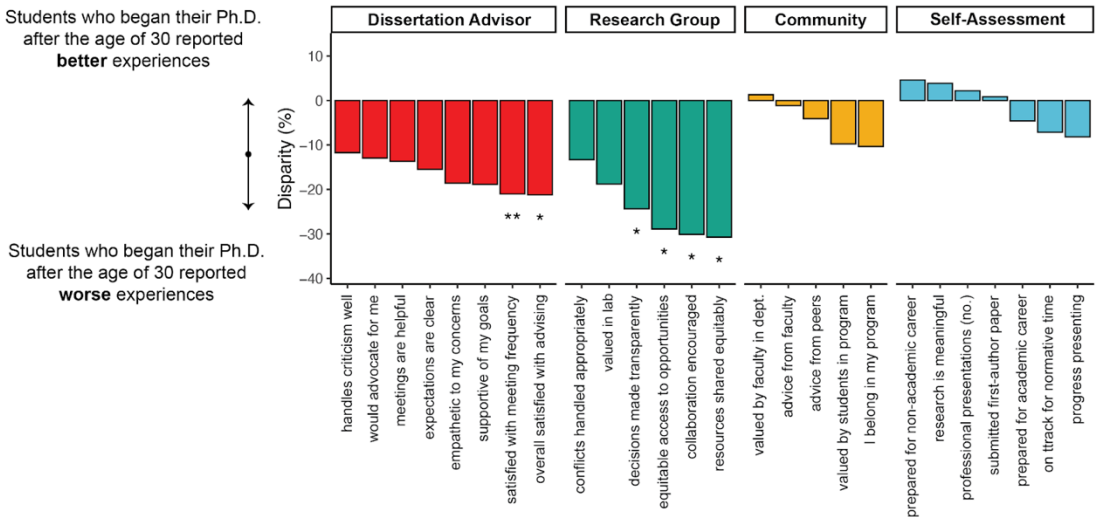


**Figure 4. Disparities in experiences of younger and older graduate students.** For each item with a quantitative response, the average difference between the response of each graduate student who started their Ph.D. after age 30 and each graduate student who started their Ph.D. before age 30 was computed. This distribution was compared to zero (the null hypothesis, that no differences exist) using a one-sample t-test with degrees of freedom equal to the number of older graduate students minus one.

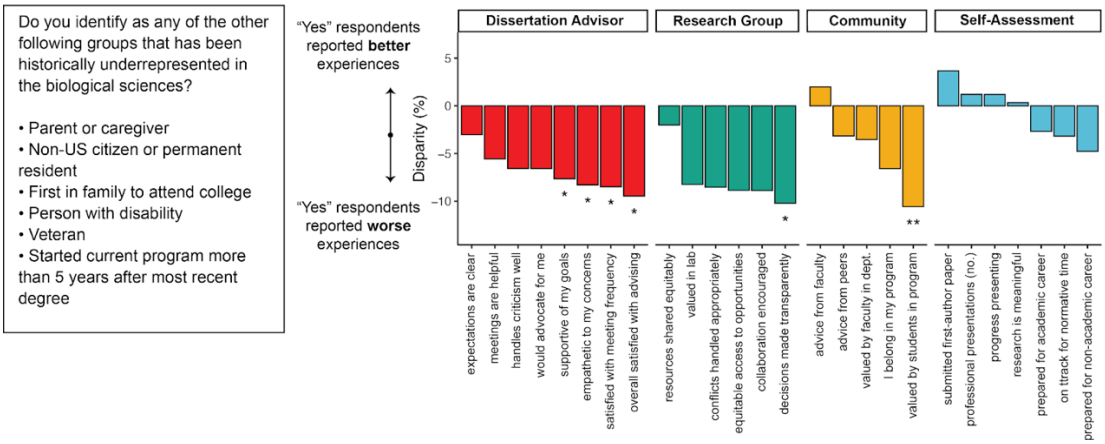


**Figure 5. Disparities in experiences of traditional and non-traditional graduate students.** For each item with a quantitative response, the average difference between the response of each non-traditional graduate student (i.e. those that answered "Yes" to the question in the left panel) and each traditional graduate student was computed. This distribution was compared to zero (the null hypothesis, that no differences exist) using a one-sample t-test with degrees of freedom equal to the number of non-traditional graduate students minus one.

1. **Gender** (female, non-binary, unlisted gender minority)
2. **Estimated age at start of program** (over 30)
3. **Representation by advisor** (no, not sure)
4. **Other underrepresented group** (parent or caregiver, non-US citizen, first-gen, disability, veteran, started program more than 5 years after most recent degree)
5. **Other identity not covered by survey** (elaborate in comments)

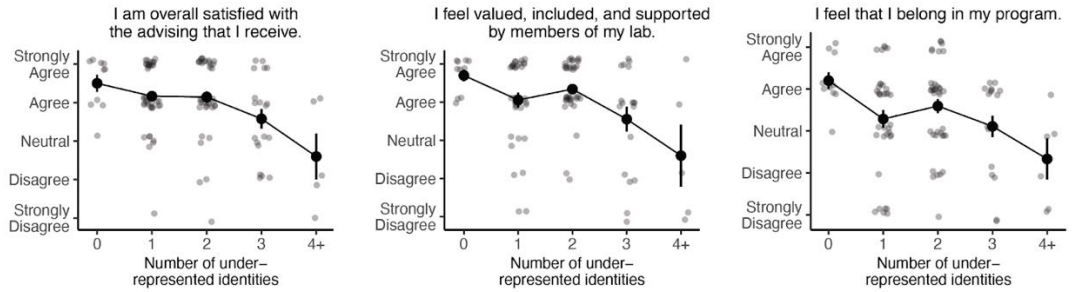


**Figure 6. Interactions between underrepresented identities.** Respondents who identified as multiple of the underrepresented identities listed in the top panel reported progressively lower satisfaction with their advisors (GLM, ß = -0.335, $p < 0.001$), inclusion and support within their labs (ß = -0.341, $p = 0.001$), and sense of belonging (ß = -0.221, $p = 0.037$) than respondents who identified as fewer underrepresented identities.

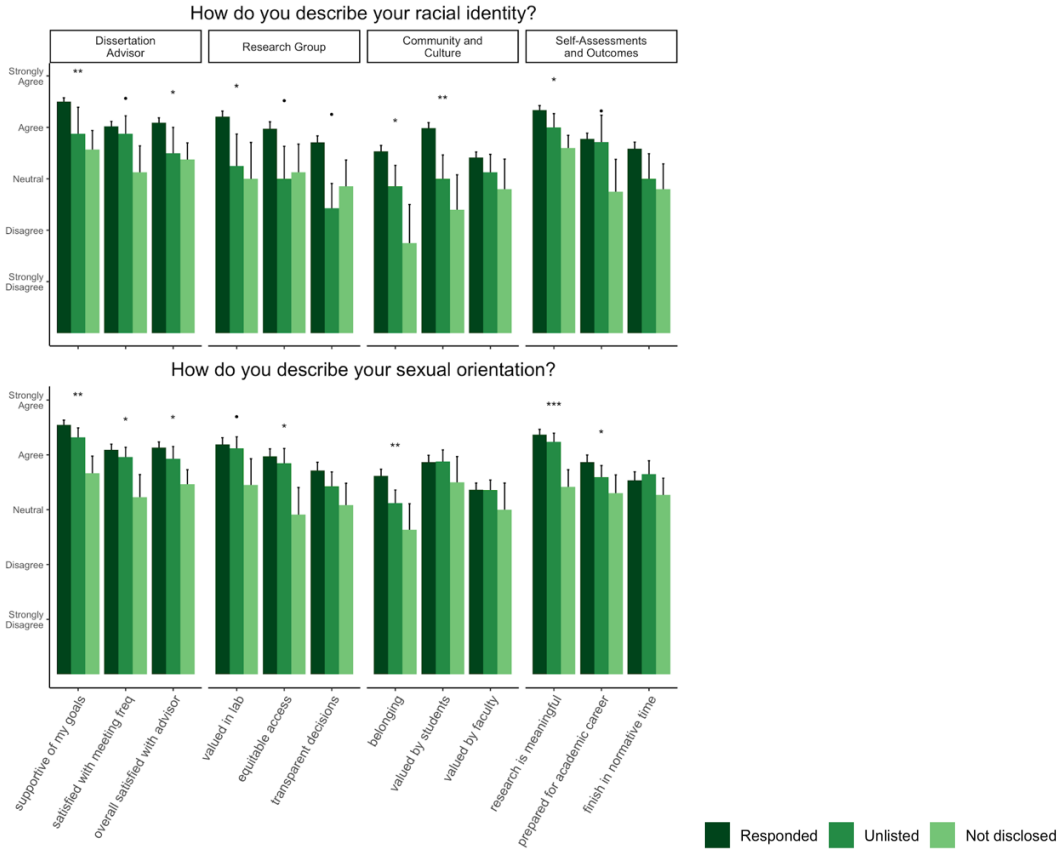


**Figure 7. Response type effects from race and sexual orientation demographic questions.** Respondents who chose either '*Unlisted*' or '*Prefer not to disclose*' in response to questions about their race (top) and sexual orientation (bottom) generally reported worse experiences with their dissertation advisor, their research group, the larger community, rated their research as less meaningful and rated themselves as less prepared for an academic career and less likely to finish in normative time. Statistical significance (cumulative link mixed models) is based on comparisons of "*Responded*" vs. "*Not disclosed*" groups.

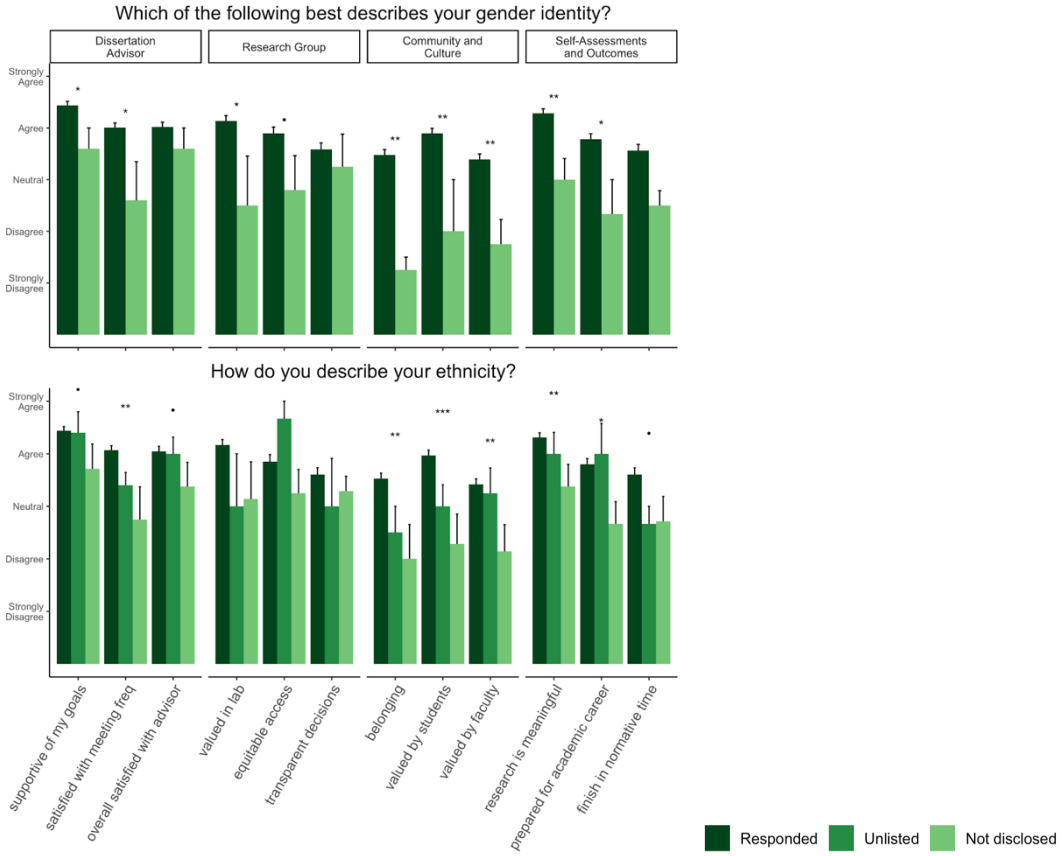


**Figure 8. Response type effects from gender and ethnicity demographic questions.** Respondents who chose either '*Unlisted*' or '*Prefer not to disclose*' in response to questions about their gender (top) and ethnicity (bottom) generally reported worse experiences with their dissertation advisor, their research group, the larger community, and additionally rated themselves as less prepared for an academic career, less likely to finish in normative time and rated their research as less meaningful. For gender identity, '*Unlisted gender minority*' and '*Prefer not to disclose*' responses are pooled (light green) because only one respondent chose '*Prefer not to disclose*'. Statistical significance (cumulative link mixed models) are based on comparisons of "*Responded*" vs. "*Not disclosed*" groups.

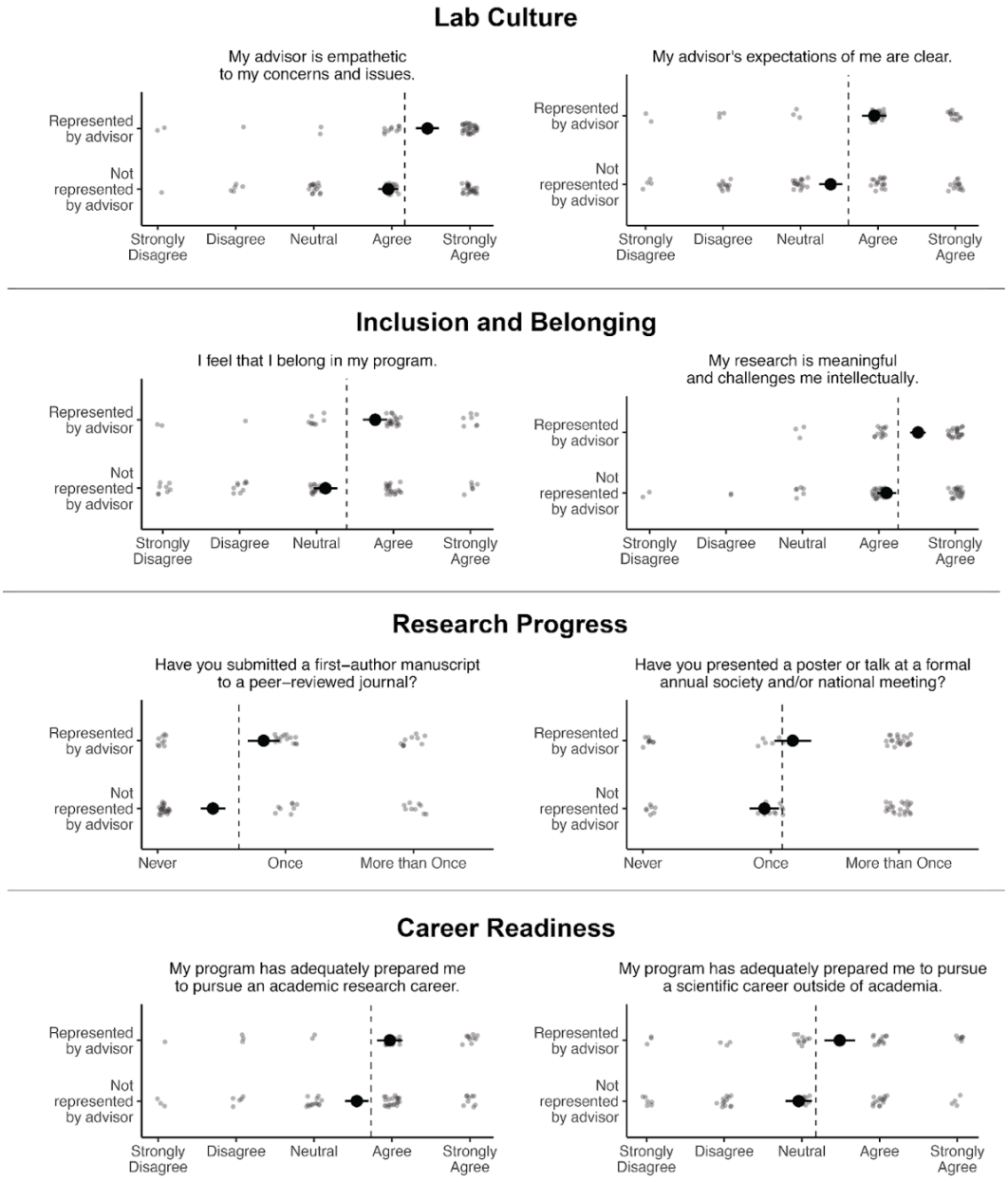


**Figure 9. Effects of demographic representation by advisor.** Respondents from historically underrepresented groups who felt their advisor shared one or more marginalized identities with them rated their advisors as more empathetic (GLM, ß = 0.503, p = 0.011) and felt they better understood what was expected of them (ß = 0.548, p = 0.015). They had a stronger sense of belonging (ß = 0.538, p = 0.017) and a stronger sense that their research was meaningful (ß = 0.410, p = 0.019). Controlling for their stage in the Ph.D. program, students who felt represented by their advisor were more likely to have submitted a first-author manuscript on their dissertation research (ß = 0.424, p = 0.006) and presented at a conference (ß = 0.324, p = 0.040) and felt more prepare d for academic (ß = 0.475, p = 0.038) and non-academic (ß = 0.667, p = 0.007) careers.

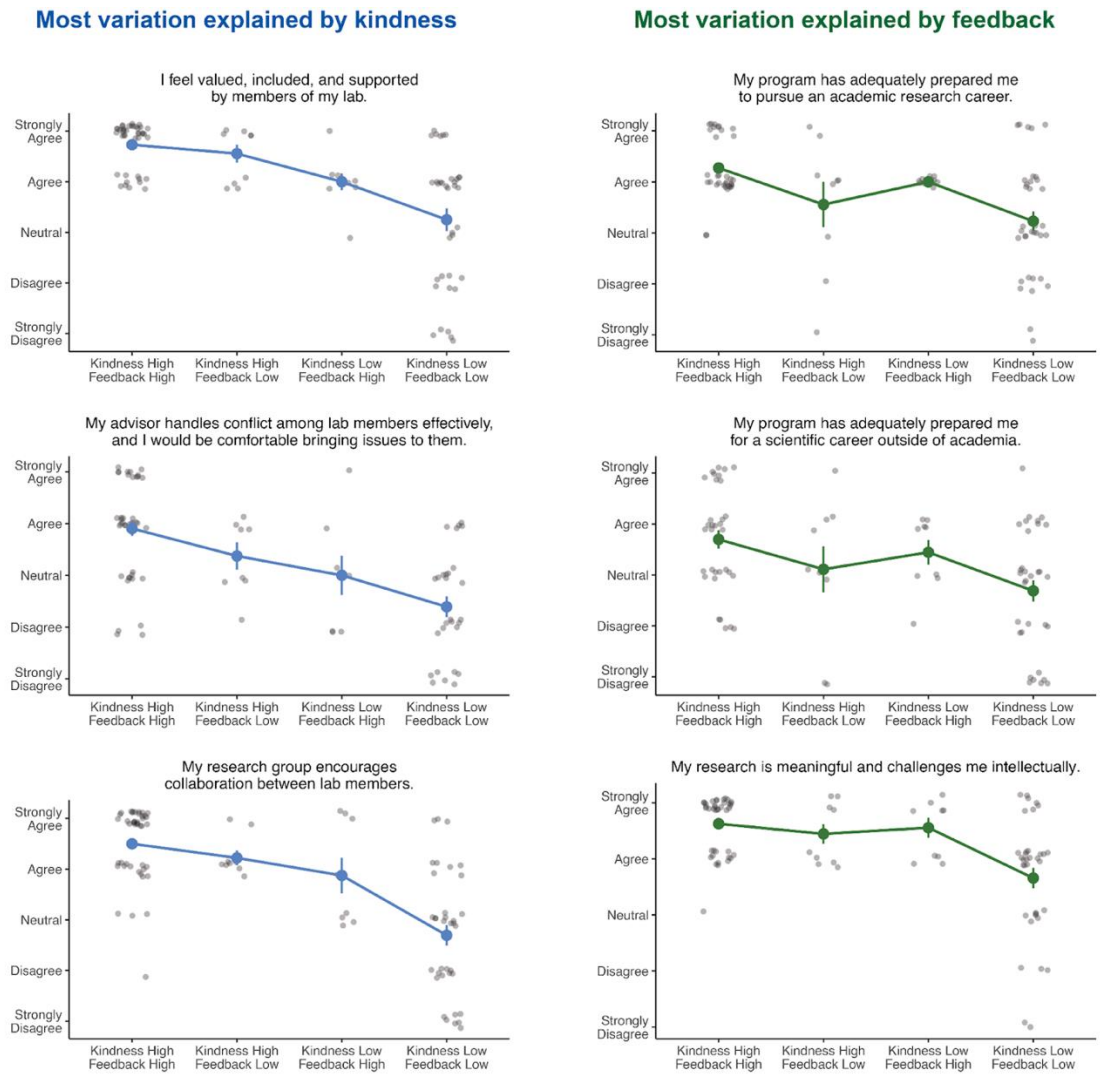


**Figure 10. Contributions of kindness and structure in advising styles to graduate student success and belonging.** An overall measure of advisor kindness was calculated based on total scores on the following items: "*My advisor is supportive of my goals and ambitions*"; "*My advisor is empathetic to my concerns and issues*"; "*My advisor would advocate for me if needed*". Similarly, an overall measure of structure and feedback was calculated based on total scores on the following items: "*My advisor's expectations of me are clear*"; "*My advisor is transparent with our lab*"; "*My meetings are constructive and helpful in setting and achieving my goals*". Both variables often contributed to explain student outcomes, but those relating to interpersonal dynamics tended to relate more strongly to advisor kindness, such as inclusion and support within the lab (GLM, kindness ß = 1.015 and $p < 0.001$, feedback n.s.), conflict resolution in the lab (kindness ß = 1.113 and $p < 0.001$, feedback ß = 0.653 and $p = 0.010$), and collaboration among lab members (kindness ß = 0.968 and $p < 0.001$, feedback ß = 0.601 and $p = 0.024$). Outcomes related to research progress and preparation tended to relate more to advisor structure and feedback, such as readiness for an academic career (kindness n.s., feedback ß = 0.668 and $p = 0.004$), readiness for a non-academic career (kindness n.s., feedback ß = 0.579 and $p = 0.040$), and feeling that their research is meaningful (kindness ß = 0.432 and $p = 0.039$, feedback ß = 0.521 and $p = 0.013$).

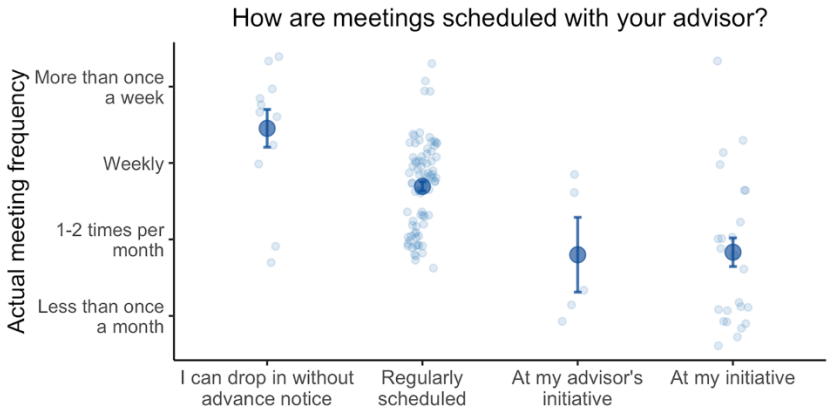


**Figure 11. Effect of how meetings are scheduled on meeting frequency.** The way meetings are scheduled between graduate students and their advisors significantly affects meeting frequency (ANOVA, *F*-value = 18.09, p < 0.0001). Here, regularly scheduled meetings are the combined values of the responses of "*Regularly scheduled, biweekly or less*" and "*Regularly scheduled, weekly or more.*" Graduate students that can drop-in without advance notice or that have regularly scheduled meetings meet, on average, more than two times per month. Students that meet at either their own or their advisor's initiative meet, on average, 1-2 times per month.

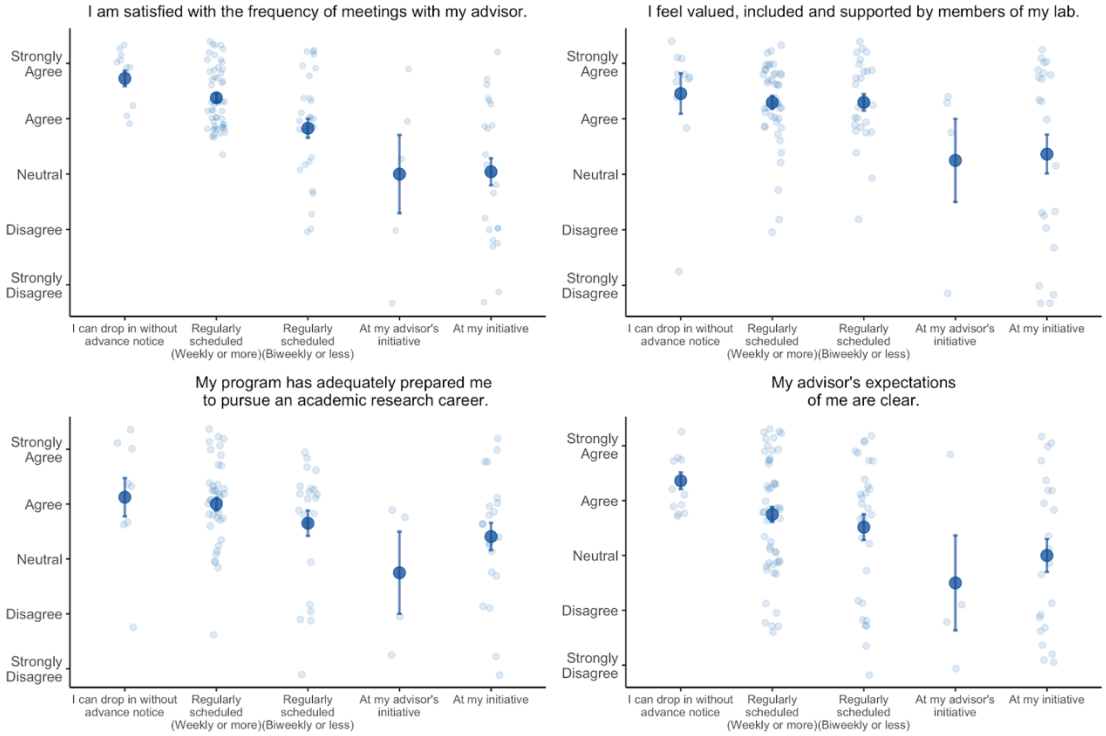


**Figure 12. Effect of how meetings are scheduled on advisor meeting satisfaction, value in lab, career preparedness and advisor's expectations.** Graduate students report higher levels of satisfaction with meetings (ANOVA, *F*-value = 14.35, p < 0.0001) as well as increased sense of value in their labs (*F*-value = 4.00, p = 0.005), preparedness for an academic career (*F*-value = 2.60, p = 0.04) and understanding of their advisor's expectations (*F*-value = 3.88, p = 0.005) when meetings are either available as drop-in or regularly scheduled.

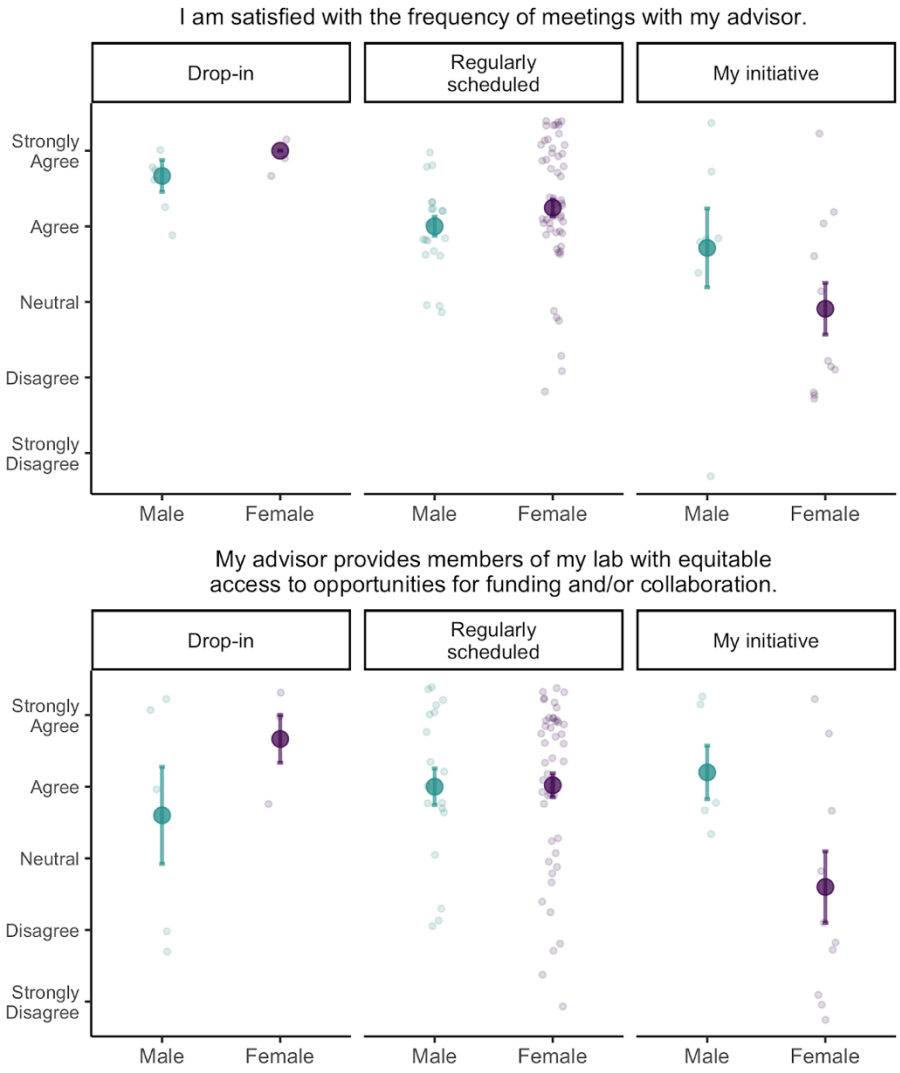


**Figure 13. Effect of how meetings are scheduled on advisor meeting satisfaction and lab equity by gender.** Female identifying respondents report differential overall meeting satisfaction (GLM, meeting satisfaction: gender overall, ß = 0.79, p = 0.052; *Regularly scheduled* vs. *At my initiative*, ß = 1.33, p < 0.0001; *Drop-in* vs. *At my initiative*, ß = 2.06, p = 0.0002; *At my initiative* vs. *Regularly scheduled* * gender, ß = -1.05, p = 0.023) and lab equity (*Drop-in* vs. *At my initiative*, ß = 2.06, p = 0.01; *Regularly scheduled* vs. *At my initiative*, ß = -1.42, p = 0.00096; *Drop-in* vs. *At my initiative* * gender, ß = -2.46, p = 0.016; *Regularly scheduled* vs. *At my initiative* * gender, ß = 1.62, p = 0.0292) when meetings are scheduled by their initiative, relative to male respondents. Regularly scheduled meetings refer to respondents that answered either "*Regularly scheduled, biweekly or less*" or "*Regularly scheduled, weekly or more.*" Respondents that identified as non-binary were excluded from this analysis due to anonymity issues.

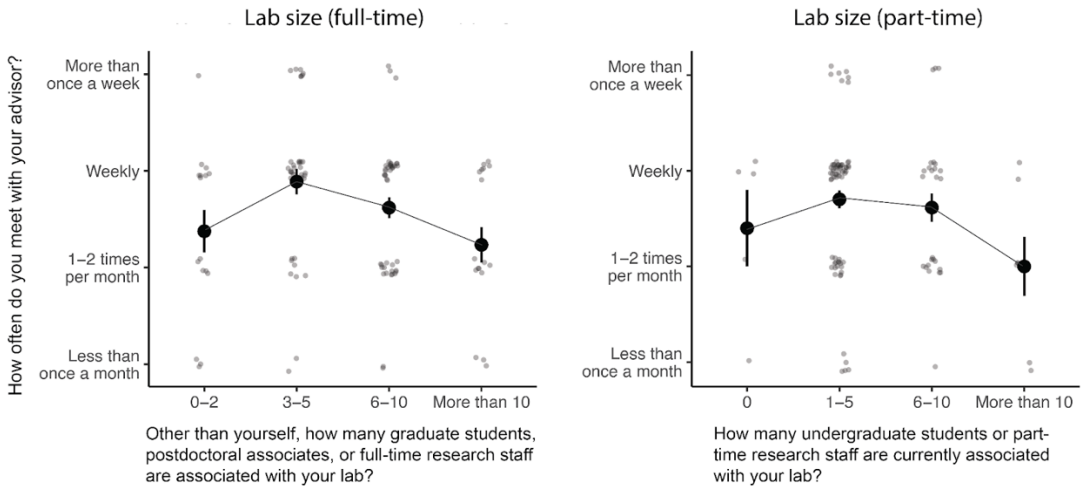


**Figure 14. Group size influences meeting frequency.** There was a significant inverse U-shaped relationship between full-time lab size and meeting frequency (quadratic regression, ß = -2.12, p = 0.007) and a significant relationship between part-time lab size and meeting frequency (quadratic regression, ß = 1.45, p = 0.059).

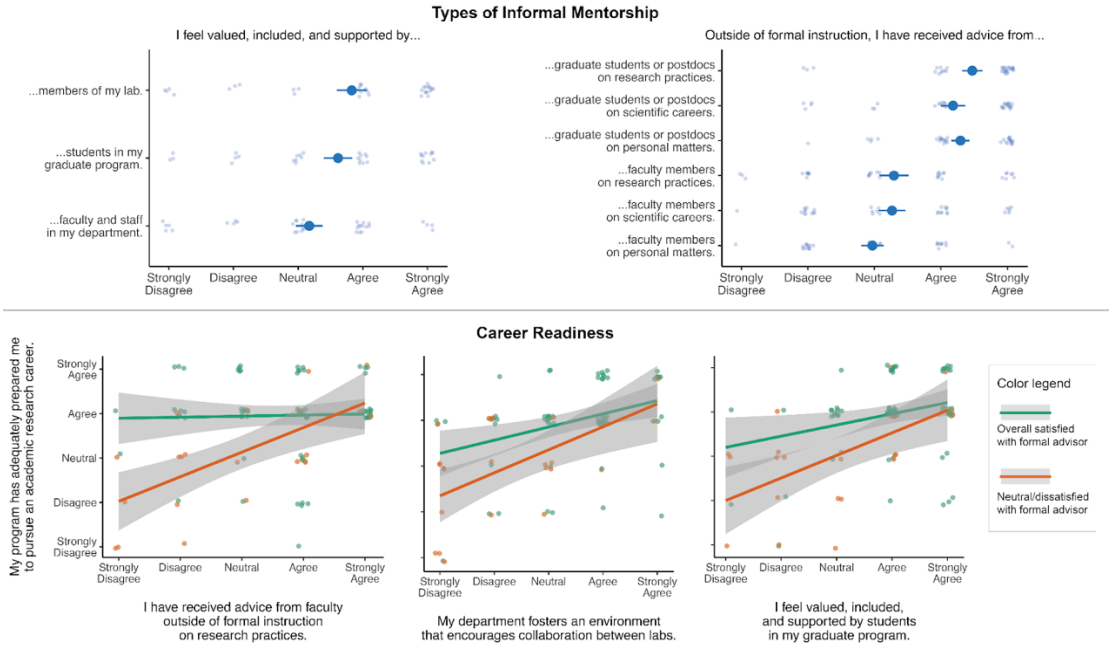


**Figure 15. Interactive effects of formal and informal mentorship.** IB graduate students generally reported high levels of support from their peers or near-peers, but less support from faculty (whether measured by feelings of inclusion or advice on research, scientific careers, or personal matters such as bias, discrimination, or work-life balance). For students dissatisfied with their formal advisors, several forms of informal mentorship such as research advice from other faculty (GLM, ß = 1.104, p = 0.006), collaboration with other labs (ß = 0.489, p = 0.034), and an inclusive departmental culture (ß = 0.804, p < 0.001) improved their self-assessed career preparedness similar to students with satisfactory advising experiences.